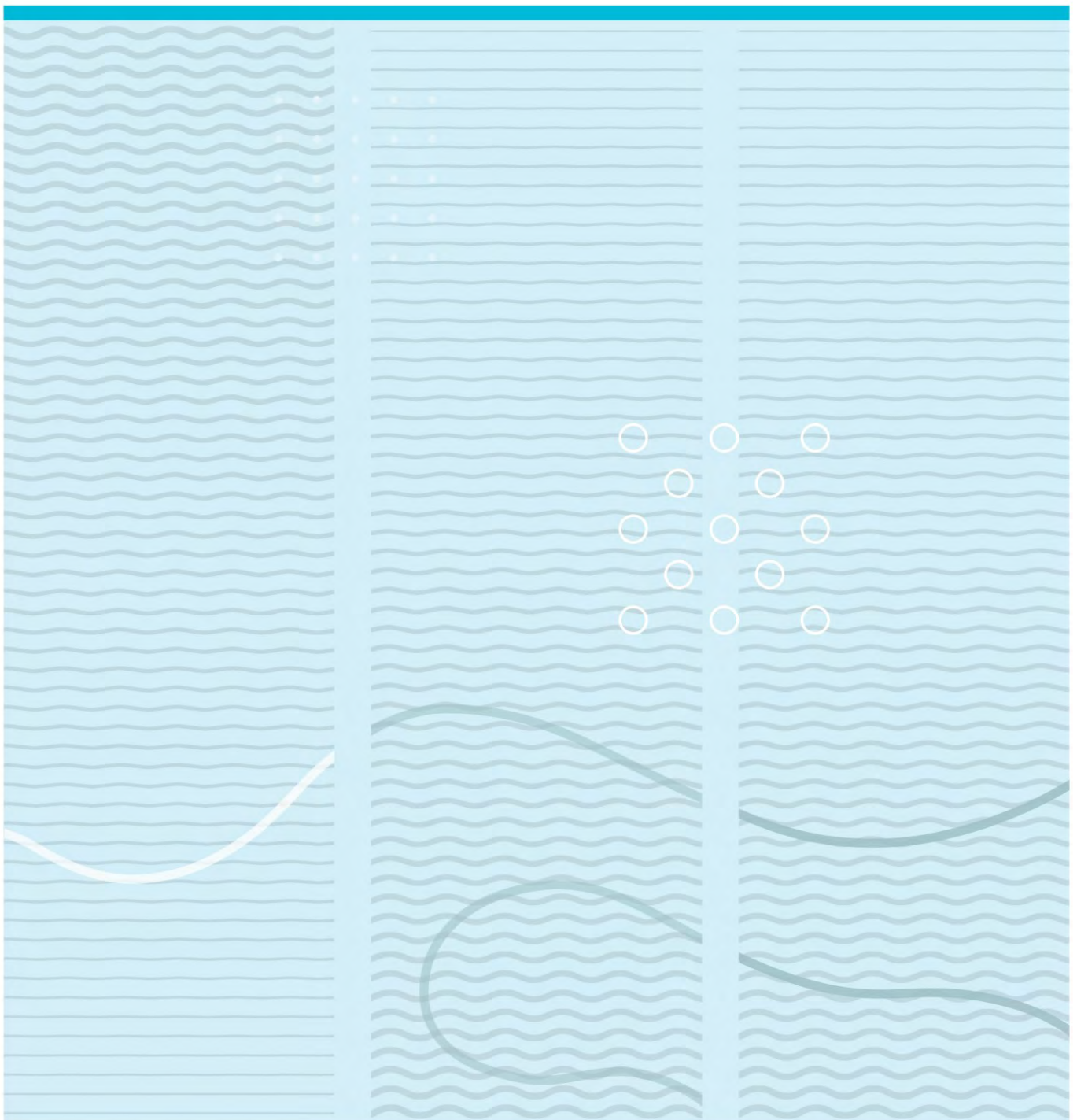


Ugwu Ambrose Anibueze

Improved oil recovery and the study of CO₂ storage in oil/gas reservoirs and aquifers



University College of Southeast Norway
Faculty of Technology
Institute of Process, Energy and Environmental Technology
PO Box 235
NO-3603 Kongsberg, Norway
<http://www.usn.no>

© 2016 Ugwu Ambrose Anibueze

This thesis is worth 30 study points

Summary

As the world's energy needs grow, several techniques have been introduced for an improved oil recovery (IOR) and secured storage of CO₂. Such techniques include the use of water injection, CO₂ for Enhanced Oil Recovery (EOR) and the application of inflow control devices (ICD) with the aim to maximize production and improve well performance. To meet global energy demand with the instability in oil price, these IOR techniques through advanced well completion and stimulation techniques have enabled commercial production in reservoirs previously abandoned by traditional recovery methods.

One of the objectives of this work is to ascertain the optimal water injection arrangement between vertical and horizontal water injection using ECLIPSE. Within this work, analyses of oil production, water breakthrough and pressure over simulation time were made. These analyses cover both cases of horizontal and vertical waterflooding in a homogeneous and a heterogeneous reservoir. In the results, it shows that the horizontal waterflooding provides longer delay in water breakthrough and increase in oil production. The increase in oil recovery achieved varies between 6% and 36% while the delay in breakthrough varies between 459 days and 1362 days.

This work also presents the mathematical models used for the implementation of ICD in ECLIPSE. A case study using reservoir conditions similar to Troll offshore Norway was simulated to illustrate the effect of ICD in a heterogeneous reservoir. The simulation result shows that with ICD completion, water breakthrough could be delayed for 262 days and water cut after 3000 days reduced by 11%. Despite the delay in water breakthrough, the oil production rate decreased. Although well productivity is reduced by approximately 42%, there is an improved degree of inflow equalization through ICD completion. Gas production was decreased by approximately 51% with ICD completion.

In addition to using CO₂ for EOR, it is crucial to store CO₂ to avoid the large contribution to global warming. It has been revealed that about 120 Giga tons of CO₂ would need to be captured and stored between 2015 and 2050 globally. Mature oil reservoirs and underlying aquifers are considered as the future solution for CO₂ storage. In this work,

literature study was carried out to have a better understanding of the storage capacity and suitability for CO₂ storage in oil/gas reservoirs and aquifers. The study shows that residual gas trapping and the dissolution in water give greater contribution to CO₂ storage than the structure trapping mechanism.

Contents

Summary	3
Foreword	8
Nomenclatures	9
1 Introduction	12
1.1 Background	13
1.2 Scope of work.....	13
1.3 Limitation	14
2 Improved oil recovery	16
2.1 Waterflooding	16
2.1.1 The principle of waterflooding.....	17
2.1.2 The effect of residual oil saturation.....	17
2.1.3 The effect of wettability	18
2.1.4 The effect of capillary pressure.....	18
2.1.5 The effect of relative permeability	18
2.1.6 The effect of mobility	19
2.2 The application of ICD.....	19
2.2.1 Orifice-type ICD.....	20
2.2.2 Advanced well completion	20
3 CO₂ storage	22
3.1 CO ₂ capture	22
3.2 CO ₂ transport	23
3.3 CO ₂ storage in geological formation	24
3.3.1 Storage in depleted oil and gas fields.....	25
3.3.2 Storage in saline aquifers	25
3.4 Vision for CO ₂ storage.....	26
3.5 CO ₂ trapping mechanism.....	27
3.5.1 Physical trapping mechanism.....	27
3.5.2 Chemical trapping mechanism.....	28
3.6 CO ₂ storage capacity in Nordic region	28
4 ECLIPSE model	30
4.1 Relative permeability model	31

4.2	ICD model.....	33
4.2.1	Pressure drop.....	33
4.2.2	Emulsion viscosity.....	34
4.3	CO ₂ storage Model	36
4.3.1	Storage in depleted oil reservoir	36
4.3.2	Storage in Aquifers	38
5	ECLIPSE simulation	42
5.1	General simulation procedure	42
5.2	Waterflooding.....	42
5.2.1	Geometry	43
5.2.2	Reservoir conditions	44
5.2.3	Initial conditions	45
5.3	Application of ICD	46
5.3.1	Geometry	47
5.3.2	Assumptions.....	48
5.3.3	Reservoir conditions	48
5.3.4	Initial conditions	49
6	Result and discussion	50
6.1	Homogeneous waterflooding	50
6.1.1	Result for the base case (Homogeneous)	50
6.1.2	Result for water injection of 500m ³ /day (Homogenous)	52
6.1.3	Result for water injection of 1000m ³ /day (Homogenous)	55
6.1.4	Result for water injection of 1500m ³ /day (Homogenous)	58
6.1.5	Result for water injection of 2000m ³ /day (Homogenous)	61
6.1.6	Result for water injection of 2500m ³ /day (Homogeneous)	64
6.1.7	Overall Pressure Trend (Homogeneous)	67
6.1.8	Water production (Homogeneous)	69
6.1.9	Oil production rate (Homogeneous)	70
6.1.10	Accumulated oil production (Homogeneous).....	71
6.1.11	Oil saturation distribution (Homogeneous)	73
6.1.12	Oil-water front progression (Homogeneous).....	75
6.2	Heterogeneous waterflooding.....	76

6.2.1	Result of the base case (Heterogeneous).....	76
6.2.2	Result at water injection of 500m ³ /day (Heterogeneous)	78
6.2.3	Result at water injection of 1000m ³ /day (Heterogeneous)	81
6.2.4	Result at water injection of 1500m ³ /day (Heterogeneous)	84
6.2.5	Result at water injection of 2000m ³ /day (Heterogeneous)	87
6.2.6	Result at water injection of 2500m ³ /day (Heterogeneous)	90
6.2.7	Overall pressure trend (Heterogeneous)	93
6.2.8	Overall water cut (Heterogeneous)	95
6.2.9	Overall oil production rate (Heterogeneous)	97
6.2.10	Accumulated oil production	98
6.2.11	Gas production.....	100
6.3	Application of ICD	103
6.3.1	Reservoir pressure	103
6.3.2	Water production	103
6.3.3	Oil Production	104
6.3.4	Gas Production.....	106
7	Conclusion.....	108
	References	110
	List of tables and charts	113
	Annexes	116

Foreword

This work focuses on the improved oil recovery and study of CO₂ storage in oil/gas reservoirs and aquifers using ECLIPSE Reservoir Simulator in fulfilment of Master's thesis FMH606. This research topic is interesting and two papers have been accepted for publication for EUROSIM conference 2016 from the results presented herein. See Annex 9 for details.

I would like to thank the management of University College of Southeast Norway and Inflow Control AS for the opportunity created to work on this interesting topic. My gratitude also goes to Professor Britt Margrethe Emilie Moldestad at University College of Southeast Norway for good supervision and support. I would also thank my wife Chinazor Monalisa Ugwu for her love. I would also like to acknowledge my friend Cornelius Agu of University College of Southeast Norway for his assistance.

Porsgrunn/3rd June, 2016

Ugwu Ambrose Anibueze

Nomenclatures

Notation	Description	Units
a	Volume fraction	[-]
A	Area	[m ²]
B	Formation volume factor	[-]
C	Effective Storage coefficient	[-]
C _s	Dissolution co-efficient	[-]
E _D	Unit displacement efficiency	[-]
E _r	Oil recovery factor	[-]
G _f	Possible mass source of phase f	[-]
h _s	Enthalpy for possible sources	[kJ/kg]
H	Pressure Head	[Pa]
k	Effective permeability	[D]
k _r	Relative permeability	[-]
M	Mobility ratio	[-]
M _t	Theoretical storage capacity of CO ₂	[Mt]
P	Pressure	[Pa]
P _{sat}	Saturation pressure	[bar]
q	Flux	[m/s]
Q	Volume flow rate	[m ³ /s]
R _s	Gas-oil ratio	[-]
R _{so}	Residual oil saturation	[-]
R _u	CO ₂ utilization co-efficient	[-]
R _v	Oil-gas ratio	[-]
S	Saturation	[-]
S _{oi}	Initial oil saturation	[-]
S _{orw}	Residual oil saturation	[-]
S _{wc}	Connate water saturation	[-]
t	Time	[sec]
T	Transmissibility	
T _c	Critical temperature	[K]
v	Velocity	[m/s]

V	Volume	[m ³]
V _p	Pore volume	[m ³]
V _r	Rock volume	[m ³]
Z	Vertical position	[m]
$\frac{N}{G}$	Net Gross	[-]
R _w ^{CO₂}	Solubility of CO ₂	[kg _{CO₂} /m ³ _{H₂O}]
API	American Petroleum Institute	
CO ₂	Carbon dioxide	

Abbreviation **Description**

CSS	Carbon Capture and Storage
EOR	Enhanced Oil Recovery
IEA	International Energy Agency
MMP	Minimum Miscibility Pressure
ICD	Inflow Control Devices
IOOP	Original Oil in Place
IOR	Improved Oil Recovery

Symbol **Description** **Units**

β	Momentum transfer coefficient	[kg/(m ³ s)]
λ	Mobility	[Pa.s]
Φ	Porosity	[-]
ρ	Density	[kg/ m ³]
μ	Viscosity	[cP]
γ	Specific gravity	[-]

Operators **Description**

Δ	Increment
$\frac{d}{d}$	Ordinary derivative
$\frac{\delta}{\delta}$	Partial derivative
∫	Integral

Subscripts **Description**

c	Component index
g	Gas
i	Phase
j	Connection
o	Oil
p	Phase
s	Solid (Rock)
w	Well
x	X-direction
y	Y- direction
z	Z- direction
l,k,f	Phase index

1 Introduction

The method for oil recovery can be divided into primary, secondary and tertiary techniques. In primary recovery method, the natural driving mechanisms such as water drive from underlying aquifers are used to extract the oil to the surface. This recovery mechanism can maintain sufficient pressure difference between reservoir and production well to move the oil to the surface. The recovery factor achieved with primary mechanism is between 10% and 15% original oil in place (OOIP) [1].

While the underground pressure in the oil reservoir is sufficient to force the oil to the surface, it is necessary to apply an advanced completion technology such as the use of inflow control device to manage the fluid flow through the reservoir. Inflow control devices slow water and gas encroachment and reduces amount of bypassed reserves [2]. With this advanced completion through stimulation techniques, it is feasible to continue commercial production in previously abandoned reservoirs [3].

Over the lifetime of the well the pressure will fall, and at some point where the underground pressure is not sufficient to force the oil to the surface. After natural reservoir drive diminishes, secondary recovery technique such as waterflooding can be applied. Typical recovery factor is between 20 to 40% OOIP [1]. Waterflooding is widely used as external agent to increase the pressure in the reservoir. The water injection process requires power and could be capital intensive to install pumps and turbines on offshore platforms. With these financial risks, it is necessary to ascertain the optimal water injection arrangement between vertical and horizontal water injection.

Tertiary oil recovery such as the use of CO₂ for enhanced oil recovery is used to increase the mobility of the oil in order to increase extraction. The typical recovery factor for this mechanism is between 30 and 60% OOIP [1]. In addition to using CO₂ for EOR, it is crucial to store CO₂ to avoid the large contribution to global warming. Carbon capture and storage (CCS) remains a critical greenhouse gas reduction solution[4]. With CCS advancement, massive deployment of new technology and effective CO₂ storage facilities is required.

1.1 Background

Several studies have shown that considerable amount of oil still remains in the reservoir after the well shutdown. With this challenge, petroleum industry is continuously looking for new technologies to improve oil recovery and to optimize operation. The main drawbacks faced by the industry are low oil recovery factor, depletion of oil production, gas coning and water coning.

As reservoirs mature, secondary recovery method such as waterflooding can be used to maintain reservoir pressure and increase sweep efficiency. Water Injection can be done through a horizontal or vertical well. It is important to ascertain the best injection method for an optimum oil recovery. Also with this secondary recovery method, water production could exceed the oil production before the reservoir is exhausted. The cost of handling the produced water is high and demands that water production to should be minimized. One increasing popular approach is to use inflow control devices that slow water and gas breakthrough and reduces amount of bypassed reserves [2].

CO₂ is used for Enhanced Oil Recovery (EOR) in fields with high amount of residual oil. In addition to using CO₂ for EOR, it is crucial to store CO₂ to reduce contribution to global warming. Mature oil reservoirs and underlying aquifers are considered as the future solution for CO₂ storage. A better understanding of the storage capacity and suitability for CO₂ storage in reservoirs and aquifers is required.

1.2 Scope of work

The main objective of this thesis is to simulate the effect of waterflooding and implement an inflow control device towards an improved oil recovery. Also the study of CO₂ storage in oil/gas reservoirs and aquifers was also covered. This thesis is structured in seven chapters covering the following topics.

- *Introduction (Chapter one)*: An overview, objectives and scope of the project are presented.
- *Improved oil recovery (Chapter two)*: the theory of waterflooding and the application of passive inflow control device are presented.

- *CO₂ storage (Chapter three)*: Literature study for CO₂ storage and EOR is treated.
- *ECLIPSE Model (Chapter four)*: the mathematical models used in ECLIPSE for the simulation of waterflooding, implementation of inflow control device and CO₂ storage and EOR are described.
- *ECLIPSE simulation (chapter five)*: the simulated parameters, reservoir conditions, geometry and procedures for waterflooding and the application of ICD are discussed.
- *Result and discussion (chapter six)*: The simulated results obtained are presented and discussed.
- *Conclusion (chapter seven)*: Finally, the significant contribution of this work is described and the recommendations for further work are given.

The task and work plan for achieving the above objective are given in Annex 1.

1.3 Limitation

In this thesis, some areas were not covered but may be considered in future work due to the following reasons.

- Limited resources

Although the simulation model for CO₂-EOR and storage was studied, there was no license to run the simulation. Also due to time constraint, advanced well bore completions were not considered to improve to the wellbore flow and its interaction with the reservoir region.

- Insufficient reservoir information

There was no adequate geological and geophysical data to build reservoir models for reserves estimation and fluid flow simulation. In this study, a lot of assumptions and simplifications of reservoir parameters were made. Although results are in agreement with theory, the real reservoir behavior may not be fully represented.

- Non flexibility of ECLIPSE simulation algorithms

Due to the implicit nature of ECLIPSE, It is not possible for a user to modify original program, assumptions and the in-built mathematical models. Owing to this, simulation results may not be accurate.

2 Improved oil recovery

The oil industry has long applied techniques such as waterflooding and the use of inflow control devices to improve oil and gas recovery. Research and development on emerging IOR projects in a quest to keep producing from mature reservoirs is necessary in order to meet global energy demand.

2.1 Waterflooding

Waterflooding is a secondary method of oil recovery where water is injected into the reservoir with the aim to increase reservoir pressure and thereby increasing oil production [5]. Waterflooding was first practiced for pressure maintenance after primary depletion and has since become the most widely adopted IOR technique [6]. It is now commonly applied at the beginning of reservoir development [6].

With water injection, the reservoir pressure is sustained and oil is pushed towards the production well. The oil-water front progresses toward the production well until water breaks through into the production stream. With the increasing water production, the oil production rate diminishes, until the time when the recovery is no longer profitable and the production is brought to an end [7]. Up to 35% oil recovery could be achieved economically through waterflooding [7]. Figure 2-1 depicts a typical horizontal and vertical waterflooding arrangement respectively.

Water can be injected through a vertical or a horizontal well. Determining the optimal position and orientation of the wells has a potentially high economic impact [8]. One major difference between the horizontal and vertical water injection is the water breakthrough behavior. Asheim studied the optimization of vertical well waterflooding processes with fixed well locations [9] while Brouwer & Jansen studied the optimization of waterflooding using a horizontal injection [10]. In both cases, delay in water breakthrough improves production rate. Also from literature, it has been shown that water breakthrough can be delayed by changing the position of the injection well profiles [10]. Studies also revealed that the use of horizontal well, delays the water breakthrough and improves the vertical sweep efficiency [11].

2.1.1 The principle of waterflooding

The principal reason for waterflooding is to increase the oil production rate and improve oil recovery. This is achieved through voidage replacement to support the reservoir pressure and sweep or displace oil from the reservoir towards the production well [12]. The efficiency of such displacement depends on many factors like oil viscosity, density and rock characteristics. Reservoir screening is necessary for the technical and economic success of waterflooding.

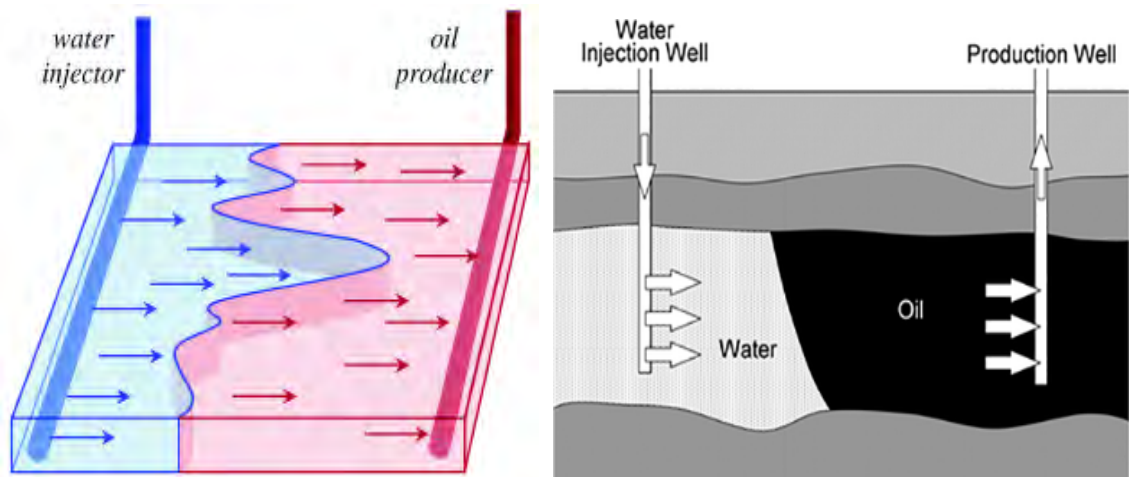


Figure 2-1 Typical horizontal and vertical waterflooding[5, 7]

2.1.2 The effect of residual oil saturation

Residual oil saturation and connate water saturation are very important numbers in waterflooding. The connate water saturation is the lowest water saturation found in situ and determines how much oil is present initially, while the residual oil saturation indicates how much of the original oil in place (OOIP) will remain in the pores after sweeping the reservoir with injected water [12]. Equation (2-1) represents the unit-displacement efficiency with the condition that the oil formation volume factor is the same at the start and the end of the waterflooding [12].

$$E_D = 1 - \frac{S_{orw}}{S_{oi}} \quad (2-1)$$

where E_D is the unit displacement efficiency S_{oi} is the initial oil saturation and S_{orw} is the residual oil saturation.

The residual oil saturation can be obtained for equation (2-2)

$$S_{orw}=1 - S_{wc} \quad (2-2)$$

where S_{wc} is the connate water saturation

2.1.3 The effect of wettability

The wettability of a reservoir rock can be defined as the tendency of a fluid to spread on, or to adhere to a solid surface in the presence of another immiscible fluid [13]. In an oil- water system it is a measure of the preference the rock has for either oil or water [14]. Changes in wettability influence the capillary pressure, irreducible water saturation, relative permeability and water flood behavior [14]. Maximum oil production rate by waterflooding is normally achieved at water-wet conditions shortly after water breakthrough [15].

2.1.4 The effect of capillary pressure

Capillary pressure is the pressure difference existing across the interface separating two immiscible fluids in porous media. Capillary pressure determines the amount of recoverable oil for waterflooding applications through imbibition process for water wet reservoir [11].

2.1.5 The effect of relative permeability

The Relative permeability is the ratio of the effective permeability to the absolute permeability of each phase. It is expressed for a specific saturation of the phases in equation (2-3):

$$k_{r,i} = \frac{k_i}{k} \quad (2-3)$$

where $k_{r,i}$ is the phase relative permeability, k is the total effective permeability and k_i is the phase effective permeability.

Relative permeability affects the unit displacement efficiency and how much of the OOIP will be recovered before the waterflooding economic limit is reached. When the interfacial tension between oil and gas phases decreases, the relative permeability values change [16], which influences the oil and gas recovery as well as the reservoir pressure.

2.1.6 The effect of mobility

Mobility, λ is described as the ratio between the endpoint effective permeability and the fluid viscosity, μ . It shows how easy the fluid is flowing through a porous medium [17]. Mobility ratio, M , plays an important role during waterflooding. It can be defined as the ratio between the mobility of the displacing fluid (water) and the displaced fluid (oil) as expressed in equation (2-4) [17]:

$$M = \frac{\lambda_{(\text{displacing})}}{\lambda_{(\text{displaced})}} = \frac{k_{r(\text{displacing})} \cdot \mu_{(\text{displaced})}}{k_{r(\text{displaced})} \cdot \mu_{(\text{displacing})}} \quad (2-4)$$

where M is the mobility ratio, λ is the mobility, k_r is the relative permeability, μ is the viscosity. The subscripts displacing and displaced represent the displacing phase and the displaced phases respectively.

Mobility ratio is considered to be either favorable if the value is less than or equal to unity or unfavorable if the value is greater than unity [12]. Favorable mobility ratio means that the displaced phase (oil) can move more quickly than the displacing phase (water) through the reservoir rock.

2.2 The application of ICD

The rate of inflow to a horizontal well can vary along the completion length due to some reasons such as frictional pressure losses or heterogeneity in reservoir permeability. These variations reduce oil sweep efficiency and the ultimate recovery. Owing to this, it is necessary to manage fluid flow through the reservoir in order to maximize oil recovery along horizontal wells and reduce bypassed reserves [2]. One increasingly popular approach is to use inflow control devices that delay water and gas breakthrough into the well. Inflow control devices balance the inflow coming from the reservoir toward the wellbore by introducing an extra pressure drop.

The challenges introduced by reservoir heterogeneity with horizontal wells tends to increase with increasing well length [18]. Completions with long intervals often have significantly uneven specific inflow distribution along their length. These inflow variations cause premature water or gas breakthrough and should be minimized [19]. Advanced well completions have been demonstrated as solution to these challenges.

Inflow Control Devices (ICDs) is an established type of advanced completions that provide passive inflow control [20]. ICDs are widely used and can be considered to be a mature well completion technology. One of the challenges is the variation in rock properties. Fluid specific inflow rate tends to increase with increasing well length [3]. ICDs are static and usually installed at the beginning of the production life. An alternative technology is the use of autonomous inflow control device with the ability of closing off the flow interval in an event of water or gas breakthrough [1].

2.2.1 Orifice-type ICD

The orifice ICD incorporates a given number of orifices of known diameter and flow characteristics. This design is very similar to nozzle-based design. The orifices are part of the ICD chamber while the nozzles are perforated directly on the base pipe. The orifices perforated on ICD chamber provide required pressure drop [18].

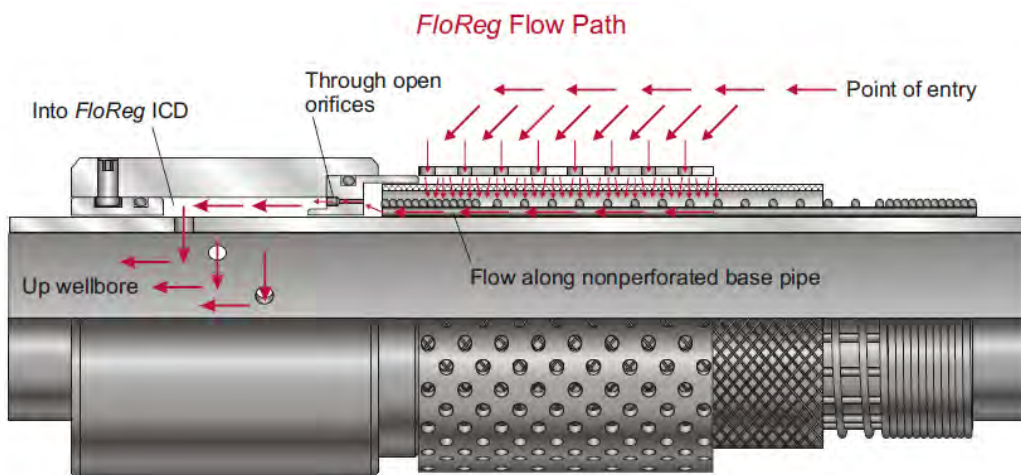


Figure 2-2 Oriface ICD [18]

2.2.2 Advanced well completion

The use of an advanced completion technology has proven to be a practical solution to the flow variation in horizontal wells [23]. The two major types of advanced completions are Interval Control Valves [22] and Inflow Control Devices [23]. With the installation of these devices along the wellbore, the inflow is controlled by restricting fluid flow from annulus into tubing. The settings and distribution of these restrictions

are designed to enhance sweep efficiency and restrict unwanted water or gas production.

ICD work by imposing a pressure drop between the sandface and the tubing to equalize drawdown across the completion. Some ICDs can change their response according to the properties of the inflowing fluid. Since ICDs behave as a choke, overall flowrate will be reduced unless the bottomhole pressure is reduced or injection pressure increased [21].

3 CO₂ storage

Historically, CO₂ accounts for the largest expense associated with EOR projects [24]. Most projects are designed for an effective CO₂ storage in oil recovery process[24]. The commercial challenges associated with CO₂ storage and EOR are numerous [25]. Additional energy and cost is incurred to recycle produced the CO₂ during EOR process. A CCS project involving CO₂-EOR known as CCS-EOR has been developed to improve emission control and secure storage of CO₂ saline aquifers [26]. Climate and energy policies required to enable every stakeholder adhere to the the rules and regulations. At present, however, the extent to which CO₂-EOR can contribute to emission reduction goals is unclear [26]. Despite the uncertainty associated with CCS-EOR, it is expected to offer means to offset the costs [26]. CCS process depends fundamentally on the production process and industrial facility. A typical CCS process is illustrated in figure 4-1.

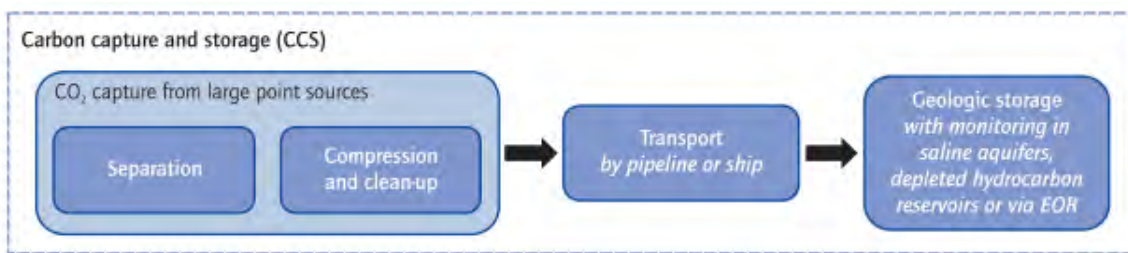


Figure 3-1 Standard CCS process[27]

3.1 CO₂ capture

In Traditionally, CO₂ can be captured in four different ways namely: post-process caputre, syngas/hydrogen capture, oxy-fuel combustion and inherent separation. In Post-process capture, CO₂ is separated from a mixture of gases (eg. flue gas) at the end of the production process. Syngas/hydrogen capture is an indirect process where syngas, a mixture of hydrogen, carbon monoxide and CO₂, can be captured from fossil fuels or biomass. The CO₂ can be furhter removed, leaving a combustible fuel, feedstock or reducing agent. Oxy-fuel combustion involves the use of oxygen in place of air during combustion to yield a flue gas of high CO₂ concentration [26]. Inherent separation involves the generation of concentrated CO₂ during production process. Some of the

large-scale CO₂ capture projects categorised by sector, capture potential, storage type and estimated start date are shown in figure 3-2.

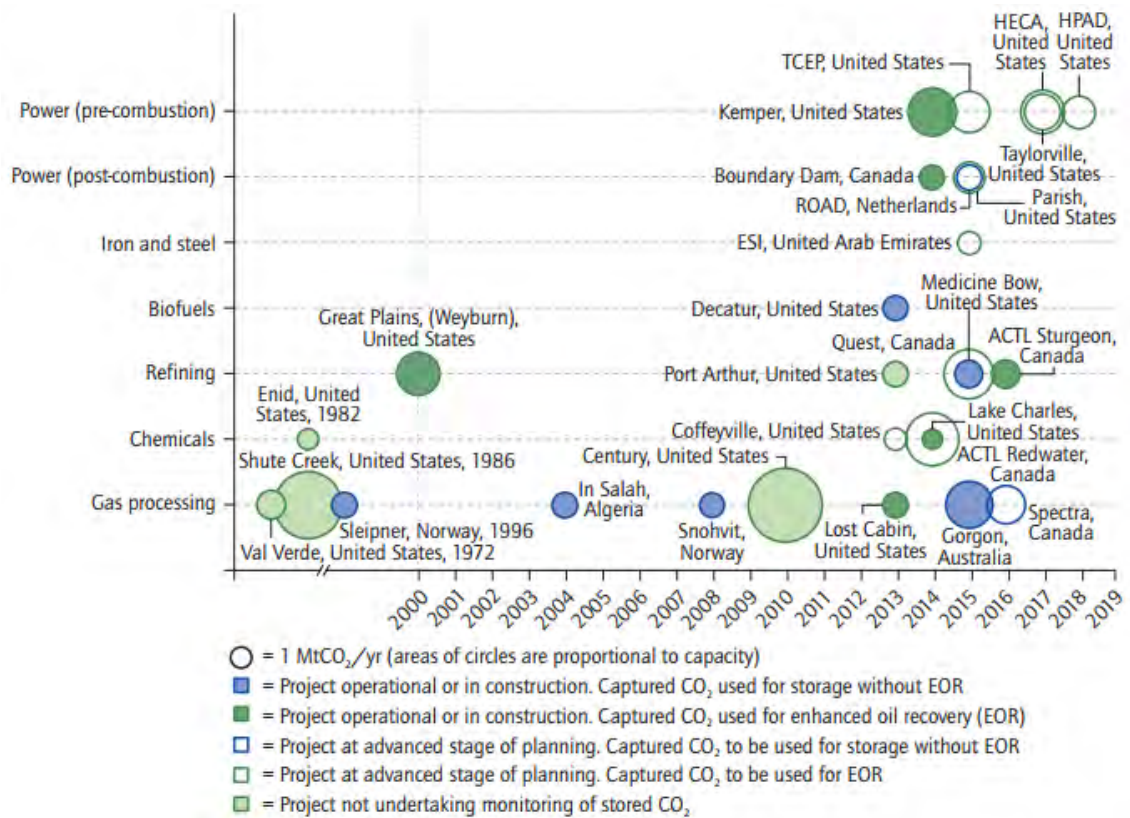


Figure 3-2 Large-scale CO₂ capture projects [27]

3.2 CO₂ transport

Transport of CO₂ in pipelines is a mature technology with more than 6 000 km of CO₂ pipes installed in the United States [27]. Guidance for the design and operation of CO₂ pipelines that supplements existing technical standards for pipeline transport of fluids was released in 2010 [28]. CO₂ can also be transported by ship, but in small quantities. Understanding of the technical requirements and conditions for CO₂ transport by ship has improved recently [29]. To achieve CCS deployment at the scales, it will be necessary to link CO₂ pipeline networks and shipping transportation infrastructure to allow access to lowest-cost storage capacity [28].

3.3 CO₂ storage in geological formation

Geological storage or geo-sequestration of CO₂ is considered to be one of the important routes for mitigating global warming [30, 31]. Geological storage of CO₂ involves the injection of CO₂ into appropriate geologic formations. The main goal of geological storage is to store CO₂ underground for a sufficient period of time. The minimum required retention time for the CO₂ should exceed few thousand years or the annual leakage rate of CO₂ should not exceed 0.01% of the injected CO₂ [32]. The storage depth is typically between one and three kilometres under the ground [33]. Storage should incorporate an effective monitoring facility of injected CO₂ [33]. Suitable geologic formations include saline aquifers, depleted oil and gas fields, oil fields with CO₂-EOR potential, and coal seams with potential for enhanced coal-bed methane (ECBM) recovery. Storage in other types of geologic formations and for other purposes, such as enhanced gas recovery or geothermal heat recovery is possible [27]. Figure 3-3 shows different geological formations for a secure CO₂ storage.

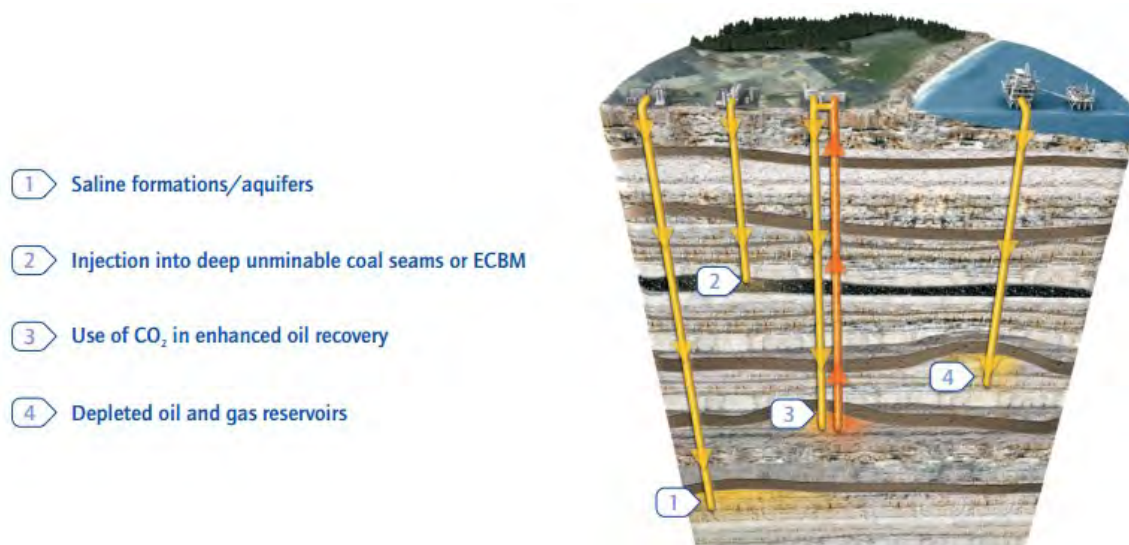


Figure 3-3 CO₂ Storage overview[27]

According to the report provided by the International Energy Agency in 2009, saline aquifers has the largest worldwide storage potential of 10,000Gt of stored CO₂ [34]. The storage capacity of oil and gas fields is estimated to be ten times less than saline aquifer [34].

3.3.1 Storage in depleted oil and gas fields

Sequestration of CO₂ in depleted gas and oil fields can be performed when reservoir pressure has become sufficiently low and no gas/oil can be produced naturally. The injection of CO₂ in such fields can continue until the pressure of the reservoir reaches its initial value. Therefore the lower the initial reservoir pressure, the more suitability for CO₂ storage. In this perspective, depleted gas fields are preferred over depleted oil field. The gas that is removed during the production process lowers the pressure in the reservoir. Depleted gas fields make about 90% of the total storage potential in oil and gas fields [34]. According to IEA report, storage potential of CO₂ in gas fields is nearly 800 Gt, meanwhile for oil fields it is only about 30Gt of CO₂ [34]. The geology and sealing properties contributes to storage capacity. However, limited capacity and unavailability of geographic site can be treated as disadvantages for using oil and gas reservoirs for CO₂ storage [35].

Oil fields are preferable as CO₂ storage sites for combined CCS and CO₂-EOR projects [30]. Only 90% to 95% of CO₂ produced along with oil from a field is injected back to the reservoir in a closed loop during CO₂-EOR [36]. Jilin oilfield in the northeast China is one of the largest projects where CO₂-EOR is combined with further CO₂ sequestration to the aquifer. During four working years, 200 000 tons of CO₂ was injected in the reservoir using CO₂-miscible flooding method as much as 80% of injected CO₂ was stored in the reservoir [30].

3.3.2 Storage in saline aquifers

The majority of CCS projects all over the world are based on CO₂ storage in deep saline aquifers. Availability of saline aquifers with high capacity makes them preferential over the oil and gas fields. The drawback of using aquifers as CCS is a lack of knowledge in geology and lithology of aquifers. High investments are needed in order to identify feasibility of using selected aquifers. Higher risks of leakage and uncertainty of storage capacity also accompany the exploitation of aquifers [37].

Sleipner and Snøhvit fields are examples of large scale CSS projects where CO₂ is injected to the aquifers in order to mitigate global warming. Both Sleipner and Snøhvit fields are operated by Statoil and each of them store approximately one million tonnes

of CO₂ per year. Sleipner project was triggered in 1996 in the North Sea. It is considered to be the first industrial scale CSS project where an aquifer is used as storage formation. In the Sleipner field, CO₂ is injected to the Utsira Sand that is characterized with high permeability (~2D) and porosity (up to 0.4) rocks [32]. The Snøhvit field was triggered in 2007 in northern Norway in the Barents Sea. This project was started as a result of high CO₂ emission taxes from gas and oil fields in Norway. Initially CO₂ was injected in Tubåen Formation, but in 2011 injection to this formation was stopped due to fast pressure increase. Up to date, Stø Formation is used as storage formation in Snøhvit field. The Stø formation is characterized with 0.7 D permeability and 0.2 porosity [32].

3.4 Vision for CO₂ storage

The projection for CO₂ storage according to the International Energy Agency (IEA) is shown in figure 3-4 [38]. From the figure, a total cumulative mass of approximately 120 Gt of CO₂ would need to be captured and stored between 2015 and 2050 in order to keep the global temperature rise within 2°C [38]. To achieve this goal, storage capacity will be a valuable asset for the private and public sectors[4]. Large-scale transportation networks with the capability of transporting billions tonnes of CO₂ annually between capture facilities and storage sites should be available to achieve this vision.

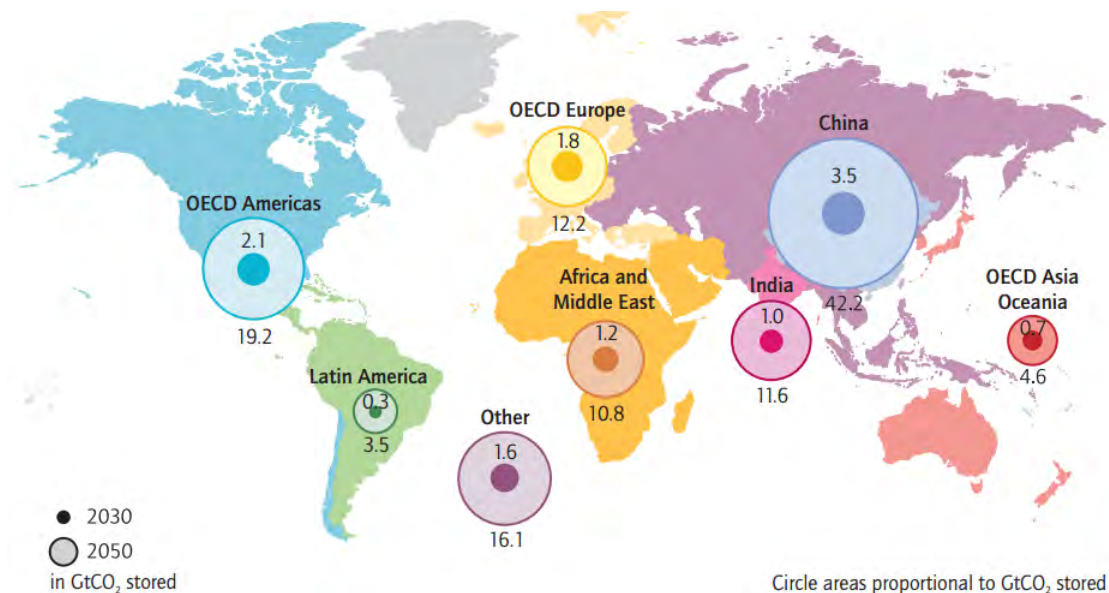


Figure 3-4 IEA Vision for Cumulative CO₂ captured between 2015 and to 2050 [38]

3.5 CO₂ trapping mechanism

Carbon dioxide is trapped in reservoirs through chemical and physical mechanisms. Physical trapping mechanisms have greater contribution in CO₂ storage pathways. The main CO₂ trapping mechanisms are depicted in figure 3-5.

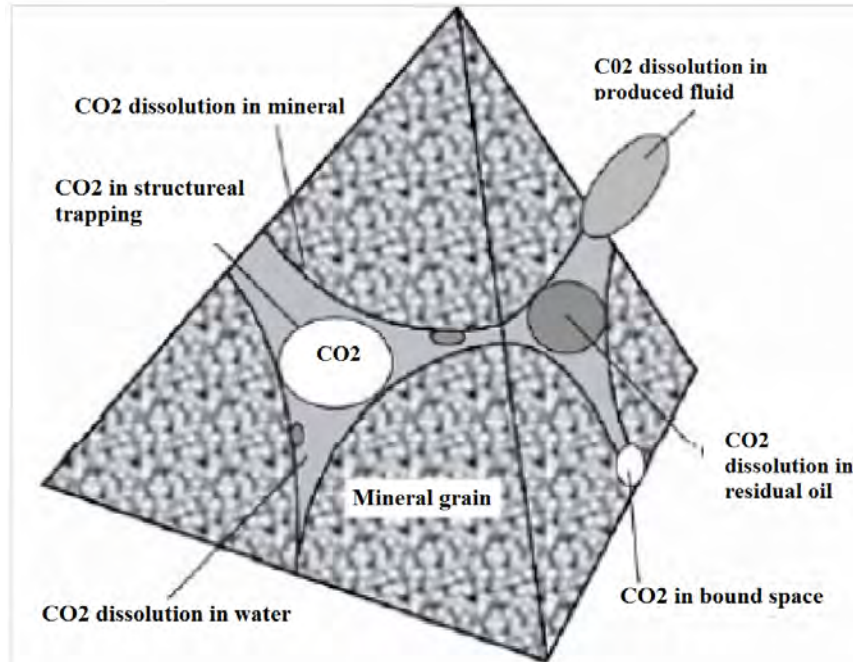


Figure 3-5 CO₂ trapping mechanisms[35]

3.5.1 Physical trapping mechanism

- **Strati-graphical and structural trapping:** Free CO₂ may migrate within the reservoir due to naturally occurring buoyancy forces and pressure gradient. However, migration of CO₂ might be limited due to impermeable barriers, i.e. cap-rocks. Layers of halite and mudstone are examples of low permeable barriers where CO₂ is retained due to strati-graphical and structural trapping [31, 32].
- **Residual gas (saturation) trapping:** In this mechanism, CO₂ may remain trapped in small pores at irreducible water saturation. This occurs due to capillary forces and adsorption on the surface of the mineral [31, 32, 39].

3.5.2 Chemical trapping mechanism

Chemical mechanisms are those processes where CO₂ is dissolved in subsurface fluids. Several types of chemical mechanisms play role in CO₂ storage [31, 32, 39]

- **Dissolution trapping:** In this mechanism, CO₂ that is injected to the reservoir dissolves in the formation water and become retained inside the reservoir brine. This mechanism is assumed to be the safest CO₂ trapping mechanism inside the reservoir [31, 32].
- **Mineral trapping:** Mineral trapping may be formed due to chemical reaction between CO₂ and the rock matrix. CO₂ interacts with water and minerals that are naturally occurring in formation rocks. As a result of this reaction, solid carbonate minerals and aqueous complexes are formed. However the contribution of mineral trapping is very limited due to its very slow reaction rate [31, 32, 39].
- **Adsorption trapping:** After CO₂ is dissolved in subsurface fluid it can be absorbed on the mineral surfaces. This process is known as adsorption trapping [39].

3.6 CO₂ storage capacity in Nordic region

According to CO₂ Storage Atlas provided by the Norwegian Petroleum Directorate [40], the highest CO₂ storage capacity in the Nordic region is the Utsira and the Skade formations. Both of them are estimated to store about 15.8 Gt CO₂ (see Figure 3-6).

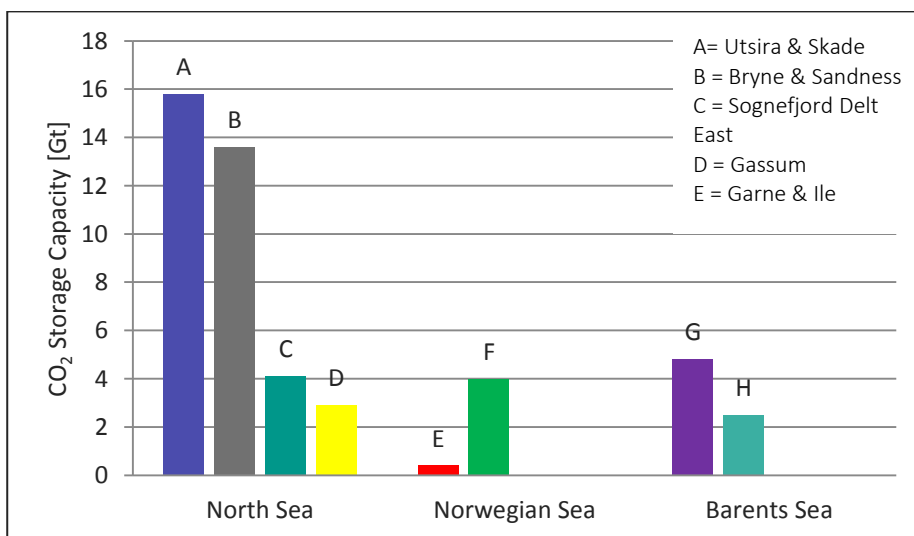


Figure 3-6 Storage capacity of largest aquifers in Nordic region

Bryne and Sandnes Formations are the second largest aquifers. Up to date, storage capacity of Barents Sea and Norwegian Sea aquifers do not exceed 4Gt of CO₂ storage capacity [40].

CO₂ storage capacity depends mainly on the following parameters [32, 37]:

- Cap rock properties:
 - Lateral continuity
 - Thickness
 - Resistance for high capillary entry pressure
 - Resistance for chemical degradation
- Reservoir properties:
 - Rock type
 - Pressure (depth more than 800 m)
 - Porosity (more than 0.1)
 - Permeability (more than 200 mD)
 - Thickness (more than 20 m)
 - Salinity (more than 30 000 mg/L)
- The nature of reservoirs rock boundaries:
 - Affect the pressure build up during injection.

4 ECLIPSE model

In ECLIPSE Reservoir simulation is a form of numerical modeling used to quantify and interpret physical phenomena with the ability to predict future performance. ECLIPSE flow model is shown in figure 4-1.

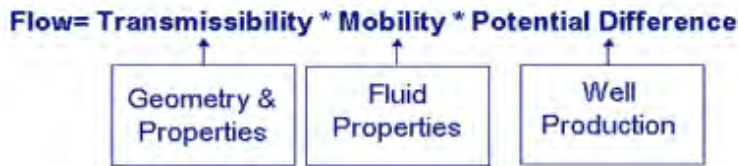


Figure 4-1 ECLIPSE flow model [15]

The simulation process involves dividing the reservoir into several discrete units in three dimensions, and modeling the progression of reservoir and fluid properties through space and time in a series of discrete steps [15]. Equations (4-1) – (4-7) are solved for each cell and each time step which are a combination of the material balance equation and Darcy's law [16].

Darcy's law (without gravity term) is expressed as:

$$q = -\frac{k}{\mu} \nabla P \quad (4-1)$$

where q is the flux, k is the permeability; μ is the viscosity and ∇P is the pressure gradient.

Material Balance is expressed as:

(Mass Flux = Accumulation + Injection/Production):

$$-\nabla \cdot M = \frac{\partial}{\partial t} (\phi \rho) + Q \quad (4-2)$$

where M is the mobility ratio, ϕ is the porosity, ρ is density and Q is volume flow rate.

Simulator Flow Equation (with gravity term) is expressed as:

$$\nabla \cdot [\lambda (\nabla P - \gamma \nabla Z)] = \frac{\partial}{\partial t} \left(\frac{\phi}{\beta} \right) + \frac{Q}{\rho} \quad (4-3)$$

$$\lambda = -\frac{k}{\mu \beta} \quad (4-4)$$

where μ is mobility, t is time, β is momentum transfer coefficient, γ is relative gravity and Z is vertical position.

Well Model is expressed as:

$$q_{p,j} = T_{wj} M_{p,j} (P_j - P_w - H_{wj}) \quad (4-5)$$

$$M_{o,j} = \frac{K_{o,j}}{B_{o,j} \cdot \mu_{o,j}} + R_v \frac{K_{g,j}}{B_{g,j} \cdot \mu_{g,j}} \quad (4-6)$$

$$M_{g,j} = \frac{K_{g,j}}{B_{g,j} \cdot \mu_{g,j}} + R_s \frac{K_{o,j}}{B_{o,j} \cdot \mu_{o,j}} \quad (4-7)$$

where T is the transmissibility, P is the pressure, H is the pressure head, B is the formation volume factor, R_s is the gas-oil ratio and R_v is the oil-gas ratio. The subscripts p is phase, j is connection, w is well, o is oil and g is gas

4.1 Relative permeability model

In this study, Corey model is used to define relative permeability curves of water and oil. This model is based on combination of Burdine approach of calculating relative permeability of wetting and non-wetting phases by Corey. Corey model sometimes might be called also Brooks and Corey model. If the pore size distribution index is less than 2 than model is called Corey model, if greater than two it is called Brooks and Corey model [41]. Equation 4-8 represents Corey model for predicting relative permeability of water [42].

$$k_{rw} = k_{rwoc} \left(\frac{S_w + S_{wir}}{1 - S_{wir} + R_{so}} \right)^{n_w} \quad (4-8)$$

where k_{rw} is relative permeability of water, k_{rwoc} is an end point of water at its maximum saturation, S_w is water saturation, S_{wir} is irreducible water saturation, R_{so} is residual oil saturation and n_w is Corey fitting parameter for water.

The model used to estimate predicting the relative permeability of oil is presented in equation (4-9) [42].

$$k_{row} = k_{rowc} \left(\frac{S_w + R_{so} - 1}{S_{wir} + R_{so} - 1} \right)^{n_{ow}} \quad (4-9)$$

Where k_{row} is the oil relative permeability for water-oil system, k_{rowc} is an end point of oil in water at irreducible water saturation and n_{ow} is the fitting parameter for oil.

The model used to estimate predicting the relative permeability of gas is presented in equations (4-10) and (4-11).

$$k_{rog} = k_{rocw} \cdot \left(\frac{1 - S_{org} - S_{wc} - S_g}{1 - S_{org} - S_{wc}} \right)^{n_{og}} \quad (4-10)$$

$$k_{rg} = k_{rgro} \cdot \left(\frac{S_g - S_{gc}}{1 - S_{org} - S_{wc} - S_{gc}} \right)^{n_g} \quad (4-11)$$

where k_{rog} is the oil relative permeability to gas, k_{rocw} is the relative permeability of oil zero gas saturation and k_{rg} is the gas relative permeability. S_{org} is the residual saturation of gas, S_{wc} is the connate water saturation, S_g is gas saturation, S_{gc} is the critical gas saturation, n_g is the Corey exponent for the gas phase and n_{og} is the Corey exponent for oil and gas phase.

See Annex 4 for the relative permeability data used for the simulation. Figure 4-2 shows the relative permeability used for the simulation.

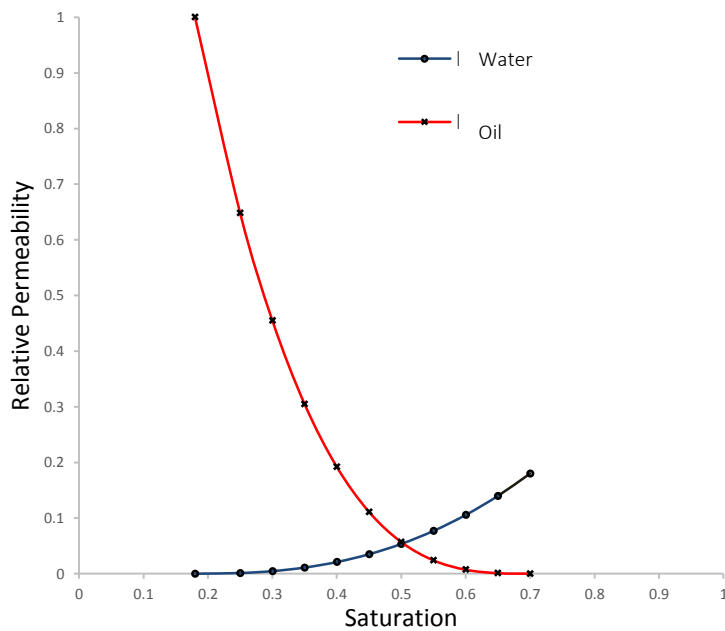


Figure 4-2 The relative permeability curve used for the simulation

4.2 ICD model

This In ECLIPSE, ICD is used to control the inflow profile along a horizontal well or branch by imposing an additional pressure drop between the sand face and the tubing. The device is placed around a section of the tubing and diverts the fluid inflowing from the adjacent part of the formation through a sand screen and then into a spiral before it enters the tubing [43].

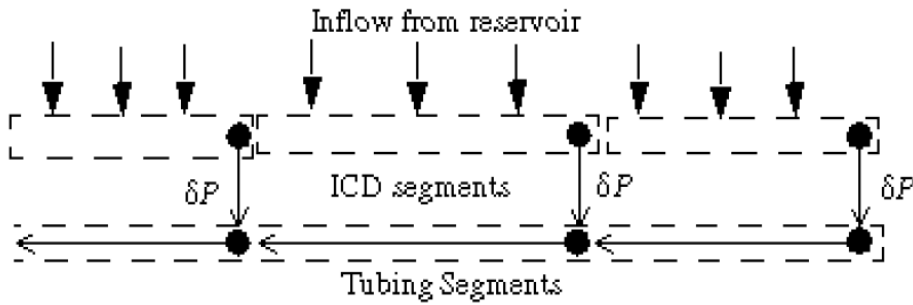


Figure 4-3 ICD segments along the well[44]

4.2.1 Pressure drop

The pressure drop across the device is calculated from calibration data, adjusted to allow for the varying density and viscosity of the reservoir fluid flowing through the device. The pressure drop equation is shown in equation (4-12) below [44].

$$\Delta P = \left(\frac{\rho_{cal} \cdot \mu_{mix}}{\rho_{mix} \cdot \mu_{cal}} \right)^{1/4} \cdot \frac{\rho_{mix}}{\rho_{cal}} \cdot K \cdot q^2 \quad (4-12)$$

Here ρ_{mix} is the density of the fluid mixture in the segment at local conditions and ρ_{cal} is the density of the fluid used to calibrate the ICD. μ_{mix} is the viscosity of the fluid mixture in the segment at local conditions and μ_{cal} is the viscosity of the fluid used to calibrate the ICD. K is the base strength of the ICD defined in equation (4-13).

$$K = \frac{a_{sICD}}{\rho_{cal}} \quad (4-13)$$

where a_{sICD} is defined as the strength of the ICD, q is the volume flow rate of fluid mixture through the ICD at local conditions, which is equal to the volume flow rate

through the ICD segment multiplied by a scaling factor that depends on the length of the device.

The density of the fluid mixture at local segment conditions is given in equation (4-14)

$$\rho_{\text{mix}} = \alpha_o \cdot \rho_o + \alpha_w \cdot \rho_w + \alpha_g \cdot \rho_g \quad (4-14)$$

where $\alpha_{o,w,g}$ is the volume fraction of the free oil, water, gas phases at local conditions and $\rho_{o,w,g}$ is the density of the oil, water, gas phases at local conditions [44].

The viscosity of the fluid mixture at local segment conditions is given in equation (4-15).

$$\mu_{\text{mix}} = (\alpha_o + \alpha_w) \cdot \mu_{\text{emul}} + \alpha_g \cdot \mu_g \quad (4-15)$$

where μ_{emul} is the viscosity of the oil-water emulsion at local conditions and μ_g is the gas viscosity at local conditions. The calculation of μ_{emul} is described in "Emulsion viscosity" section [44].

To include a series of these devices in a multi-segment well, the devices should be represented by segments branching off the tubing as shown in Figure 4-3. The grid block connections are located in the ICD segments instead of the segments representing the well tubing. The ICD segments should be given a very small length (of the order, say, of the wellbore radius). This length is not used in the pressure loss calculations, but it influences the location of the connections of the grid block in the reservoir. The ICD segments were given the same depth as their 'parent' tubing segments, so that there will be no hydrostatic head across them [45]. The pressure loss across an ICD segment is reported as the friction pressure loss; the acceleration pressure loss is set to zero.

4.2.2 Emulsion viscosity

The emulsion viscosity is a function of the local phase volume fractions in the segment and has differing functional forms at low water in liquid fractions (when oil is the continuous phase) and high water in liquid fractions (when water is the continuous

phase) [44]. A critical water in liquid fraction as shown in figure 4-4 is used to select between equations (4-16) and (4-17) below.

$$\mu_{wio} = \mu_o \cdot \left(\frac{1}{1 - \left(\frac{0.8415}{0.7480} \alpha_{wl} \right)} \right)^{2.5} \quad (4-16)$$

$$\mu_{oiw} = \mu_w \cdot \left(\frac{1}{1 - \left(\frac{0.6019}{0.6410} \alpha_{ol} \right)} \right)^{2.5} \quad (4-17)$$

where μ_{wio} is the water-in-oil emulsion viscosity (when oil is the continuous phase), μ_{oiw} is the oil-in-water emulsion viscosity (when water is the continuous phase) and μ_o is the oil viscosity at local conditions. μ_w is the water viscosity at local conditions, α_{wl} is the local water in liquid fraction and α_{ol} is the local oil in liquid fraction.

The water-in-oil viscosity is subject to an upper limit expressed as a maximum ratio of water-in-oil viscosity to oil viscosity.

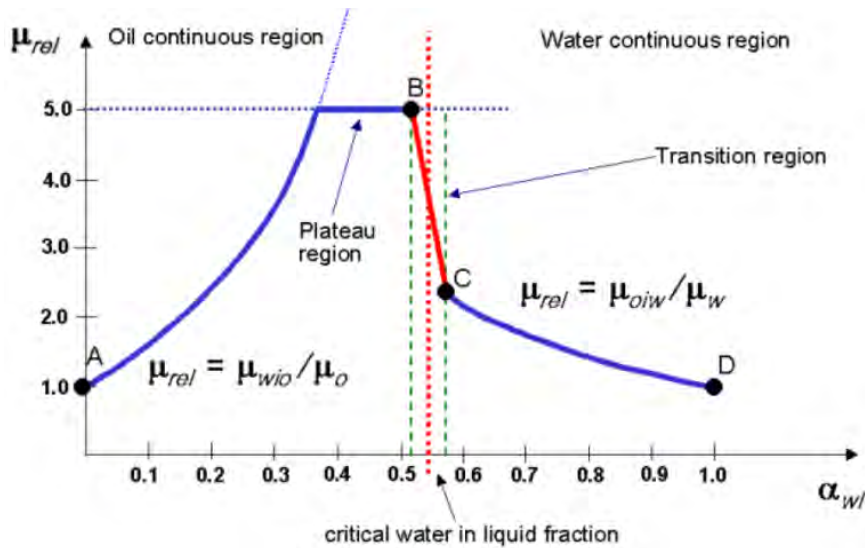


Figure 4-4 Phase transition region about the critical water in liquid fraction[44]

This usually results in a 'plateau' region within which the water-in-oil viscosity is at its maximum permitted value as shown schematically in Figure 4-4, with the maximum viscosity ratio set at 5.0 [44]. This upper limit also applies to the oil-in-water viscosity, but is less commonly encountered. At the critical water in liquid fraction there is a jump in emulsion viscosity as the continuous phase changes. Such a discontinuity would

cause stability problems in the simulator and a transition region is defined about the critical water in liquid fraction to avoid this. In this region the emulsion viscosity is linearly interpolated between the water-in-oil and oil-in-water viscosities at the edges of the region; the viscosity is thus a continuous function of the water in liquid fraction. This transition region is presented schematically in Figure 4-4, with the linear interpolation shown in red between points B and C [44].

4.3 CO₂ storage Model

In ECLIPSE there are several options available in order to study the storage of CO₂ under various conditions. These storage options include; storage in depleted oil/gas reservoir, storage in aquifers and storage in Coal Bed Methane reservoirs. In this work, the model for storage of CO₂ in depleted oil/gas reservoir and aquifers was considered.

4.3.1 Storage in depleted oil reservoir

“CO2SOL” is a three-phase compositional option for simulating CO₂ EOR and storage in depleted oil reservoirs. The gas/oil composition is not restricted to CO₂ but only CO₂ is considered soluble in water. CO₂ partitioning between the oil and gas phases is calculated by a fugacity equilibration method. A cubic equation of state is used to model oil and gas phase densities and fugacities [44]. The amount of CO₂ dissolved in water, and other aqueous phase properties, are computed using solubility data.

The CO₂ solution algorithm allows carbon dioxide to dissolve in the aqueous phase. This The basic model is a fugacity function for aqueous CO₂ which is constructed to match solubility data and which takes the form as shown in equation (4-18) [44]:

$$f_{\text{CO}_2}^{\text{A}} = P_{\text{aCO}_2} \phi_{\text{CO}_2}(P) \quad (4-18)$$

Where P_{aCO_2} is the partial pressure of CO₂ and $\phi(P)$ is the fugacity coefficient function. The phase equilibrium between the aqueous CO₂ and the hydrocarbon phases is then defined by the conditions that the fugacity values are equal. It is also possible to construct a CO₂ aqueous phase Gibbs energy contribution.

The function $\phi(P)$ is constructed by considering a pure CO₂ aqueous mixture. The gas phase fugacity is obtained using the equation of state. The initial CO₂ concentration may not be in exact equilibrium with the hydrocarbon phases and initial flash modifies the input values slightly.

Water component properties

After computing the CO₂ aqueous mole fraction using the phase equilibrium algorithm mentioned previously, the saturated formation volume factor FVF_{sat} , the water compressibility c_{sat} , the water viscosity μ_{sat} and the water saturation pressure P_{sat} can be calculated using the CO₂-saturated water properties tables or using linear interpolation. The formation volume factor FV at pressure is calculated from equation (4-19) [44].

$$\frac{1}{FVF} = \frac{1}{FVF_{sat}} \cdot (1 + X_c + 0.5X_c^2) \quad (4-19)$$

where the compressibility term X_c is given in equation (4-18).

$$X_c = c_{sat} \cdot (P - P_{sat}) \quad (4-20)$$

Density

The reservoir density of water can be calculated from equation (4-21).

$$\frac{\rho_s}{MW} \cdot \frac{MW_r}{FVF} \quad (4-21)$$

Where ρ_s is the surface density, MW is the molecular weight of pure water, FVF is the formation volume factor, MW_r is the molecular weight of water in the reservoir calculated using equation (4-22).

$$MW_r = AMF_{CO_2} \cdot MW_{CO_2} + (1 - AMF_{CO_2}) \cdot MW \quad (4-22)$$

where AMF_{CO_2} is aqueous mole fraction of CO₂ and water, MW_{CO_2} is the molecular weight of CO₂.

4.3.2 Storage in Aquifers

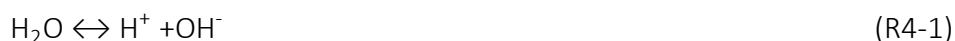
In ECLIPSE, CO₂ storage in aquifers can be implemented using “CO2STORE” option. With this option, three phases are considered: a CO₂-rich phase (gas phase), a water-rich phase (liquid phase) and a solid phase. This option gives accurate mutual solubilities of CO₂ in water (xCO₂) and water in the CO₂-rich phase (yH₂O). Salts are described as components of the liquid/solid phase. The mutual solubilities of CO₂ and H₂O are calculated to match experimental data for typical CO₂ storage conditions: typically 12-250°C and up to 600 bars. They are calculated based on fugacity equilibration between water and a CO₂ phase. Water fugacity is obtained by Henry's law, while CO₂ fugacity is calculated using a modified Redlich Kwong equation of state [44]. Allowed component names are currently CO₂, H₂O and the salts NaCl, CaCl₂ and CaCO₃ [44].

Table 4-1 Components of ECLIPSE CO2STORE option[44]

Component name	Phases
CO2	Aqueous/Gas
H2O	Aqueous/Gas
NACL	Aqueous/Solid
CACL2	Aqueous/Solid
CACO3	Aqueous/Solid

Phase splitting

The partitioning of CO₂ and H₂O in the aqueous and gas phase follows the procedure given by Spycher and Pruess [44]. The salts are assumed to stay in the aqueous phase unless the SOLID option is activated. With the “SOLID” option the components NaCl, CaCl₂ and CaCO₃ can be present in both the aqueous phase and the solid phase according to the following equilibrium reactions (R4-1) to (R4-7).





If only NaCl is present, a simplified procedure can be used and the maximum NaCl solubility in the aqueous phase using equation (4-23) [44].

$$\text{WtNaCl} = 26.218 + 0.0072T + 0.000106T^2 \quad (4-23)$$

where WtNaCl is the maximum solubility value of NaCl and T is the temperature in °C.

It is recommended that the “SOLIDMMS” keyword is used in order to model the decrease in mobility as a function of the solid saturations. The gas and aqueous saturations are normalized to be between zero and unity, so the two phase water and gas relative permeability curves can be used. However it should be noted that the effective fluid volume “FV” is given in equation (4-24) [44].

$$\text{FV} = (1 - S)\text{PV} \quad (4-24)$$

where PV is the pore volume and S is the solid saturation. It is possible to specify a target solid saturation change for each time step. A small value will usually enhance the stability.

Activity coefficient models

The CO₂ and H₂O activity coefficients are computed using Margules expressions are given in equations (4-25) – (4-28) [44].

$$\ln(\gamma_{\text{H}_2\text{O}}) = (A_M - 2A_{M^{\text{H}_2\text{O}}})x_{\text{CO}_2}^2 \quad (4-25)$$

$$\ln(\gamma_{\text{CO}_2}) = 2A_{M^{\text{CO}_2}x_{\text{H}_2\text{O}}^2} \exp(\gamma_{\text{CO}_2}') \quad (4-26)$$

where:

$$A_M = 0 \quad (T \leq 100^\circ\text{C}) \quad (4-27)$$

$$A_M = a \cdot (T - 100) + b \cdot (T - 100)^2 \quad (T > 100^\circ\text{C}) \quad (4-28)$$

In these expressions, a and b are regressed parameters, x_{CO_2} and $x_{\text{H}_2\text{O}}$ denote the aqueous phase mole fractions. The CO_2 activity coefficient is modified for salting out effects by γ_{CO_2}' . This requires additional model like the Rumpf et. al 1994 model which is applicable up to 160°C [44].

Density

The gas density is obtained by a cubic equation of state tuned to accurately give the density of the compressed gas phase, following Spycher and Pruess [44]. A modified Redlich- Kwong equation of state is used, where the attraction parameter is made temperature dependent in equation (4-29).

$$P = \left(\frac{RT_K}{V - b_{\text{mix}}} \right) - \left(\frac{a_{\text{mix}}}{T_K^{1/2} V(V + b_{\text{mix}})} \right) \quad (4-29)$$

where V is the molar volume, P is the pressure, T_K the temperature in Kelvin, R is the universal gas constant and a_{mix} and b_{mix} are the attraction and repulsion parameters.

The transition between liquid CO_2 and gaseous CO_2 will lead to rapid density changes for the CO_2 -rich phase. The simulator uses a narrow transition interval between the liquid state and gaseous state. For the brine density, the first approach is to compute the density of pure water.

pH calculation

The pH is calculated from equation (4-30).

$$\text{pH} = -\log(\zeta_H \cdot m_H) \quad (4-30)$$

where ζ_H is the activity coefficient of the H^+ ion and m_H is the molality of the H^+ ion.

Analytic water aquifers

An analytic water aquifer should be defined to contain only the “H₂O” component. It is possible to modify the aquifer composition using the “AQSTREAM” keyword. Any component is allowed to leave or enter the reservoir.

5 ECLIPSE simulation

ECLIPSE has been considered as a good simulation tool for more than twenty years because of its functionalities, robustness, speed, parallel scalability, and unmatched platform coverage [46]. ECLIPSE uses the finite volume method [2] to solve material and energy balance equations for petroleum reservoir. The black oil, compositional, thermal and streamline reservoir simulators in ECLIPSE make it capable to solve different simulation needs. In this section, blackoil model is used to simulate waterflooding and the application of inflow control device for an improved oil recovery. The relative permeability data used for all simulations is presented in figure 4-2.

With the blackoil model, the following assumptions were made:

- Oil and gas phases are represented by multi-component mixtures.
- Assumes the reservoir fluids are at all temperatures, pressures.
- Composition and time can be represented by EOS.

5.1 General simulation procedure

The general ECLIPSE simulation procedure can be summarized in these steps:

- Divide the reservoir into several cells.
- Provide basic data for each cell.
- Position wells within the cells.
- Specify well production rates as a function of time.
- Solve the equations to yield the pressure and saturation for each block, as well as the production of each phase from each well

5.2 Waterflooding

Simulations were carried out for 3653 days (3653 days) by injecting water at a constant rate through a horizontal and a vertical well respectively. A homogeneous and a heterogeneous reservoir was considered. In both cases, water was injected at the same depth as the production well. Also the same lateral distance was maintained between

the injection well and the production well for both cases. Different simulations were performed by varying water injection rate from 500m³/day to 2500m³/day. A base case without water injection was considered for reference.

5.2.1 Geometry

Rectangular reservoir geometry was considered with the dimension 900m x 900m x 70m. Figures (5-1) – (5-3) show the reservoir geometry used for homogenous and the heterogeneous cases as indicated in the captions. The reservoir heterogeneous was achieved by varying the effective permeability between 0.1 and 1Darcy. The horizontal production (P1) and injection (INJW) wells are 800m long respectively while the length of the vertical injection well (INJW) is 40m.

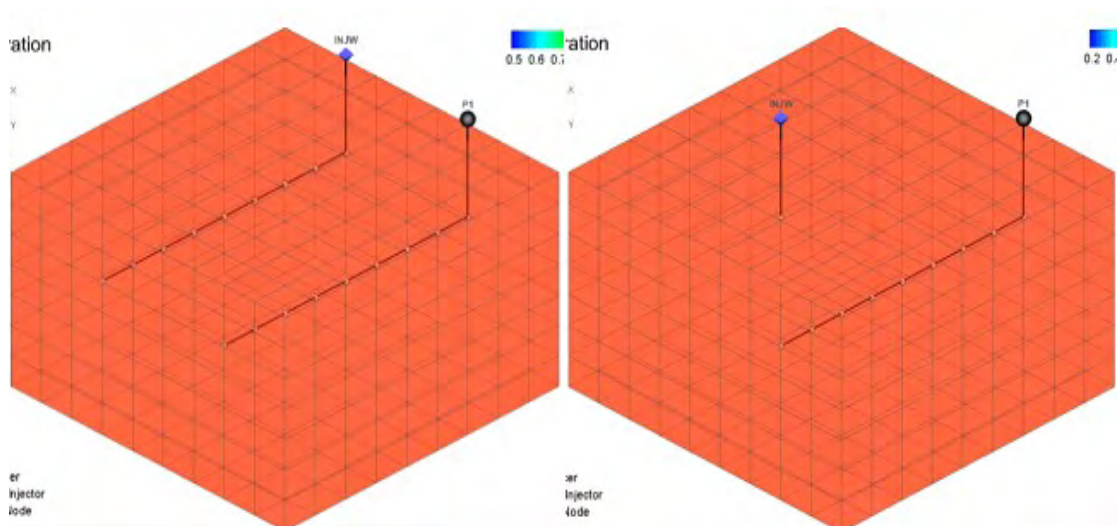


Figure 5-1 Reservoir geometry for horizontal and vertical injection(Homogenous)

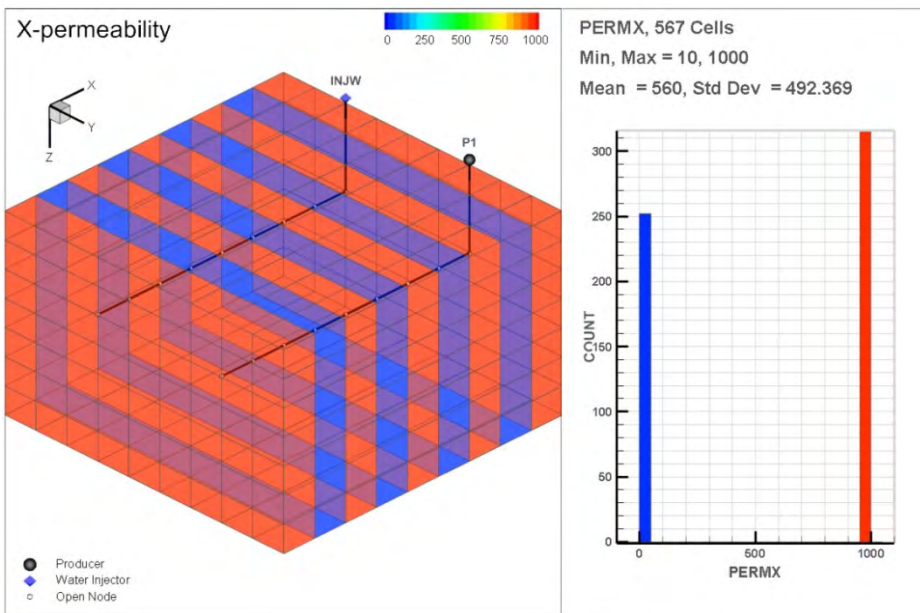


Figure 5-2 Reservoir geometry for the horizontal injection case (Heterogenous)

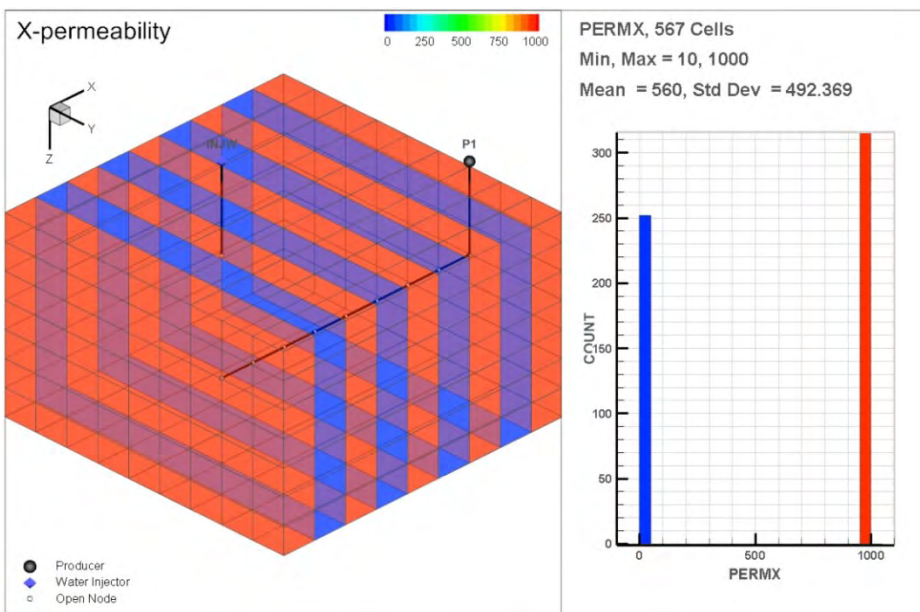


Figure 5-3 Reservoir geometry for the vertical injection (Heterogenous)

5.2.2 Reservoir conditions

The reservoir is homogeneous and consists of water-wetted rock. Although the reservoir fluid consists of live black oil, gas production was not considered for simplicity. The composition of oil components is assumed to be constant relative to pressure and time. It is also assumed that the reservoir fluid is Newtonian and that Darcy's law applies. The reservoir conditions used for the simulation are summarized in Table 5-1. See Annexes 5 and 6 for the PVT of the reservoir fluid.

Table 5-1 Reservoir conditions for waterflooding

Parameter	Value	Unit
Components	Oil, water and gas	-
Wettability	Water-wetted	-
Porosity	0.25	-
X and Y Permeability (homogeneous)	1	Darcy
X and Y Permeability (heterogeneous)	0.1 - 1	Darcy
Z Permeability (All)	0.1	Darcy
Rock compressibility @ 10Bar	5.0E-5	/Bar
Oil gravity	35	°Api
Residual oil saturation	0.3	-
Oil viscosity @ 320Bar	3	cP
Water Density	1000	kg/m ³
Water viscosity	0.5	cP
Connate water saturation	0.2	-
Gas density	1	kg/m ³
Total simulation time	3653 (3653 days)	days
No of Grids	567 (9x9x7)	-

5.2.3 Initial conditions

Initially, the reservoir is assumed to be in hydrostatic equilibrium consisting of only oil.

Table 5-2 shows the initial conditions considered during the simulation.

Table 5-2 Initial conditions for waterflooding

<i>Initial condition</i>	<i>Value</i>	<i>Unit</i>
Reservoir pressure	320	Bar
Bottomhole pressure	310	Bar
Bubble point pressure	182	Bar
Oil saturation	1	-
Water saturation	0	-
Gas saturation	0	-

5.3 Application of ICD

In this simulation, the effect of ICD completion on oil, water and gas production was investigated. Also the reservoir pressure trend recovery was discussed. A base case without ICD completion was considered as reference.

A case study was considered with reservoir conditions similar to the Troll field, Norway to illustrate the effect of ICD on oil recovery, reservoir sweep, delay in water breakthrough and decrease in water cut. Troll is a large subsea offshore Norway. The challenge is to drill and complete well in a way that gas and water do not have easy access to the production well [20]. The main oil reservoir at Troll is the Late Jurassic Sognefjord Formation. This formation consists of Sandstone and siltstone with thickness of about 160m. The porosity vary between 30 -35% and permeability between 1 – 20D. The reservoir driving mechanism is mainly gas expansion and water drive. Horizontal wells are located close to the oil-water contact in order to reduce gas breakthrough[20].

Simulation was carried out for 3000 days. Water drive was achieved by connecting analytical aquifer (Fetkovich aquifer) at the bottom of the reservoir. Frictional pressure drop and variation in permeability will lead to non-uniform inflow profile along the production well [47]. ICDs are set at two segments along the production open hole section to distribute downhole pressure to optimize fluid inflow along the entire production interval. Water saturation profile shown in Fig. 4 indicates that more water is produced at the 225m and 375m positions of the production well due to high permeability at these positions. To reduce water breakthrough, ICDs were placed at these positions. Each ICD joint is about 12m in length and about 3mm nozzle diameter. A base case without water ICD was considered for reference.

19 Oct 2016 K=4

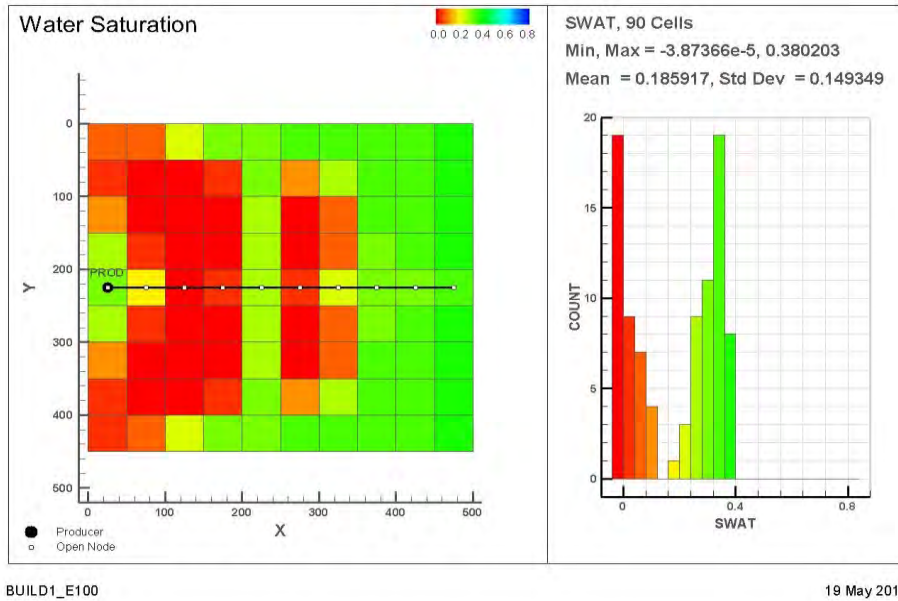


Figure 5-4 Location of ICD along the well

5.3.1 Geometry

Rectangular reservoir geometry was considered with the dimension 500m x 450m x 70m. The multi-segment horizontal production (PROD) well is of length 450m. The reservoir is heterogeneous with varying permeability between 1 and 20 Darcy. The areas of high permeability represents defeat in the reservoir see Fig. 5 and 6.

1 Jan 2026

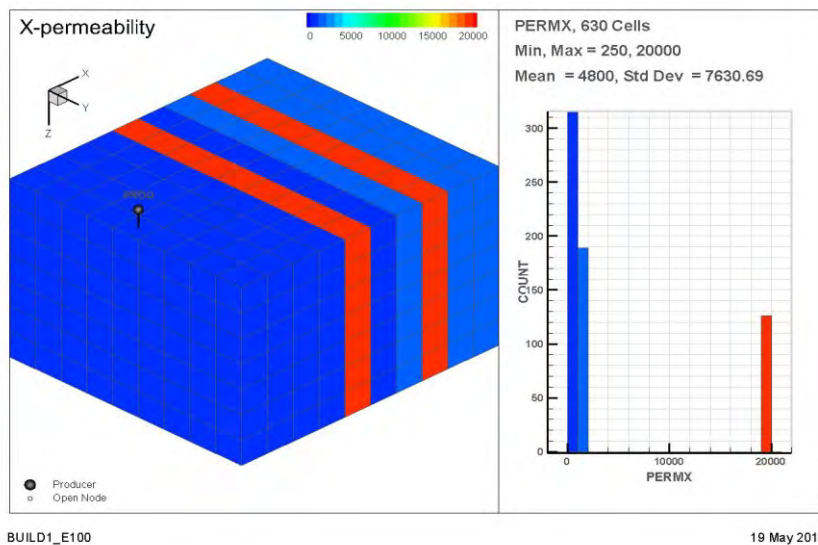


Figure 5-5 Reservoir geometry showing the distribution of X and Y permeability

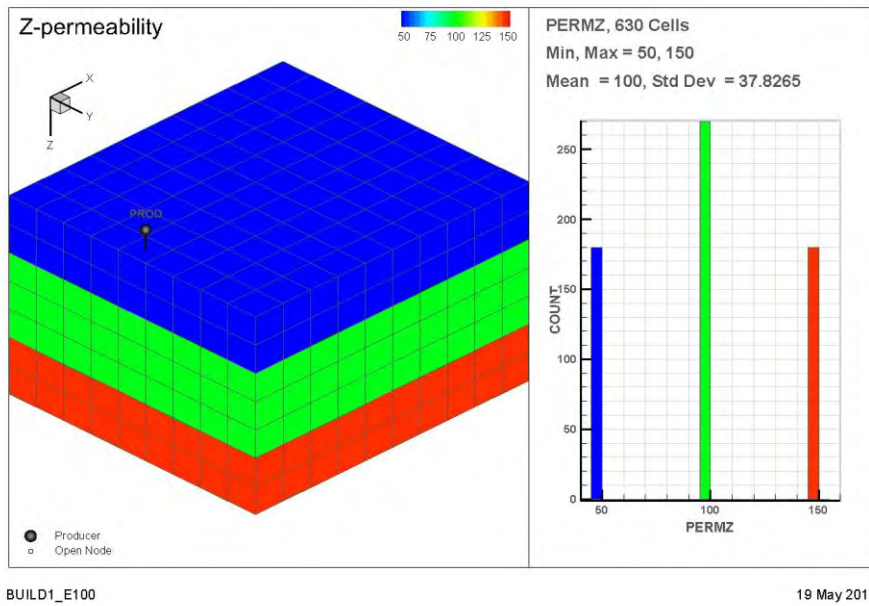


Figure 5-6 Reservoir geometry showing the distribution of Z-permeability

5.3.2 Assumptions

The following assumptions were made regarding the inflow:

- Darcy's law applies to the flow through the reservoir.
- The flow into the well is at steady or pseudo-steady state.
- The distance between the well and the reservoir boundary is longer than the length of the well length.

The following assumptions were made about the ICDs:

- There is no flow in the annulus parallel to the base pipe. This means that fluid flows from reservoir directly through ICD screens into the base pipe [48].
- ICDs installed are of the same strength. This is the most common type of ICD application due to the relative simplicity of its design and installation operation [20]. This is done in order to reduce the operational risks [49, 50].

5.3.3 Reservoir conditions

The reservoir is heterogeneous and consists of water-wetted rock. Although the reservoir fluid consists of live black oil, gas production was not considered for simplicity. The composition of oil components is assumed to be constant relative to pressure and

time. It is also assumed that the reservoir fluid is Newtonian and that Darcy's law applies. The reservoir conditions used for the simulation are summarized in Table 5-3.

Table 5-3 Reservoir conditions for ICD simulation

Parameter	Value	Unit
Components	Oil, water and gas	-
Wettability	Water-wetted	-
Porosity	0.30	-
X and Y Permeability	0.1 – 20	Darcy
Z Permeability	0.1-1	Darcy
Rock compressibility @ 10Bar	5.0E-5	/Bar
Oil gravity	35	°Api
Residual oil saturation	0.3	-
Oil viscosity @ 320Bar	10	cP
Water Density	1000	kg/m ³
Water viscosity	0.5	cP
Connate water saturation	0.2	-
Gas density	1	kg/m ³
Well length	450	m
Target well flow rate	2000	Sm ³ /day
ICD Length	12	m
ICD Strength	0.00021	bar/(Rm ³ /day) ²
ICD nozzle diameter	3	mm
No of Grids	630 (10x9x7)	-

5.3.4 Initial conditions

Initially, the reservoir is assumed to be in hydrostatic equilibrium consisting of only oil. The initial pressure is greater than the bubble point and water has much higher mobility than oil. The initial condition for the simulation is the same as presented in Table 5-2.

6 Result and discussion

The simulation results for waterflooding (homogenous and heterogeneous) and the application of ICD are discussed in this section.

6.1 Homogeneous waterflooding

Simulation of waterflooding with horizontal and vertical water injection were carried out for 3653 day by varying water injection rate from $500\text{m}^3/\text{day}$ to $2500\text{m}^3/\text{day}$. In this simulation, analysis of the oil production rate, water cut, reservoir pressure, accumulated oil production and recovery factor were made for the horizontal and vertical waterflooding. A base case without water injection was also considered as reference. Simulation result for the homogenous case is summarised in Annex 3. This is an ideal case and results for each case show the effect of the waterflooding on oil recovery. Also the nature of water-front progression was shown with the homogeneous case.

6.1.1 Result for the base case (Homogeneous)

Figure 6-10 shows how the oil production rate, water cut and reservoir pressure change with time without water injection for the horizontal and vertical injection arrangement respectively. From figure 6-11, the drawdown pressure of 0.6bar is available which is not sufficient for oil production. From figure 6-12, it shows that the saturation after ten years in the reservoir is 100%.

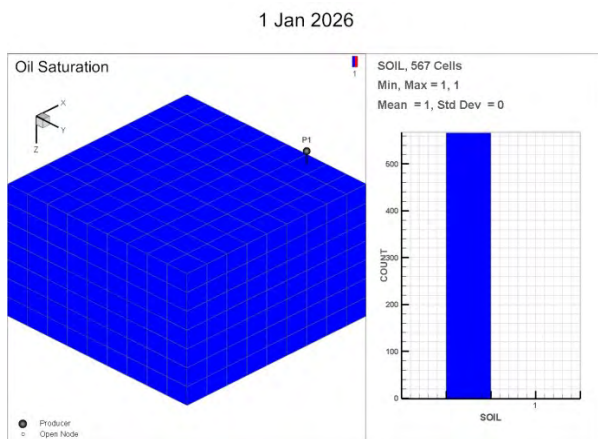


Figure 6-1 Final oil saturation of the base case (homogeneous)

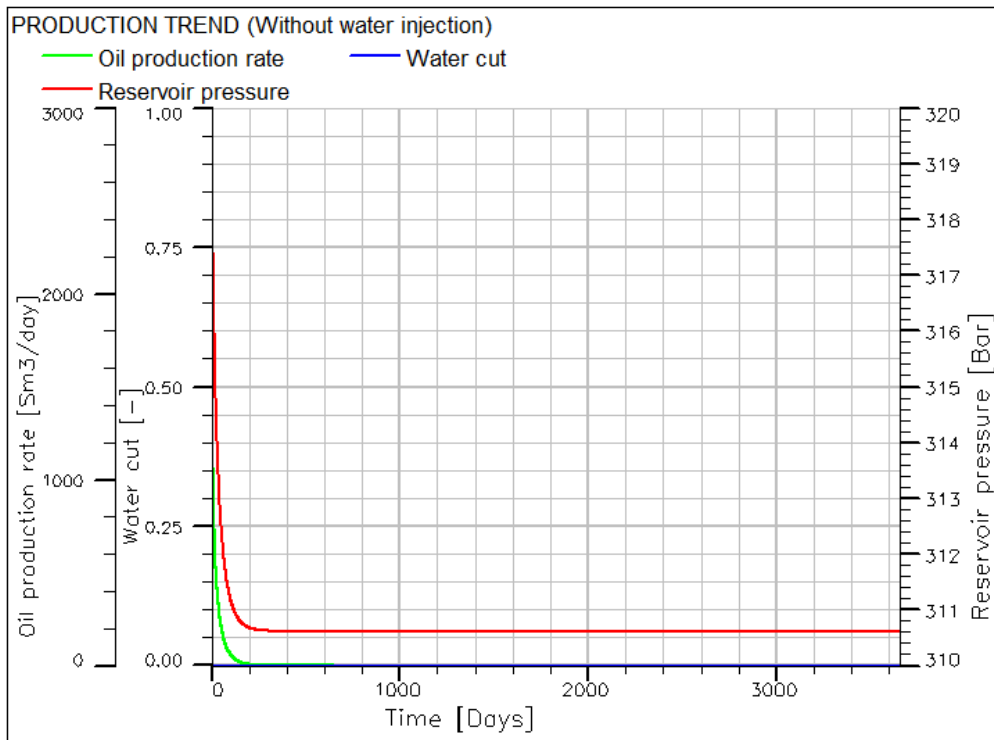


Figure 6-2 Production trend for the base case (homogeneous)

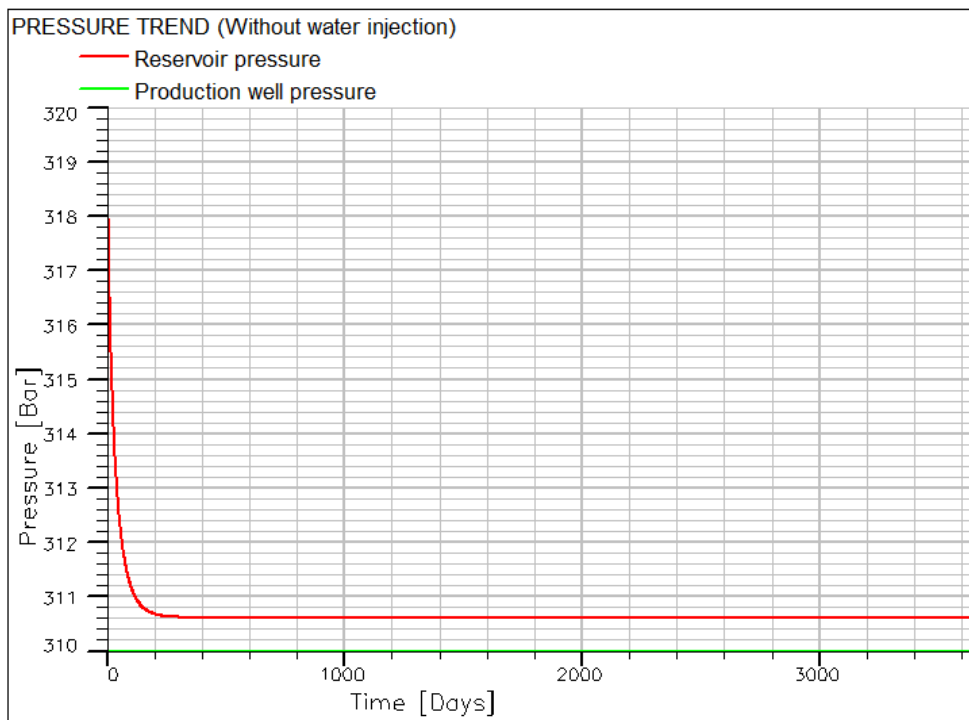


Figure 6-3 Pressure trend for the base case (homogeneous)

6.1.2 Result for water injection of 500m³/day (Homogenous)

Figure 6-4 shows how the oil production rate, water cut and reservoir pressure change with time at water injection rate of 500m³/day for the horizontal and vertical injection arrangement respectively. From the start to the 100th day, the oil production rate decreases sharply from 3832m³/day to approximately 388m³/day for the horizontal case while the vertical case decreases from about 3832m³/day to approximately 389m³/day. This sharp drop in the production rate could be due to transient effect of start-up. The oil production rate of 372m³/day is maintained from the 120th day to the 3653rd day for the horizontal case while the vertical case maintains oil production rate of 371m³/day till water breakthrough at the 3391st day. The oil production rate is further reduced to approximately 369m³/day for the vertical case and this rate is maintained till the end of the 3653rd day. The total oil production at the end of 3653rd day is about 1,391,437Sm³ for the horizontal and 1,309,863 for the vertical case. Water breakthrough time is around 3,391days with water cut of 0.01 at end of the 3653rd day for the vertical case while there is no water breakthrough for the horizontal case.

Figure 6-4 also shows a sharp decrease in the reservoir pressure to about 312bar at the 100th day for both cases due to start-up. The reservoir pressure of about 312bar is maintained throughout the simulation period for both cases. The final reservoir pressure at the 3653rd day is 311.81bar for the horizontal case and 311.78bar for the vertical case. From figure 6-5 it can be shown that an average drawdown pressure of about 2bar is achieved through horizontal injection and 1.8bar achieved through vertical injection. Figure 6-5 also shows that lower differential injection pressure of about 0.8bar is required for the horizontal case while the vertical case requires higher differential injection pressure of about 8bar.

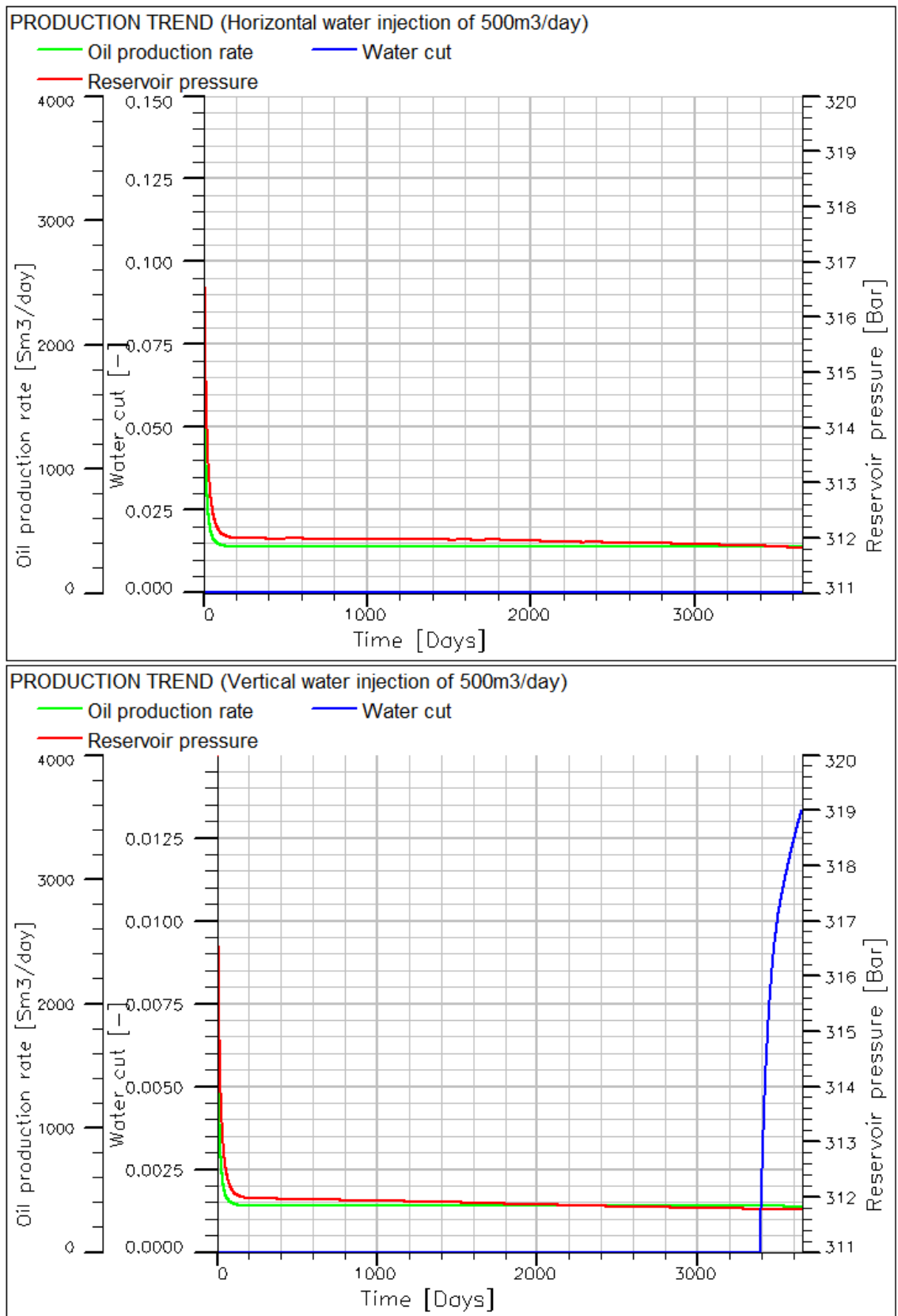


Figure 6-4 Production trend for water injection of 500m³/day (homogeneous)

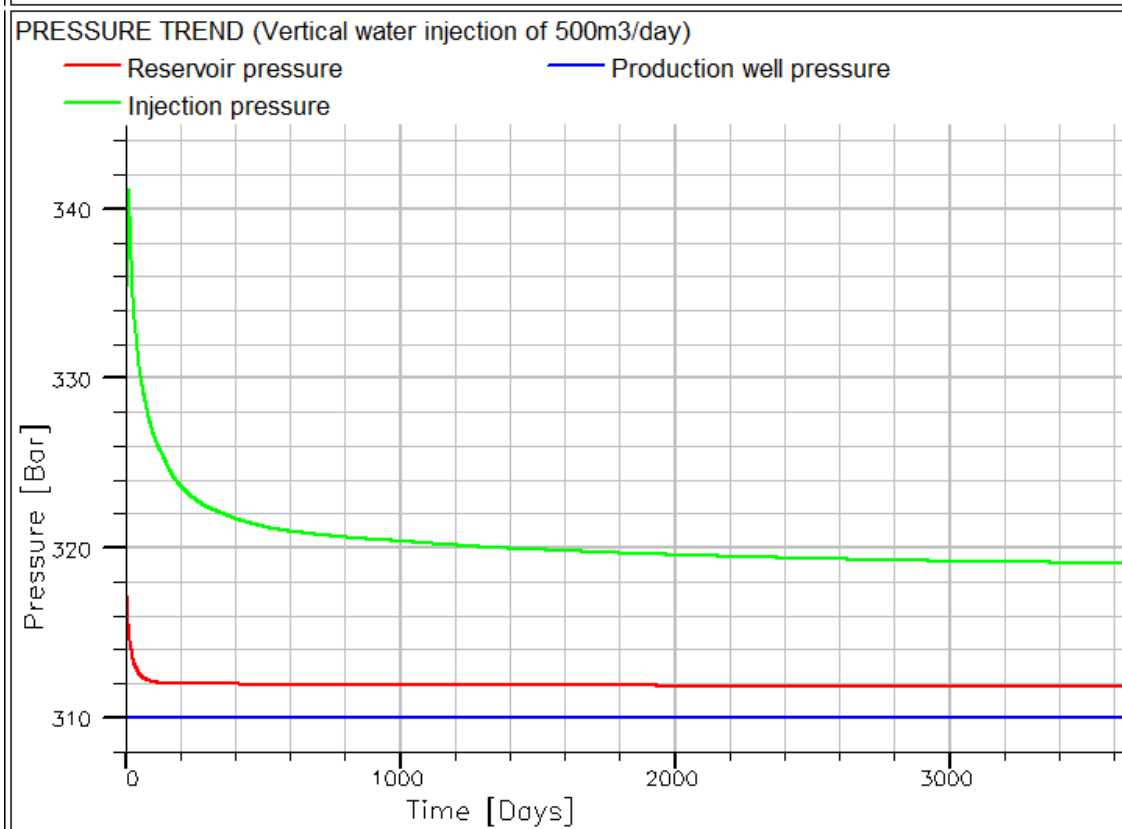
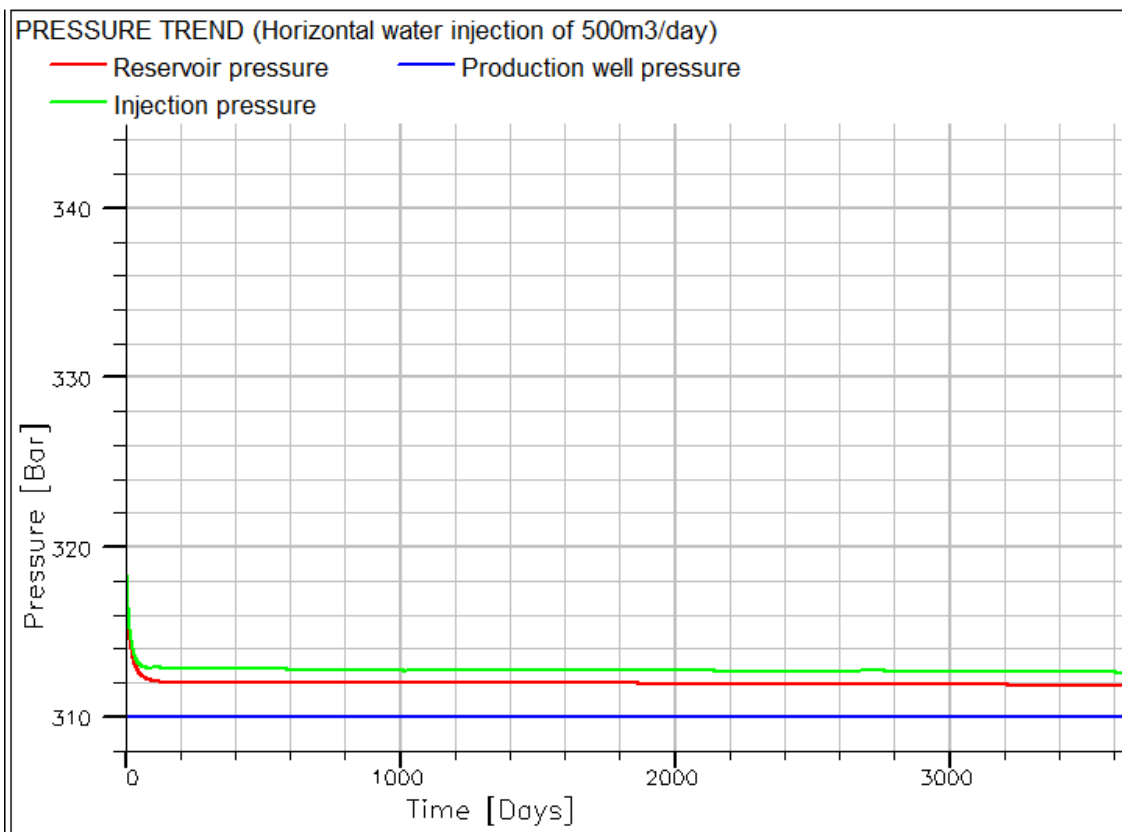


Figure 6-5 Pressure trend for water injection of 500m³/day (homogeneous)

6.1.3 Result for water injection of 1000m³/day (Homogenous)

Figure 6-6 shows how the oil production rate, water cut and reservoir pressure change with time at water injection rate of 1000m³/day for the horizontal and vertical injection arrangement respectively. From the start to the 100th day, oil production rate decreases from 3842m³/day to approximately 758m³/day for the horizontal case while the vertical case decreases from 3841m³/day to approximately 757m³/day. For the horizontal case, oil production of 745m³/day is maintained for about 2600 days until further decrease at the 2700th day due to water breakthrough. The oil production rate of about 745m³/day is maintained for a shorter period of 1238 days for the vertical case until further decrease at the 1338th day due to water breakthrough. At the end of 3653rd day, oil production rate for the horizontal case is approximately 485m³/day while that of the vertical case is approximately 503m³/day. The total oil produced at the end of 3653rd day is about 2,552,601m³ for the horizontal case and about 2,492,110m³ for the vertical case. Water breakthrough time is about 2700 days for the horizontal injection and the 1338 days for the vertical case. At the end of the 3653rd day, the water cut is 0.42 for the horizontal case and 0.39 for the vertical case.

Figure 6-6 also shows a sharp decrease in reservoir pressure to about 313.46bar at the 100th day due to start-up for horizontal injection while the vertical case decreases to 313.43bar at the 100th day due to start-up. The reservoir pressure of about 313bar is maintained for 2600 days for horizontal injection and 1238 days for the vertical injection. For the two cases, it is observed that the reservoir pressure increases sharply immediately after water breakthrough due to the propagation of water wave. The final reservoir pressure at the end of the 3653rd day is about 313.54bar for the horizontal case and 313.16bar for the vertical case. From figure 6-7, it can be shown that an average drawdown pressure of about 3.8bar is achieved through horizontal water injection while approximately 3.5bar achieved with vertical water injection. Figure 6-7 also shows that lower differential injection pressure of 2bar is required for the horizontal case while the vertical case requires higher differential injection pressure of approximately 19bar.

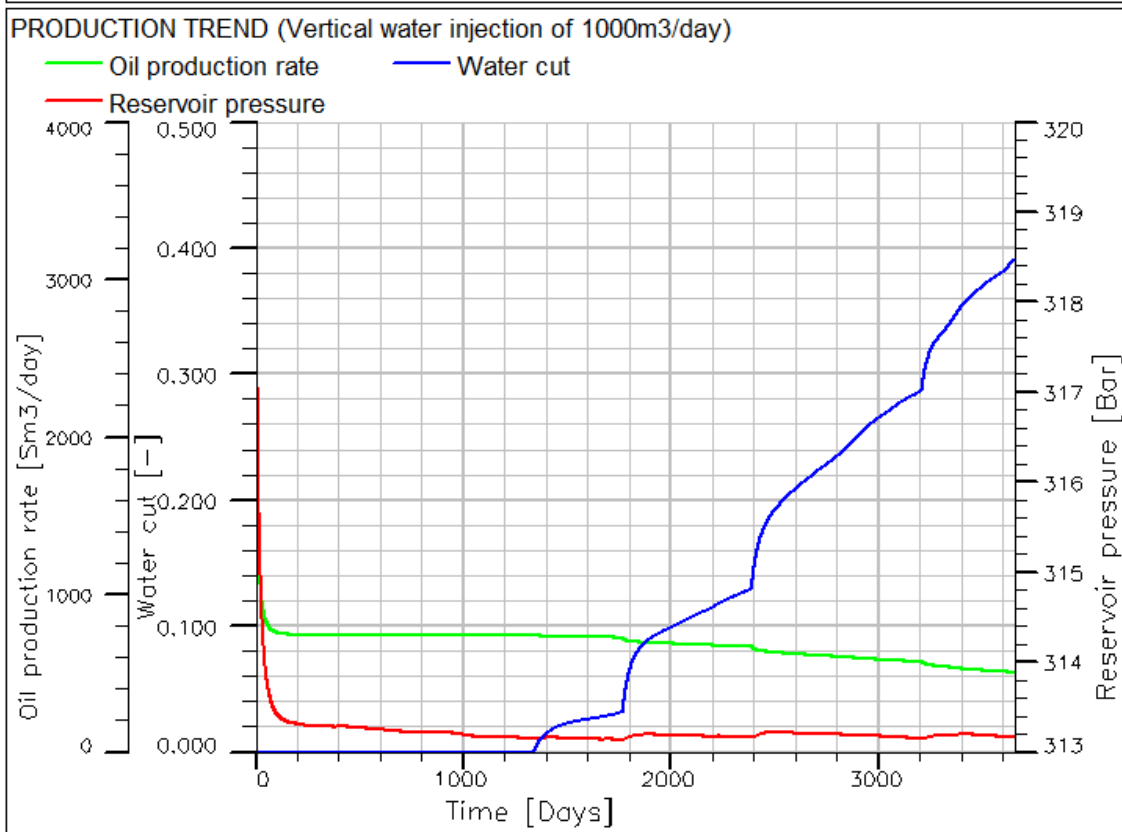
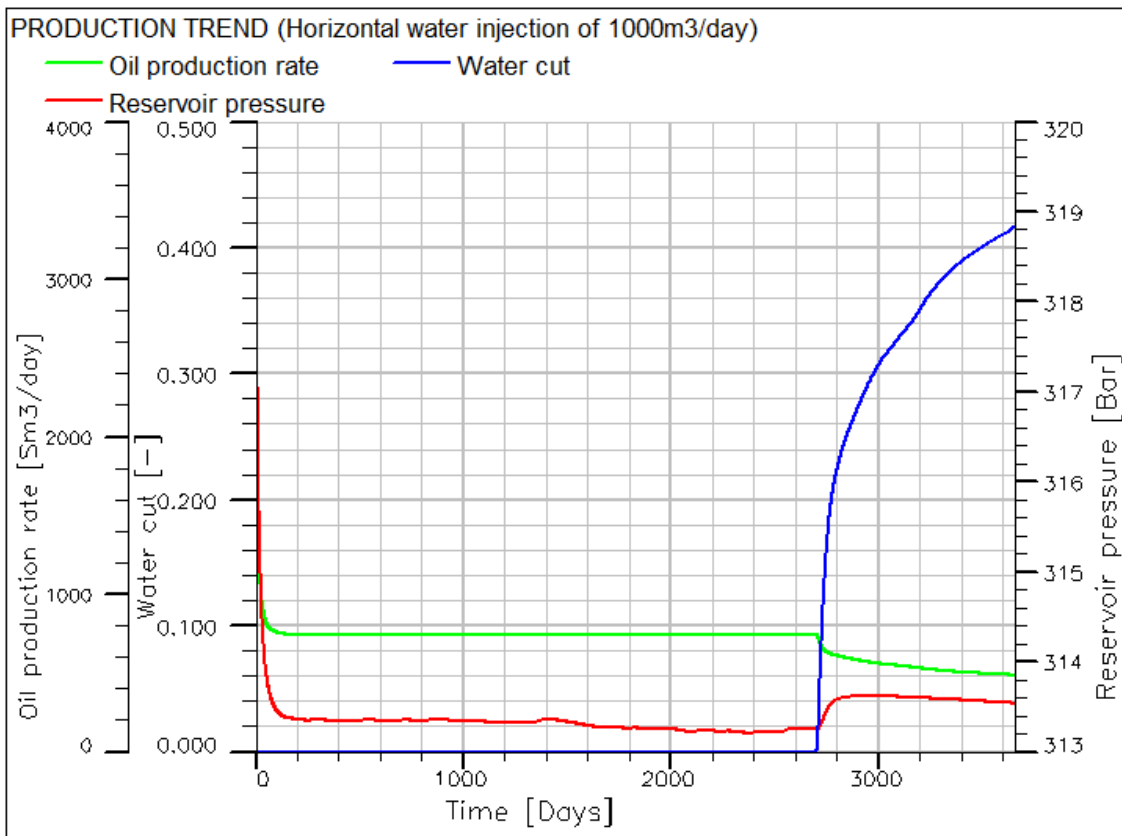


Figure 6-6 Production trend for water injection of 1000m³/day (homogeneous)

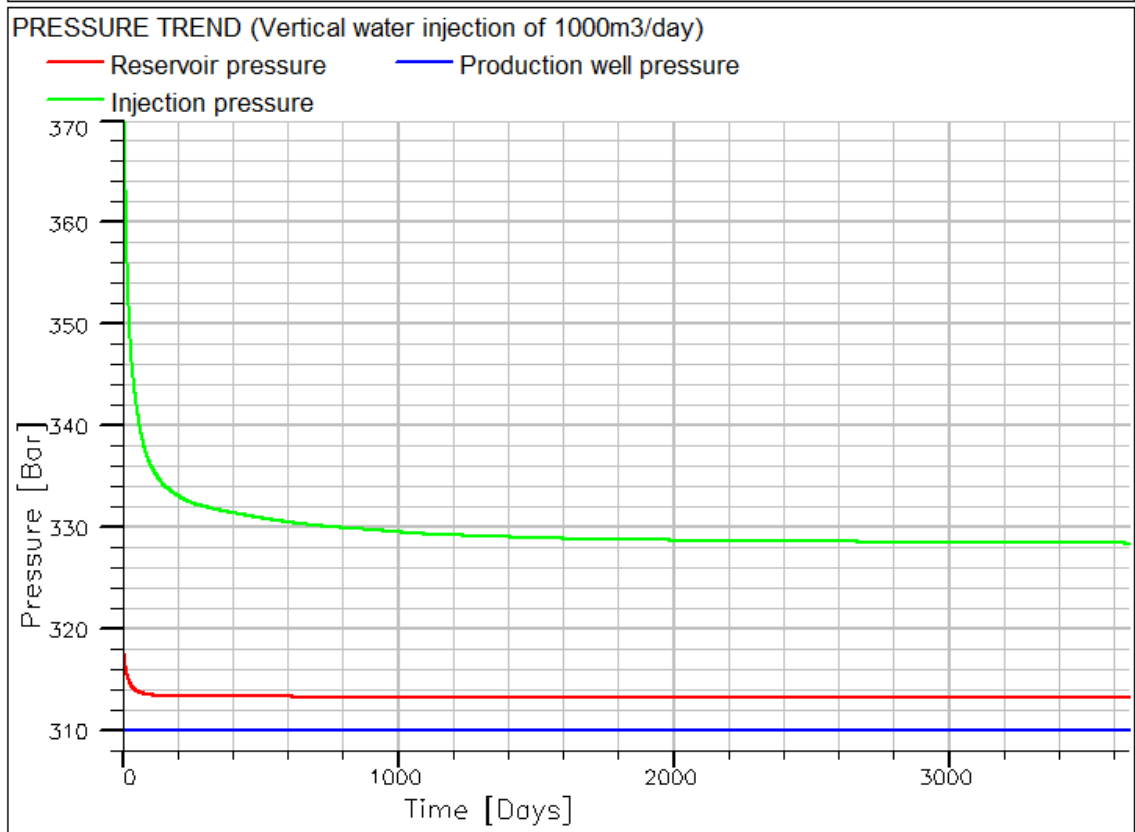
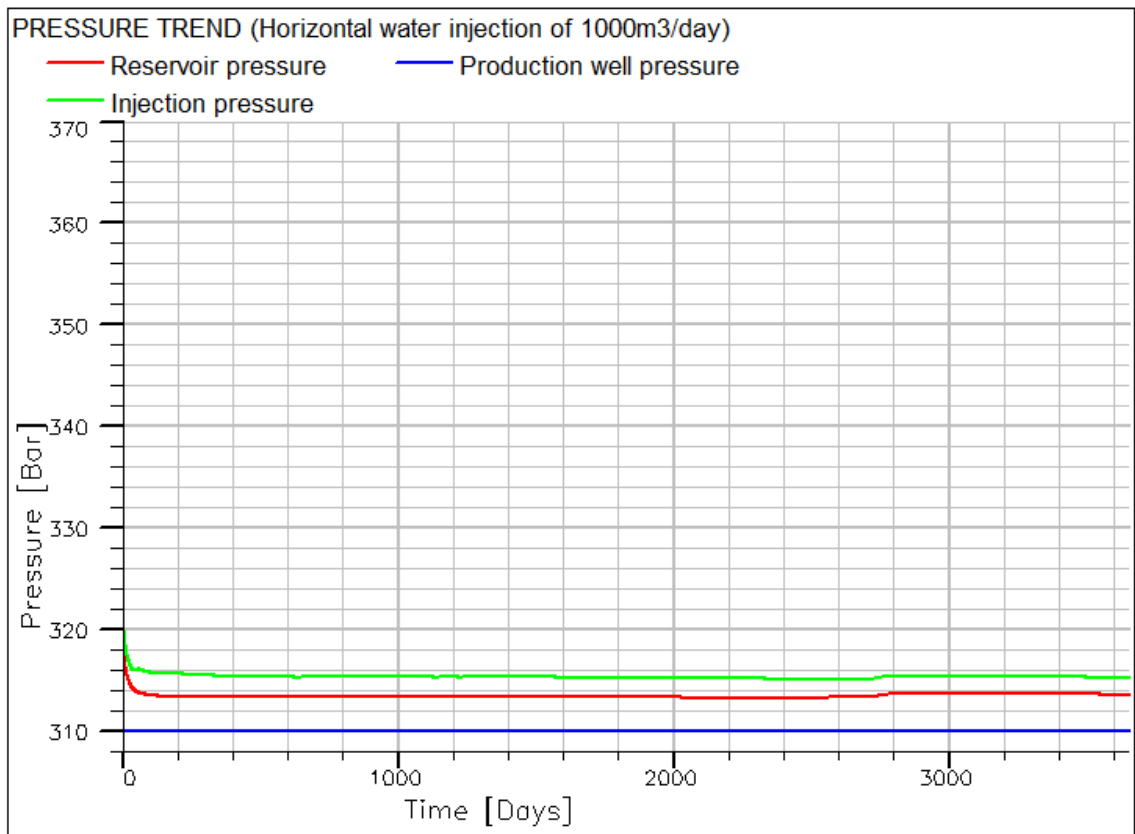


Figure 6-7 Pressure trend for water injection of 1000m³/day (homogeneous)

6.1.4 Result for water injection of 1500m³/day (Homogenous)

Figure 6-8 shows how the oil production rate, water cut and reservoir pressure change with time at water injection rate of 1500m³/day for the horizontal and vertical injection arrangement respectively. From the start to the 100th day, oil production rate decreases from 3852m³/day to approximately 1125m³/day for the horizontal case while the vertical case decreases from 3852m³/day to approximately 1127m³/day. For the horizontal case, oil production rate of approximately 1113m³/day is maintained for about 1591 days until further decrease at the 1691st day due to water breakthrough. Higher oil production rate of about 1115m³/day is maintained for a shorter period of 692 days for the vertical case until further decrease at the 792nd day due to water breakthrough. At the 3653rd day, oil production rate for the horizontal case is approximately 350m³/day while that of the vertical case is approximately 418m³/day. The total oil produced at the end of 3653rd day is about 3,013,196m³ for the horizontal case and about 3,056,921m³ for the vertical case. Water breakthrough time is 1691 days for the horizontal injection and 792 days for the vertical case. At the end of the 3653rd day, the water cut is 0.75 for the horizontal case and 0.69 for the vertical case.

Figure 6-8 also shows a sharp decrease in reservoir pressure to about 314.80bar at the 100th day due to start-up for horizontal injection while the vertical injection also shows a sharp decrease to about 314.75bar at the 100th day due to start-up. The reservoir pressure of approximately 315bar is maintained for 1591 days before water breakthrough for the horizontal case. There is a further increase in the reservoir pressure with water through for the horizontal case which maintains the reservoir pressure to 314.58bar at the end of the 3653rd day. Different trend was observed for the vertical case. Reservoir pressure continues to decrease for the vertical case, even with water breakthrough with final value of 314.26bar at the end of the simulation day. From figure 6-9, it can be shown that an average drawdown pressure of about 5bar is achieved through horizontal water injection while approximately 4.5bar is achieved with vertical water injection. Figure 6-9 also shows that lower differential injection pressure of 3bar is required for the horizontal case while the vertical case requires higher differential injection pressure of 25bar.

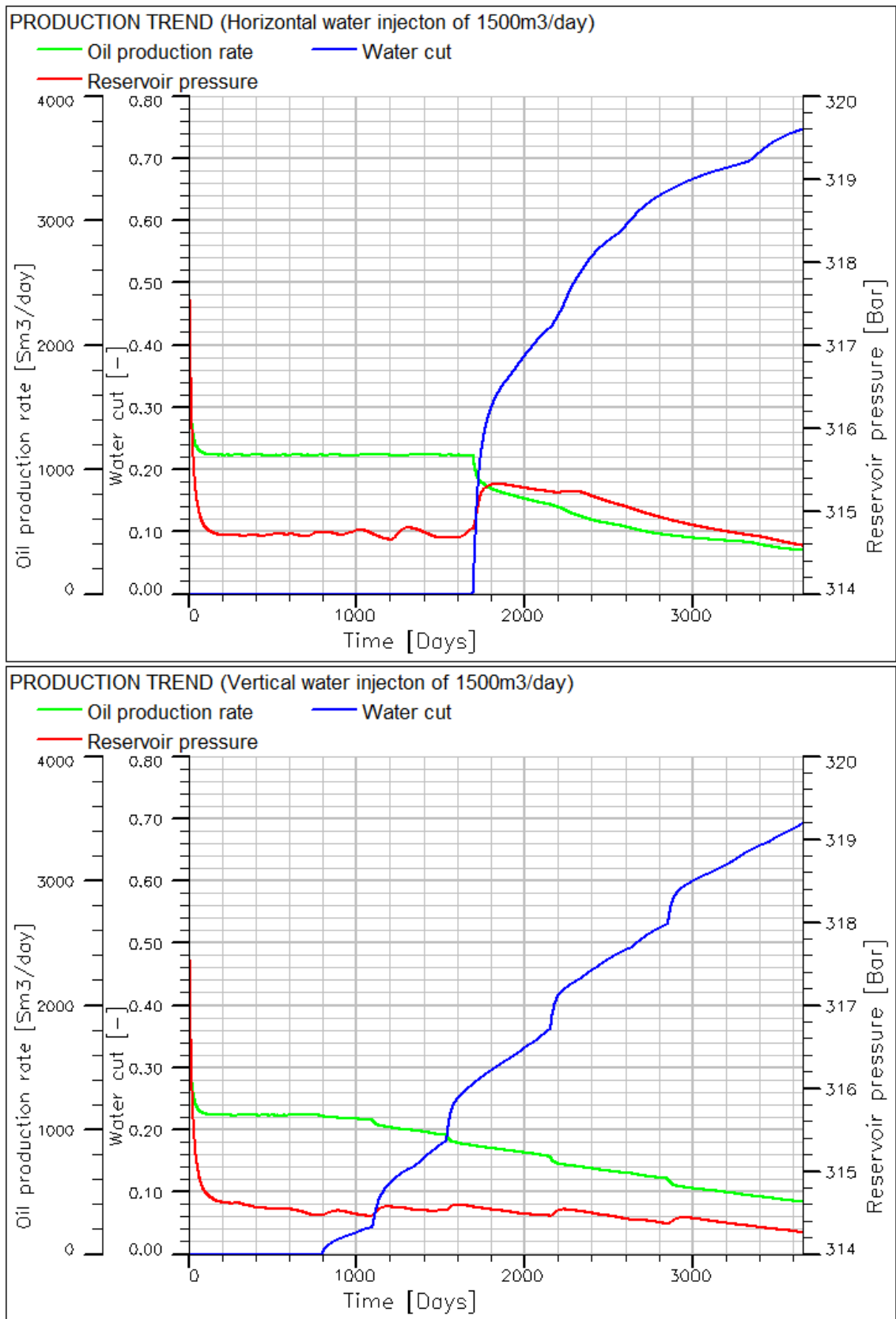


Figure 6-8 Production trend for water injection of 1500m³/day (homogeneous)

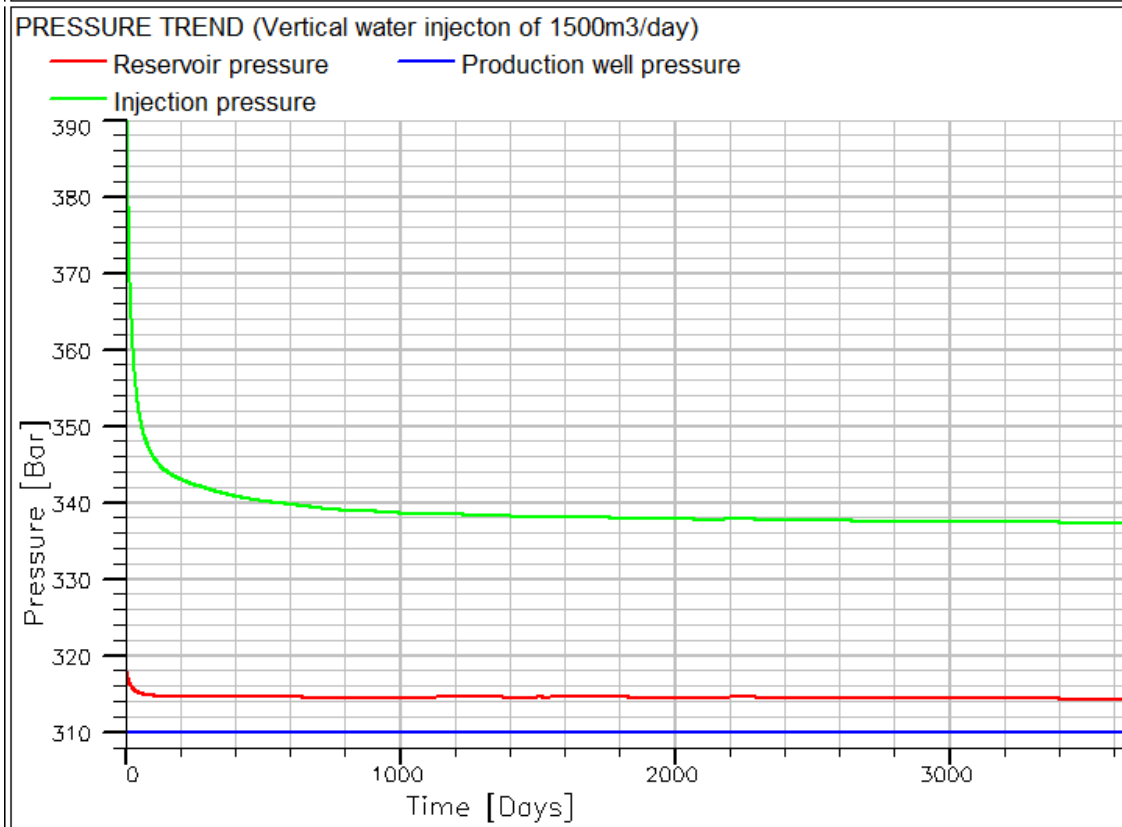
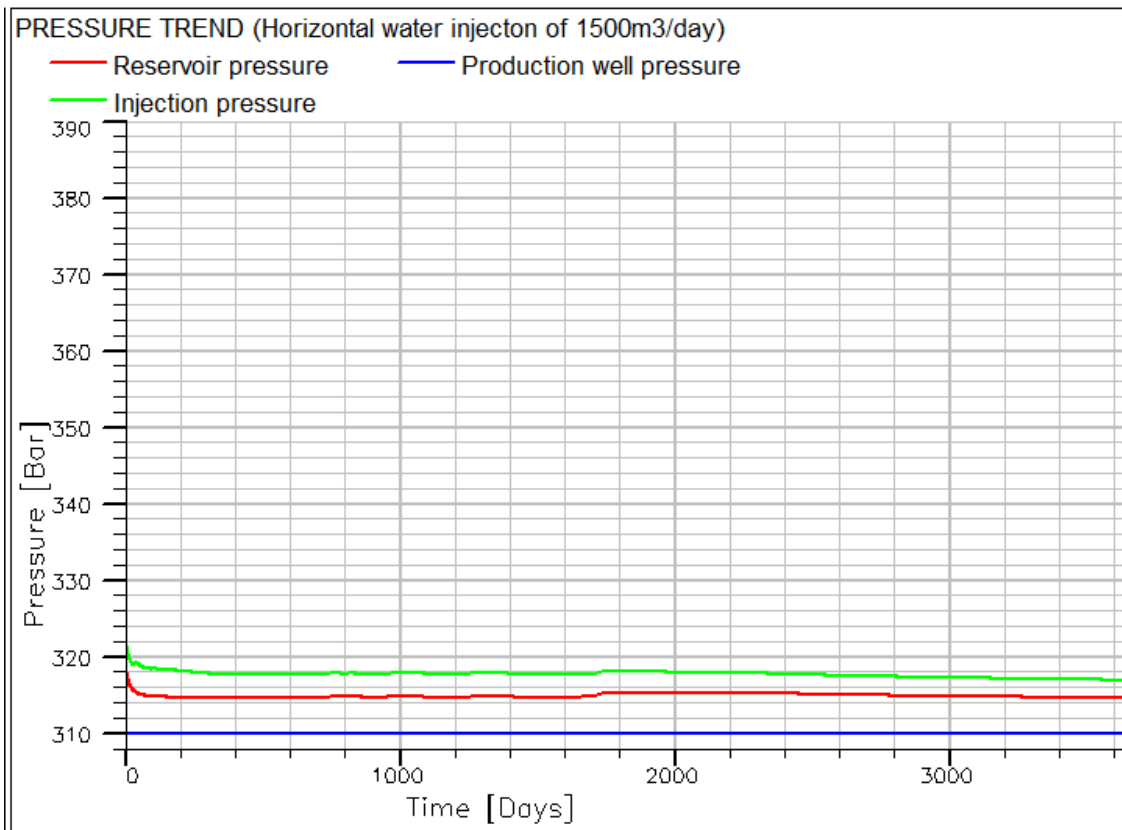


Figure 6-9 Pressure trend for water injection of 1500m³/day (homogeneous)

6.1.5 Result for water injection of 2000m³/day (Homogenous)

Figure 6-10 shows how the oil production rate, water cut and reservoir pressure change with time at water injection rate of 2000m³/day for the horizontal and vertical injection arrangement respectively. From the start to the 100th day, oil production rate decreases from 3862m³/day to approximately 1496m³/day for the horizontal case while the vertical case decreases from 3862m³/day to approximately 1499m³/day. For the horizontal case, oil production rate of approximately 1488m³/day is maintained for about 1079 days until further decrease at the 1179th day due to water breakthrough. Approximately the same oil production rate of about 1488m³/day is maintained for a shorter period of 458 days for the vertical case until further decrease at the 558th day due to water breakthrough. At the 3653rd day, oil production rate for the horizontal case is approximately 333m³/day while that of the vertical case is approximately 388m³/day. The total oil produced at the end of 3653rd day is about 3,236,492m³ for the horizontal case and about 3,378,713m³ for the vertical case. Water breakthrough time is 1691 days for the horizontal injection and the 792 days for the vertical case. At the 3653rd day, the water cut is 0.75 for the horizontal case and 0.69 for the vertical case.

Figure 6-10 also shows a sharp decrease in reservoir pressure to about 316.15bar at the 100th day due to start-up for horizontal injection while the vertical injection also shows sharp decreased to 316.06bar at the 100th day due to start-up. Reservoir pressure of approximately 316bar is maintained for 10179 days before water breakthrough for the horizontal case. There is a further increase in the reservoir pressure with water through for the horizontal case with reservoir pressure at the end of the 3653rd day maintained to 315.53bar. Different trend is observed for the vertical case. The reservoir pressure continues to decrease even with water breakthrough with final value of 315.07bar at the end of the simulation day for the vertical injection. From figure 6-11, it can be shown that an average drawdown pressure of about 7.5bar is achieved through horizontal water injection while approximately 7bar is achieved with vertical water injection. Figure 6-11 also shows that lower differential injection pressure of 5bar is required for the horizontal case while the vertical case requires higher differential injection pressure of 39bar.

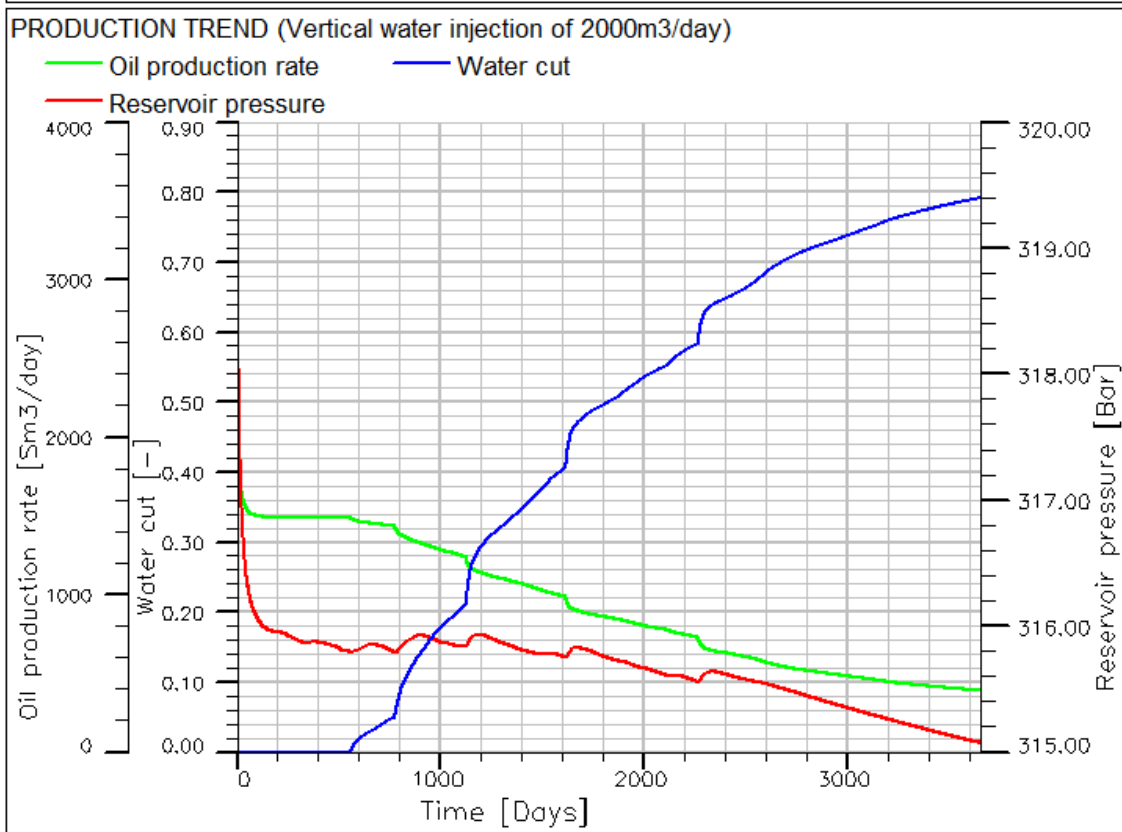
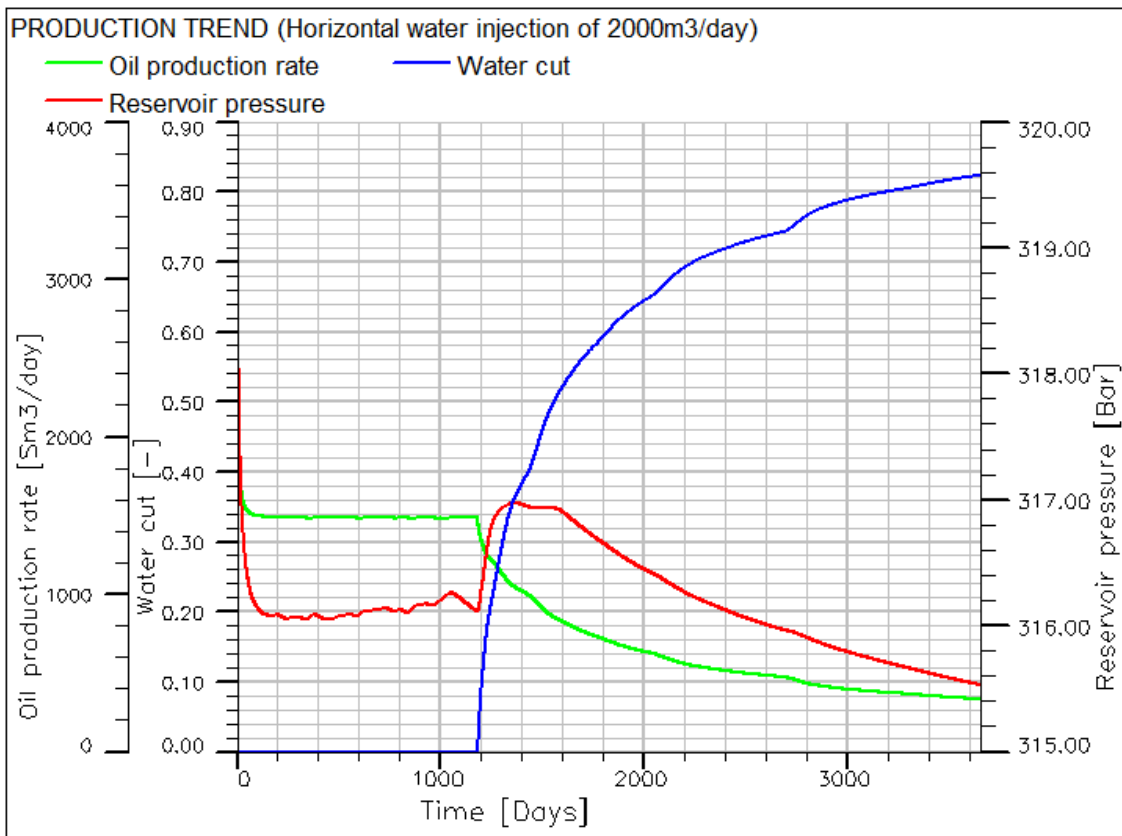


Figure 6-10 Production trend for water injection of 2000m³/day (homogeneous)

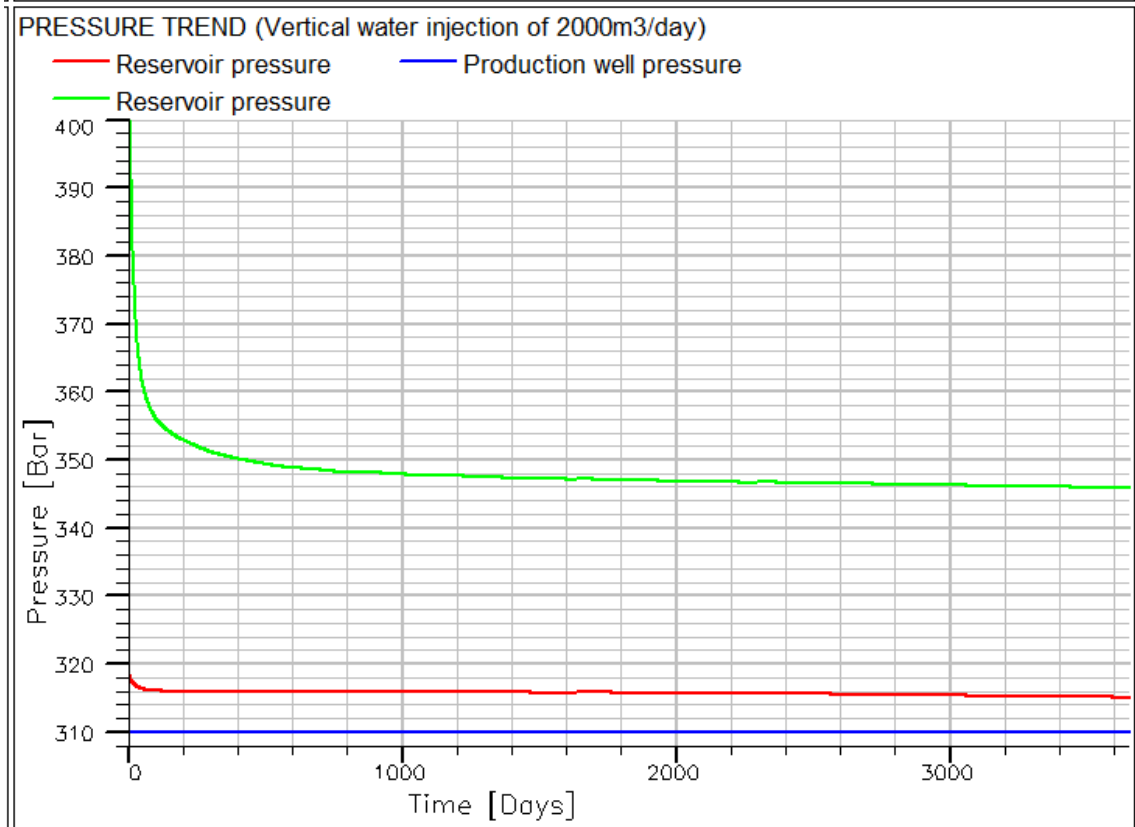
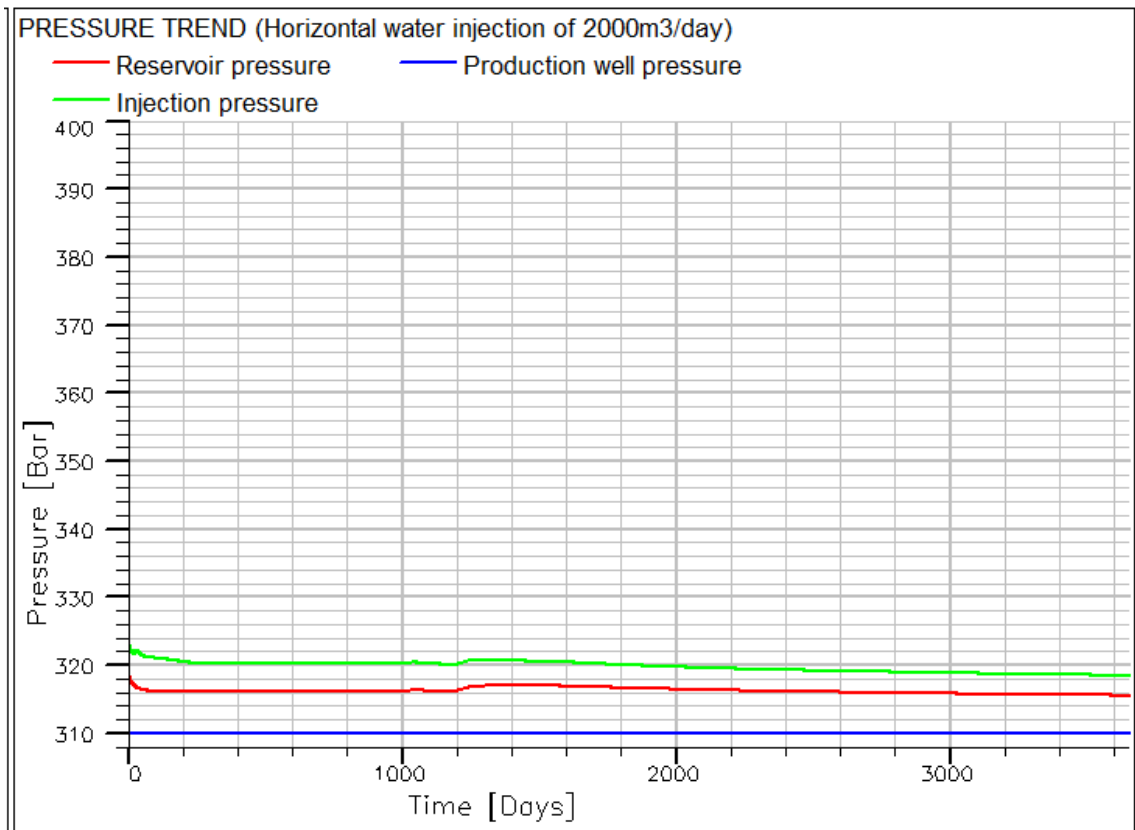


Figure 6-11 Pressure trend for water injection of 2000m³/day (homogeneous)

6.1.6 Result for water injection of 2500m³/day (Homogeneous)

Figure 6-12 shows how the oil production rate, water cut and reservoir pressure change with time at water injection rate of 2500m³/day for the horizontal and vertical injection arrangement respectively. From the start to the 100th day, oil production rate decreases from 3872m³/day to approximately 1869m³/day for the horizontal case while the vertical case decreases from 3872m³/day to approximately 1870m³/day. For the horizontal case, oil production rate of approximately 1869m³/day is maintained for about 790 days until further decrease at the 890th day due to water breakthrough. Approximately oil production rate of about 1870m³/day is maintained for a shorter period of 331 days for the vertical case until further decrease at the 431st day due to water breakthrough. At the 3653rd day, oil production rate for the horizontal case is approximately 307m³/day while that of the vertical case is approximately 342m³/day. The total oil produced at the end of 3653rd day is about 3,386,664m³ for the horizontal case and about 3,600,575m³ for the vertical case. Water breakthrough time is 890 days for the horizontal injection and the 431 days for the vertical case. At the 3653rd day, the water cut is 0.87 for the horizontal case and 0.86 for the vertical case.

Figure 6-12 also shows a sharp decrease in reservoir pressure to about 317.45bar at the 100th day due to start-up for horizontal injection while the vertical injection also shows sharp decreased to 317.36bar at the 100th day due to start-up. For the horizontal case, the reservoir pressure increases to approximately 317.62 at the 890th day. With the water breakthrough, the reservoir pressure increases higher due to the propagation of water wave and maintains value of 316.41bar at the end of the 3653rd day. For the vertical case, the reservoir pressure continues to decrease even with water breakthrough with final value of 315.81bar at the end of the simulation day. From figure 6-13, it can be shown that an average drawdown pressure of about 8.5bar is achieved through horizontal water injection while approximately 7.5bar is achieved with vertical water injection. Figure 6-13 also shows that lower differential injection pressure of 6bar is required for the horizontal case while the vertical case requires higher differential injection pressure of 45bar.

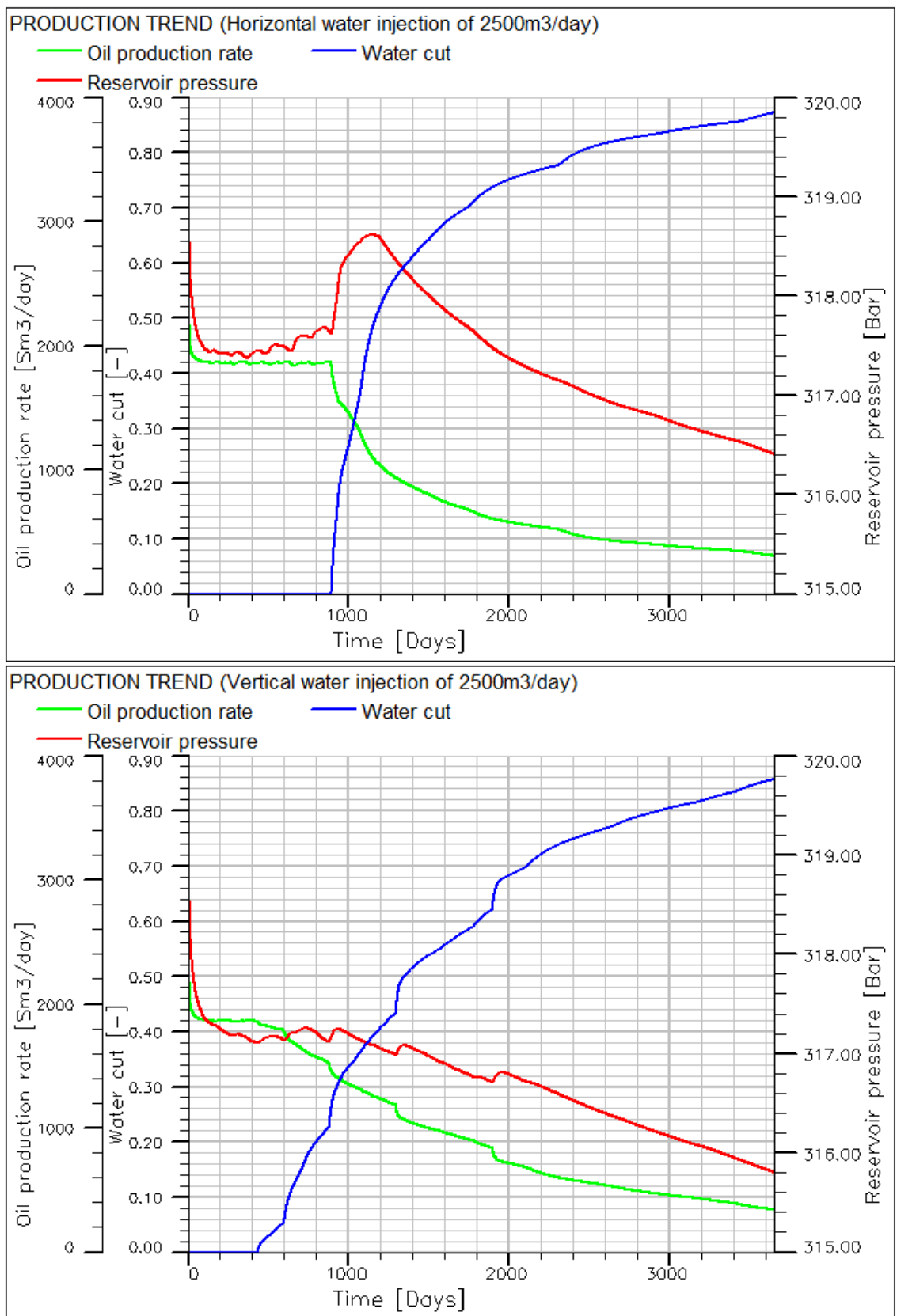


Figure 6-12 Production trend for water injection of 2500m³/day (homogeneous)

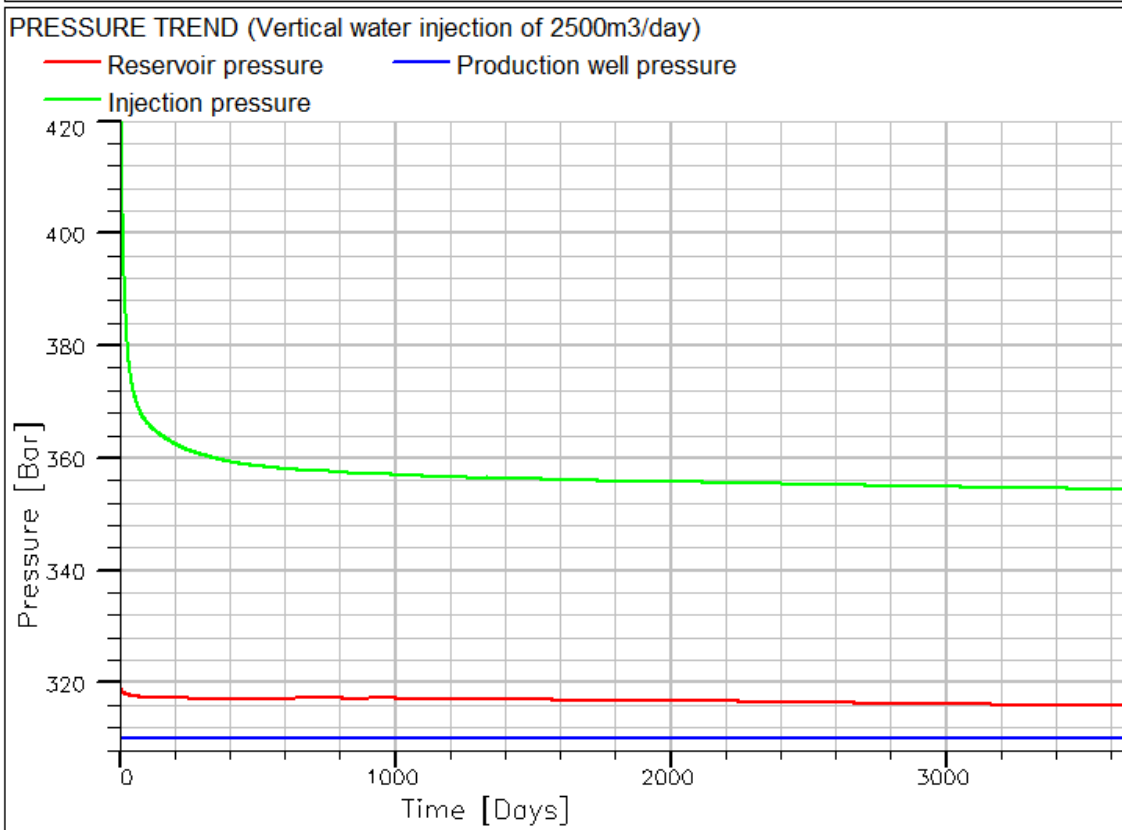
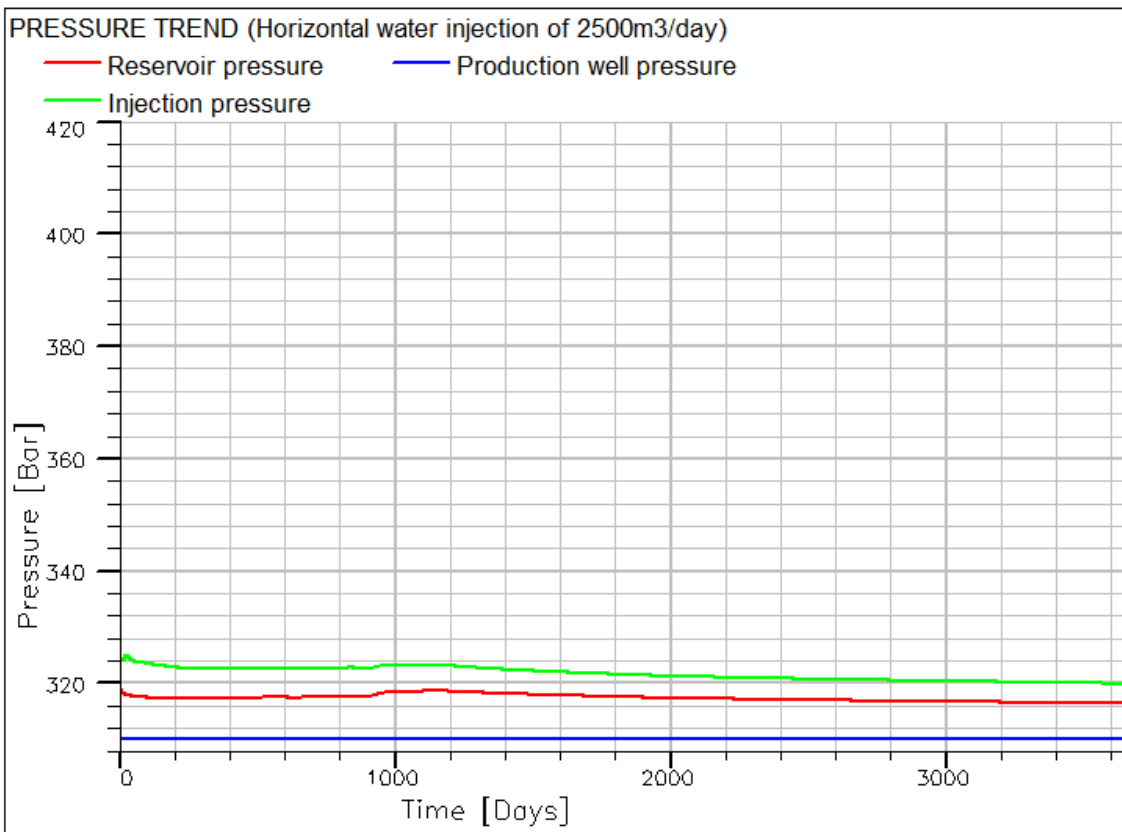


Figure 6-13 Pressure trend for water injection of 2500m³/day (homogeneous)

6.1.7 Overall Pressure Trend (Homogeneous)

Figure 6-14 shows the simulated reservoir pressure trend.

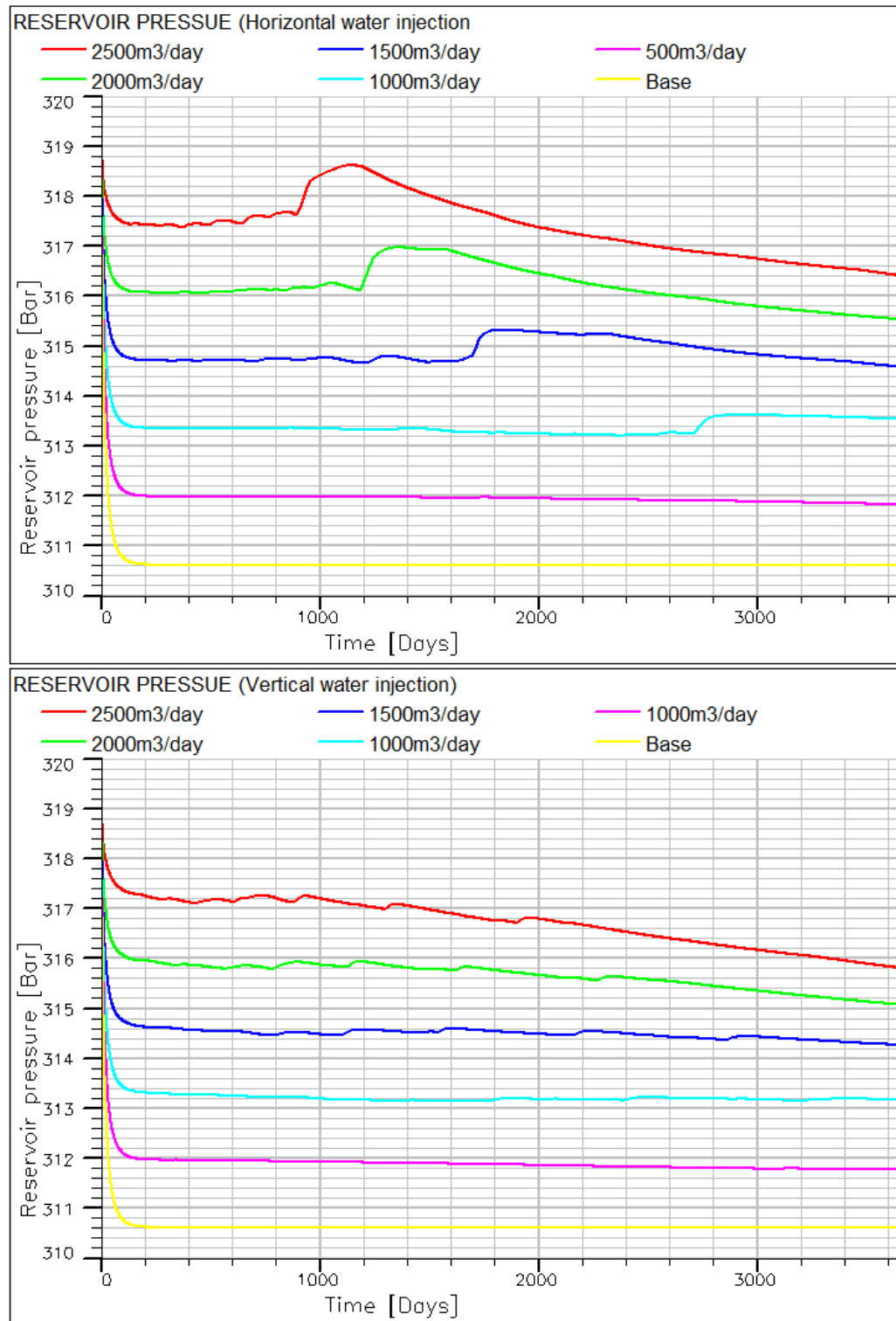


Figure 6-14 Plot of overall reservoir pressure against time (homogeneous)

From figure 6-14, the reservoir pressure drop with horizontal injection is between 6% and 14% less than for the vertical case. This is because of the gravitational pressure

drop with the vertical arrangement which does not affect the horizontal injection. Also lower flow velocity is obtained with horizontal injection due to several perforations unlike the vertical injection with one opening for the same injection flow rate. With less flow velocity of the horizontal injection, frictional pressure loss would be less than the case of vertical injection. This phenomenon also accounts for the higher injection pressure with the vertical injection compared with the horizontal injection as can be shown in figure 6-15. From the result, it can be shown that the differential injection pressure required for horizontal injection is between 87% and 96% less than vertical injection. This implies that less energy and cost is required for horizontal waterflooding compared with the vertical arrangement. Also from figure 6-14, it shows that the drawdown pressure achieved through waterflooding using horizontal injection is higher between 7% and 13% compared with the vertical injection case. The highest percentage increase in the drawdown pressure was observed with injection rate of 2500m³/day.

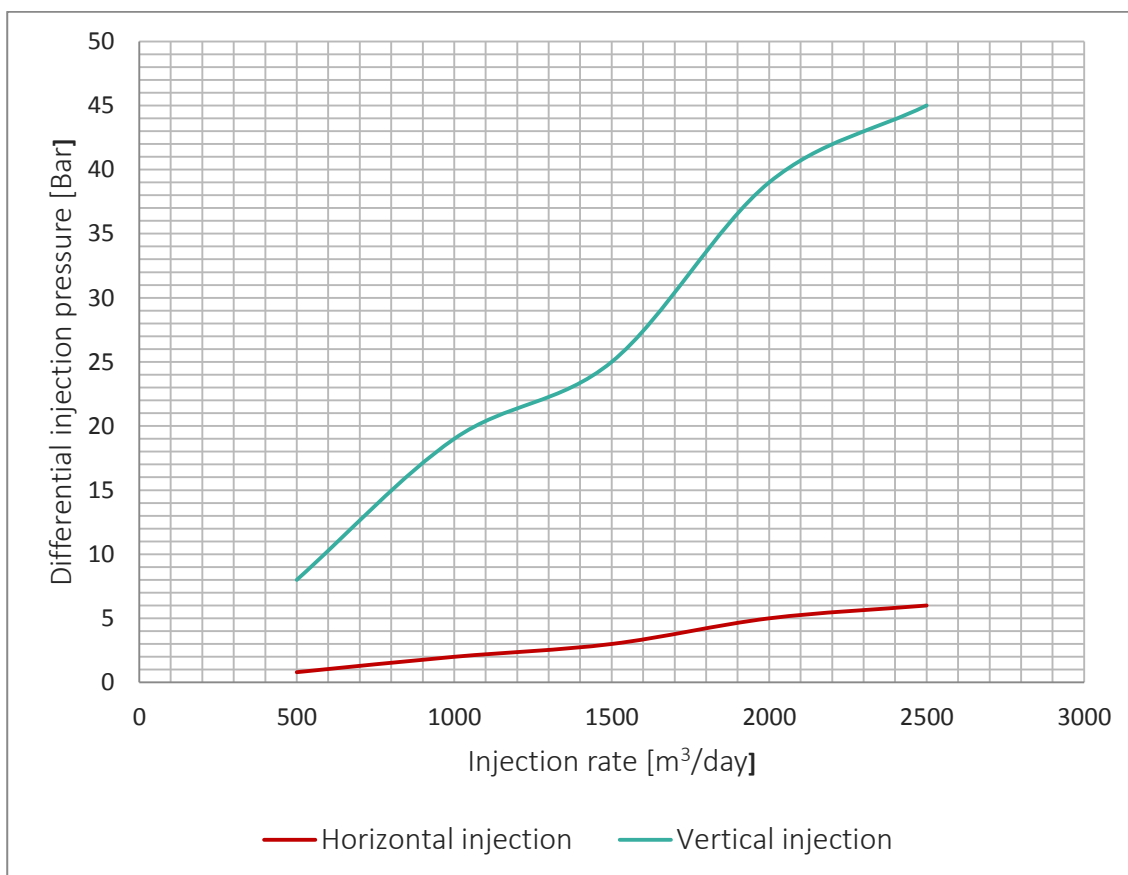


Figure 6-15 Plot of differential injection pressure against injection rate (homogeneous)

6.1.8 Water production (Homogeneous)

The trend of water cut is shown in Figure 6-16. Relative permeability affects water cut trend.

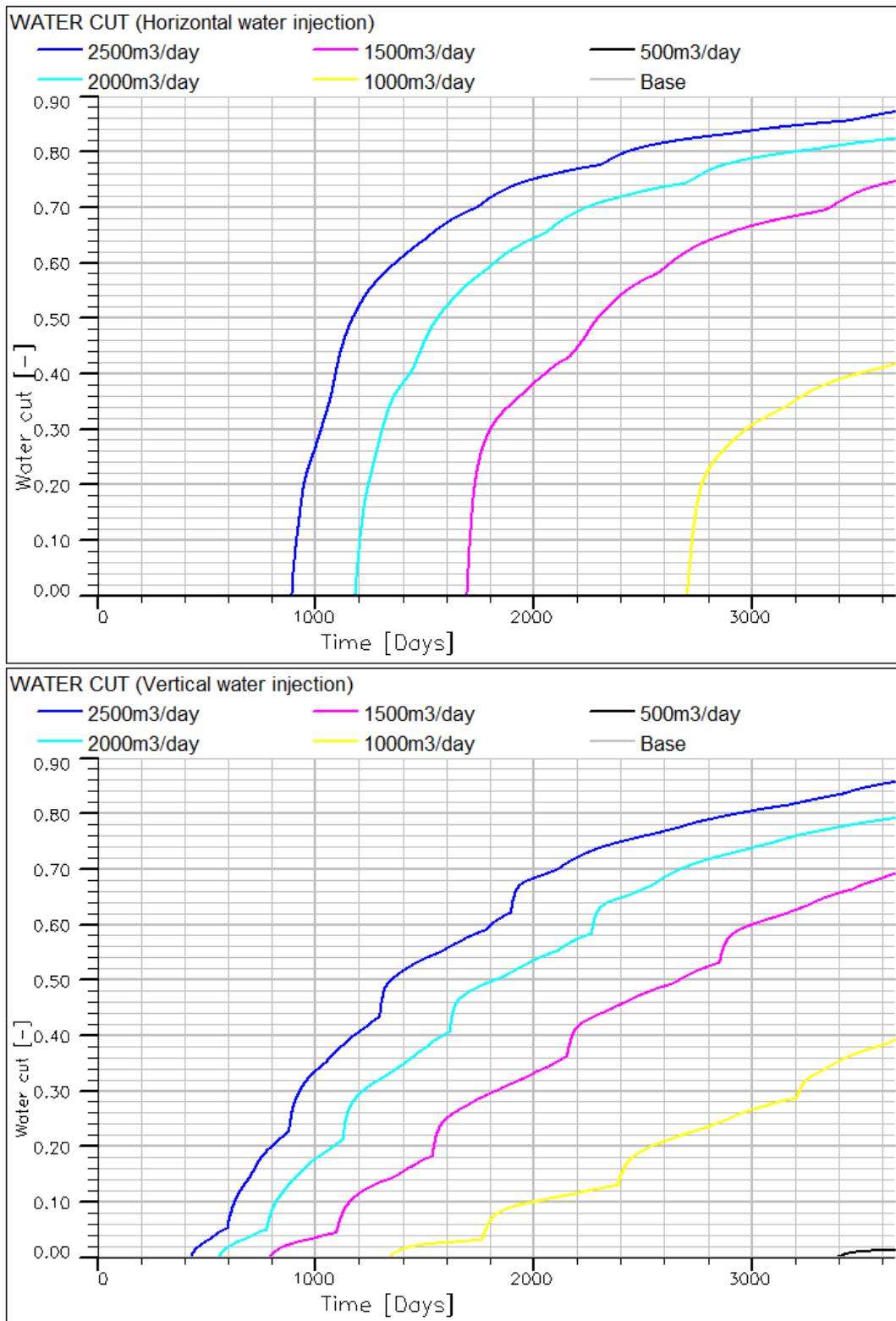


Figure 6-16 Plot of overall water cut against time (homogeneous)

It was observed that water breakthrough is delayed between 459 days and 1362 days with horizontal case compared with the vertical case. This delay in water breakthrough could be attributed to less flow velocity with horizontal injection compared with the vertical injection. With this, it takes longer time to push water into the production well for the horizontal injection than the vertical injection. Despite of the late water breakthrough, the water cut after 3653 days is higher using horizontal flooding in all the cases. This may be attributed to the higher drawdown pressure observed with the horizontal injection than the vertical injection. With higher drawdown pressure, water with lower viscosity flows more into the production well than oil.

This result conforms with theoretical relative permeability trend for multi-phase flow. During oil production, the saturation of oil in the reservoir decreases while the water saturation increases. This causes the relative permeability of oil to decrease while relative permeability of water increases. From Darcy law, with the increase in relative permeability, the volumetric water flow of water in the reservoir will continue to increase and eventually water starts flowing more into the production well.

6.1.9 Oil production rate (Homogeneous)

Figure 6-10 shows the oil production rate for horizontal and vertical water injection respectively. At the beginning, the flow rate is maintained at constant level until the breakthrough occurs. Thereafter the oil flow rate decreased and the flow rate starts to fluctuate with time. This fluctuations is due to the multiphase flow after the breakthrough. This can be explained using the concept of relative permeability and Darcy's law for multiphase flow. With waterbreak through, the oil saturation reduces while water saturation increases. This reduces the relative permeability and flow rate of oil in the reservoir. Volumetric flow rate also depends on the the viscosities of each component. With oil having more viscosity values than water and gas, the flow rate would reduce after breakthrough. The result shows that horizontal waterflooding maintains higher oil production rate for a longer period until water breaks through. After water breakthrough, the production rate drops more for horizontal waterflooding than the vertical case. This may be attributed to the higher drawdown pressure of the horizontal waterflooding case compared with the vertical case. The production rate for

the base case is very low compared to the cases with waterflooding. This is in agreement that waterflooding improve the oil production rate [6].

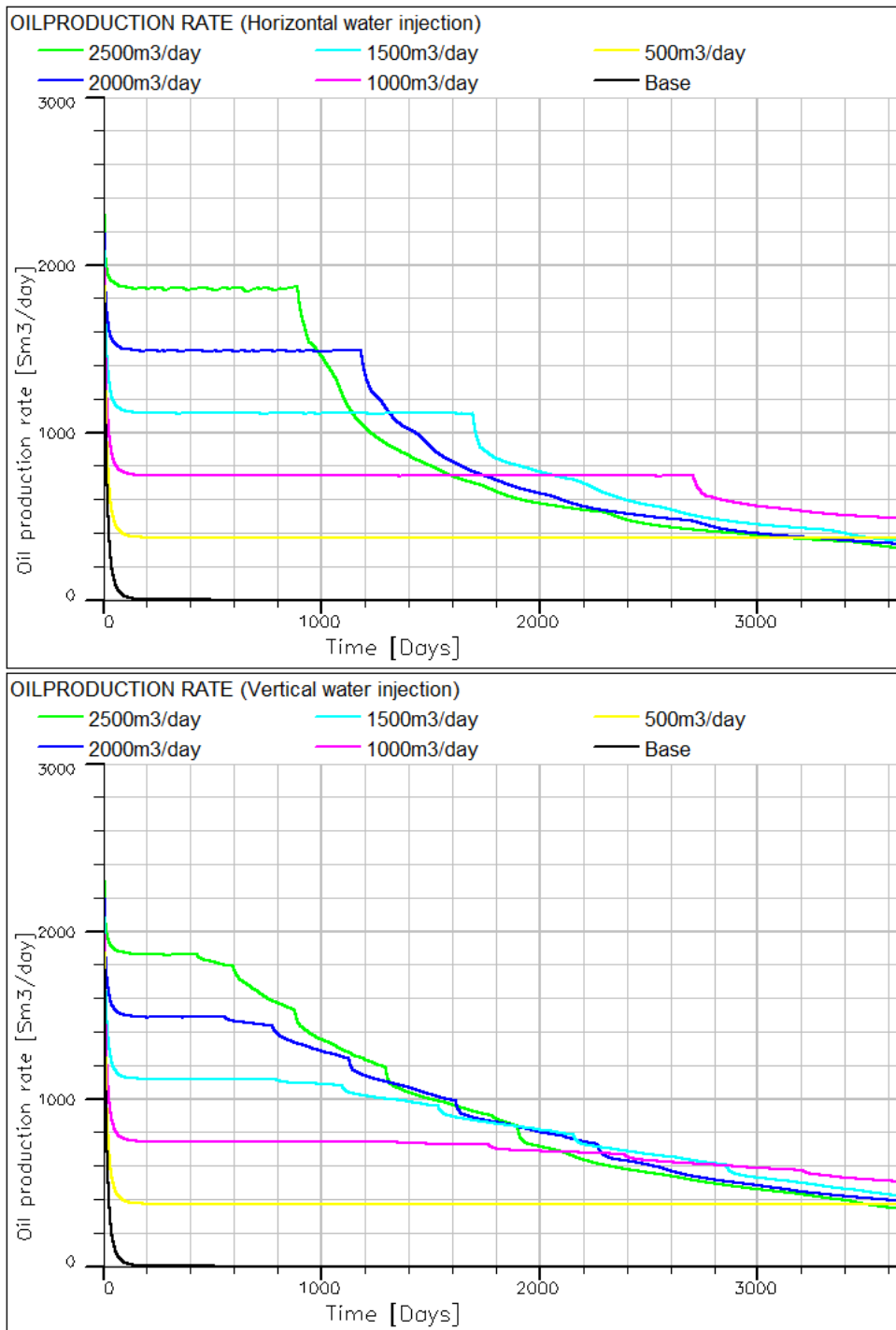


Figure 6-17 Plot of overall oil production rate against time (homogeneous)

6.1.10 Accumulated oil production (Homogeneous)

Figure 6-10 shows the accumulated oil production trend. The plot shows that despite the delay in water breakthrough, the accumulated oil production with horizontal flooding is slightly less than the vertical flooding. This may be attributed to more water

production in the horizontal arrangement compared with the vertical arrangement as discussed earlier.

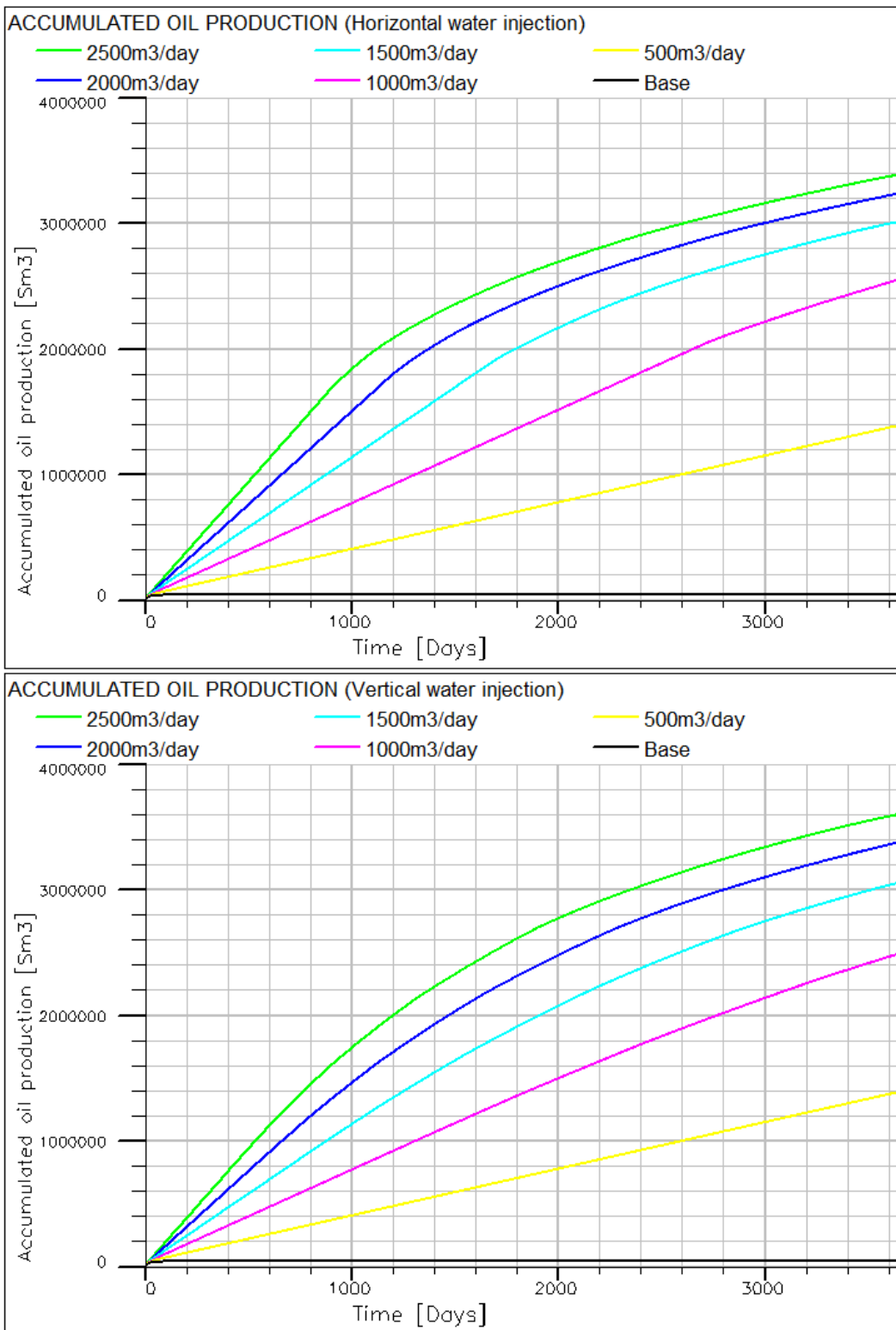


Figure 6-18 Plot of accumulated oil production against time(homogenous)

The plot of the recovery factor against injection rate shown in Figure 6-19 indicates that the recovery factor with horizontal flooding is less than the vertical flooding may be due to more water production. See summary of results in Annex 2.

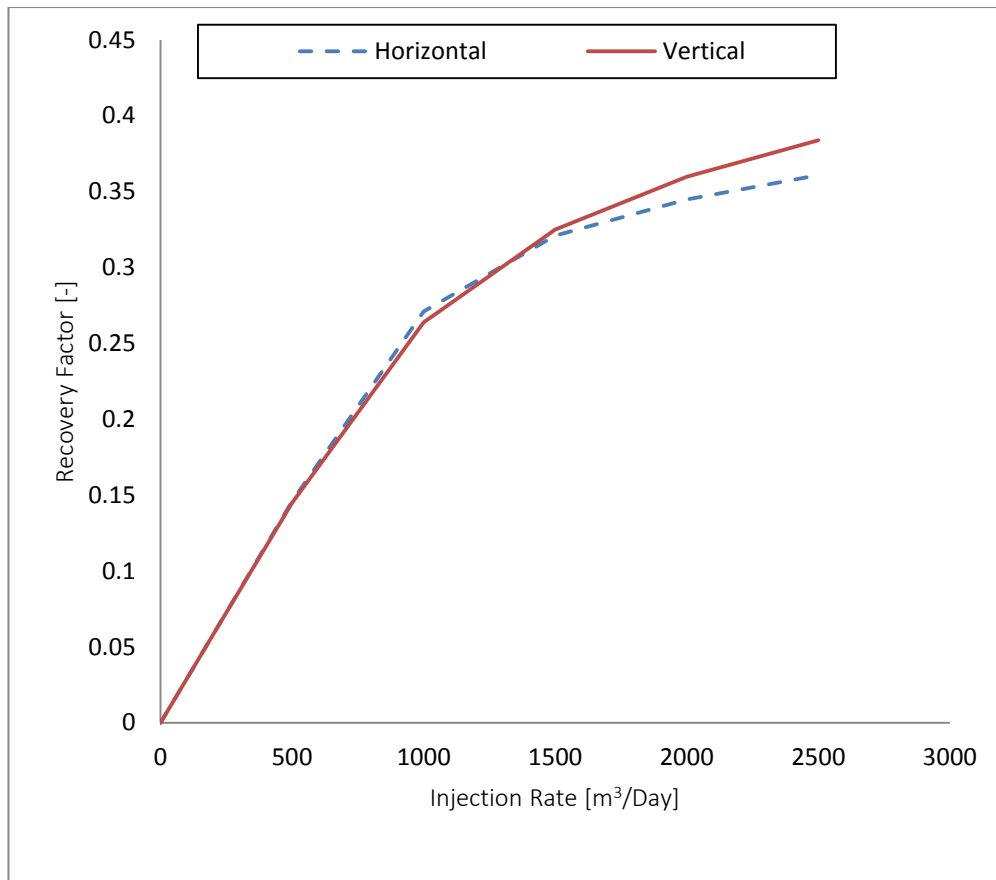
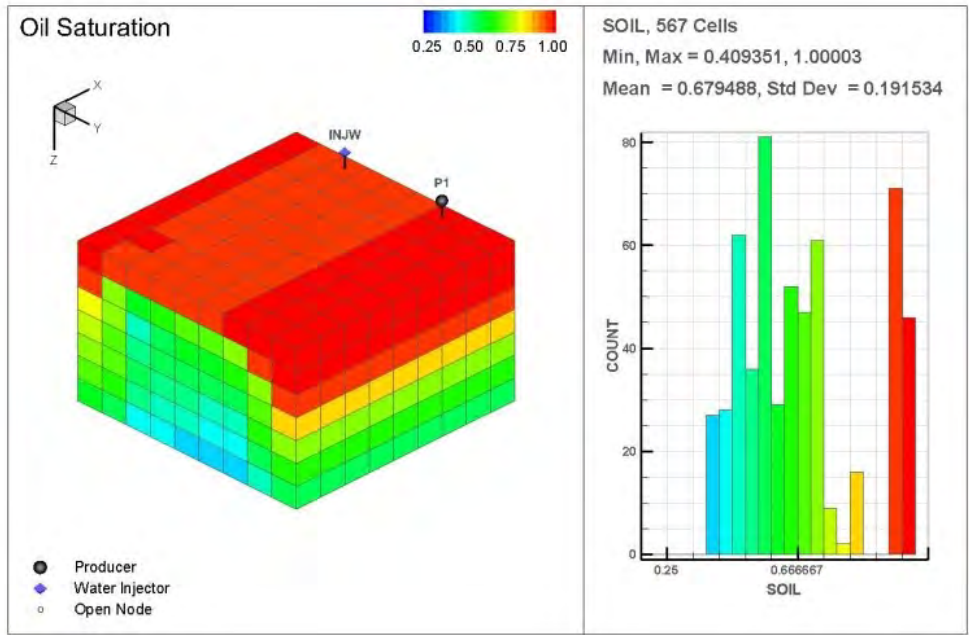


Figure 6-19 Plot of recovery factor against injection rate (homogeneous)

6.1.11 Oil saturation distribution (Homogeneous)

The case for water injection at 1500m³/day is chosen to illustrate how oil saturation is distributed in the reservoir over time for horizontal and vertical water injection respectively. Initially, the oil saturation is 1 for both cases as shown in Figure 5-1. Figure 6-20 shows the oil saturation distribution for horizontal injection after ten years. It can be seen that about 32% oil recovery was achieved through waterflooding. Figure 6-21 shows the oil saturation distribution for vertical injection after ten years. About 33% oil recovery was achieved through waterflooding. See Annex 7 for other oil saturations.

1 Jan 2026

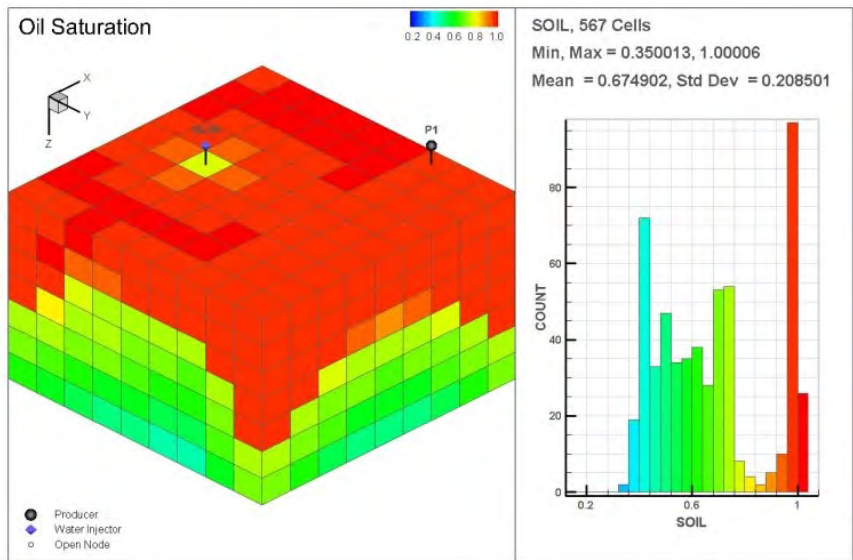


BUILD1_E100

14 Apr 2016

Figure 6-20 Oil saturation for horizontal injection after 3653 days (homogeneous)

1 Jan 2026



BUILD1_E100

14 Apr 2016

Figure 6-21 Oil saturation for vertical injection after 3653 days (homogeneous)

6.1.12 Oil-water front progression (Homogeneous)

The case for water injection at $1500\text{m}^3/\text{day}$ is used to illustrate how water displaces oil and sweeps oil towards the production well in the reservoir. Figure 6-22 shows the plan view of the oil-water front progression for the horizontal and vertical water injection after two years. The oil-water front progression after ten years is shown in Figure 6-23. From the plot, it can be seen that the oil saturation reduced due to more sweep by water injection. In general, result shows that oil-water front progresses laterally for horizontal flooding and radially for vertical flooding

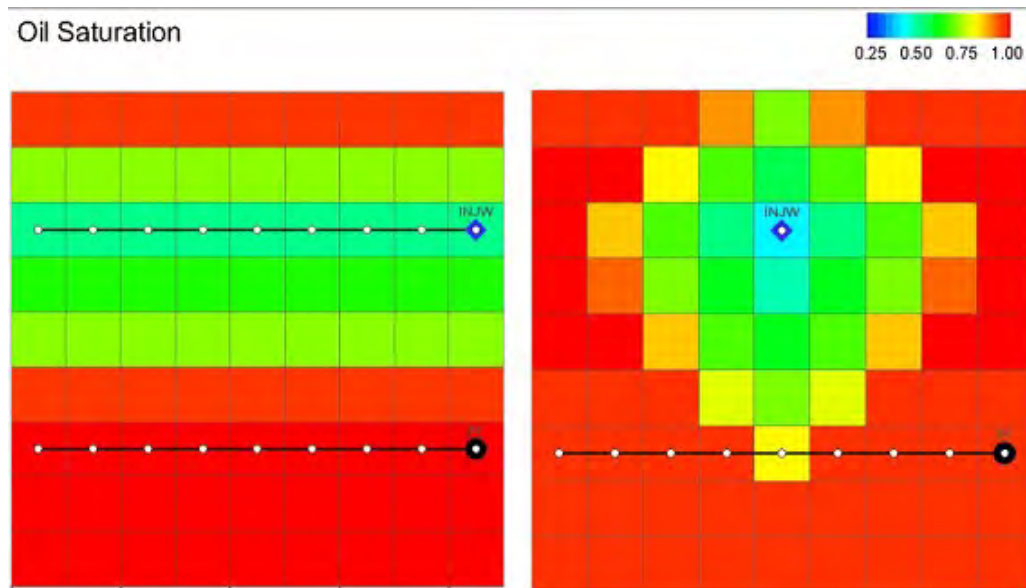


Figure 6-22 Plan view of oil-water front progression after 2 years (homogeneous)

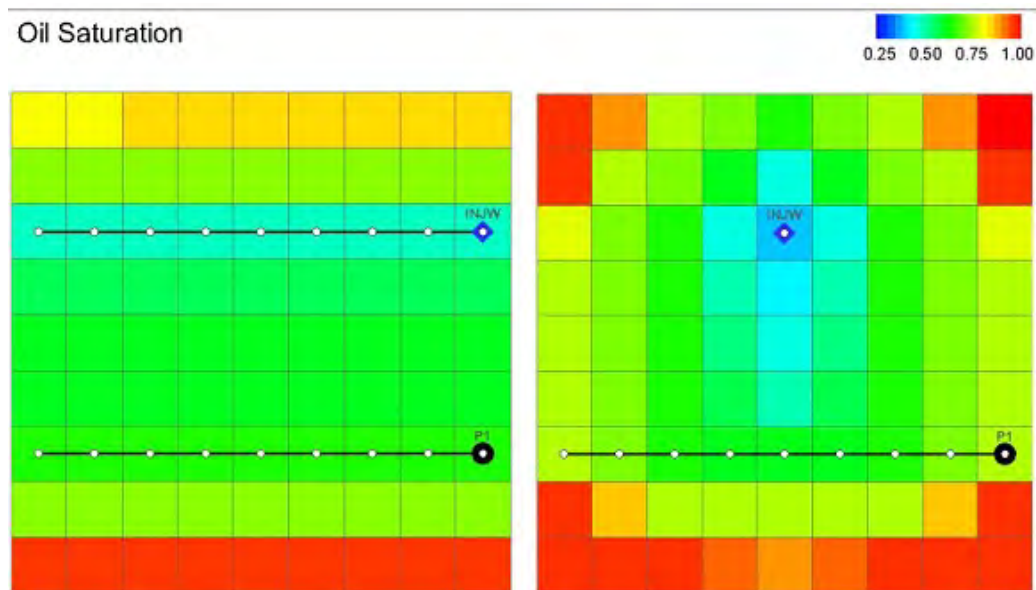


Figure 6-23 Plan view of oil-water front progression after 3653 days (homogeneous)

6.2 Heterogeneous waterflooding

Simulation of waterflooding with horizontal and vertical water injection was carried out for 3653 day by varying water injection rate from 500m³/day to 2500m³/day. In this simulation, analysis of the oil production rate, water cut, reservoir pressure, accumulated oil production and recovery factor were made for the horizontal and vertical waterflooding. A base case without water injection was also considered as reference.

6.2.1 Result of the base case (Heterogeneous)

Figure 6-24 shows how the oil production rate, water cut and reservoir pressure change with time without water injection for the horizontal and vertical injection arrangement respectively. From figure 6-25, the drawdown pressure of 0.6bar is available which is not sufficient for oil production. From figure 6-26, it shows that the saturation after ten years in the reservoir is 100%.

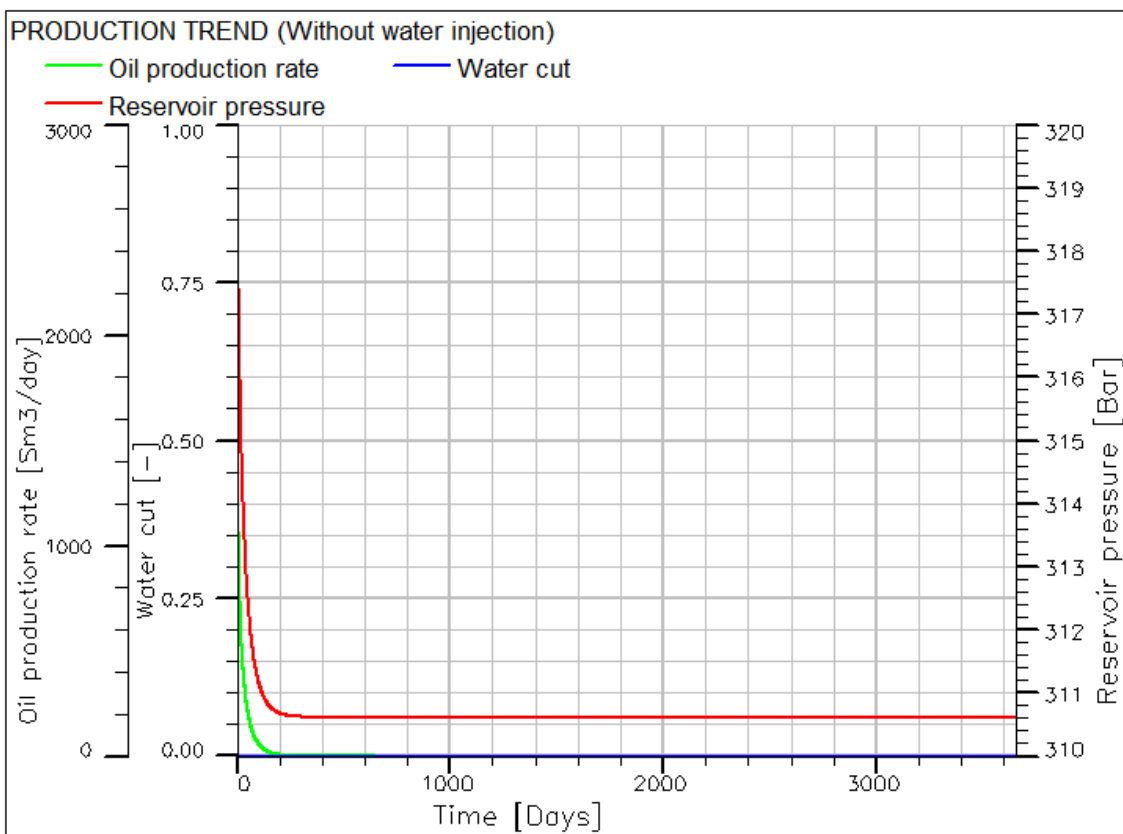


Figure 6-24 Production trend for the base case (heterogeneous)

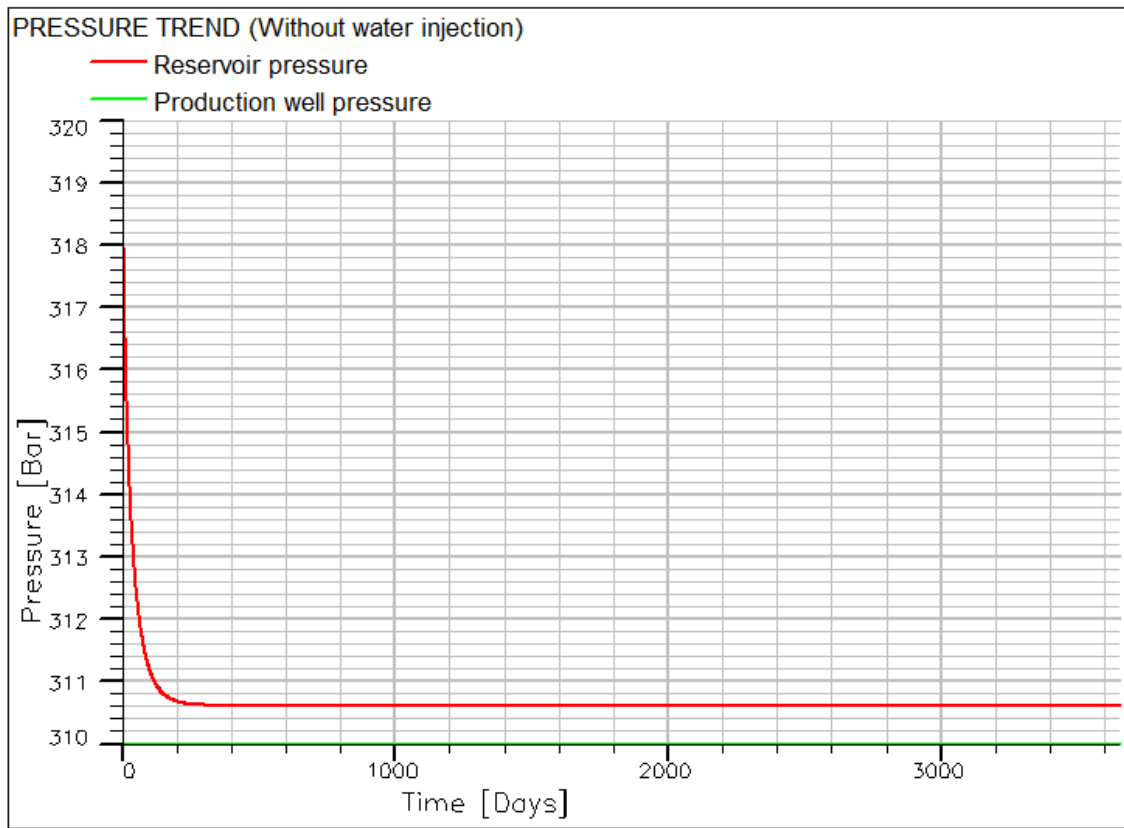


Figure 6-25 Pressure trend for the base case (heterogeneous)

1 Jan 2026

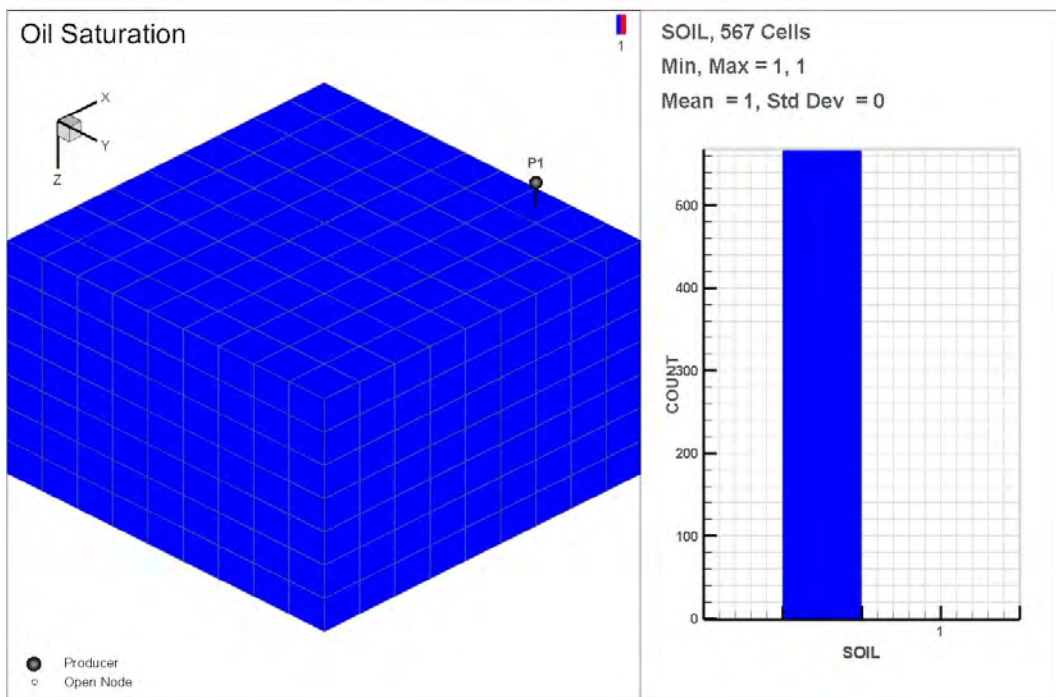


Figure 6-26 Final oil saturation of the base case (heterogeneous)

6.2.2 Result at water injection of 500m³/day (Heterogeneous)

Figure 6-27 shows how the oil production rate, water cut and reservoir pressure change with time at water injection rate of 500m³/day. From the start to the 200th day, oil production rate decreases sharply from 2367m³/day to approximately 376m³/day for the horizontal case while the vertical case decreases from about 2367m³/day to approximately 376m³/day. The oil production rate of 376m³/day is maintained for 2945 days for the horizontal case until further decrease at the 3143rd day due to water breakthrough. The oil production rate of 376m³/day is maintained for shorter period of 400 days for the vertical case until further decrease at the 600th day due to water breakthrough. At the end of 3653rd day, the production rate for the horizontal case is approximately 293m³/day while the vertical case is about 153m³/day. Water breakthrough time is 3143 days for the horizontal injection and 600 days for the vertical case. At the end of 3653rd day, the water cut is 0.27 for the horizontal case and 0.66 for the vertical case.

Figure 6-27 also shows a sharp decreased in reservoir pressure to about 313.06bar at the 200th day due to start-up for horizontal injection while the vertical injection also shows sharp decreased to 313.15bar at the 200th day due to start-up. The reservoir pressure of about 313bar was maintained for 2943 days for horizontal injection and 400 days for the vertical injection. For the two cases, it was observed that the reservoir pressure increased sharply immediately after water breakthrough due to the propagation of water wave. The final reservoir pressure at the 3653rd day is 313.3bar for the horizontal case and 312.39bar for the vertical case. From figure 6-28 it can be shown that an average drawdown pressure of about 3bar was achieved through horizontal water injection while approximately 2.7bar achieved with vertical water injection. Figure 6-28 also shows that lower injection differential pressure of 1.6bar is required for the horizontal case while the vertical case requires higher injection differential pressure of 13bar.

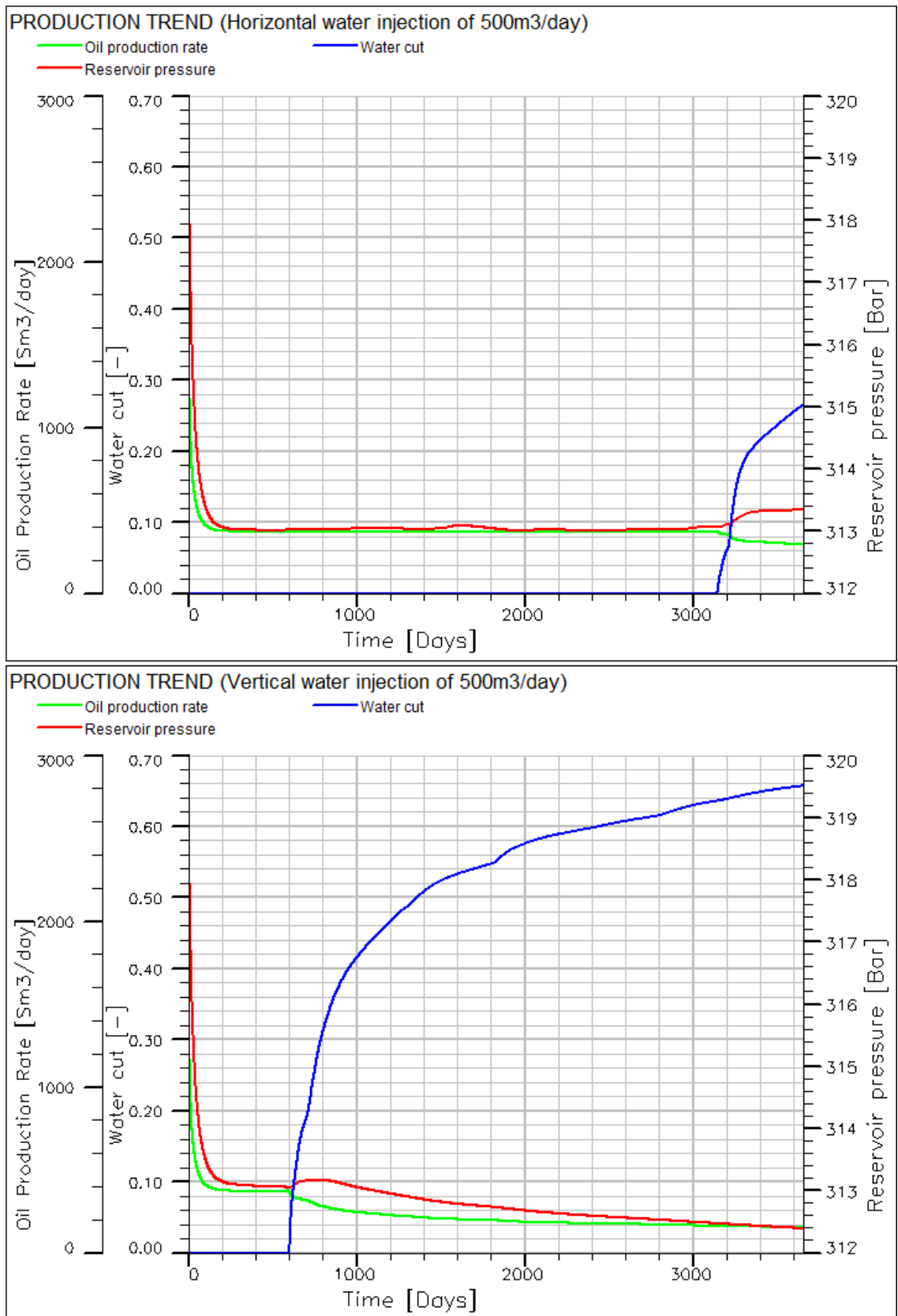


Figure 6-27 Production trend for water injection of 500m³/day (heterogeneous)

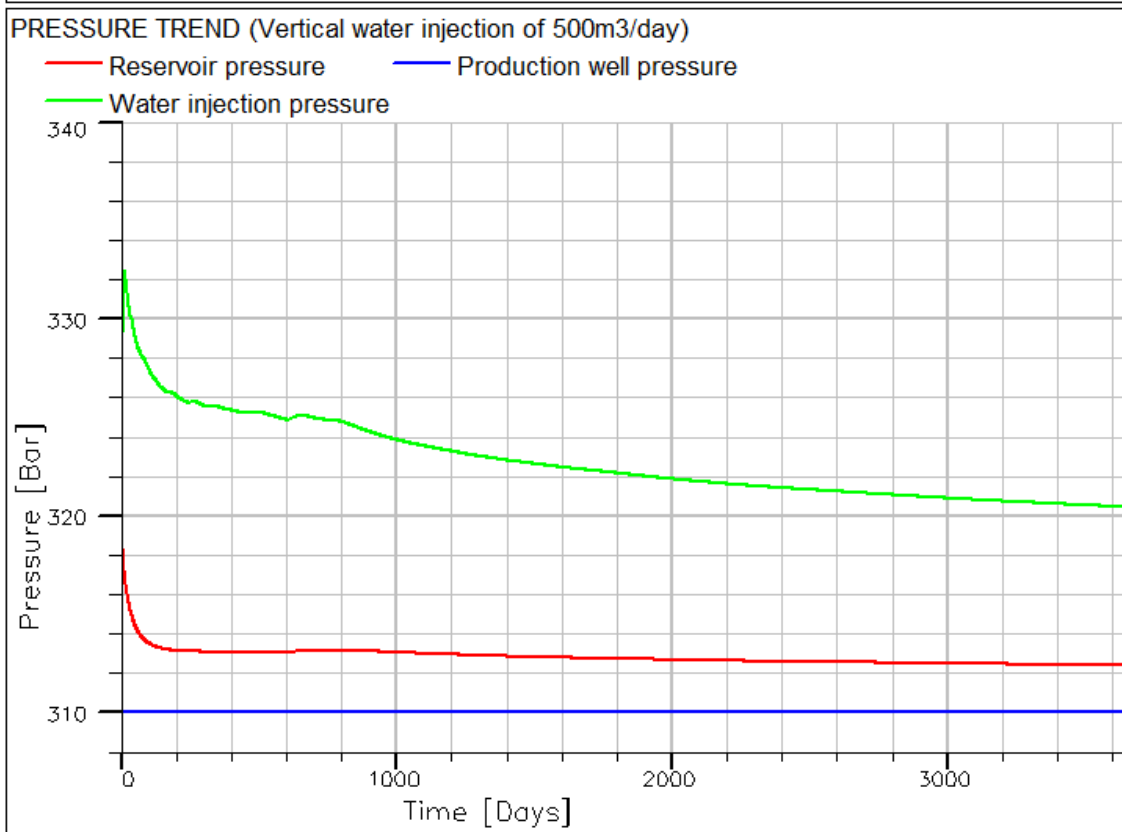
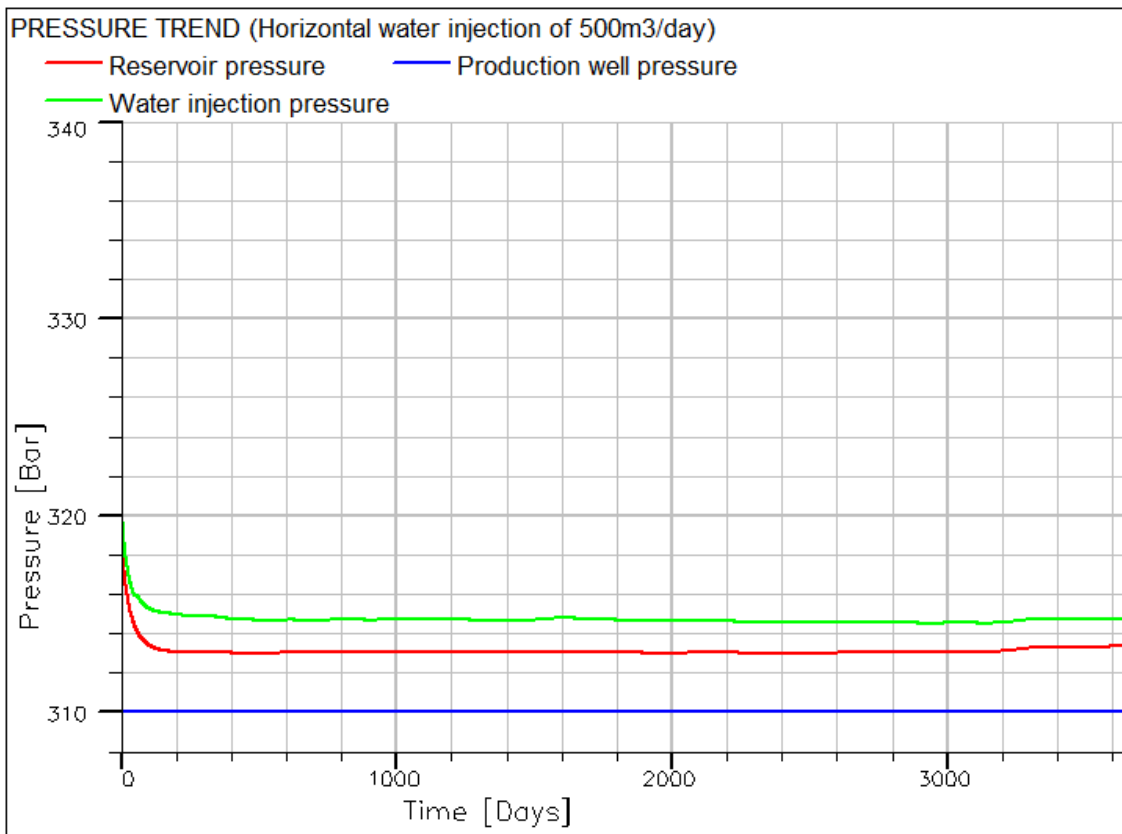


Figure 6-28 Pressure trend for water injection of 500m³/day (heterogeneous)

6.2.3 Result at water injection of 1000m³/day (Heterogeneous)

Figure 6-29 shows how the oil production rate, water cut and reservoir pressure change with time at water injection rate of 1000m³/day. From the start to the 100th day, oil production rate decreases from 2375m³/day to approximately 768m³/day and from 2376m³/day to approximately 767m³/day for the vertical case. For the horizontal case, oil production rate of 768m³/day is maintained for about 1292 days until further decrease at the 1392nd day due to water breakthrough. The same oil production rate of is maintained for shorter period of 179 days for the vertical case until further decrease at the 279th day due to water breakthrough. At the end of 3653rd day, oil production rate for the horizontal case is approximately 259m³/day while that of the vertical case is approximately 238m³/day. Water breakthrough time is 1392 days for the horizontal injection and 279 days for the vertical case. At the end of 3653rd day, the water cut is 0.72 for the horizontal case and 0.74 for the vertical case.

Figure 6-29 also shows a sharp decrease in reservoir pressure to about 315.43bar at the 200th day due to start-up for horizontal injection. Also the reservoir pressure for vertical case decreases to 315.52bar at the 200th day due to start-up. Reservoir pressure of about 315bar is maintained for 1192 days for horizontal injection and 79 days for the vertical injection. For the two cases, it is observed that the reservoir pressure increases sharply immediately after water breakthrough due to propagation of water wave. The final reservoir pressure at the end of 3653 days is 315.45bar for the horizontal case and 313.55bar for the vertical case. From figure 6-30, it can be shown that an average drawdown pressure of about 6bar is achieved through horizontal water injection while approximately 4bar achieved with vertical water injection. Figure 6-30 also shows that lower injection differential pressure of 3bar is required for the horizontal case while the vertical case requires higher injection differential pressure of 18bar.

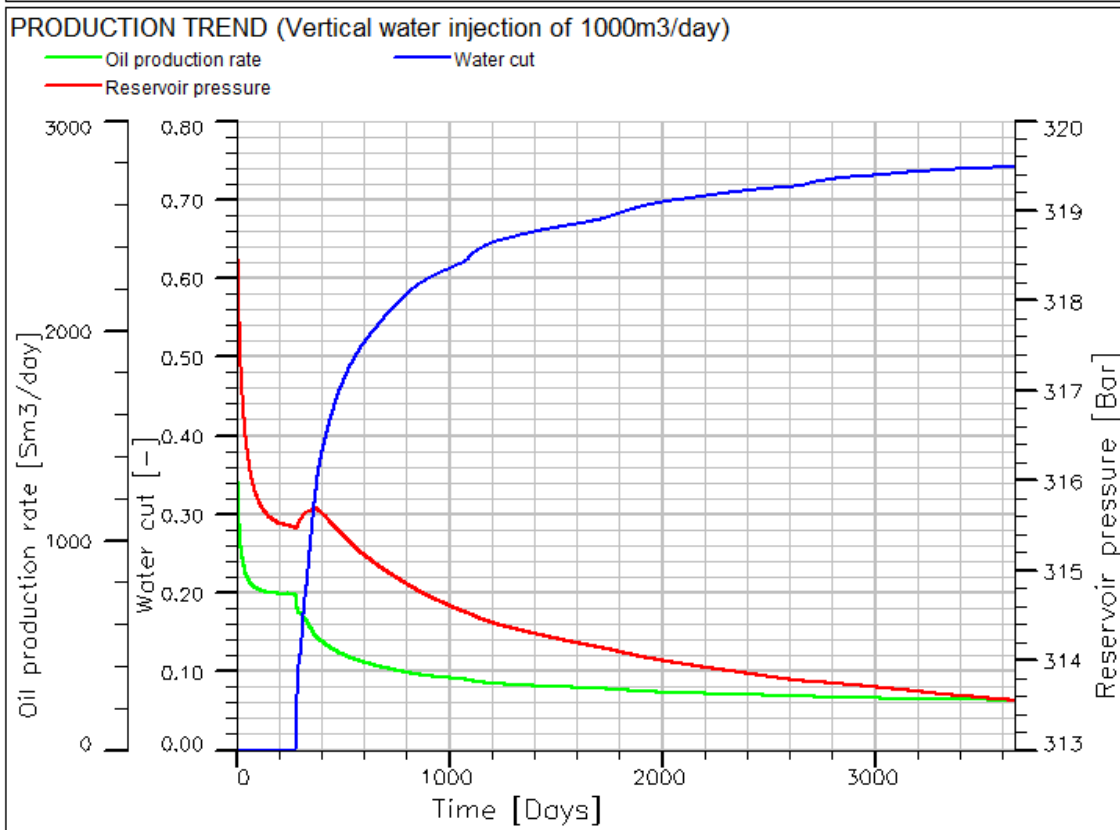
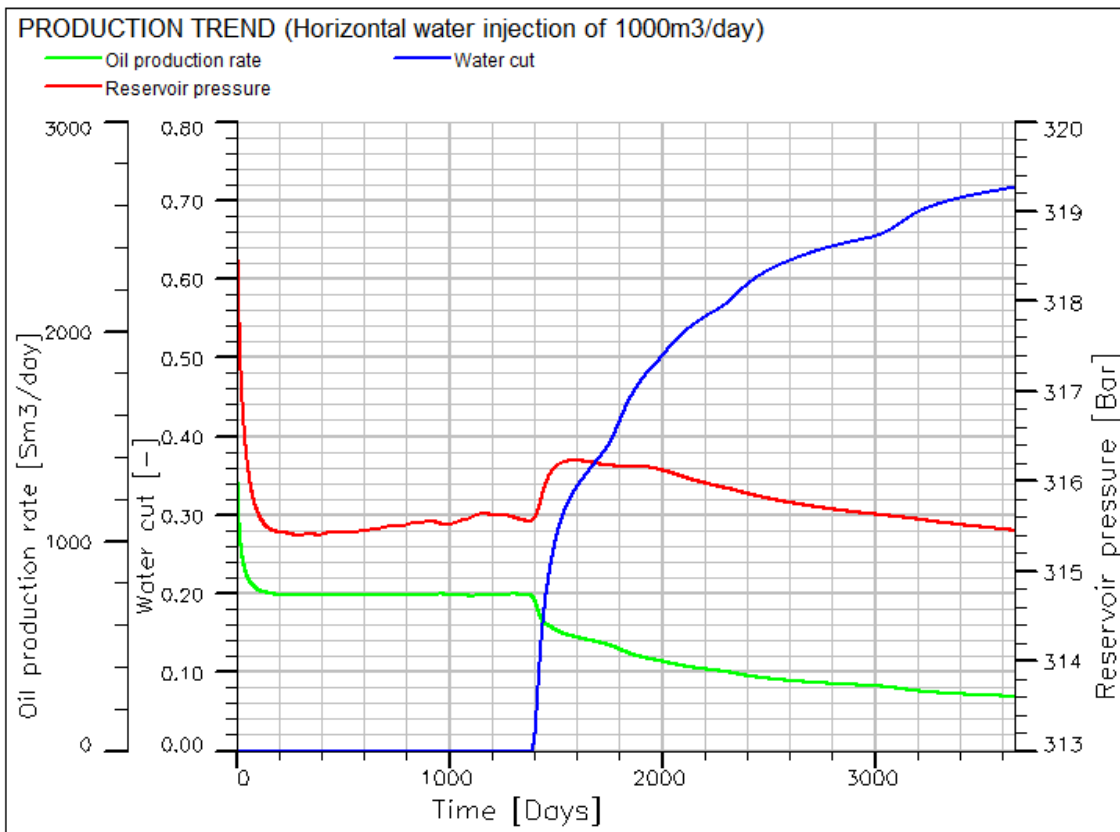


Figure 6-29 Production trend for water injection of 1000m³/day (heterogeneous)

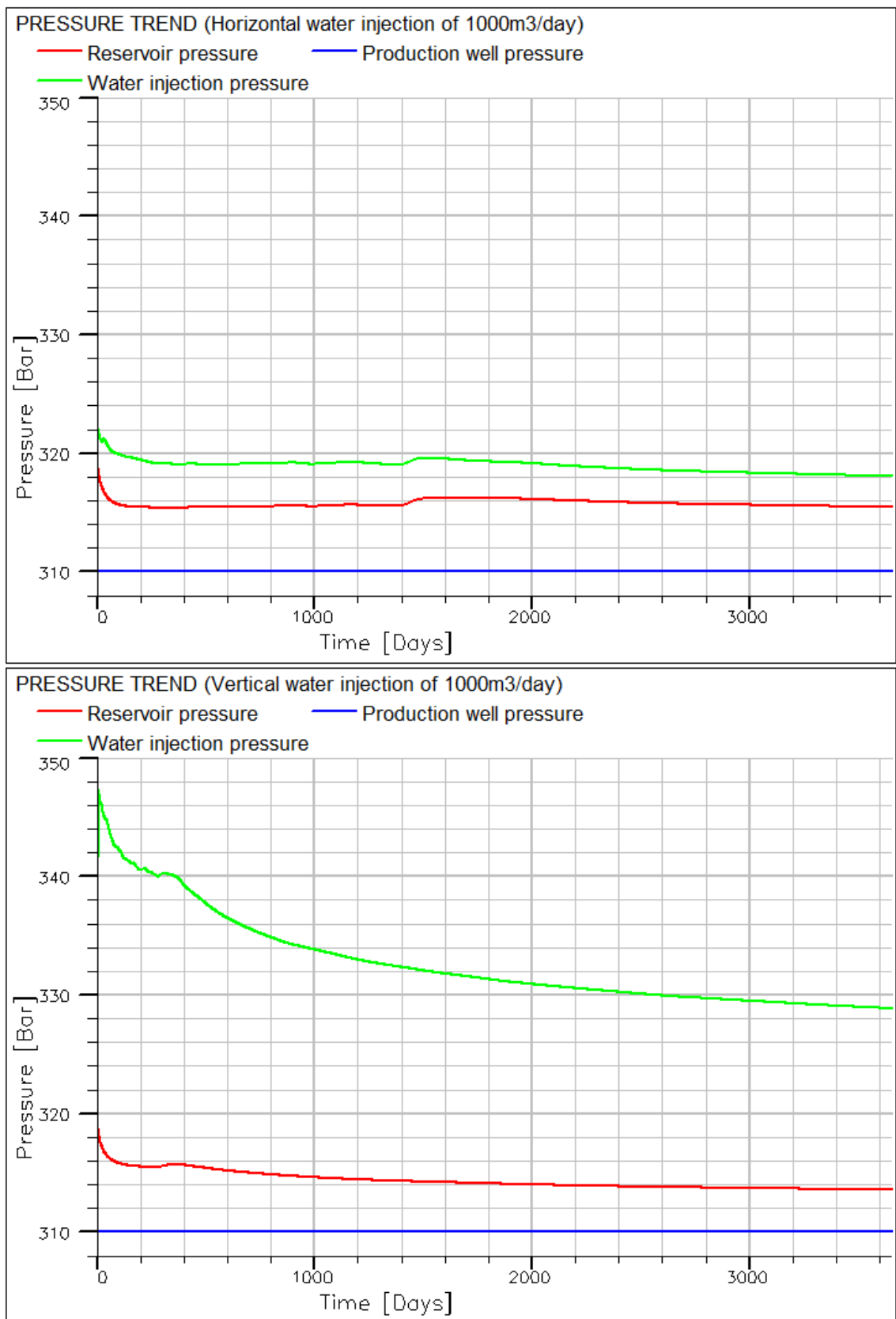


Figure 6-30 Pressure trend for water injection of 1000m³/day (heterogeneous)

6.2.4 Result at water injection of 1500m³/day (Heterogeneous)

Figure 6-31 shows how the oil production rate, water cut and reservoir pressure change with time at water injection rate of 1500m³/day. From the start to the 50th day, oil production rate decreases from 2383m³/day to approximately 1151m³/day for the horizontal case and 2387m³/day to approximately 1138m³/day for the vertical case. For the horizontal case, oil production rate of 1151m³/day is maintained for about 785 days until further decrease at the 835th day due to water breakthrough. Lower oil production rate of about 1138m³/day is maintained for a shorter period of 132 days for the vertical case until further decrease at the 182nd day due to water breakthrough. At the end of the 3653rd day, oil production rate for the horizontal case is approximately 260m³/day while that of the vertical case is approximately 324m³/day. Water breakthrough time is 835 days for the horizontal injection and the 182 day for the vertical case. At the end of the 3653rd day, the water cut is 0.82 for the horizontal case and 0.77 for the vertical case.

Figure 6-31 also shows a sharp decrease in reservoir pressure to about 317.79bar for both the horizontal and the vertical at 200th day due to start-up. The reservoir pressure increases slightly due to water injection to 318.14 between 200 and 835th day for the horizontal case. For the two cases, it is observed that the reservoir pressure increases sharply immediately after water breakthrough due to propagation of water wave. The final reservoir pressure at the end of 3653rd day is about 317.185bar for the horizontal case and 314.74bar for the vertical case. From figure 6-32, it can be shown that an average drawdown pressure of about 8bar is achieved through horizontal water injection while approximately 5bar achieved with vertical water injection. Figure 6-32 also shows that lower injection differential pressure of 4.5bar is required for the horizontal case while the vertical case requires higher injection differential pressure of 28bar.

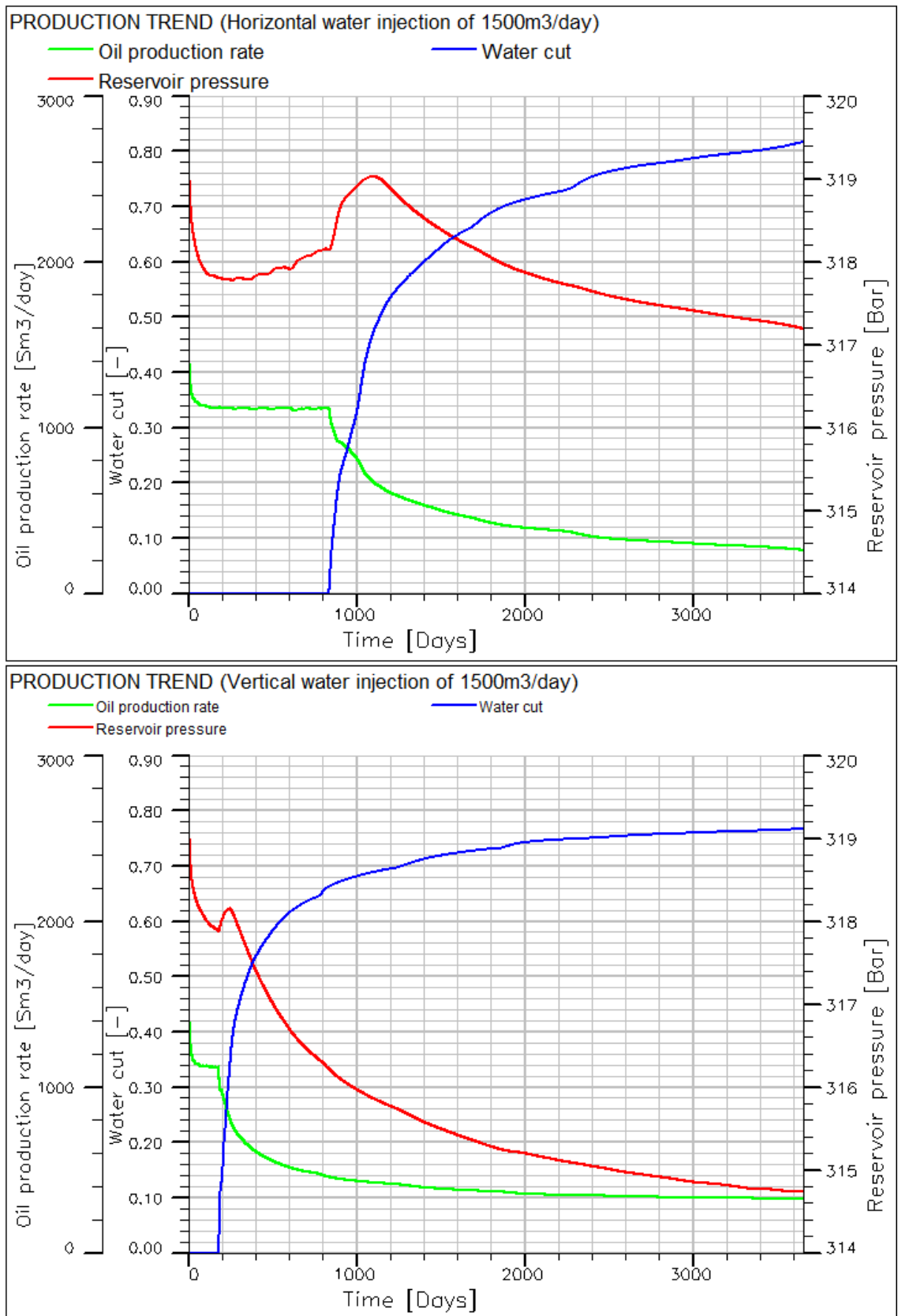


Figure 6-31 Production trend for water injection of 1500m³/day (heterogeneous)

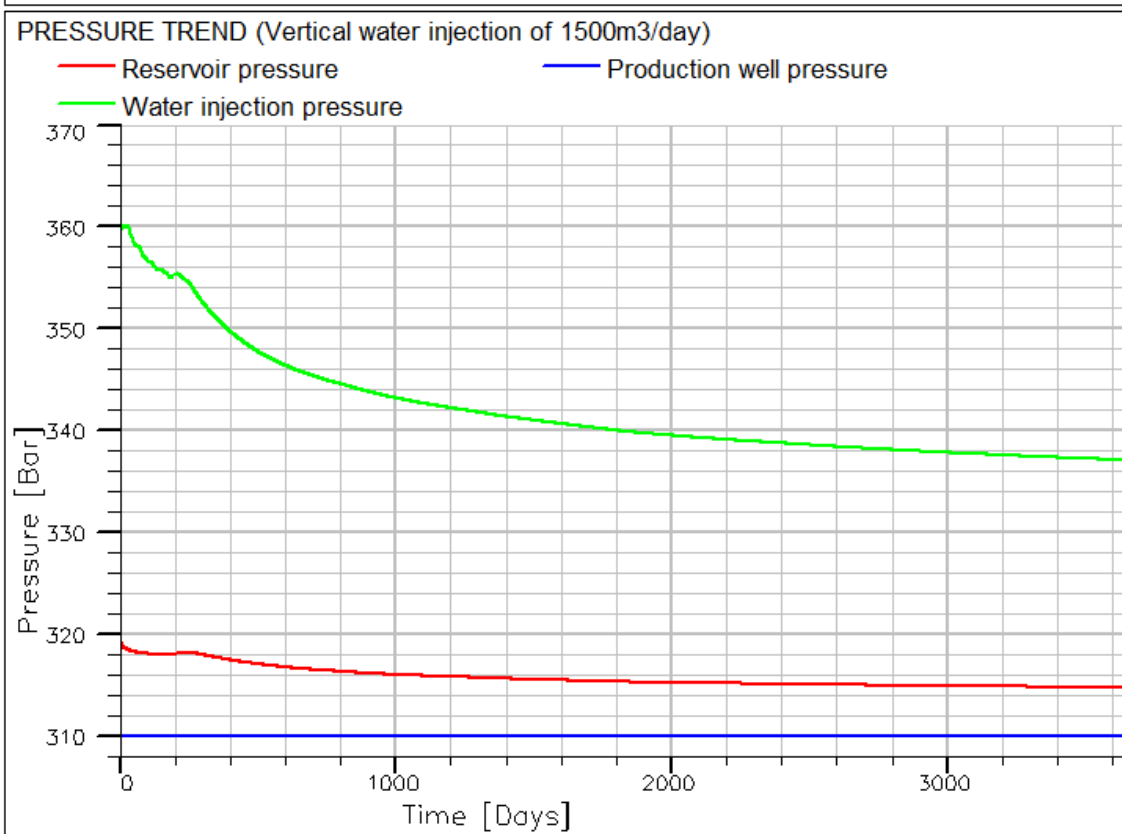
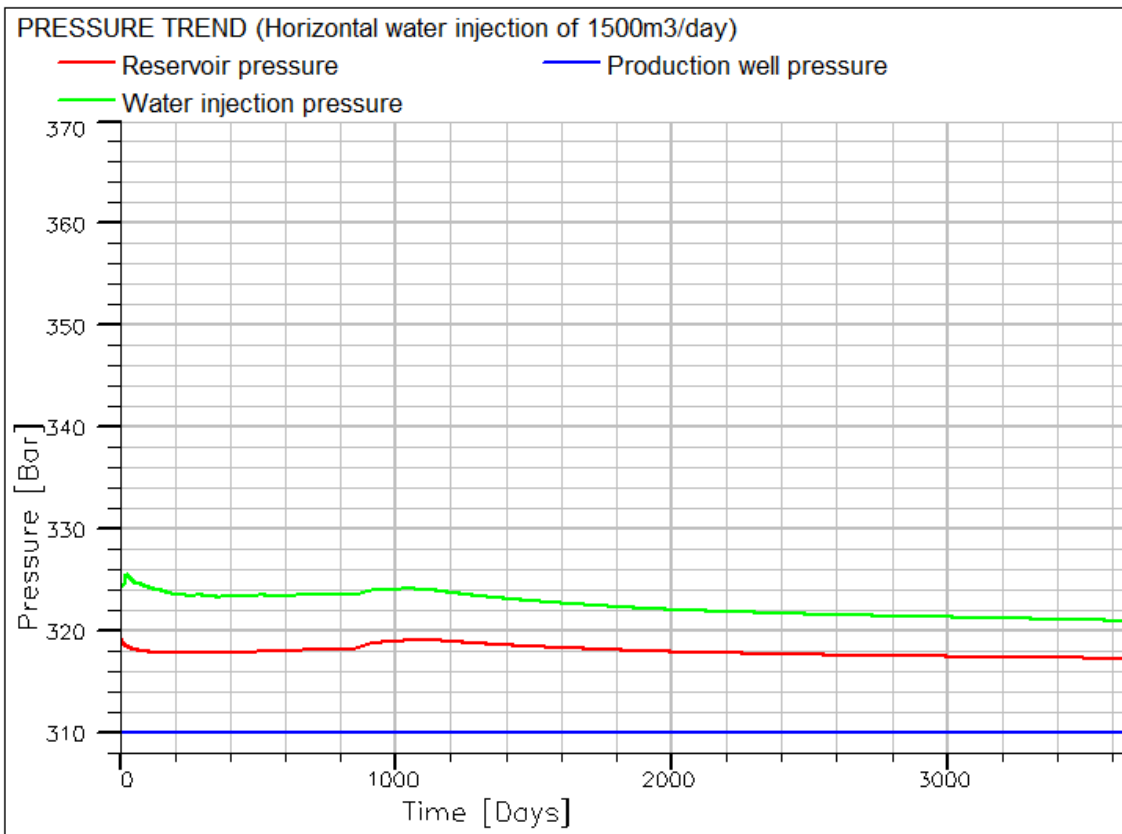


Figure 6-32 Pressure trend for water injection of 1500m³/day (heterogeneous)

6.2.5 Result at water injection of 2000m³/day (Heterogeneous)

Figure 6-33 shows how the oil production rate, water cut and reservoir pressure change with time at water injection rate of 2000m³/day. For the horizontal case, oil production rate of approximately 1500m³/day is maintained for 550days until water breakthrough at the 600th day. After 600th day, the oil production rate further decreases to about 232m³/day at the end of the 3653rd day. For the vertical injection, oil production rate increases from 1478m³/day to approximately 1493m³/day from start to the 134th day. The oil production rate at the end of the 3653rd day is 324m³/day for the vertical injection. Water breakthrough time is 600 days for the horizontal injection and the 135 days for the vertical case. At the end of the 3653rd day, the water cut is about 0.88 for the horizontal case and 0.84 for the vertical case.

Result also shows an increase in the reservoir pressure to about 320.56bar at 600th day for horizontal case and 320.23bar at the 135th day due for vertical case due to water injection. For the two cases, it is observed that the reservoir pressure increases sharply immediately after water breakthrough due to the propagation of water wave. The final reservoir pressure at the end of the 3653 days is about 318.77bar for the horizontal case and 316.12bar for the vertical case. From figure 6-34, it can be shown that an average drawdown pressure of about 9.5bar is achieved through horizontal water injection while approximately 7bar is achieved with vertical water injection. Figure 6-34 also shows that lower injection differential pressure of 6bar is required for the horizontal case while the vertical case requires higher injection differential pressure of 39bar.

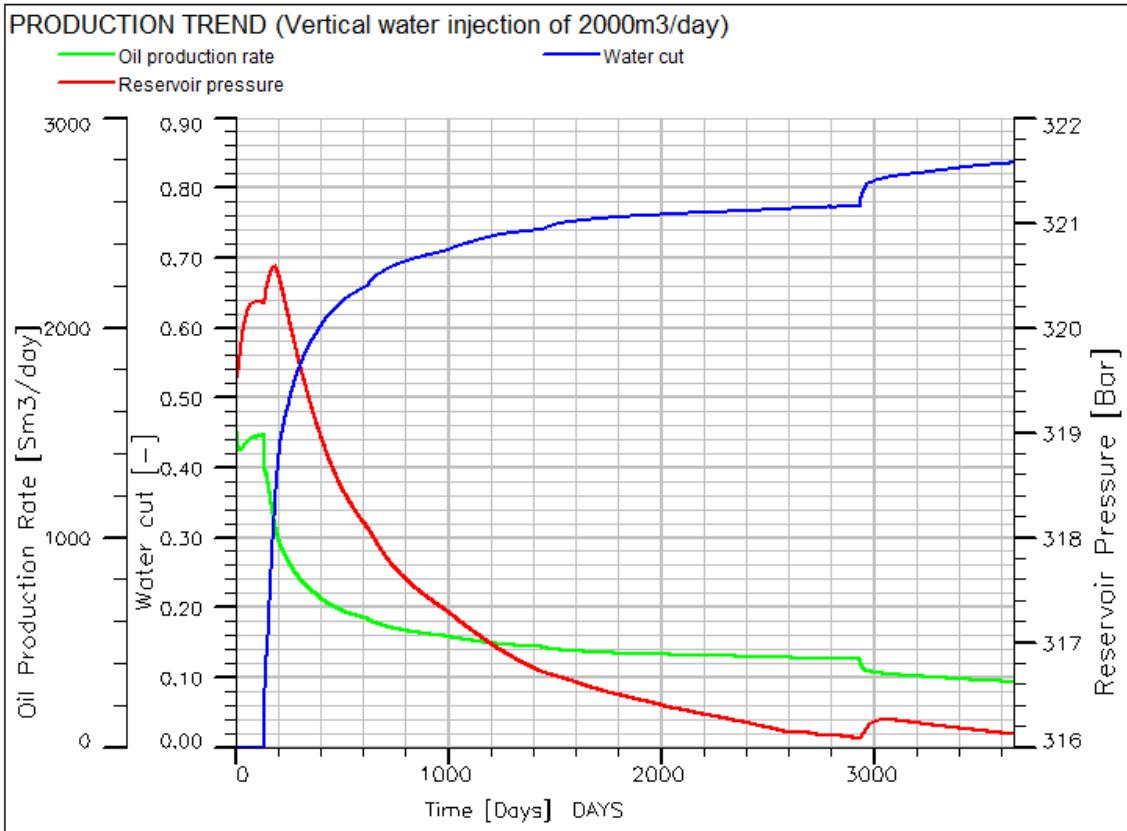
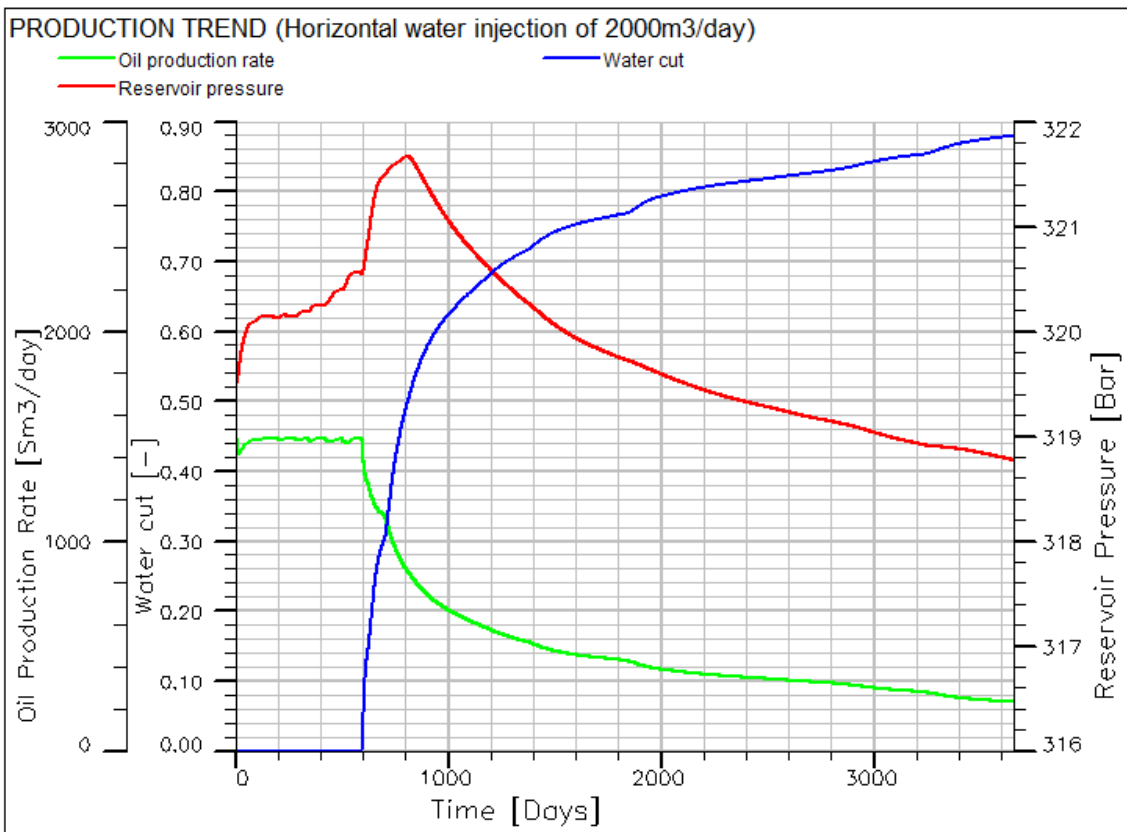


Figure 6-33 Production trend for water injection of 2000m³/day (heterogeneous)

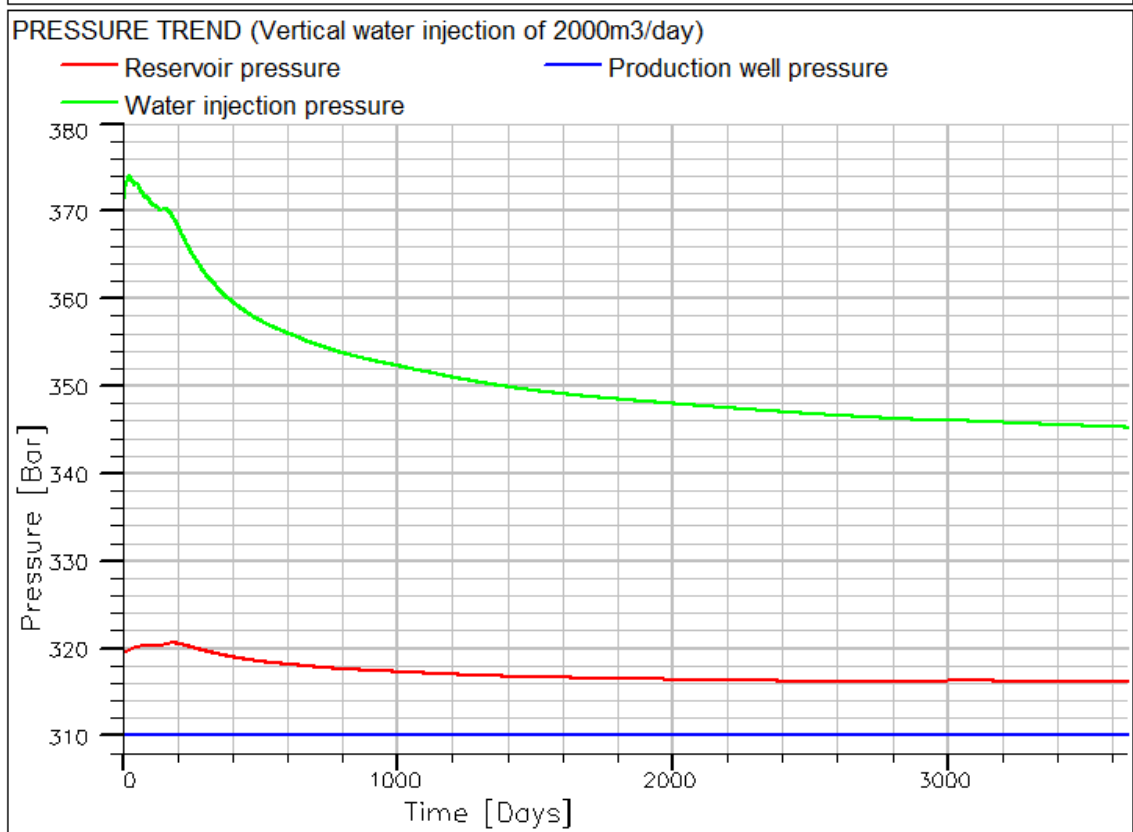
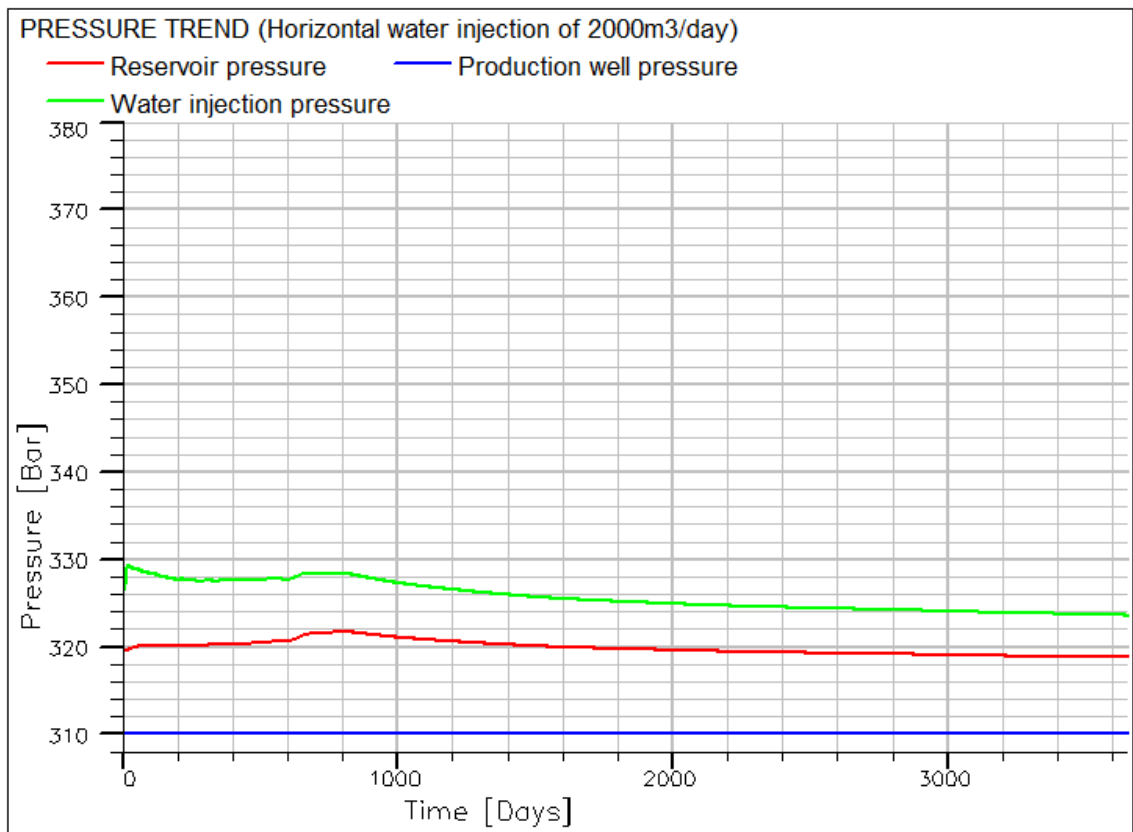


Figure 6-34 Pressure trend for water injection of 2000m³/day (heterogeneous)

6.2.6 Result at water injection of 2500m³/day (Heterogeneous)

Figure 6-35 shows how the oil production rate, water cut and reservoir pressure change with time at water injection rate of 2500m³/day. For the horizontal case, oil production rate increases from 2399 m³/day to about 1850m³/day at 110th day. This rate is maintained for almost one year until further decrease at the 462nd day due to water breakthrough. The oil production rate for the horizontal case is about 1856m³/day at the end of the 3653rd day. For the vertical injection, oil production rate increases to a maximum of 1850.23m³/day just before water breakthrough. The oil production rate for the vertical injection is about 311.66m³/day at the end of the 3653rd day. Water breakthrough time is about 462 days for the horizontal injection and the 108 days for the vertical case. At end of the 3653rd day, the water cut is 0.90 for the horizontal case and 0.87 for the vertical case.

Figure 6-35 also shows an increase in the reservoir pressure to about 322.92bar at the 462nd day for horizontal case and 322.47bar at the 108th day for vertical case due to water injection. For the two cases, it was observed that the reservoir pressure increased sharply immediately after water breakthrough due to the propagation of water wave. The final reservoir pressure at the end of 3653 days is about 320.29bar for the horizontal case and 317.26bar for the vertical case. From figure 6-36, it can be shown that an average drawdown pressure of about 12bar is achieved through horizontal water injection while approximately 9bar is achieved with vertical water injection. Figure 6-36 also shows that lower injection differential pressure of 8bar is required for the horizontal injection while the vertical injection requires higher differential injection pressure of 50bar.

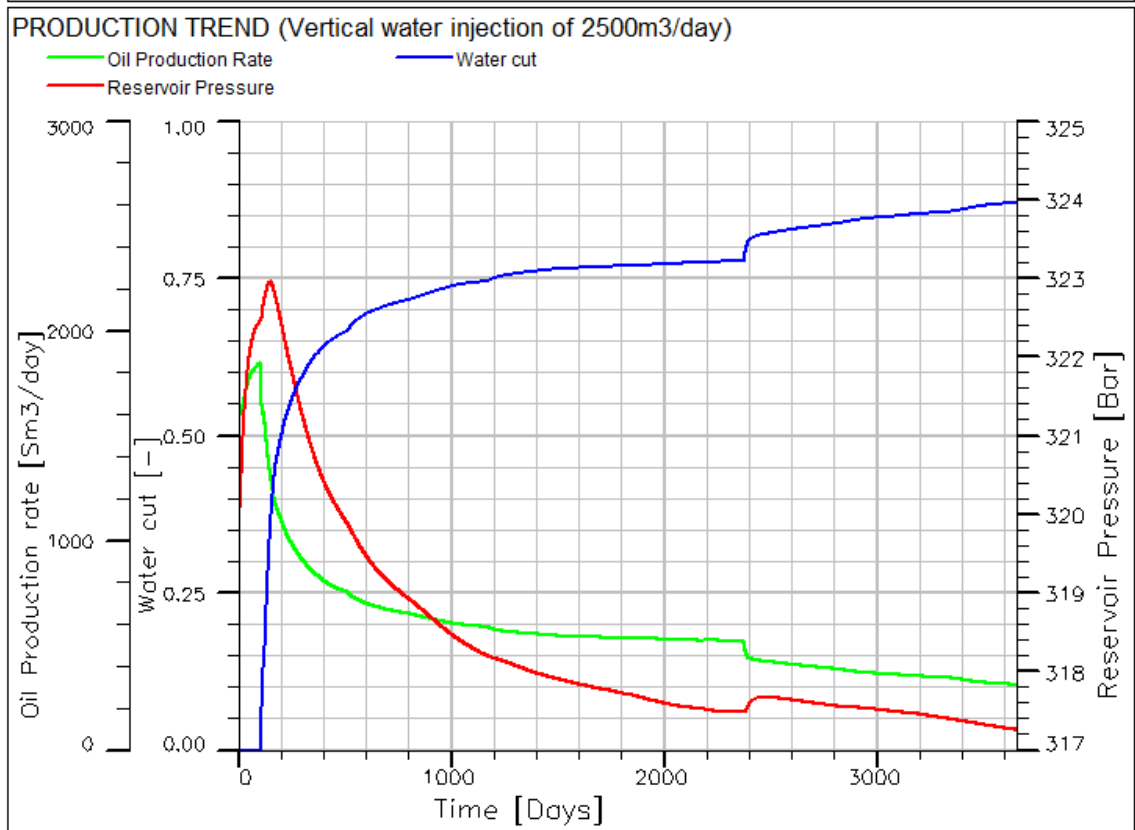
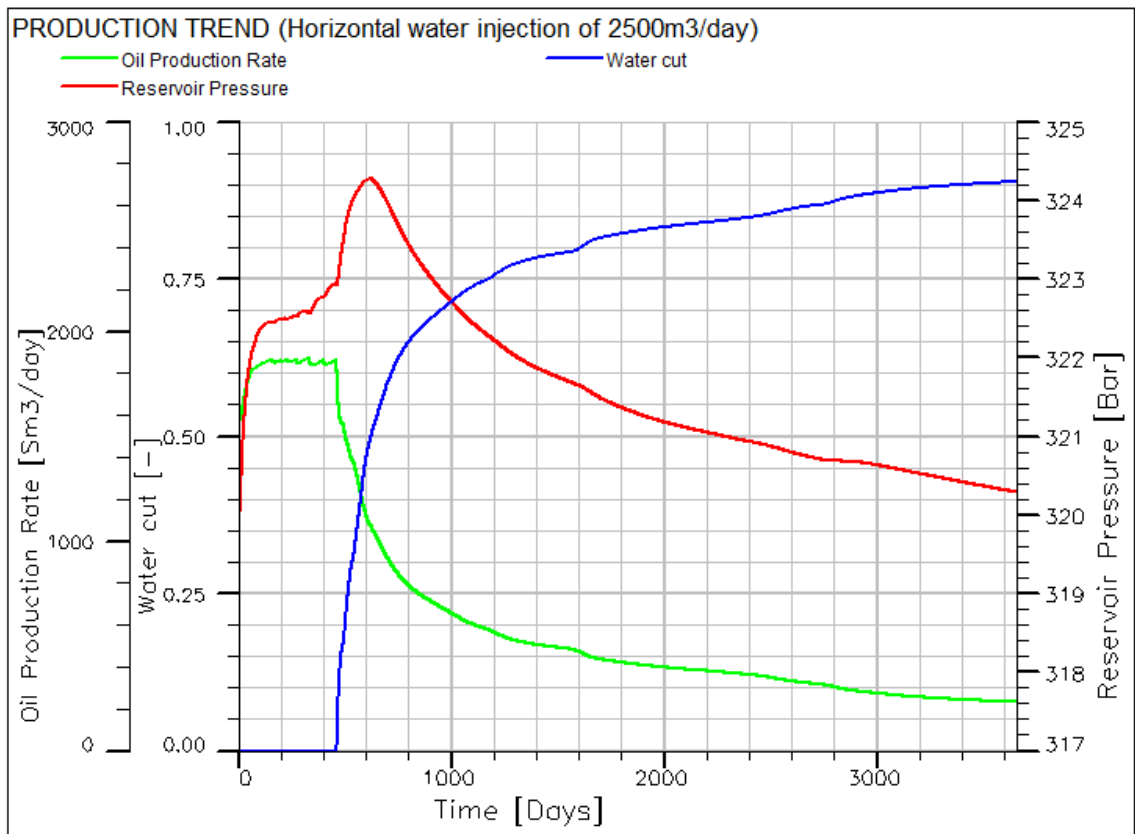


Figure 6-35 Production trend for water injection of 2500m³/day (heterogeneous)

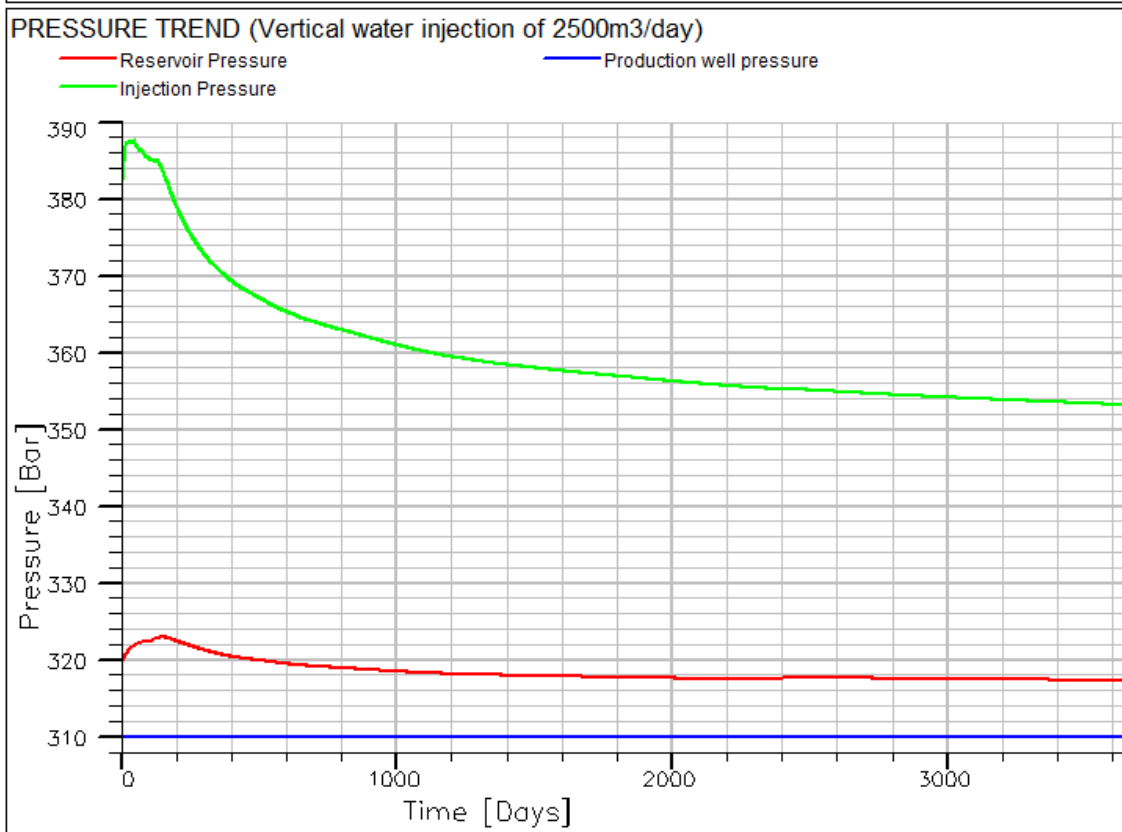
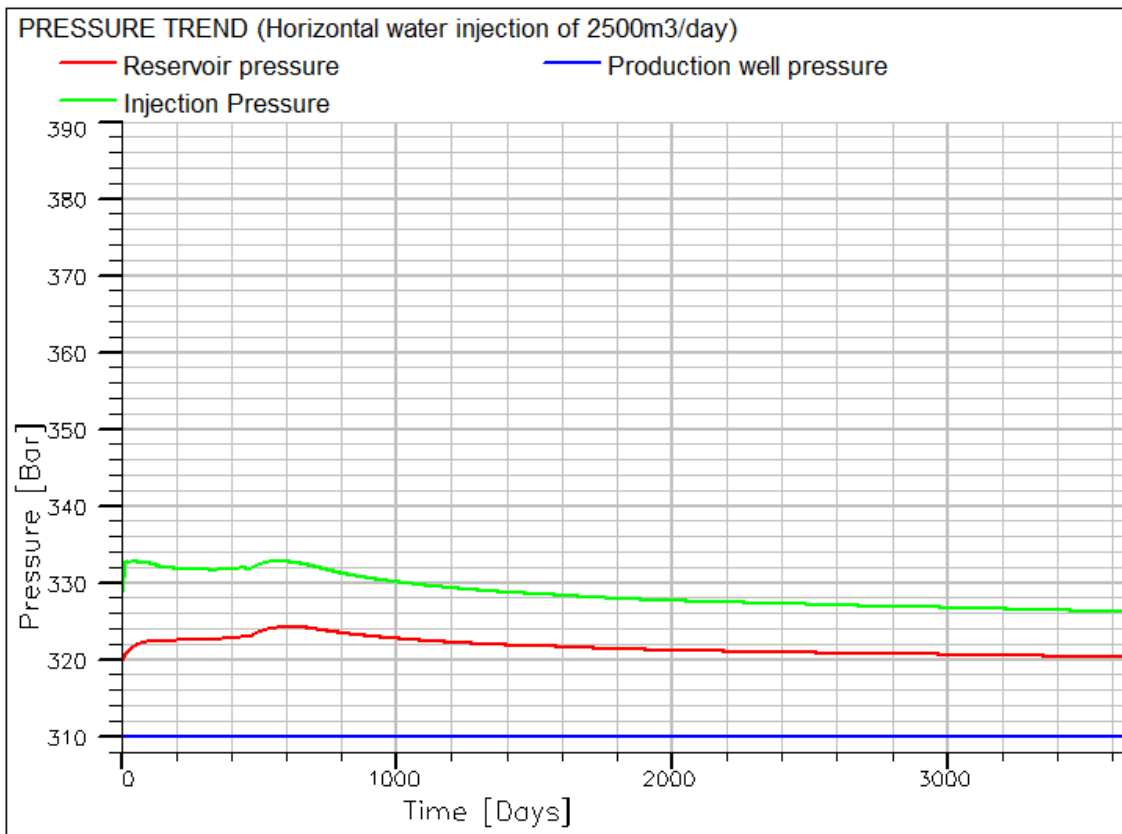


Figure 6-36 Pressure trend for water injection of 2500m³/day (heterogeneous)

6.2.7 Overall pressure trend (Heterogeneous)

Figure 6-37 shows the simulated reservoir pressure trend.

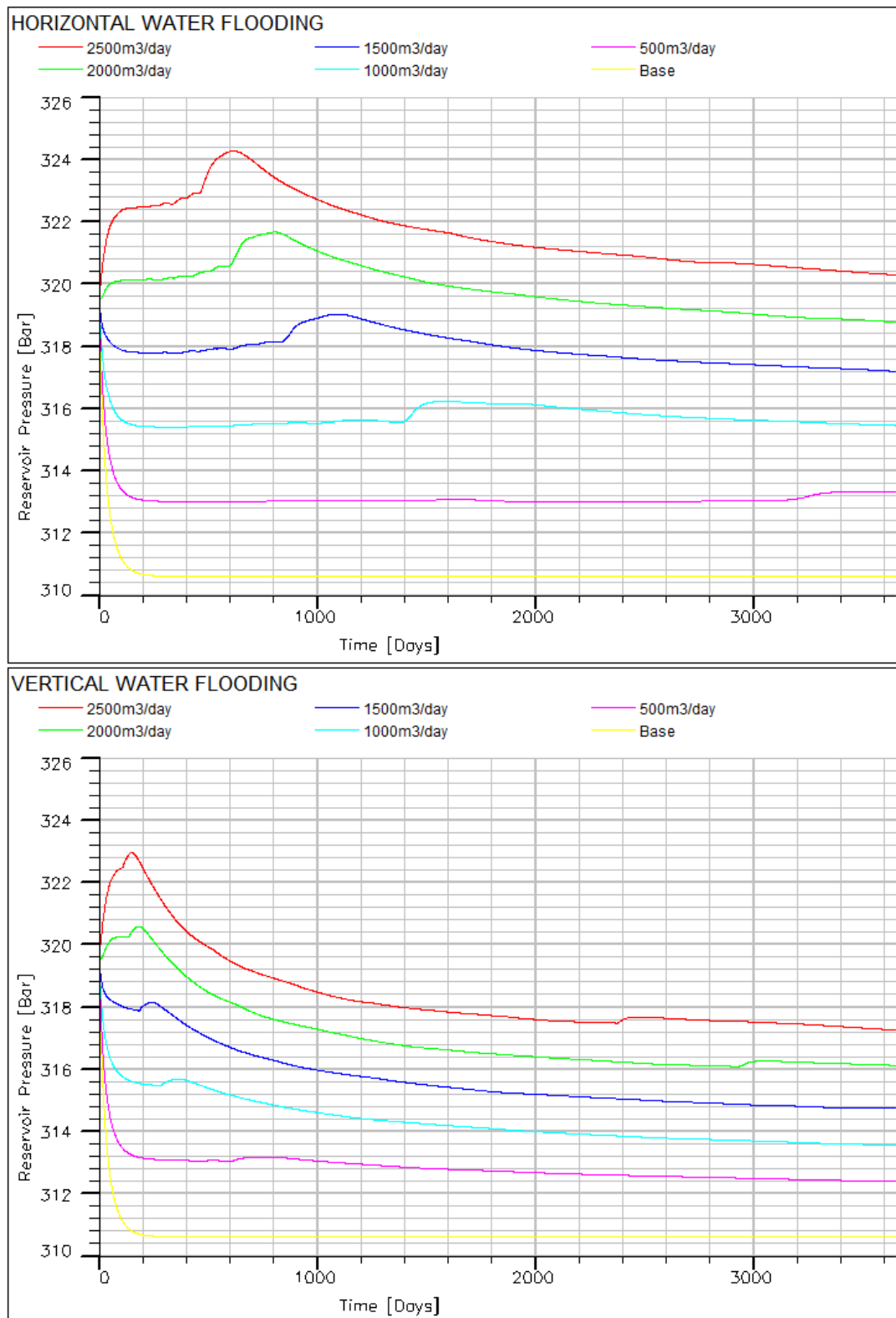


Figure 6-37 Overall reservoir pressure trend (heterogeneous)

For water injection rates between 500m³/day and 2000m³/day, the reservoir pressure drop with horizontal injection is between 10% and 63% less than that of the vertical case. For injection rates of 2500m³/day, the reservoir pressure rather increased by 0.29bar after 10year unlike the vertical case with about 2.74bar pressure drop. General observation shows that with horizontal injection, higher reservoir pressure is maintained with the horizontal case than the vertical case. This is because of the gravitational pressure drop with the vertical arrangement which does not affect the horizontal injection. Also lower flow velocity is obtained with horizontal injection due to several perforations unlike the vertical injection with one opening for the same injection flow rate. With less flow velocity of the horizontal injection, frictional pressure loss would be less than the case of vertical injection. This phenomenon also accounts for the higher injection pressure with the vertical injection compared with the horizontal injection as can be shown in figure 6-38.

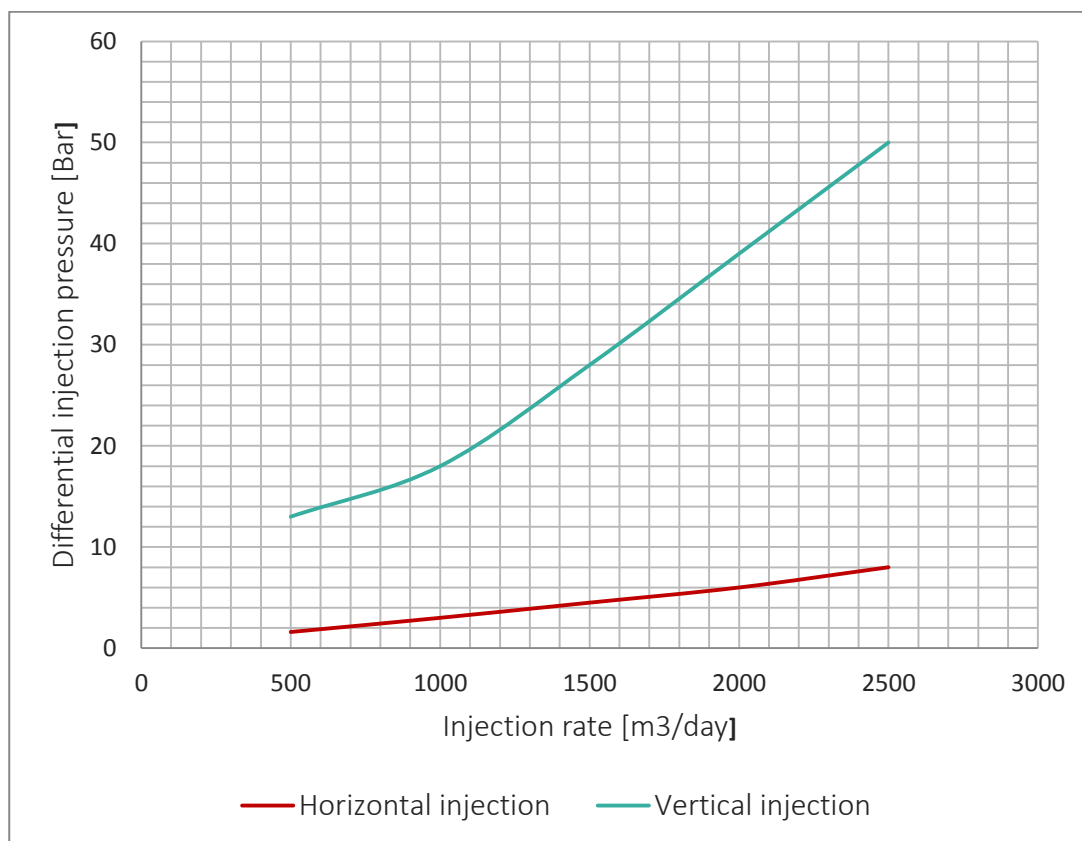


Figure 6-38 Plot of differential injection pressure against injection rate (heterogeneous)

From figure 6-38 it can be shown be shown that the injection differential required is about 83% and 87% less with horizontal injection than vertical injection. This implies

that less energy and cost is required for horizontal waterflooding than the vertical arrangement. Result also reveals that the drawdown pressure achieved through waterflooding using horizontal injection is higher between 11% and 36% compared with the vertical injection case. The highest percentage increase in the drawdown pressure was observed with injection rate of $2000\text{m}^3/\text{day}$.

6.2.8 Overall water cut (Heterogeneous)

The water cut trend is shown in Figure 6-39. Originally, water is in chemical equilibrium with oil and gas phases at the original temperature and pressure in the reservoir. With oil and gas production, the reservoir pressure and temperature changes thus perturbing the chemical equilibrium.

From the result, it is observed that water breakthrough is delayed between 354 days to 2543 days with horizontal case compared with the vertical case. This delay in water breakthrough could be attributed to less flow velocity with horizontal injection compared with the vertical injection. With this, it takes longer time to push water into the production well for the horizontal injection compared with the vertical injection. The trend shows that higher delay is water breakthrough is achieved with lower water injection rates. Between $500\text{m}^3/\text{day}$ and $1000\text{m}^3/\text{day}$ injection rate, water cut at the 3653rd day was lower with the horizontal case may be due to flow restrictions. At higher injection from $1500\text{m}^3/\text{day}$, the water cut after 3653 days is higher using horizontal flooding. This may be attributed to the higher drawdown pressure and higher influx from multiple perforations of the horizontal injection well compared with vertical injection.

This result conforms with theoretical relative permeability trend for multi-phase flow. The increase in water production is a consequence of the relative permeability behavior. With oil recovery, the saturation of oil in the reservoir decreases while the water saturation increases. This causes the relative permeability of oil to decrease while relative permeability of water increases. According to Darcy law, volumetric water flow of water in the reservoir continues to increase with the increase in the relative permeability increases. Eventually water starts flowing into the production well when

the water saturation is above the irreducible water saturation. From the result, volumetric flow rate of water supersedes that of oil very soon after water breakthrough, and continues to increase till the end time of the simulation. This is because water viscosity is lower than oil viscosity making water to flow more into the production well.

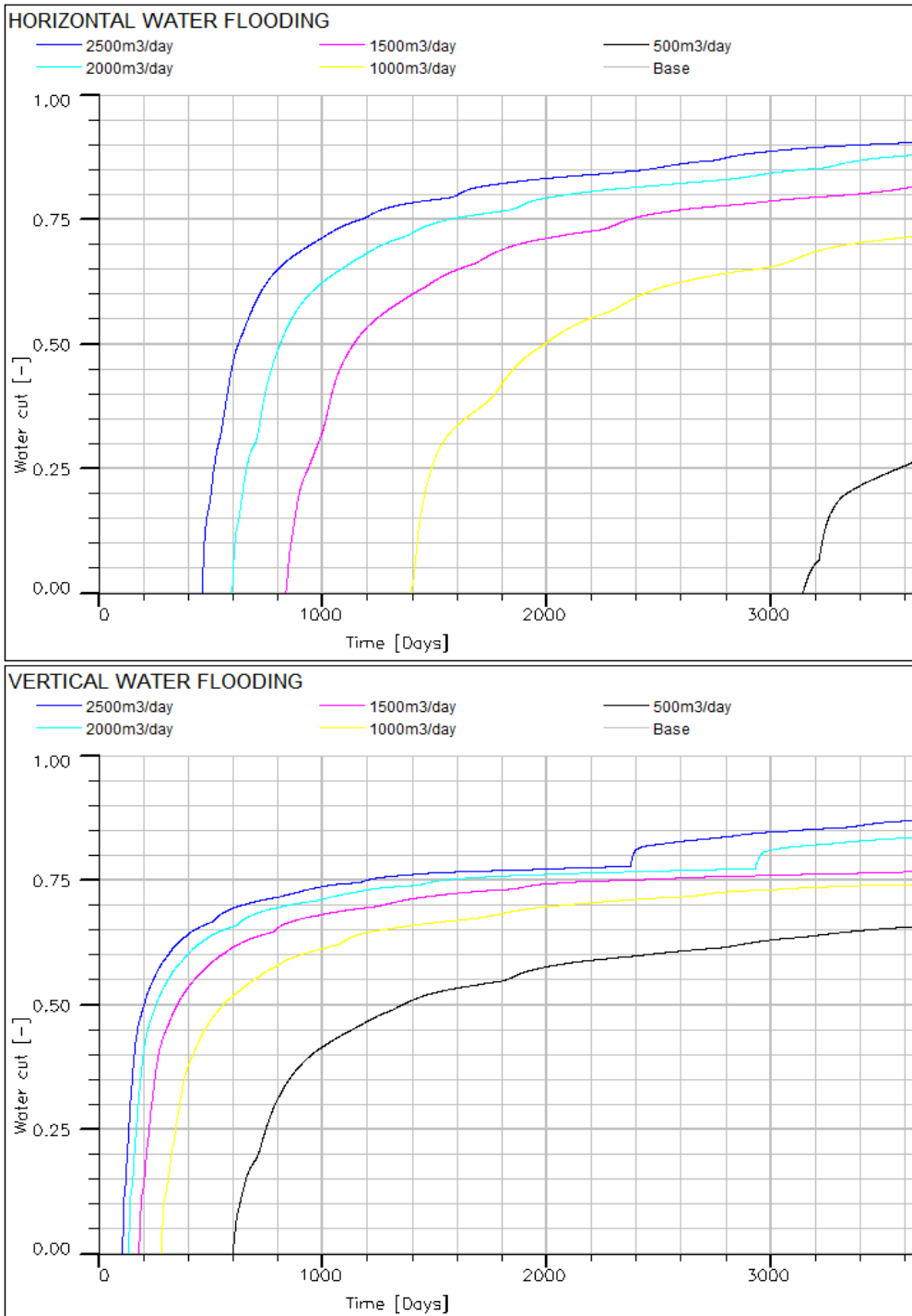


Figure 6-39 Overall water cut trend (heterogeneous)

6.2.9 Overall oil production rate (Heterogeneous)

The overall plot of the oil production rate for horizontal and vertical water injection is shown in figure 6-40.

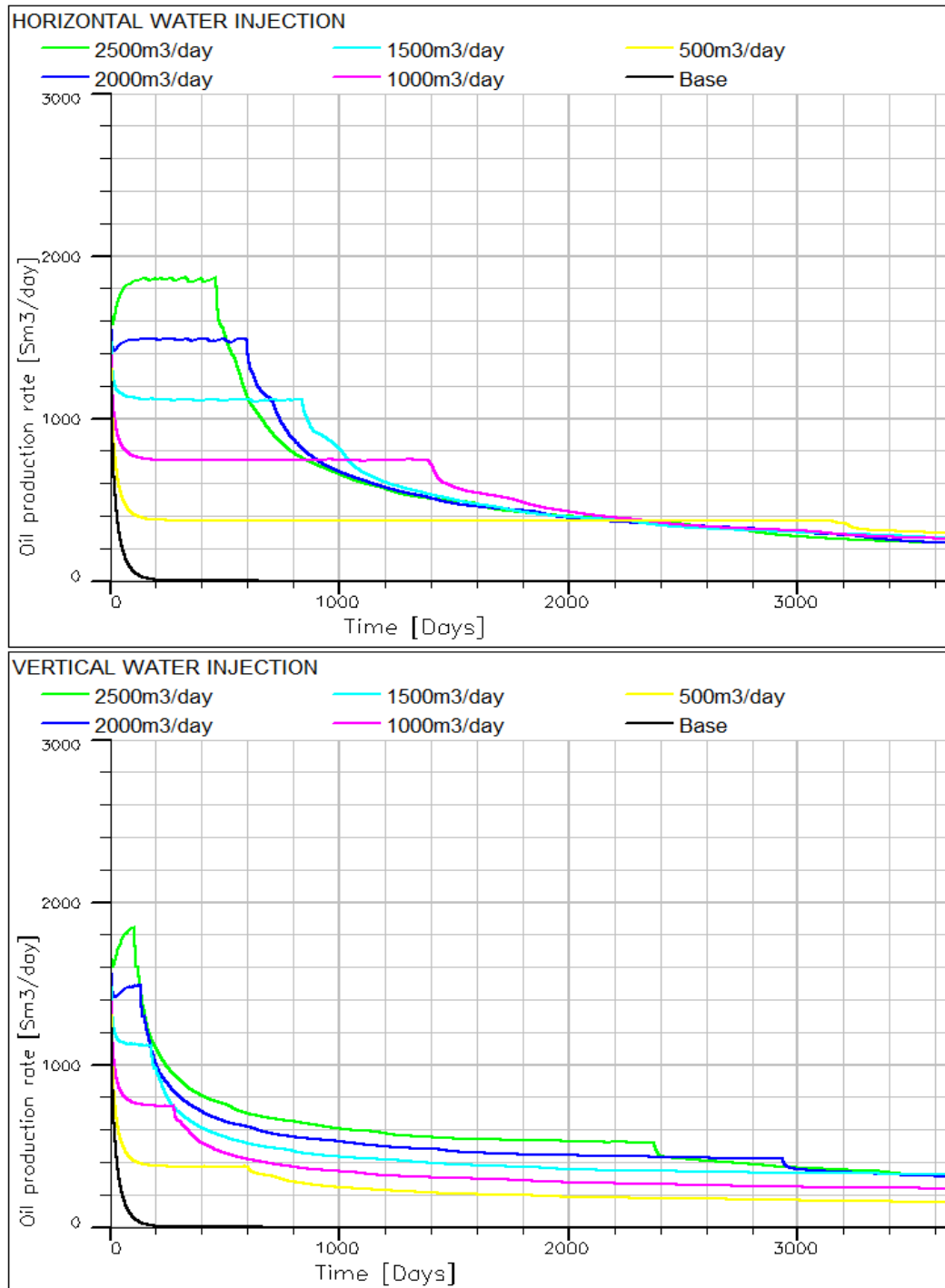


Figure 6-40 Overall oil production rate (heterogeneous)

Figure 6-40 shows the oil production rate for horizontal and vertical water injection respectively. At the beginning, the flow rate is maintained at constant level until the breakthrough occurs. Thereafter the oil flow rate decreased and the flow rate starts to fluctuate with time. This fluctuations is due to the multiphase flow after the breakthrough. This can be explained using the concept of relative permeability and Darcy's law for multiphase flow. With waterbreak through, the oil saturation reduces while water saturation increases. This reduces the relative permeability and flow rate of oil in the reservoir. Volumetric flow rate also depends on the the viscosities of each component. With oil having more viscosity values than water and gas, the flow rate would reduce after breakthrough. The result shows that horizontal waterflooding maintains higher oil production rate for a longer period until water breaks through. After water breakthrough, the production rate drops more for horizontal waterflooding than the vertical case. For both cases, oil production rate is at a maximum just before water breakthrough. The production rate for the base case is very low compared to the cases with waterflooding. This is in agreement that waterflooding improve the oil production rate [6].

6.2.10 Accumulated oil production

Figure 6-41 shows the accumulated oil production trend for the horizontal and vertical waterflooding. The plot shows that the accumulated oil production with horizontal flooding is higher for in all cases. This may be attributed to the higher drawdown pressure achieved. The plot of the recovery factor against injection rate shown in Figure 6-42 indicates that the recovery factor with horizontal waterflooding is higher than the vertical waterflooding. The curves shows that the more the injection rate, the more recovery factor.

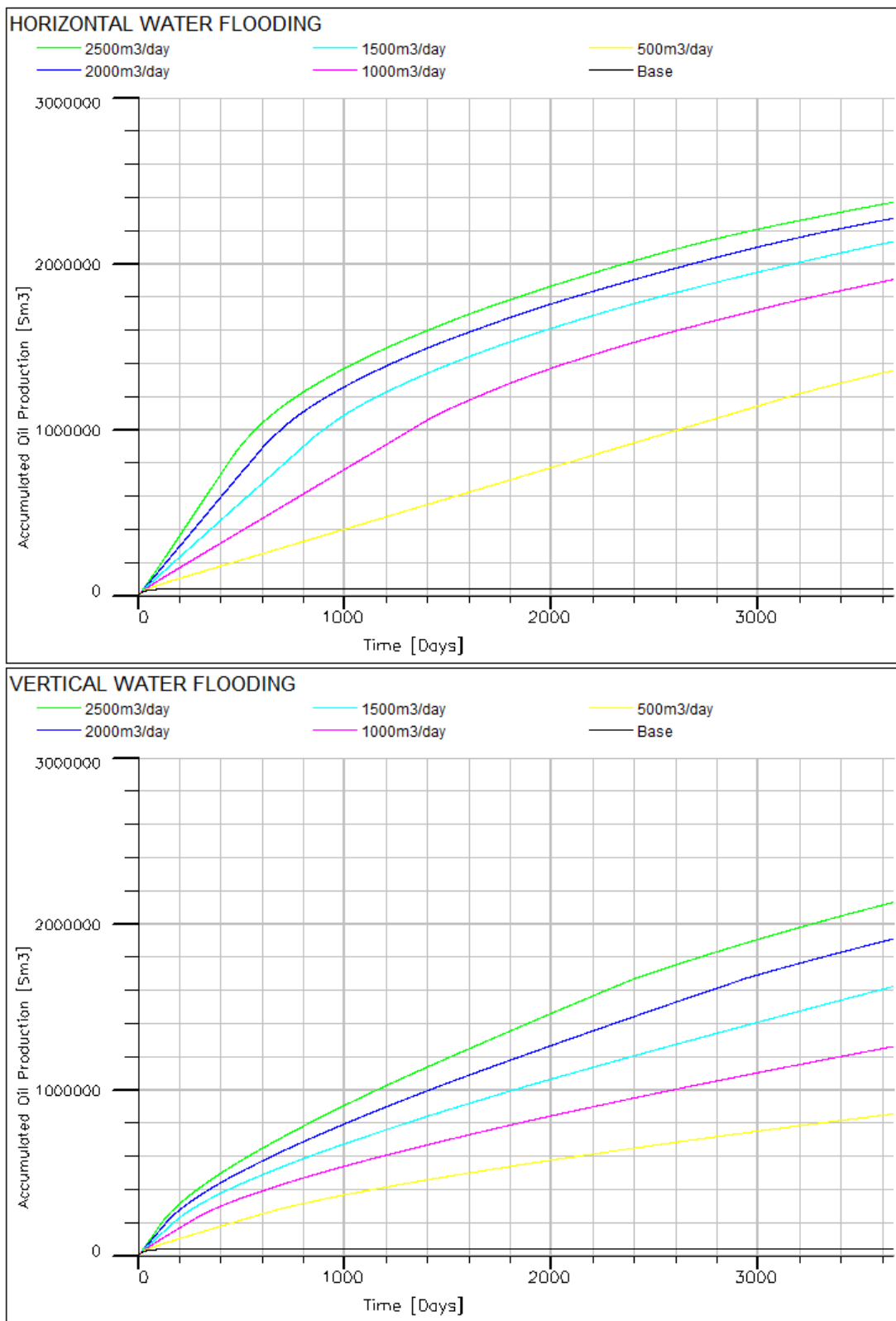


Figure 6-41 Accumulated oil production (heterogeneous)

Annex 8 shows how oil saturation distribution in the reservoir over the simulation period for a given water injection rate for both cases. See Annex 3 for summary of results.

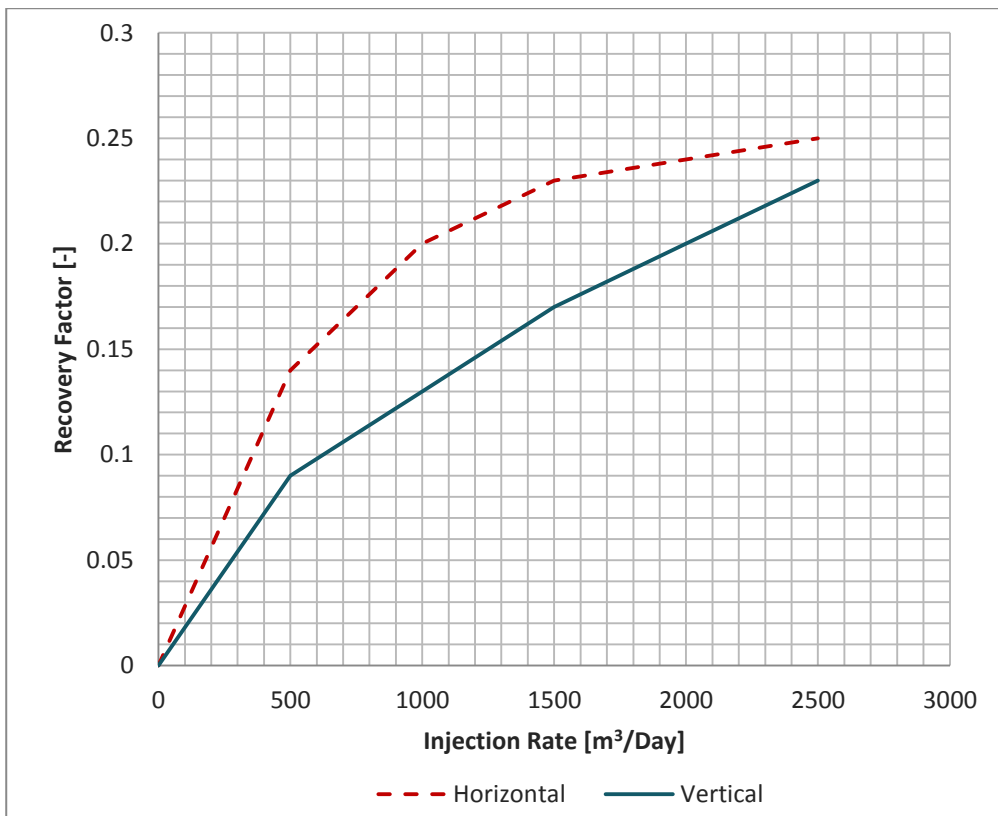


Figure 6-42 Overall recovery factor (heterogeneous)

6.2.11 Gas production

The overall plot of gas production rate and accumulated gas production for horizontal and vertical water injection are shown in figure 6-43 and figure 6-44 respectively. Figure 6-43 shows that horizontal waterflooding maintains higher gas production rate for a longer period. After water breakthrough, gas production rate drops more rapidly for horizontal waterflooding than the vertical case. This may be attributed to higher drawdown pressure and influx for the horizontal injection as opposed to the vertical case. For both cases, gas production rate is at a maximum just before water breakthrough. The production rate for the base case is very low compared to the cases with waterflooding. Figure 6-44 shows that the accumulated gas production with horizontal waterflooding is higher in all cases compared with the vertical waterflooding.

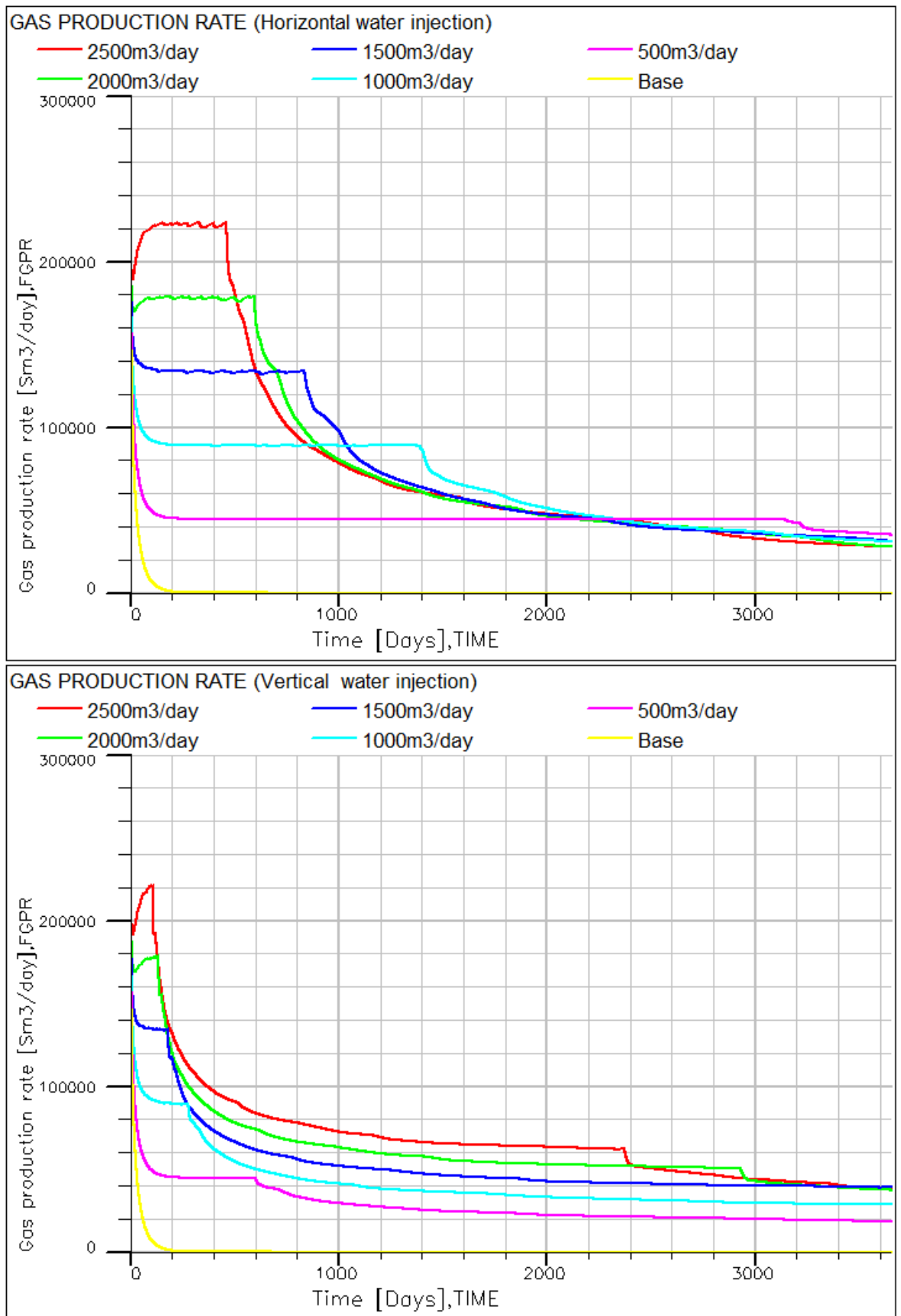


Figure 6-43 Gas production rate (heterogeneous)

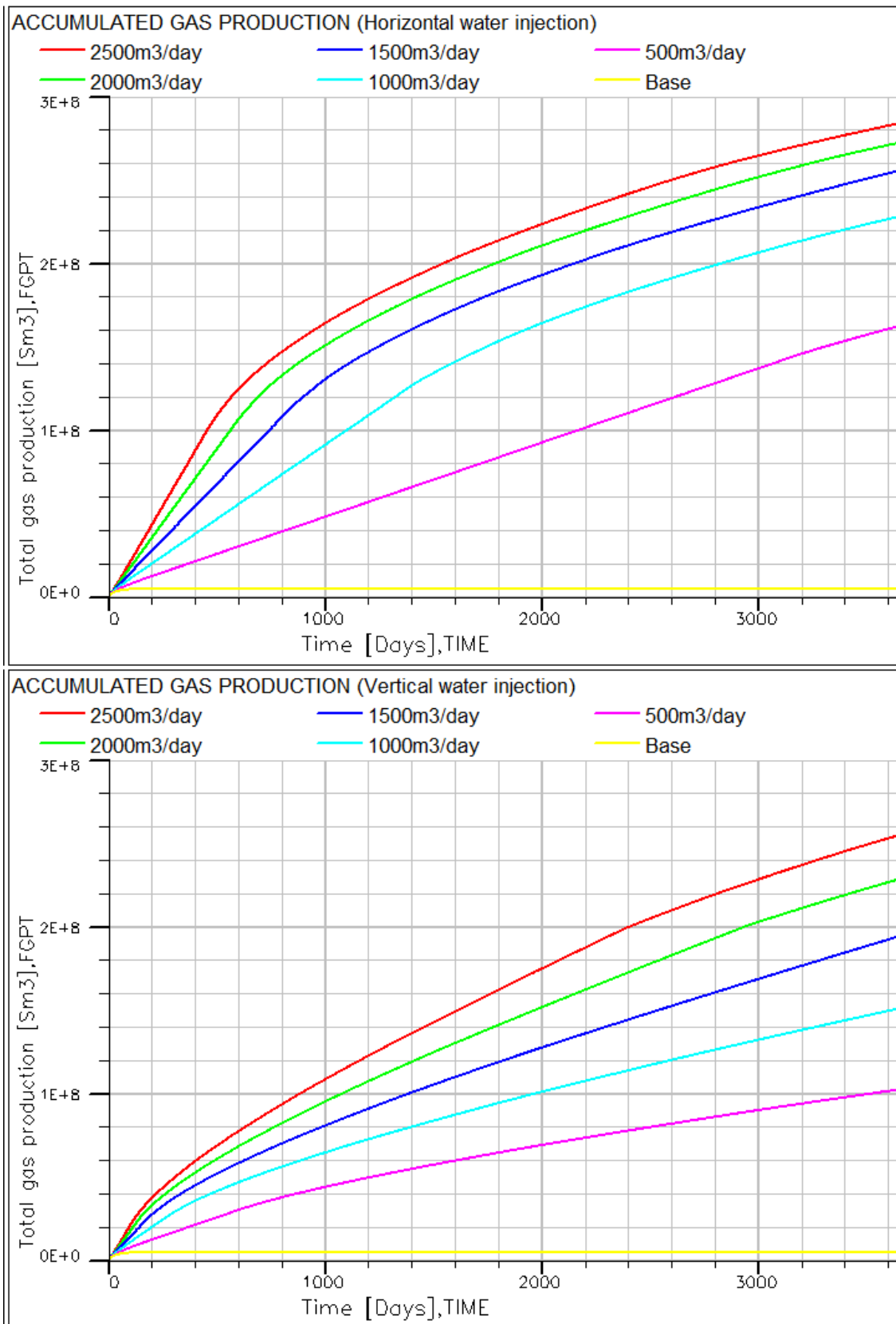


Figure 6-44 Accumulated gas production (heterogeneous)

6.3 Application of ICD

In this simulation, the effect of ICD completion on oil, water and gas production was investigated. Also the reservoir pressure trend recovery was discussed. A base case without ICD completion was considered as reference.

6.3.1 Reservoir pressure

Figure 6-45 shows the simulated reservoir pressure trend. The ratio of the total pressure drop without ICD completion to the total pressure drop with ICD is about 52. The high pressure drop for the case without ICD may be due to more reservoir depletion as a result of high water production. ICD tends to maintain the reservoir pressure by retaining water in the reservoir pore spaces.

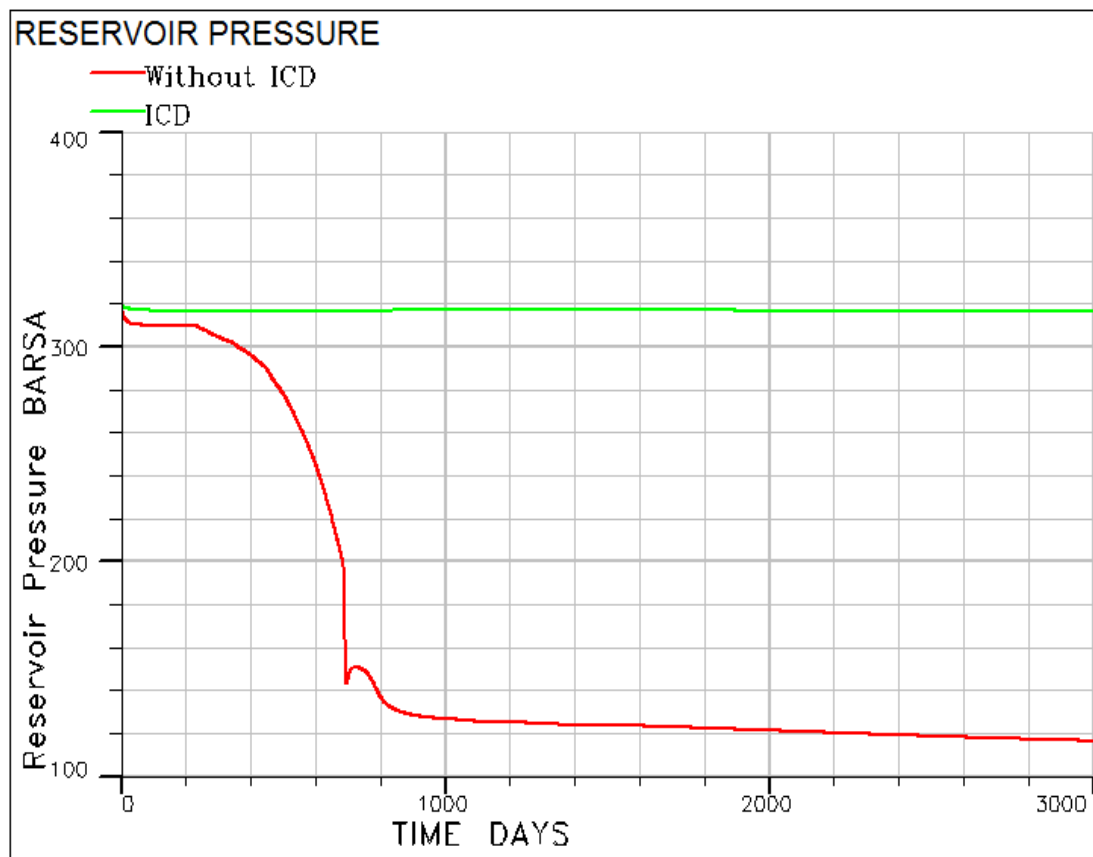


Figure 6-45 Reservoir Pressure Trend (ICD)

6.3.2 Water production

The water cut trend is shown in Figure 6-46. It is observed that water breakthrough is delayed for 262 days (about 66%) with the installation of ICD. Also the water cut is

reduced with about 11% after 3000 days with the ICD completion. This would be attributed to the restriction imposed on water flow due to the additional pressure drop with the ICD.

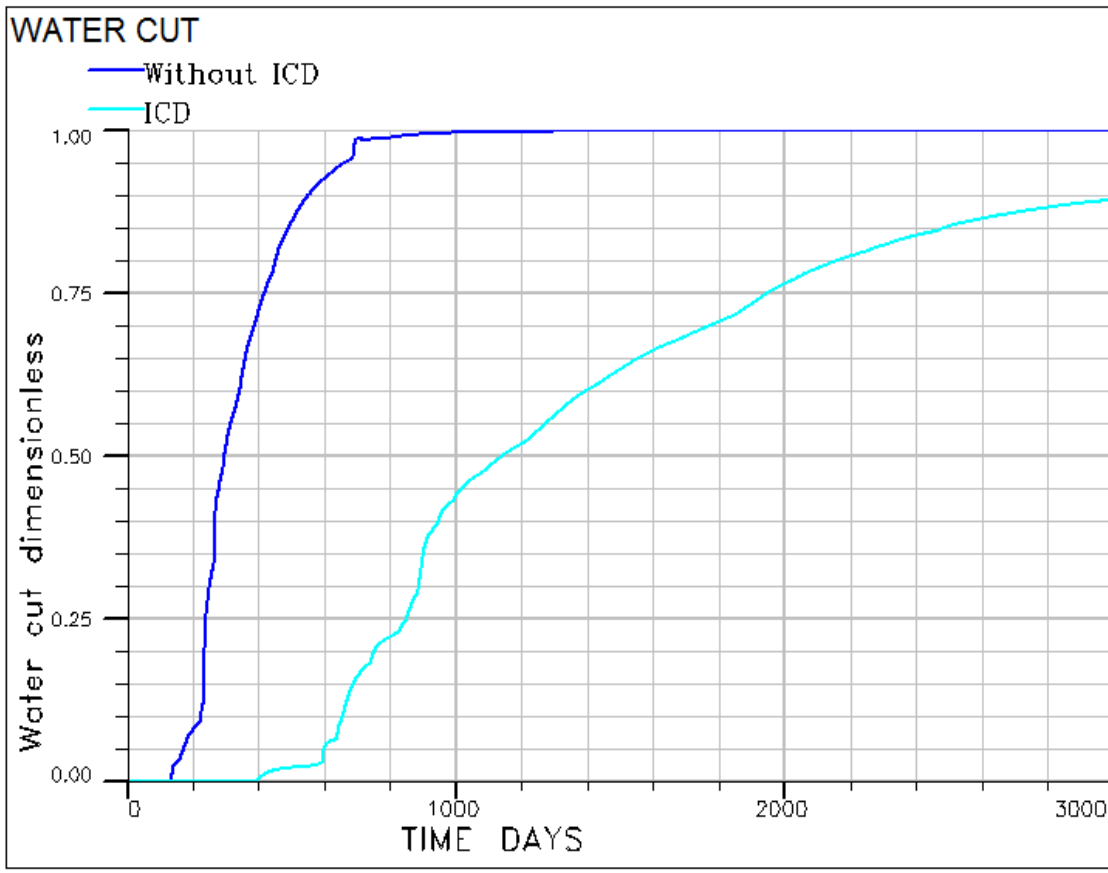


Figure 6-46 Trend of water cut

6.3.3 Oil Production

Figure 6-47 shows the oil production rate with and without ICD respectively. Although the water breakthrough is delayed with ICD, the oil production rate is lower compared with the case without ICD. After water breakthrough, the production rate drops more rapidly for the case without ICD. This may be attributed to rapid water production as there is no restriction towards water production. Shock wave was propagated at about 690th day due to sudden opening of valve to match up the production target for the case without ICD. This shock wave can lead to very high pressure buildup which could make the system to fail. With the ICD, this phenomenon is annulled through its equalization effect on flow variation making the system stable throughout the production life.

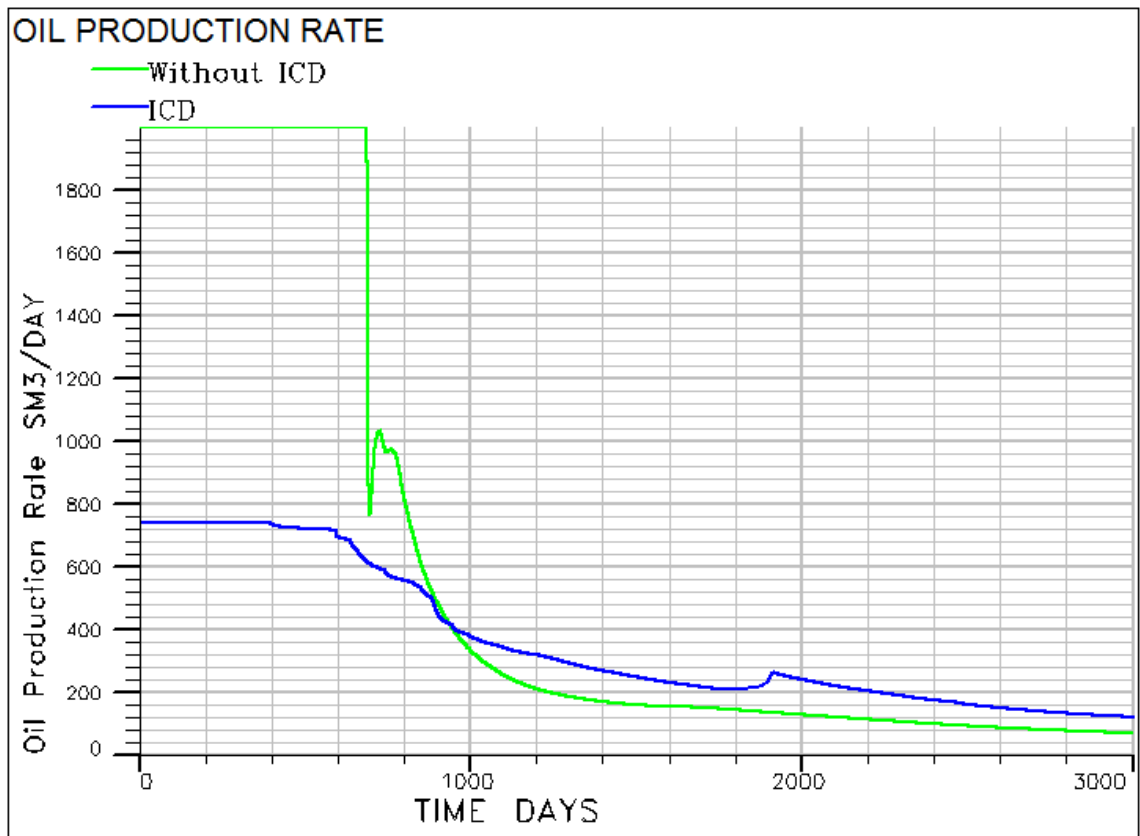


Figure 6-47 Trend of oil production rate

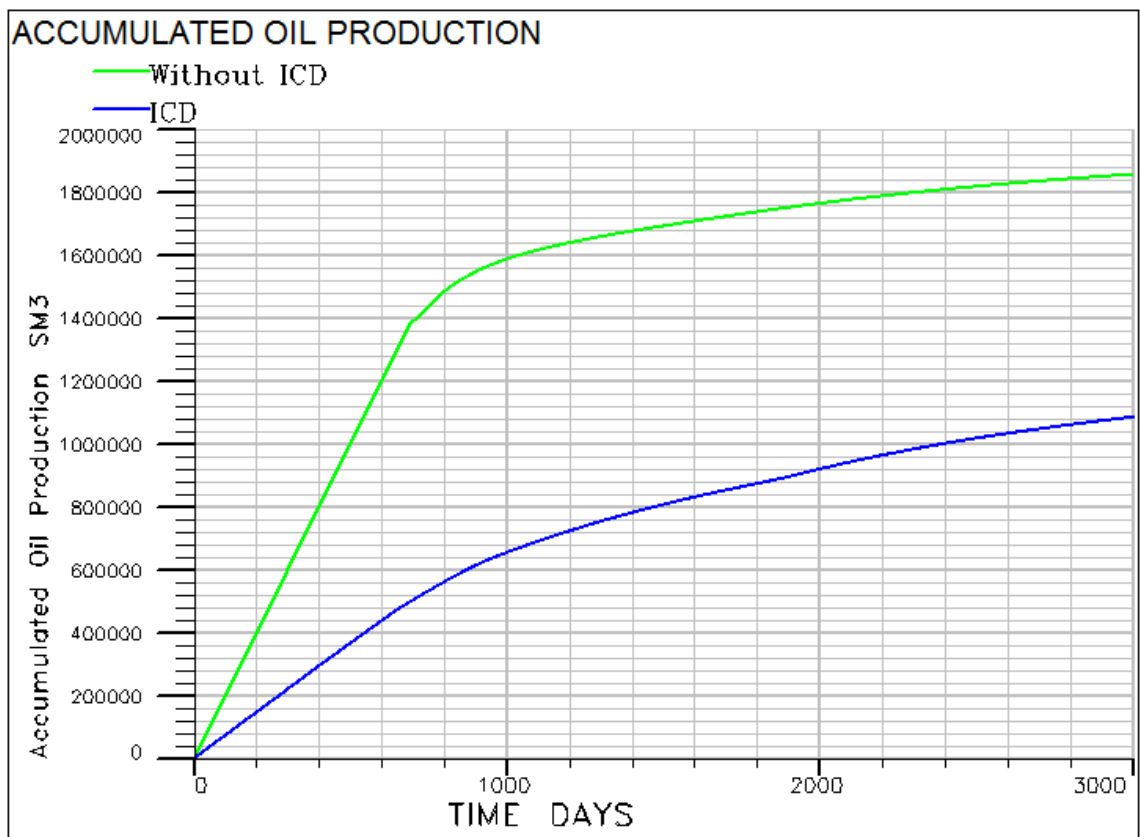


Figure 6-48 Trend of accumulated oil production

Although well productivity is reduced by approximately 42%, there is an improved degree of inflow equalization through ICD completion. The accumulated oil production is shown in Figure 6-48. From the slope, production would be sustained more and the accumulated oil production expected to be higher over a long time with ICD completion.

6.3.4 Gas Production

Figure 6-49 shows the gas production rate with ICD and without ICD completions respectively.

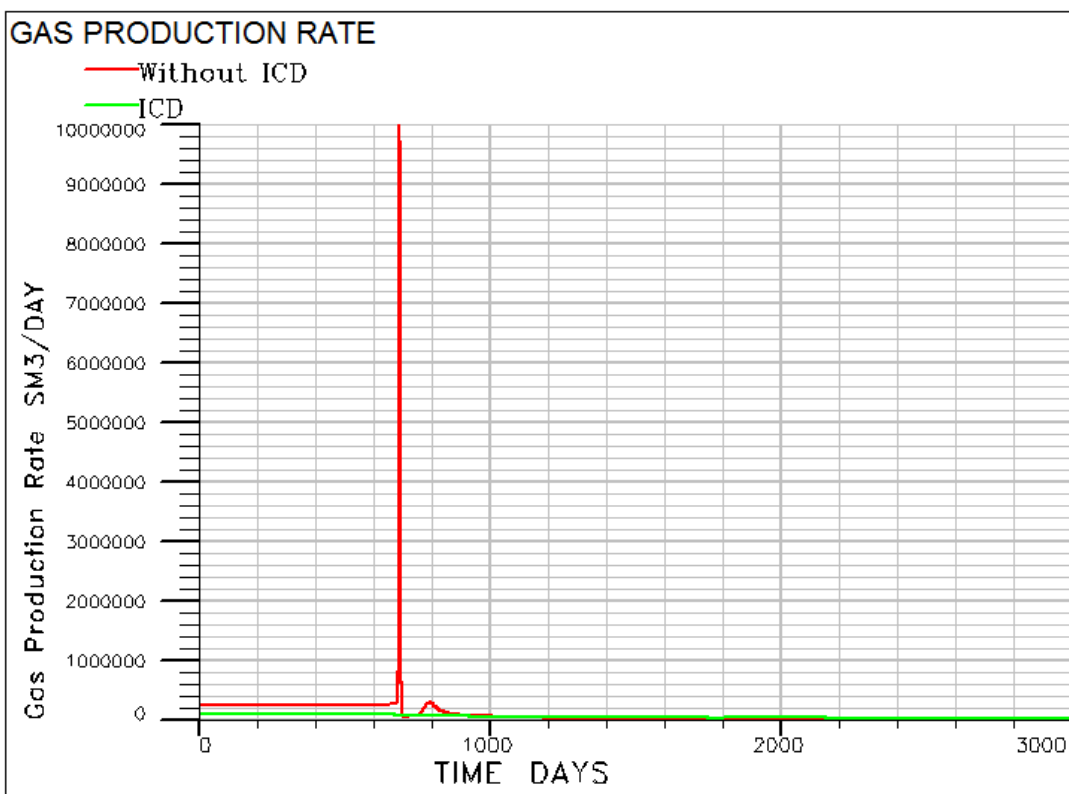


Figure 6-49 Trend of gas production rate

It can be seen that gas production rate is less with ICD completion throughout the production life. This may be attributed to rapid water production in the case without ICD as there is no restriction towards water production. Shock wave was propagated at about 690th day due to sudden opening of valve to match up production target for the case without ICD. This shock wave can lead to system failure as result of high pressure. This shock effect is not observed with ICD completion due to the restriction imposed by additional pressure drop and the equalization effect on flow variation.

With ICD completion, the system is stable throughout the production life. There is about 51% decrease in gas production as depicted in figure 6-50 with ICD completion. This increase in gas production for the case without ICD may reduce well performance and recovery significantly as oppose to ICD completion.

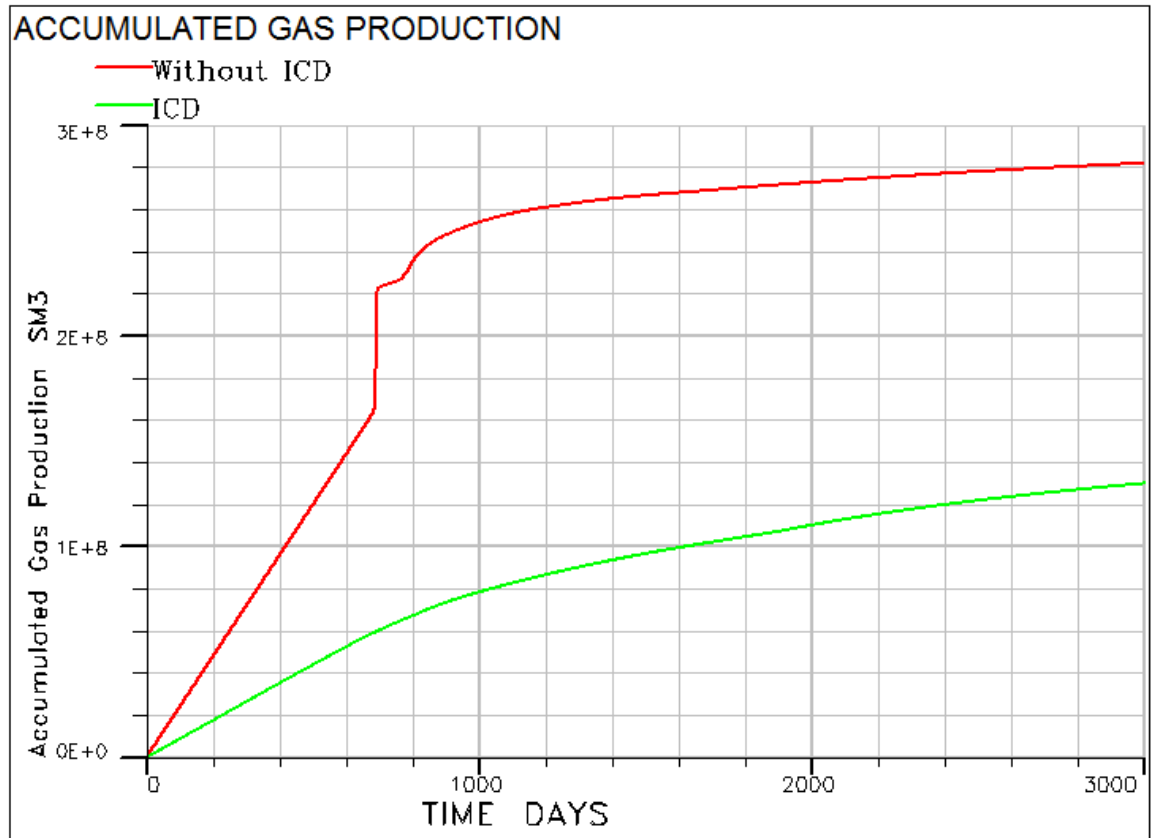


Figure 6-50 Trend of the accumulated gas production

7 Conclusion

This research was carried out to study the effect of waterflooding and inflow control device on oil recovery. Also the study CO₂ storage in oil/gas reservoirs and aquifers was covered.

For the waterflooding, analysis of pressure, water cut, oil and gas production was carried out between horizontal and vertical waterflooding. Simulation was performed over ten years (3653 days) using ECLIPSE Reservoir simulator for homogeneous and heterogeneous reservoir. Result shows that horizontal waterflooding maintains higher reservoir pressure maybe due to less frictional pressure drop and no effect of gravity. With less pressure drop, the injection pressure for horizontal waterflooding could be up to 96% less than that of the vertical waterflooding. This would imply lower operation cost and energy using using horizontal injection. Result also reveals that higher oil recovery is achieved with the horizontal injection in heterogeneous reservoirs. Also the results shows that more gas is produced with the horizontal flooding. From the result, water breakthrough could be delay with horizontal injection up to 1362 days. Despite the delay in water breakthrough, horizontal flooding accounts more water production. With the implementation of inflow control device to reduce water and gas production, oil recovery through horizontal waterflooding would more effective than vertical waterflooding.

Mathematical models used for the implementation of ICD in ECLIPSE reservoir simulator were studied. A case study using similar reservoir conditions as Troll offshore Norway was simulated to illustrate the effect of ICD in a heterogeneous reservoir. Analysis of oil, water and gas production was made within a simulation period of 3000 days. Result shows that with ICD completion, water breakthrough was delayed with 262 day and water cut after 3000 days was reduced by 11%. Despite the delay in water breakthrough, the oil production rate was reduced due to flow restriction by additional pressure drop with ICD completion. A trade-off between well productivity and inflow equalization is important. Although well productivity is reduced by approximately 42%, there is an improved degree of inflow equalization through ICD completion. Gas production was decreased by approximately 51% with ICD completion. With this reduction in gas production, well performance and ultimate recovery would improve.

Result also indicates that the case with ICD completion sustains the reservoir pressure as water is forced to occupy the pore spaces of the reservoir. It can be inferred that although ICD delays water and gas breakthrough, it could not stop the breakthrough. It would be appropriate to apply autonomous inflow control device instead, to stop gas and water breakthrough.

Finally, the literature study carried out on storage capacity and suitability of CO₂ storage in oil/gas reservoirs and aquifers. The study shows that the physical trapping mechanism could have more contribution in CO₂ storage than chemical trapping mechanism.

This thesis is not to some extent exhaustive due to limited resources and time constraints. The following areas are therefore recommended for future work:

- Provision of license for the simulation of CO₂ EOR and storage.
- Access to more reservoir details for more realistic simulations.
- Comparison of the simulated results with experiment data to validate claims.
- PVT analysis and modeling of reservoir fluid should be incorporated for more realistic models.
- Provision of Near Wellbore license for the implementation of advanced completions and improvement of the wellbore flow.
- Provision of flux boundary license for the implementation of pressure and flux boundary conditions.
- More simulations to study the effect of other inflow control devices for gas and water breakthrough.

References

- [1] T. A. Jelmert, N. Chang, L. Høier, S. Pwaga, C. Iluore, Ø. Hundseth, *et al.*, "Comparative Study of Different EOR Methods," *Norwegian University of Science & Technology, Trondheim, Norway*, 2010.
- [2] T. Ellis, A. Erkal, G. Goh, T. Jokela, S. Kvernstuen, E. Leung, *et al.*, "Inflow Control Devices—Raising Profiles," *Oilfield Review*, vol. 21, pp. 30-37, 2009.
- [3] D. Krinis, D. E. Hembling, N. J. Al-Dawood, S. A. Al-Qatari, S. Simonian, and G. Salerno, "SS-Optimizing Horizontal Well Performance In Non-Uniform Pressure Environments Using Passive Inflow Control Devices," in *Offshore Technology Conference*, 2009.
- [4] I. S. A. E. Outlook, "International Energy Agency (IEA)," *Organisation for Economic Cooperation and Development (OECD): Paris, France*, 2013.
- [5] G. E. P. LLC. (2016). *Waterflooding*. Available: <http://www.gtnenergypartners.com/technology/waterflooding>
- [6] N. Morrow and J. Buckley, "Improved oil recovery by low-salinity waterflooding," *Journal of Petroleum Technology*, vol. 63, pp. 106-112, 2011.
- [7] G. Van Essen, M. Zandvliet, J. Jansen, D. Hof, P. M. Van, and O. Bosgra, "Robust optimization of oil reservoir flooding," in *Computer Aided Control System Design, 2006 IEEE International Conference on Control Applications, 2006 IEEE International Symposium on Intelligent Control, 2006 IEEE*, 2006, pp. 699-704.
- [8] W. Bangerth, H. Klie, M. Wheeler, P. Stoffa, and M. Sen, "On optimization algorithms for the reservoir oil well placement problem," *Computational Geosciences*, vol. 10, pp. 303-319, 2006.
- [9] M. Zandvliet, M. Handels, G. van Essen, R. Brouwer, and J.-D. Jansen, "Adjoint-based well-placement optimization under production constraints," *SPE Journal*, vol. 13, pp. 392-399, 2008.
- [10] D. Brouwer, J. Jansen, S. Van der Starre, C. Van Kruijsdijk, and C. Berentsen, "Recovery increase through waterflooding with smart well technology," in *SPE European Formation Damage Conference*, 2001.
- [11] R. Baker, "Reservoir management for waterfloods-Part II," *Journal of Canadian Petroleum Technology*, vol. 37, 1998.
- [12] S. o. P. Engineers. (2014, Microscopic Efficiency of Waterflooding. Available: <http://petrowiki.org/Waterflooding>
- [13] W. Owens and D. Archer, "The effect of rock wettability on oil-water relative permeability relationships," *Journal of Petroleum Technology*, vol. 23, pp. 873-878, 1971.
- [14] W. G. Anderson, "Wettability literature survey part 5: the effects of wettability on relative permeability," *Journal of Petroleum Technology*, vol. 39, pp. 1,453-1,468, 1987.
- [15] P. Jadhunandan and N. R. Morrow, "Effect of wettability on waterflood recovery for crude-oil/brine/rock systems," *SPE reservoir engineering*, vol. 10, pp. 40-46, 1995.
- [16] Y. Al-Wahaibi, C. Grattoni, and A. Muggeridge, "Drainage and imbibition relative permeabilities at near miscible conditions," *Journal of Petroleum Science and Engineering*, vol. 53, pp. 239-253, 2006.
- [17] T. Ydstebø, "Enhanced Oil Recovery by CO₂ and CO₂-Foam in Fractured Carbonates," 2013.

- [18] V. Birchenko, A. I. Bejan, A. Usnich, and D. Davies, "Application of inflow control devices to heterogeneous reservoirs," *Journal of Petroleum Science and Engineering*, vol. 78, pp. 534-541, 2011.
- [19] J. Hallundbæk and P. Hazel, "Inflow control in a production casing," ed: Google Patents, 2010.
- [20] K. H. Henriksen, E. I. Gule, and J. R. Augustine, "Case Study: The Application of Inflow Control Devices in the Troll Field," in *SPE Europec/EAGE Annual Conference and Exhibition*, 2006.
- [21] B. YOUNGS, K. NEYLON, and J. HOLMES, "Multisegment well modeling optimizes inflow control devices," *World oil*, vol. 231, 2010.
- [22] C. H. Gao, R. T. Rajeswaran, and E. Y. Nakagawa, "A literature review on smart well technology," in *Production and Operations Symposium*, 2007.
- [23] F. T. Al-Khelaiwi, V. M. Birchenko, M. R. Konopczynski, and D. Davies, "Advanced wells: a comprehensive approach to the selection between passive and active inflow-control completions," *SPE Production & Operations*, vol. 25, pp. 305-326, 2010.
- [24] IEA/UNIDO, "Technology Roadmap: Carbon Capture and Storage in Industrial Applications," 2011.
- [25] P. Ashworth, N. Boughen, M. Mayhew, and F. Millar, "From research to action: Now we have to move on CCS communication," *International Journal of Greenhouse Gas Control*, vol. 4, pp. 426-433, 2010.
- [26] P. Jaramillo, W. M. Griffin, and S. T. McCoy, "Life cycle inventory of CO₂ in an enhanced oil recovery system," *Environmental science & technology*, vol. 43, pp. 8027-8032, 2009.
- [27] G. C. Institute, *The Global Status of CCS 2013*, 2013.
- [28] D. N. Veritas, "Assessment of measures to reduce future CO₂ emissions from shipping," ed: DNV, 2010.
- [29] P. Brownsort, "Ship transport of CO₂ for Enhanced Oil Recovery—Literature Survey," SCCS2015.
- [30] L. Zhang, B. Ren, H. Huang, Y. Li, S. Ren, G. Chen, *et al.*, "CO₂ EOR and storage in Jilin oilfield China: Monitoring program and preliminary results," *Journal of Petroleum Science and Engineering*, vol. 125, pp. 1-12, 2015.
- [31] L. Zhang, S. Ren, B. Ren, W. Zhang, Q. Guo, and L. Zhang, "Assessment of CO₂ storage capacity in oil reservoirs associated with large lateral/underlying aquifers: case studies from China," *International Journal of Greenhouse Gas Control*, vol. 5, pp. 1016-1021, 2011.
- [32] A. Chadwick, R. Arts, C. Bernstone, F. May, S. Thibeau, and P. Zweigel, "Best practice for the storage of CO₂ in saline aquifers," *British Geological Survey Occasional Publication*, vol. 14, p. 267, 2008.
- [33] A. Chadwick, R. Arts, C. Bernstone, F. May, S. Thibeau, and P. Zweigel, *Best Practice for the Storage of CO₂ in Saline Aquifers-Observations and Guidelines from the SACS and CO₂STORE projects* vol. 14: British Geological Survey, 2008.
- [34] IEA, "CO₂ Storage In Depleted Gas Fields," IEA Greenhouse Gas R&D Programme, <http://hub.globalccsinstitute.com/sites/default/files/publications/95786/co2-storage-depleted-gas-fields.pdf>, Report June 2009.

- [35] S. Pingping, L. Xinwei, and L. Qiuji, "Methodology for estimation of CO₂ storage capacity in reservoirs," *Petroleum Exploration and Development*, vol. 36, pp. 216-220, 2009.
- [36] L. S. Melzer, "Carbon dioxide enhanced oil recovery (CO₂ EOR): Factors involved in adding carbon capture, utilization and storage (CCUS) to enhanced oil recovery," *Center for Climate and Energy Solutions*, 2012.
- [37] D. Smith, "CO₂ Storage in Saline Aquifers," British Geological Survey, Applied geoscience for our changing Earth May 2010.
- [38] C. IEA, "Emissions from Fuel Combustion Highlights," *Paris, France: International Energy Agency (IEA/OECD)*, 2012.
- [39] P. I. CSLF, "final Report from the Task Force for Review and Identification of Standards for CO₂ Storage Capacity Estimation," in *Carbon Sequestration Leadership Forum, Washington DC*, 2007, p. 43.
- [40] Storage capacities of The Norwegian Continental Shelf [Online]. Available: <http://www.npd.no/Publikasjoner/Rapporter/CO2-samleatlas/7-Summary-Storage-capacities-of-The-Norwegian-Continental-Shelf/>
- [41] K. Li and R. N. Horne, "Comparison of methods to calculate relative permeability from capillary pressure in consolidated water-wet porous media," *Water resources research*, vol. 42, 2006.
- [42] ROX Help. Reservoir characteristics. [Online].
- [43] V. Mathiesen, B. Werswick, H. Aakre, and G. Elseth, "Autonomous Valve, A Game Changer Of Inflow Control In Horizontal Wells," in *Offshore Europe*, 2011.
- [44] Schlumberger, "ECLIPSE Reservoir Simulation Software - Technical Description." vol. 2013.1, ed, 2013.
- [45] C. D. Johnson and G. M. Oddie, "Flow control regulation method and apparatus," ed: Google Patents, 2004.
- [46] Schlumberger. (2015). *ECLIPSE Industry Reference Reservoir Simulator*. Available: <https://www.software.slb.com/products/eclipse>
- [47] H. Aakre, B. Halvorsen, B. Werswick, and V. Mathiesen, "Smart well with autonomous inflow control valve technology," in *SPE Middle East Oil and Gas Show and Conference*, 2013.
- [48] L.-B. Ouyang, "Practical consideration of an inflow-control device application for reducing water production," in *SPE Annual Technical Conference and Exhibition*, 2009.
- [49] V. Birchenko, K. Muradov, and D. Davies, "Reduction of the horizontal well's heel-toe effect with inflow control devices," *Journal of Petroleum Science and Engineering*, vol. 75, pp. 244-250, 2010.
- [50] K. Muradov, V. Birchenko, and D. Davies, "Modeling of the Heel-toe Effect in a Horizontal Well with Inflow Control Devices," in *12th European Conference on the Mathematics of Oil Recovery*, 2010.

List of tables and charts

Table 4-1 Components of ECLIPSE CO2STORE option[44]	38
Table 5-1 Reservoir conditions for waterflooding	45
Table 5-2 Initial conditions for waterflooding.....	45
Table 5-3 Reservoir conditions for ICD simulation.....	49
Figure 2-1 Typical horizontal and vertical waterflooding[5, 7].....	17
Figure 2-2 Oriface ICD [18].....	20
Figure 3-1 Standard CCS process[27]	22
Figure 3-2 Large-scale CO ₂ capture projects [27]	23
Figure 3-3 CO ₂ Storage overview[27]	24
Figure 3-4 IEA Vision for Cumulative CO ₂ captured between 2015 and to 2050 [38]	26
Figure 3-5 CO ₂ trapping mechanisms[35].....	27
Figure 3-6 Storage capacity of largest aquifers in Nordic region	28
Figure 4-1 ECLIPSE flow model [15].....	30
Figure 4-2 The relative permeability curve used for the simulation.....	32
Figure 4-4 ICD segments along the well[44]	33
Figure 4-5 Phase transition region about the critical water in liquid fraction[44]	35
Figure 5-1 Reservoir geometry for horizontal and vertical injection(Homogenous)	43
Figure 5-2 Reservoir geometry for the horizontal injection case (Heterogenous)	44
Figure 5-3 Reservoir geometry for the vertical injection (Heterogenous)	44
Figure 5-4 Location of ICD along the well.....	47
Figure 5-5 Reservoir geometry showing the distribution of X and Y permeability	47
Figure 5-6 Reservoir geometry showing the distribution of Z- permeability	48
Figure 6-1 Final oil saturation of the base case (homoogeneous).....	50
Figure 6-2 Production trend for the base case (homogeneous).....	51
Figure 6-3 Pressure trend for the base case (homogeneous).....	51
Figure 6-4 Production trend for water injection of 500m ³ /day (homogeneous).....	53
Figure 6-5 Pressure trend for water injection of 500m ³ /day (homogeneous).....	54
Figure 6-6 Production trend for water injection of 1000m ³ /day (homogeneous)	56
Figure 6-7 Pressure trend for water injection of 1000m ³ /day (homogeneous)	57
Figure 6-8 Production trend for water injection of 1500m ³ /day (homogeneous)	59
Figure 6-9 Pressure trend for water injection of 1500m ³ /day (homogeneous)	60

Figure 6-10 Production trend for water injection of 2000m ³ /day (homogeneous)	62
Figure 6-11 Pressure trend for water injection of 2000m ³ /day (homogeneous)	63
Figure 6-12 Production trend for water injection of 2500m ³ /day (homogeneous)	65
Figure 6-13 Pressure trend for water injection of 2500m ³ /day (homogeneous)	66
Figure 6-14 Plot of overall reservoir pressure against time (homogeneous)	67
Figure 6-15 Plot of differential injection pressure against injection rate (homogeneous)	68
Figure 6-16 Plot of overall water cut against time (homogeneous)	69
Figure 6-17 Plot of overall oil production rate against time (homogeneous).....	71
Figure 6-18 Plot of accumulated oil production against time(homogenous)	72
Figure 6-19 Plot of recovery factor against injection rate (homogeneous)	73
Figure 6-20 Oil saturation for horizontal injection after 3653 days (homogeneous)	74
Figure 6-21 Oil saturation for vertical injection after 3653 days (homogeneous)	74
Figure 6-22 Plan view of oil-water front progression after 2 years (homogeneous)	75
Figure 6-23 Plan view of oil-water front progression after 3653 days (homogeneous) .	75
Figure 6-24 Production trend for the base case (heterogeneous)	76
Figure 6-25 Pressure trend for the base case (heterogeneous)	77
Figure 6-26 Final oil saturation of the base case (heterogeneous)	77
Figure 6-27 Production trend for water injection of 500m ³ /day (heterogeneous).....	79
Figure 6-28 Pressure trend for water injection of 500m ³ /day (heterogeneous).....	80
Figure 6-29 Production trend for water injection of 1000m ³ /day (heterogeneous).....	82
Figure 6-30 Pressure trend for water injection of 1000m ³ /day (heterogeneous).....	83
Figure 6-31 Production trend for water injection of 1500m ³ /day (heterogeneous).....	85
Figure 6-32 Pressure trend for water injection of 1500m ³ /day (heterogeneous).....	86
Figure 6-33 Production trend for water injection of 2000m ³ /day (heterogeneous).....	88
Figure 6-34 Pressure trend for water injection of 2000m ³ /day (heterogeneous).....	89
Figure 6-35 Production trend for water injection of 2500m ³ /day (heterogeneous).....	91
Figure 6-36 Pressure trend for water injection of 2500m ³ /day (heterogeneous).....	92
Figure 6-37 Overall reservoir pressure trend (heterogeneous).....	93
Figure 6-38Plot of differential injection pressure against injection rate (heterogeneous)	94
Figure 6-39 Overall water cut trend (heterogeneous)	96

Figure 6-40 Overall oil production rate (heterogeneous)	97
Figure 6-41 Accumulated oil production (heterogeneous)	99
Figure 6-42 Overall recovery factor (heterogeneous)	100
Figure 6-43 Gas production rate (heterogeneous)	101
Figure 6-44 Accumulated gas production (heterogeneous)	102
Figure 6-45 Reservoir Pressure Trend (ICD)	103
Figure 6-46 Trend of water cut	104
Figure 6-47 Trend of oil production rate	105
Figure 6-48 Trend of accumulated oil production	105
Figure 6-49 Trend of gas production rate	106
Figure 6-50 Trend of the accumulated gas production	107

Annexes

Annex 1: Task description and work plan

Annex 2: Relative permeability data

Annex 3: Live oil PVT

Annex 4: Dry gas and water PVT

Annex 5: Summary of result (Homogeneous waterflooding)

Annex 6: Summary of result (Heterogeneous waterflooding)

Annex 7: Oil saturation for homogeneous waterflooding

Annex 8: Oil saturation for heterogeneous waterflooding

Annex 9: Publications

Annex 10: Summary page

Annex 1: Task description and work plan

Faculty of Technology

FMH606 Master's Thesis

Title: Improved Oil Recovery and Study of CO₂ Storage in Oil/Gas Reservoirs and Aquifers

TUC supervisor: Prof. Britt M. E. Moldestad

Co-supervisor: Vidar Mathiesen, Dr.ing

External Partner: InflowControl AS

Task background:

The oil industry uses various technologies to increase the recovery of oil from the existing reservoirs and increase the well performance. Different methods are used for this purpose. CO₂ is used for Enhanced Oil Recovery (EOR) in fields with high amount of residual oil. In addition to using CO₂ for EOR, it is crucial to store CO₂ to avoid the large contribution to global warming. Mature oil reservoirs and underlying aquifers are considered as the future solution for CO₂ storage. A better understanding of the storage capacity and suitability for CO₂ storage in reservoirs and aquifers are needed. Another method used to increase oil recovery is water injection referred to as water flooding. Water can be injected through a horizontal or a vertical well. It is important to ascertain the optimal water injection arrangement between vertical and horizontal arrangement using ECLIPSE Reservoir simulation software. Water and gas breakthrough is a major challenge in oil production. It is a mature technology to use an inflow control device to delay water and gas breakthrough and maximize ultimate recovery. ECLIPSE simulation to illustrate the implementation of ICD completion along a horizontal well is required.

Task description:

The project will focus on:

1. Literature study of Improved Oil recovery and CO₂ storage
2. Study of CO₂ storage in oil/gas reservoir and aquifers
3. ECLIPSE Simulation of water flooding and the application of ICD

Practical arrangements:

Necessary software will be provided by HSN.

Student category:

PT. The student need to have good knowledge about CO₂ storage, reservoir and near well simulation.

Signatures:

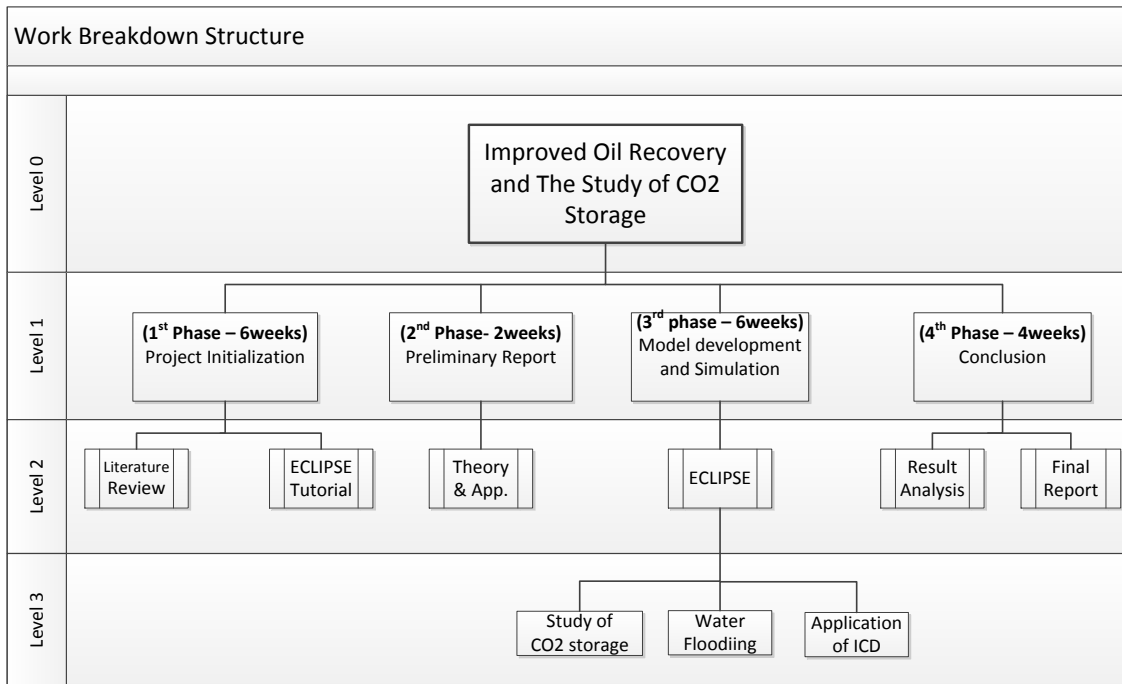
Supervisor (date and signature):

01.02.2016 Britt Moldestad

Student (date and signature):

01/02/2016 *Almogues*

Work Breakdown Structure



Annex 2: Result Summary (Homogenous)

<i>Injection Rate</i>	Water Breakthrough Time [Day]		Water cut@ 3653 day [-]	
	<i>Horizontal</i>	<i>Vertical</i>	<i>Horizontal</i>	<i>Vertical</i>
0	-	-	0.00	0.00
500M ³ /Day	-	3,391	0.00	0.01
1000M ³ /Day	2,700	1,338	0.42	0.39
1500M ³ /Day	1,691	792	0.75	0.69
2000M ³ /Day	1,179	558	0.82	0.79
2500M ³ /Day	890	431	0.87	0.86
<i>Injection Rate</i>	Pressure Drop@ 3653 day [Bar]		<i>Differential injection pressure [Bar]</i>	
	<i>Horizontal</i>	<i>Vertical</i>	<i>Horizontal</i>	<i>Vertical</i>
0	9.38	9.38	-	-
500M ³ /Day	8.19	8.22	0.8	8.0
1000M ³ /Day	6.46	6.84	2.0	19.0
1500M ³ /Day	5.42	5.74	3.0	25.0
2000M ³ /Day	4.47	4.93	5.0	39.0
2500M ³ /Day	3.59	4.19	6.0	45.0
<i>Injection Rate</i>	Accumulated Oil @ 3653 [SM³]		Recovery factor@ 3653 day [-]	
	<i>Horizontal</i>	<i>Vertical</i>	<i>Horizontal</i>	<i>Vertical</i>
0	40,918	40,918	0.000	0.000
500M ³ /Day	1,391,437	1,390,863	0.146	0.145
1000M ³ /Day	2,552,601	2,492,110	0.271	0.264
1500M ³ /Day	3,013,196	3,056,921	0.321	0.325
2000M ³ /Day	3,236,492	3,378,713	0.345	0.360
2500M ³ /Day	3,386,664	3,600,575	0.361	0.384

Annex 3: Result Summary (Heterogeneous)

Injection Rate	Water Breakthrough Time [Day]		Water cut@ 3653 day [-]	
	<i>Horizontal</i>	<i>Vertical</i>	<i>Horizontal</i>	<i>Vertical</i>
0	-	-	0.00	0.00
500M ³ /Day	3143	600	0.27	0.66
1000M ³ /Day	1392	279	0.72	0.74
1500M ³ /Day	835	182	0.82	0.77
2000M ³ /Day	600	135	0.88	0.84
2500M ³ /Day	462	108	0.90	0.87
Injection Rate	Pressure Drop@ 3653 day [Bar]		Differential injection pressure [Bar]	
	<i>Horizontal</i>		<i>Horizontal</i>	<i>Vertical</i>
0	9.38	9.38	-	-
500M ³ /Day	6.66	7.61	1.6	13.0
1000M ³ /Day	4.55	6.45	3.0	18.0
1500M ³ /Day	2.81	5.26	4.5	28.0
2000M ³ /Day	1.23	3.88	6.0	39.0
2500M ³ /Day	-0.29	2.74	8.0	50.0
Injection Rate	Accumulated Oil @ 3653 [SM³]		Recovery factor@ 3653 day [-]	
	<i>Horizontal</i>	<i>Vertical</i>	<i>Horizontal</i>	<i>Vertical</i>
0	0	0	0.000	0.000
500M ³ /Day	1,357,360	855,086	0.14	0.09
1000M ³ /Day	1,905,035	1,261,237	0.20	0.13
1500M ³ /Day	2,133,903	1,623,008	0.23	0.17
2000M ³ /Day	2,273,588	1,909,105	0.24	0.20
2500M ³ /Day	2,371,081	2,129,027	0.25	0.23

Annex 4: Relative permeability data

In this study, Corey model is used to define relative permeability curves of water and oil. Equation 4a-4d represents Corey model for predicting relative permeability of water [42].

$$k_{rw}=k_{rwoc} \left(\frac{S_w+S_{wir}}{1-S_{wir}+R_{so}} \right)^{n_w} \quad (4a)$$

where k_{rw} is relative permeability of water, k_{rwoc} is an end point of water at its maximum saturation, S_w is water saturation, S_{wir} is irreducible water saturation, R_{so} is residual oil saturation and n_w is Corey fitting parameter for water.

The model used to estimate predicting the relative permeability of oil is presented in equation (4-9) [42].

$$k_{row}=k_{rowc} \left(\frac{S_w+R_{so}-1}{S_{wir}+R_{so}-1} \right)^{n_{ow}} \quad (4b)$$

Where k_{row} is the oil relative permeability for water-oil system, k_{rowc} is an end point of oil in water at irreducible water saturation and n_{ow} is the fitting parameter for oil.

The model used to estimate predicting the relative permeability of gas is presented in equations (4-10) and (4-11).

$$k_{rog}=k_{rocw} \cdot \left(\frac{1-S_{org}-S_{wc}-S_g}{1-S_{org}-S_{wc}} \right)^{n_{og}} \quad (4c)$$

$$k_{rg}=k_{rgro} \cdot \left(\frac{S_g-S_{gic}}{1-S_{org}-S_{wc}-S_{gic}} \right)^{n_g} \quad (4d)$$

where k_{rog} is the oil relative permeability to gas, k_{rocw} is the relative permeability of oil zero gas saturation and k_{rg} is the gas relative permeability. S_{org} is the residual saturation of gas, S_{wc} is the connate water saturation, S_g is gas saturation, S_{gic} is the critical gas saturation, n_g is the Corey exponent for the gas phase and n_{og} is the Corey exponent for oil and gas phase. Table 4a shows the relative permeability data used for the simulation

Table 4a Relative permeability data

Parameter	Value
S_{wc}	0.2
S_{orw}	0.3
S_{org}	0.3
S_{gc}	0.1
n_g	2
n_w	3.5
n_{ow}	3.0
n_{og}	4
R_{so}	0.3
S_{wir}	0.2

Annex 5: Live Oil PVT

Reports from file BUILD1_E100.PRT

```

1          ***** 2
PVTO  AT  0.00 DAYS *PRODUCTIONCASE          * ECLIPSE VERSION 2013.1
REPORT 0  1 JAN 2016 * RUN                    * RUN AT 08:15 ON 04 APR 2016
          *****
  
```

OIL PVT FUNCTIONS TABLE 1

RS	PRESSURE	BO	VO
SM3/SM3	BARSA	RM3/SM3	CP
5.247	20.00	1.1776	3.0000
	100.00	1.1401	3.0000
	150.00	1.1231	3.0000
	200.00	1.1090	3.0000
	250.00	1.0971	3.0000
	300.00	1.0870	3.0000
	331.65	1.0812	3.0000
	350.00	1.0781	3.0000
	400.00	1.0703	3.0000
	450.00	1.0633	3.0000
	500.00	1.0571	3.0000
52.085	100.00	1.3922	3.0000
	150.00	1.3531	3.0000
	200.00	1.3233	3.0000
	250.00	1.2994	3.0000
	300.00	1.2797	3.0000
	331.65	1.2689	3.0000
	350.00	1.2630	3.0000
	400.00	1.2487	3.0000
	450.00	1.2363	3.0000
	500.00	1.2252	3.0000
89.117	150.00	1.5425	3.0000
	200.00	1.4952	3.0000
	250.00	1.4591	3.0000
	300.00	1.4301	3.0000
	331.65	1.4144	3.0000
	350.00	1.4061	3.0000
	400.00	1.3859	3.0000
	450.00	1.3685	3.0000
	500.00	1.3533	3.0000
137.043	200.00	1.7330	3.0000
	250.00	1.6756	3.0000
	300.00	1.6314	3.0000

	331.65	1.6081	3.0000
	350.00	1.5959	3.0000
	400.00	1.5664	3.0000
	450.00	1.5415	3.0000
	500.00	1.5201	3.0000
204.562			
	250.00	2.0016	3.0000
	300.00	1.9295	3.0000
	331.65	1.8926	3.0000
	350.00	1.8736	3.0000
	400.00	1.8285	3.0000
	450.00	1.7911	3.0000
	500.00	1.7594	3.0000
317.856			
	300.00	2.4637	3.0000
	331.65	2.3976	3.0000
	350.00	2.3641	3.0000
	400.00	2.2866	3.0000
	450.00	2.2240	3.0000
	500.00	2.1721	3.0000
477.910			
	331.65	3.1539	3.0000
	350.00	3.0954	3.0000
	400.00	2.9625	3.0000
	450.00	2.8578	3.0000
	500.00	2.7727	3.0000
486.566			
	350.00	3.1540	3.0000
	400.00	3.0583	3.0000
	450.00	2.9566	3.0000
	500.00	2.8681	3.0000
510.576			
	400.00	3.1541	3.0000
	450.00	3.0555	3.0000
	500.00	2.9636	3.0000
535.771			
	450.00	3.1543	3.0000
	500.00	3.0590	3.0000
562.210			
	500.00	3.1544	3.0000
	550.00	3.0592	3.0000

Annex 6: Dry gas and water PVT

```

1          ***** 3
PVDG AT 0.00 DAYS *PRODUCTIONCASE          * ECLIPSE VERSION 2013.1
REPORT 0 1 JAN 2016 * RUN                    * RUN AT 08:15 ON 04 APR 2016
          *****
  
```

 DRY GAS PVT DATA TABLE 1

PRESSURE	BG	VG
BARSA	RM3/SM3	CP
20.00	0.0798	0.0139
100.00	0.0153	0.0165
150.00	0.0103	0.0184
200.00	0.0079	0.0207
250.00	0.0065	0.0232
300.00	0.0056	0.0258
331.65	0.0052	0.0276
350.00	0.0050	0.0285
400.00	0.0046	0.0310
450.00	0.0042	0.0334
500.00	0.0040	0.0357

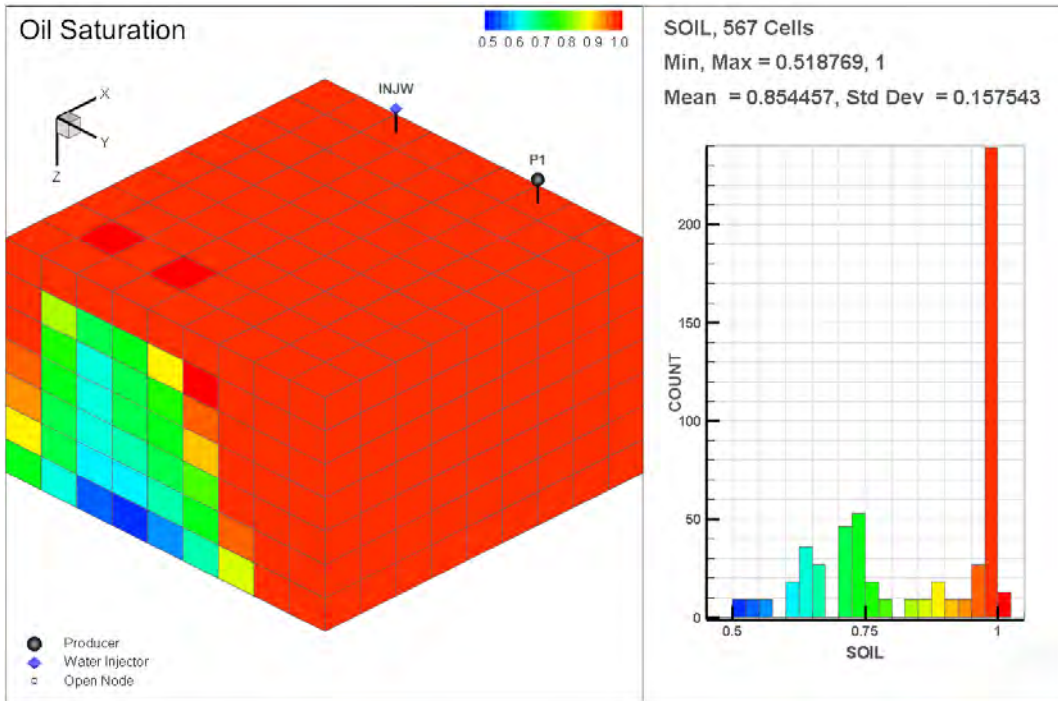
PVTW (Water PVT Properties)

BARSA	RM3/SM3	1/BARS	CF
Water PVT Properties			
Reference pressure (Pref)	<input type="text" value="400"/>	<input type="text" value="bar"/>	<input type="button" value="v"/>
Water FVF at Pref	<input type="text" value="1.13579"/>	<input type="text" value="m3/sm3"/>	<input type="button" value="v"/>
Water compressibility	<input type="text" value="0.00011"/>	<input type="text" value="/bar"/>	<input type="button" value="v"/>
Water viscosity at Pref	<input type="text" value="0.5"/>	<input type="text" value="cp"/>	<input type="button" value="v"/>
Water viscosibility	<input type="text" value="0.00011"/>	<input type="text" value="/bar"/>	<input type="button" value="v"/>

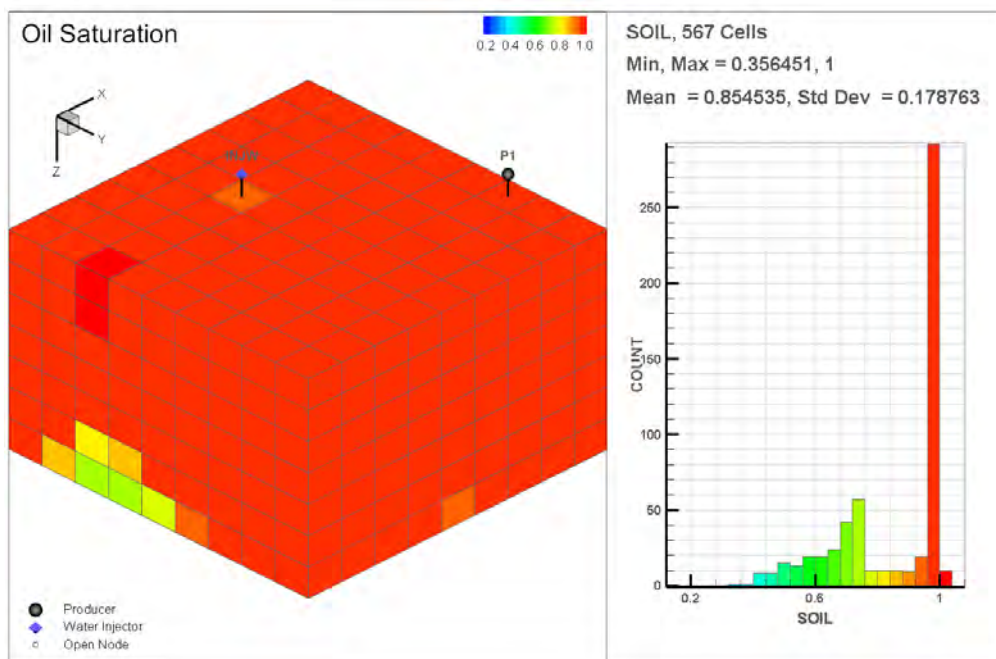
Annex 7: Oil saturation (Homogeneous)

Injection rate of 500m³/day: Homogeneous case at the 3653rd day

1 Jan 2026



1 Jan 2026

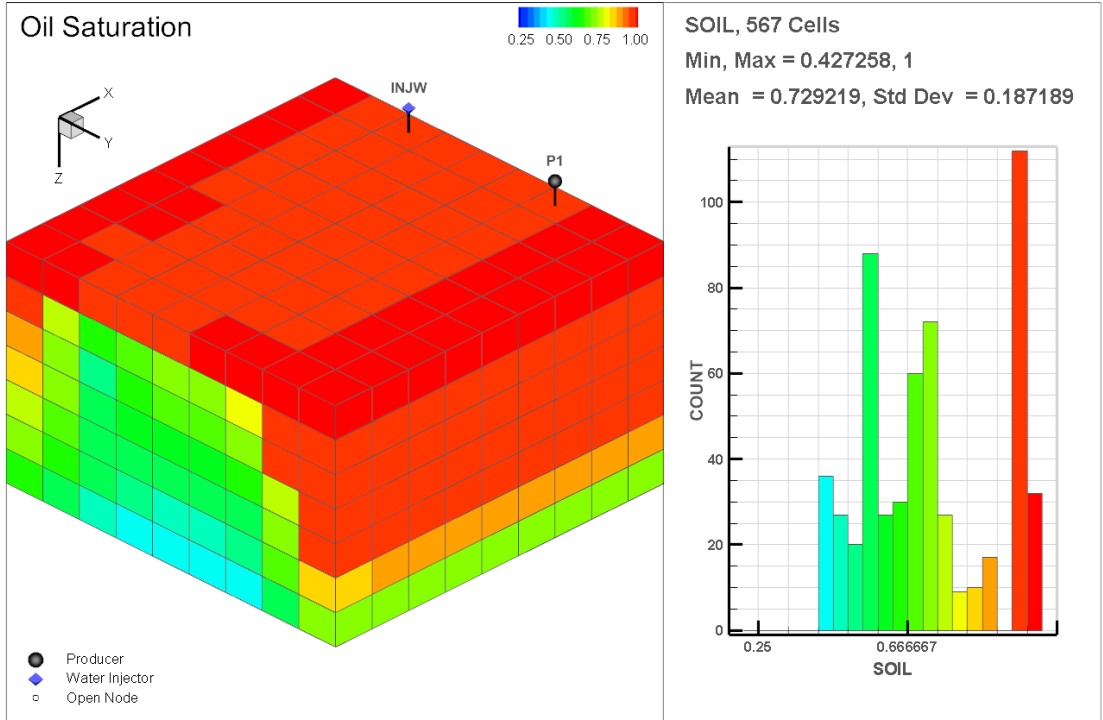


BUILD1_E100

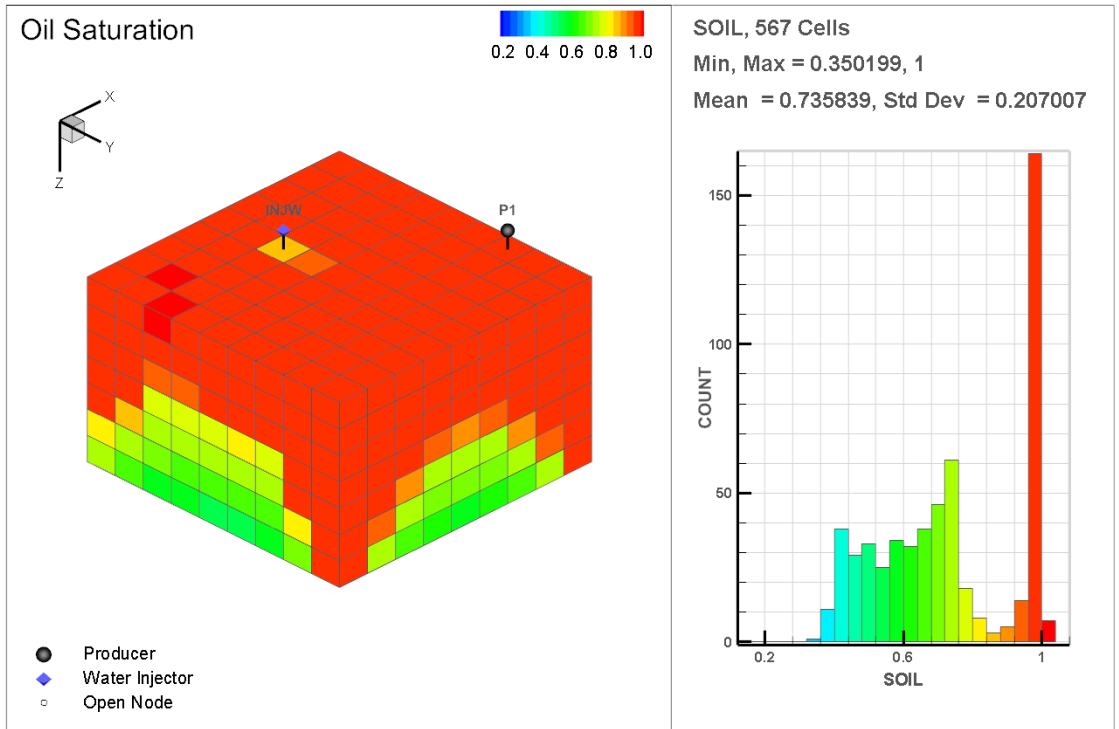
01 Jun 2016

Injection rate of 1000m³/day: Homogeneous case at the 3653rd day

1 Jan 2026

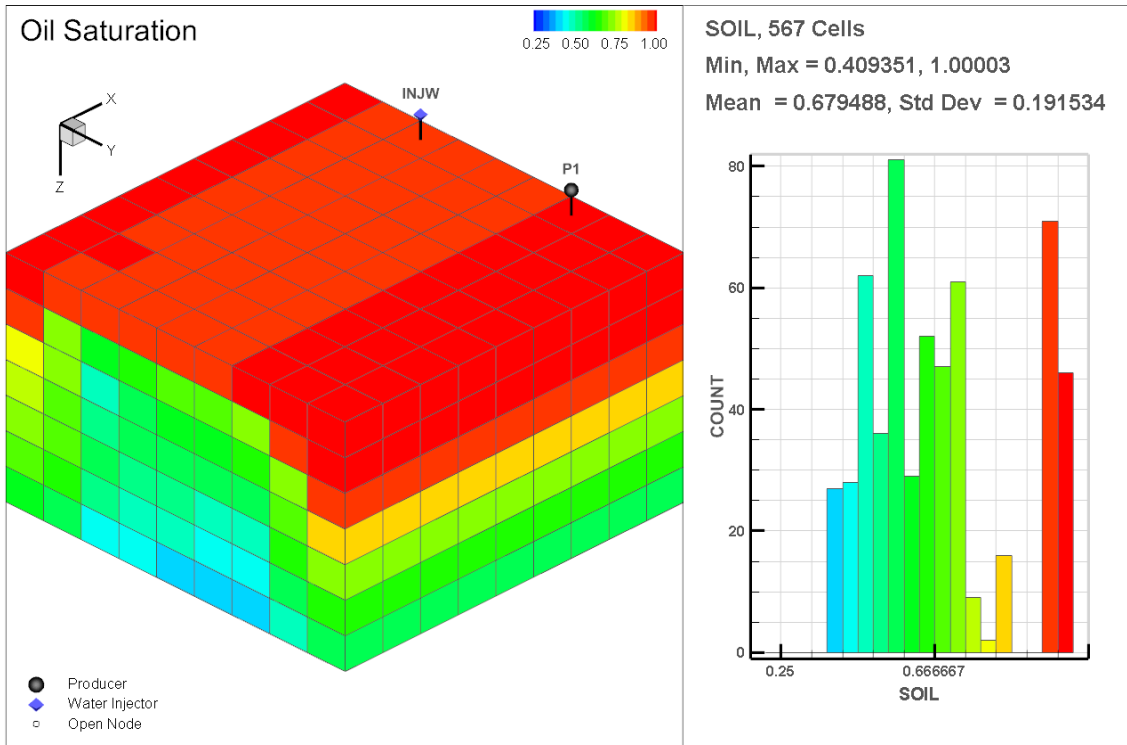


1 Jan 2026

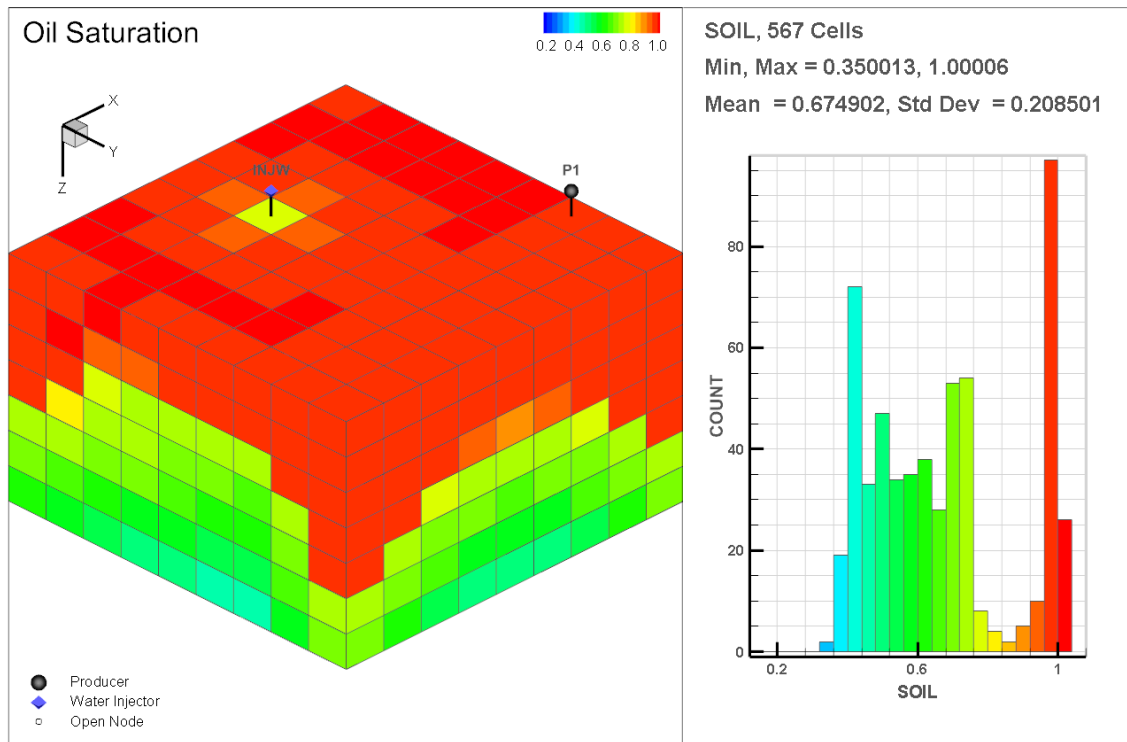


Injection rate of 1500m³/day: Homogeneous case at the 3653rd day

1 Jan 2026

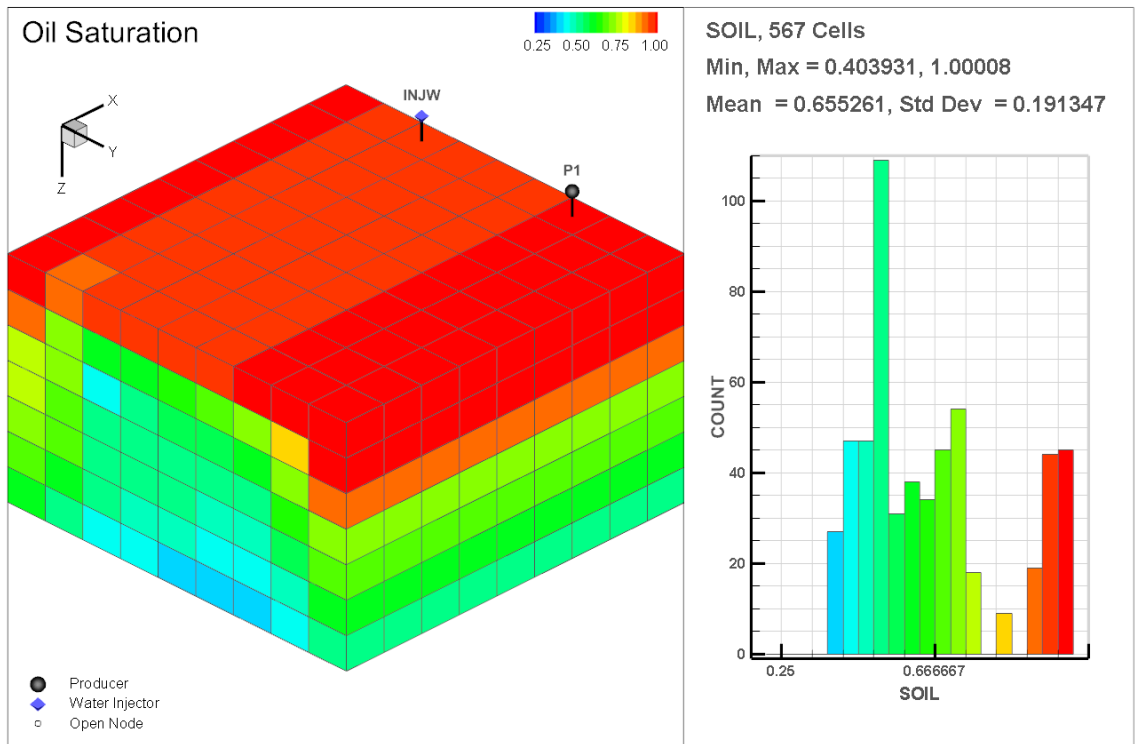


1 Jan 2026

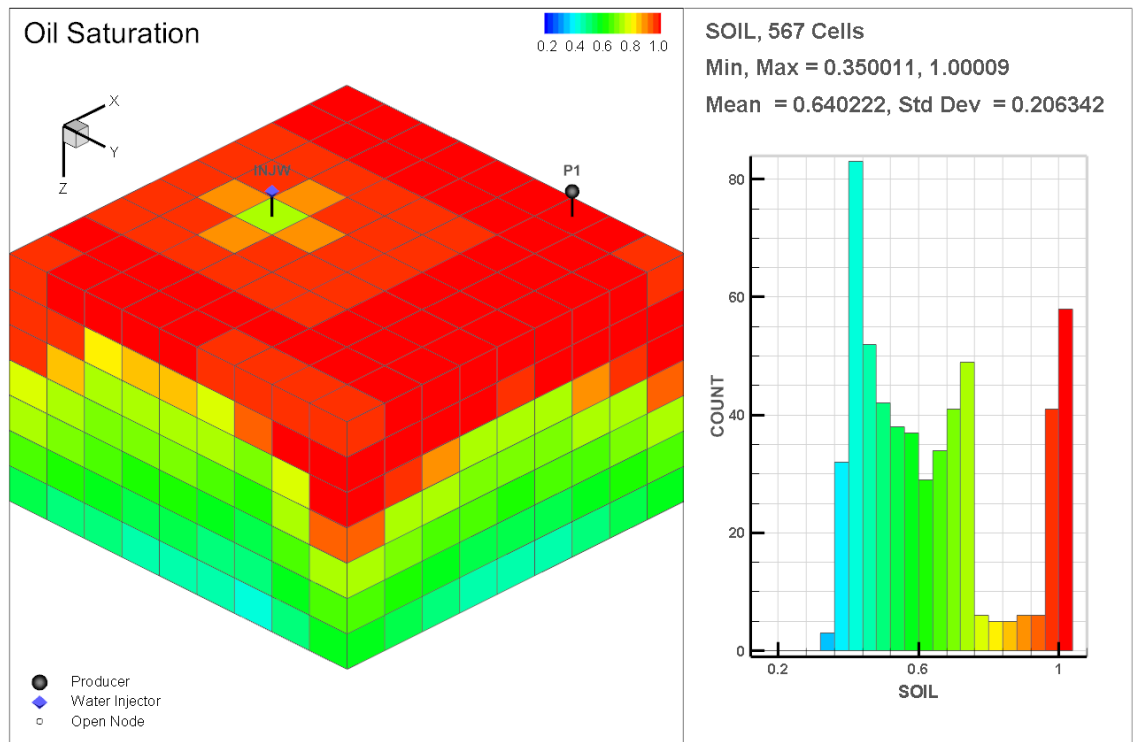


Injection rate of 2000m³/day: Homogeneous case at the 3653rd day

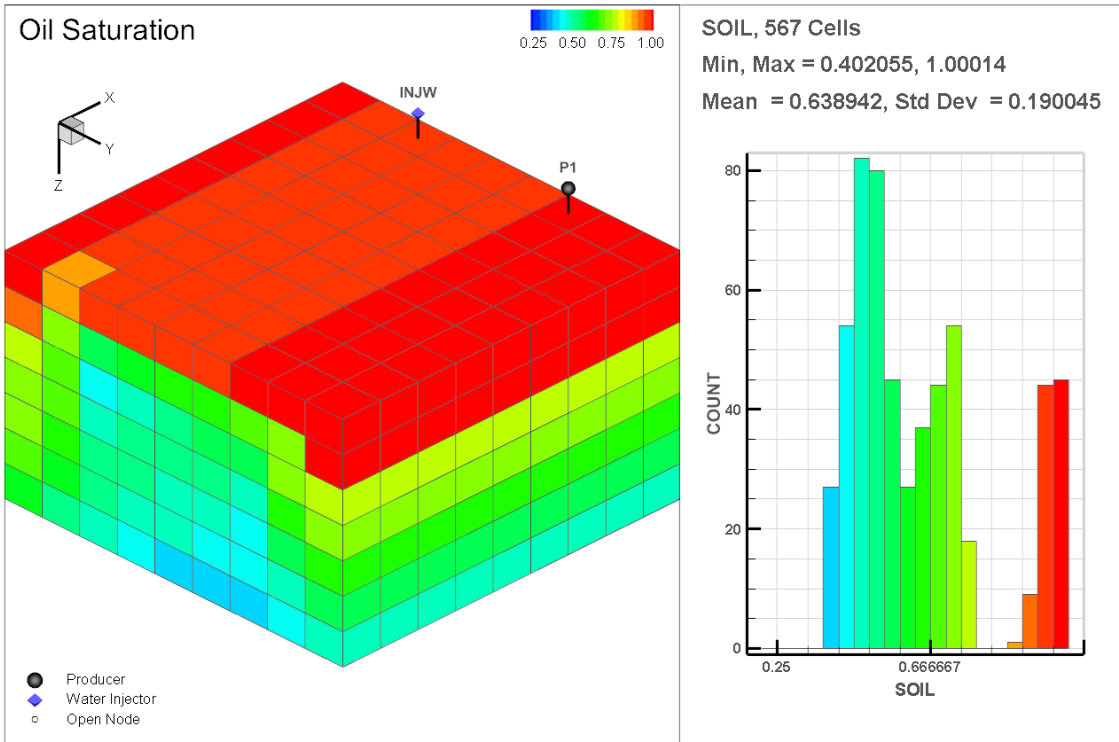
1 Jan 2026



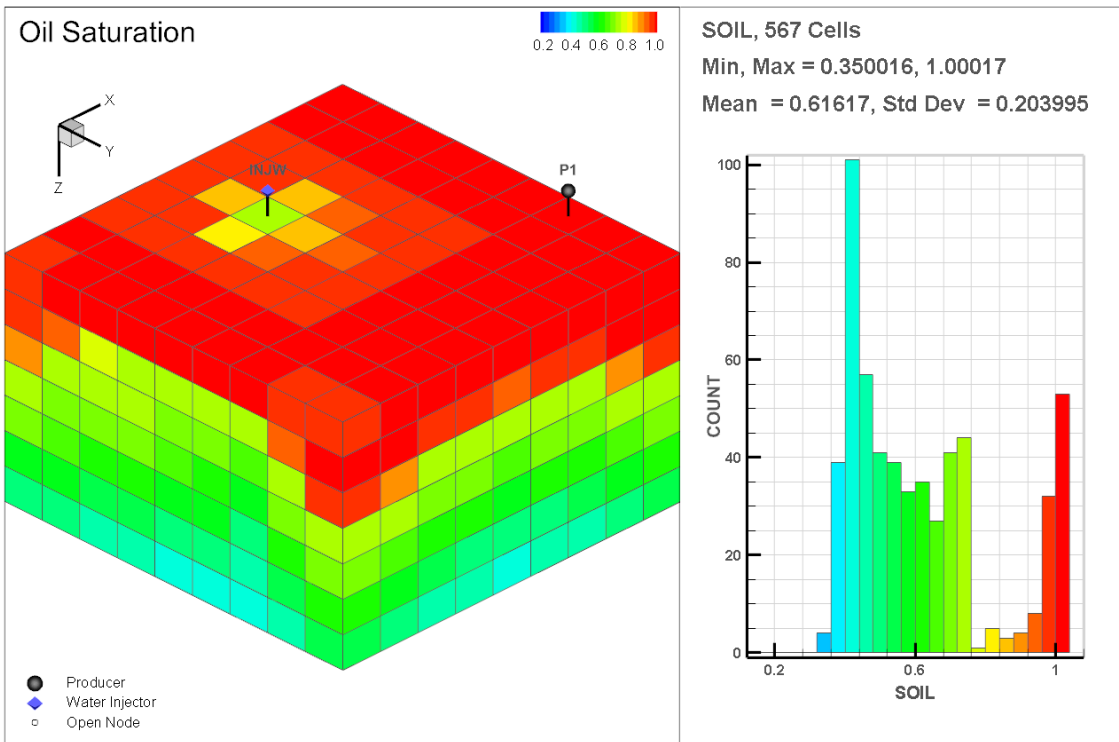
1 Jan 2026



Injection rate of 2500m³/day: Homogeneous case at the 3653rd day
 1 Jan 2026



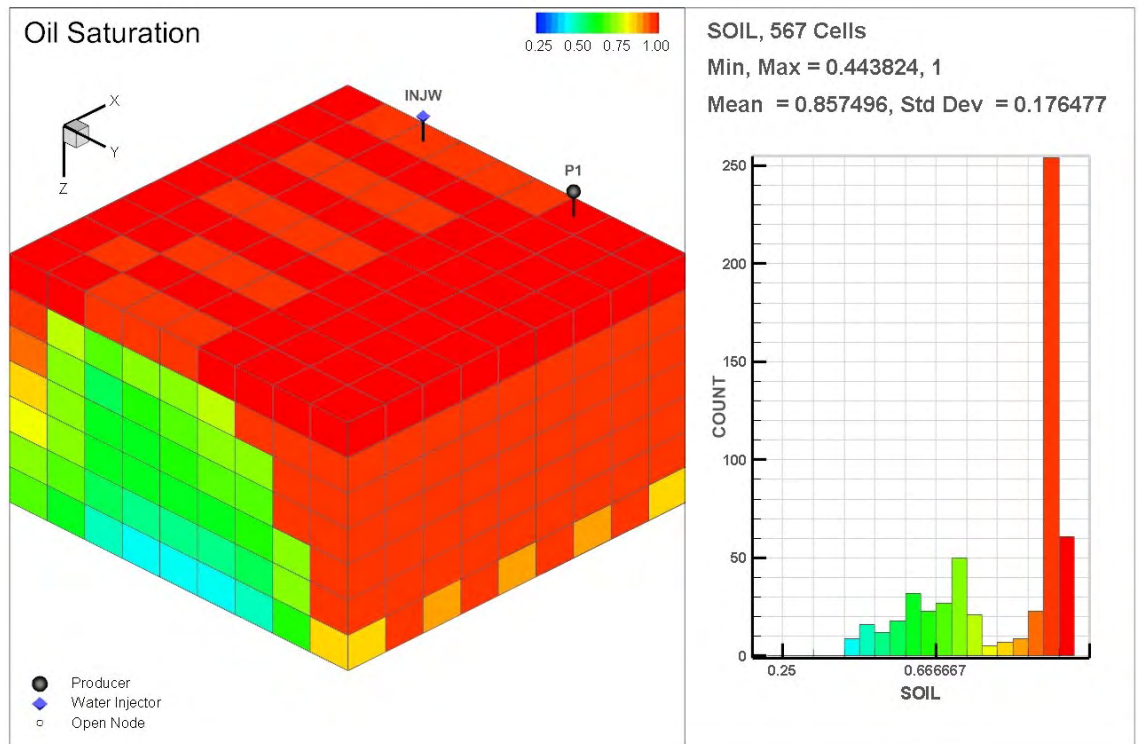
1 Jan 2026



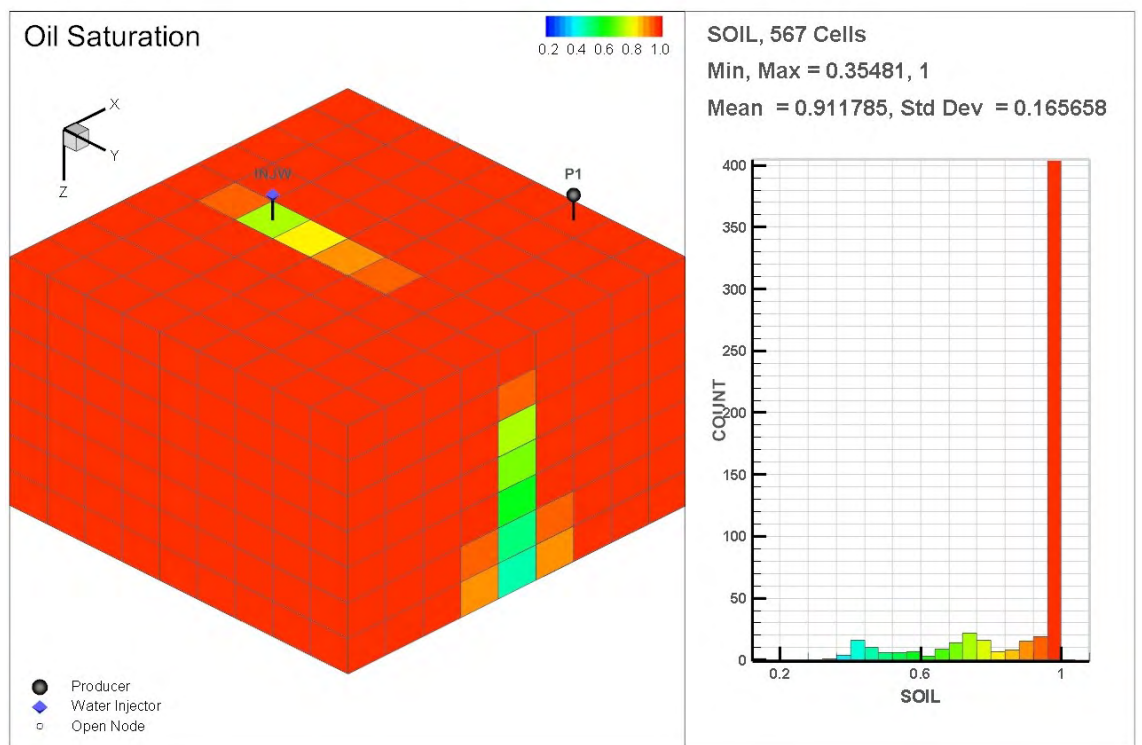
Annex 8: Oil saturation (Heterogeneous)

Injection rate of 500m³/day: Heterogeneous case at the 3653rd day

1 Jan 2026

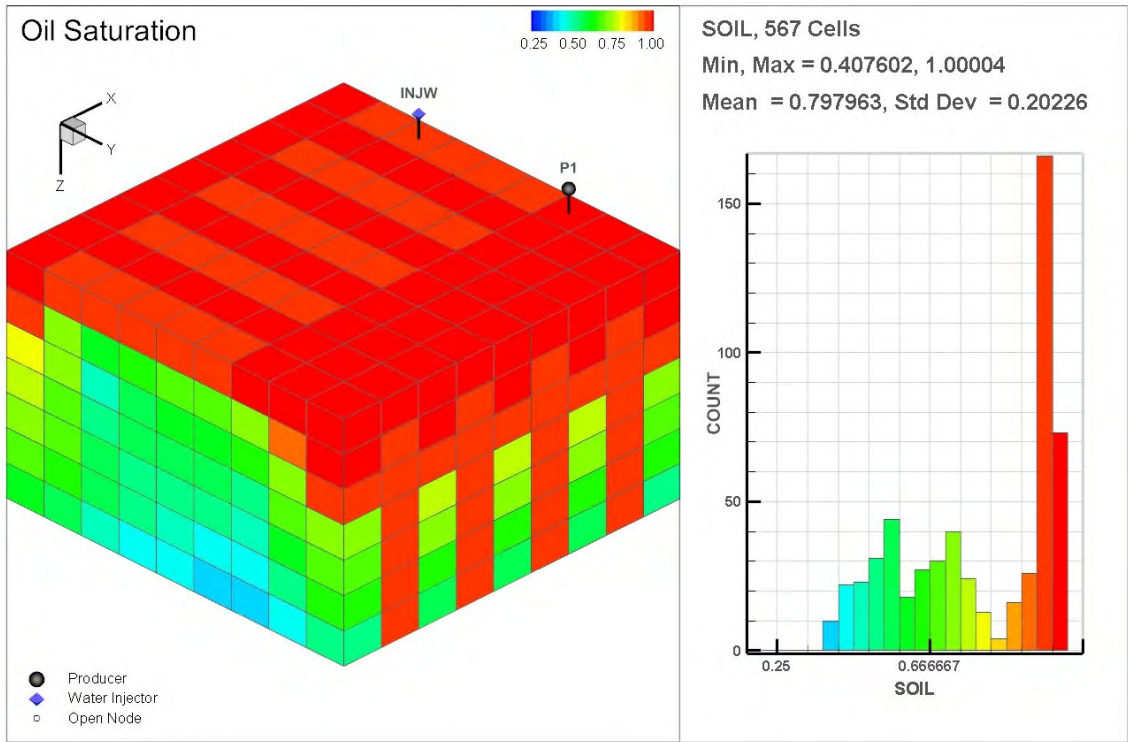


1 Jan 2026

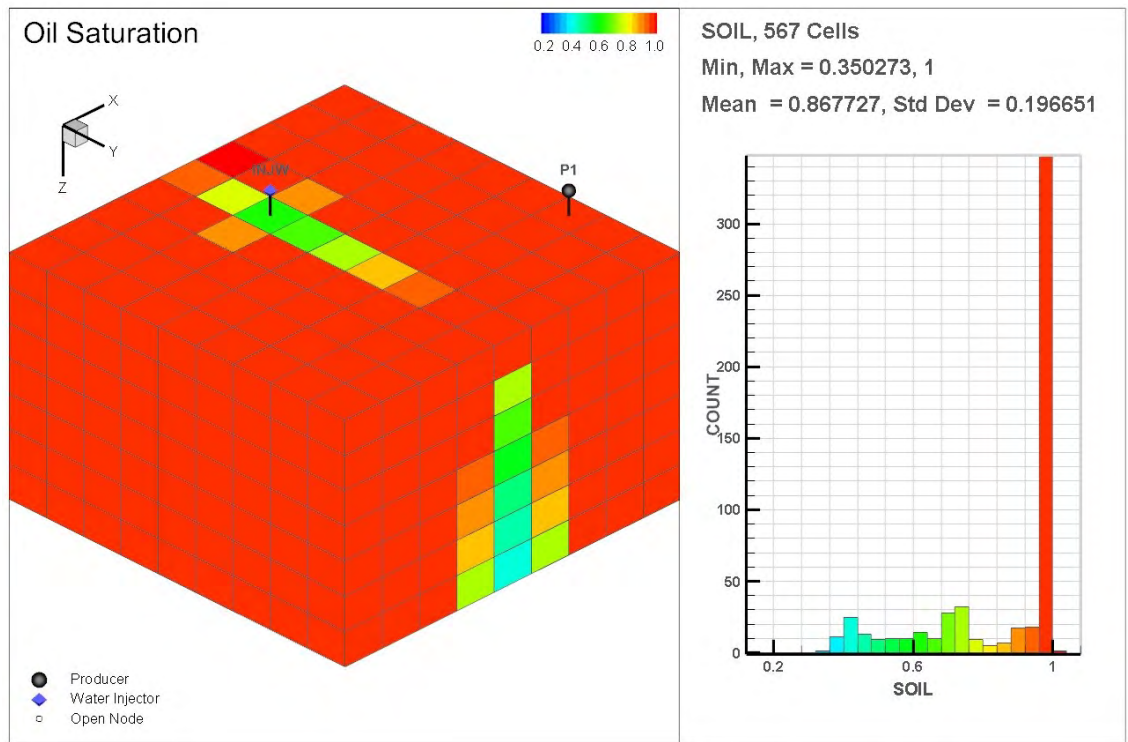


Injection rate of 1000m³/day: Heterogeneous case at the 3653rd day

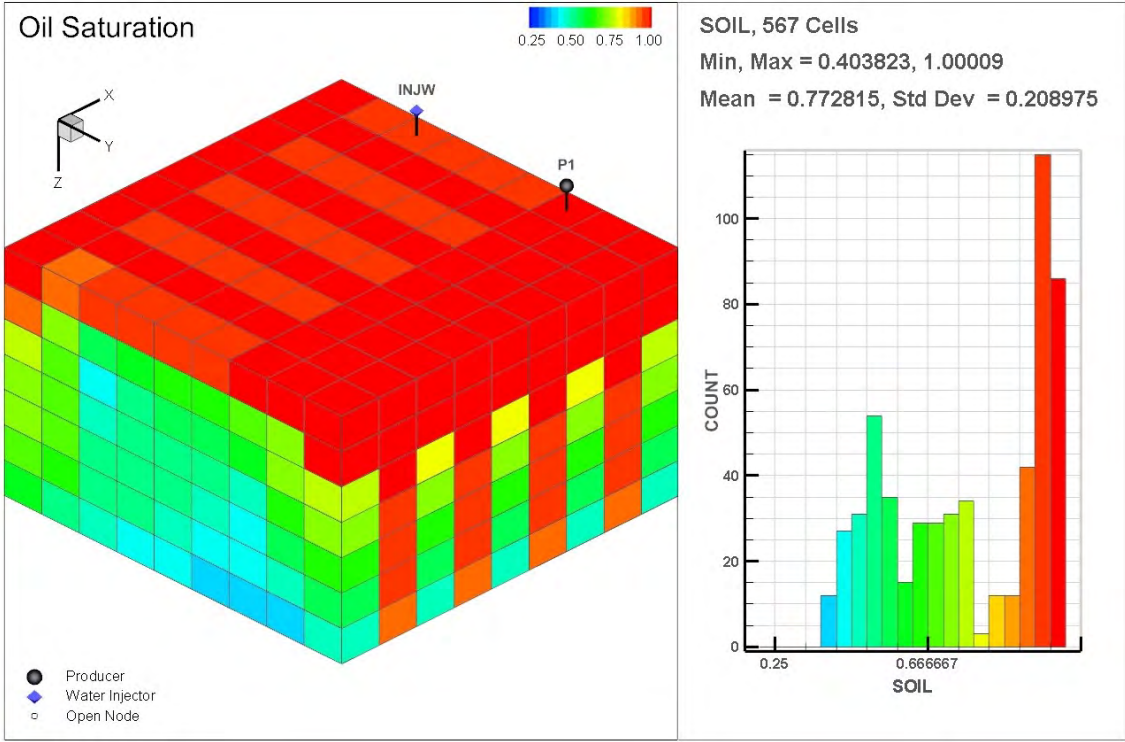
1 Jan 2026



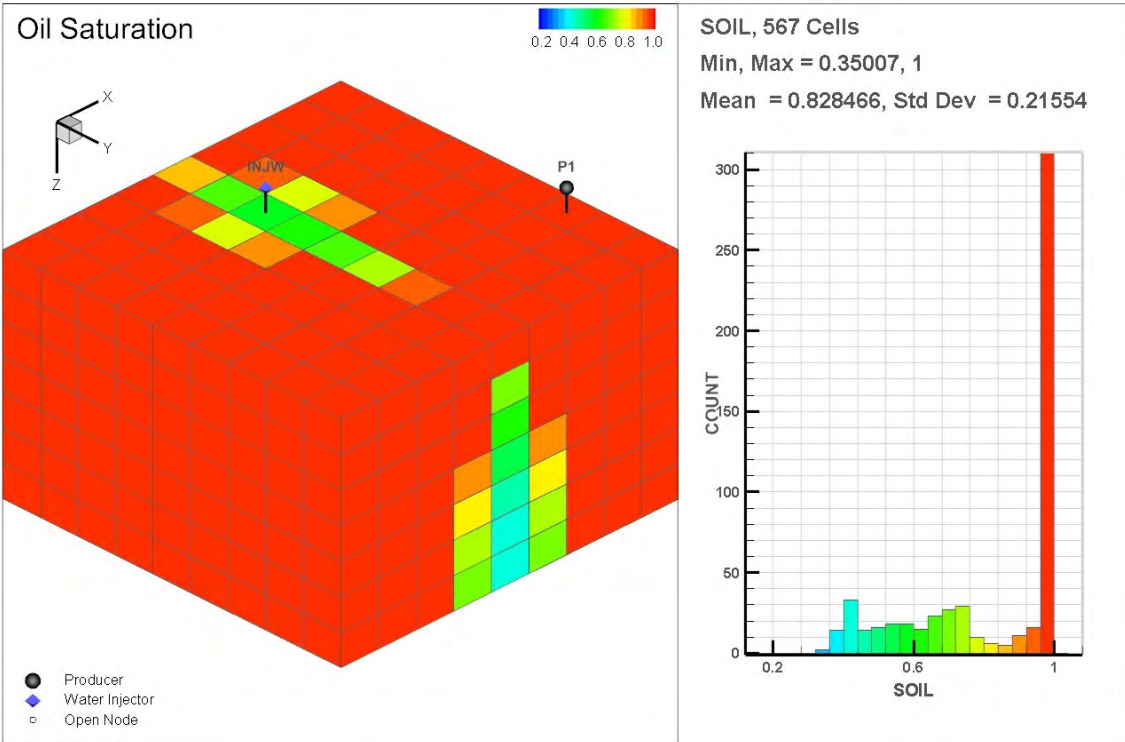
1 Jan 2026



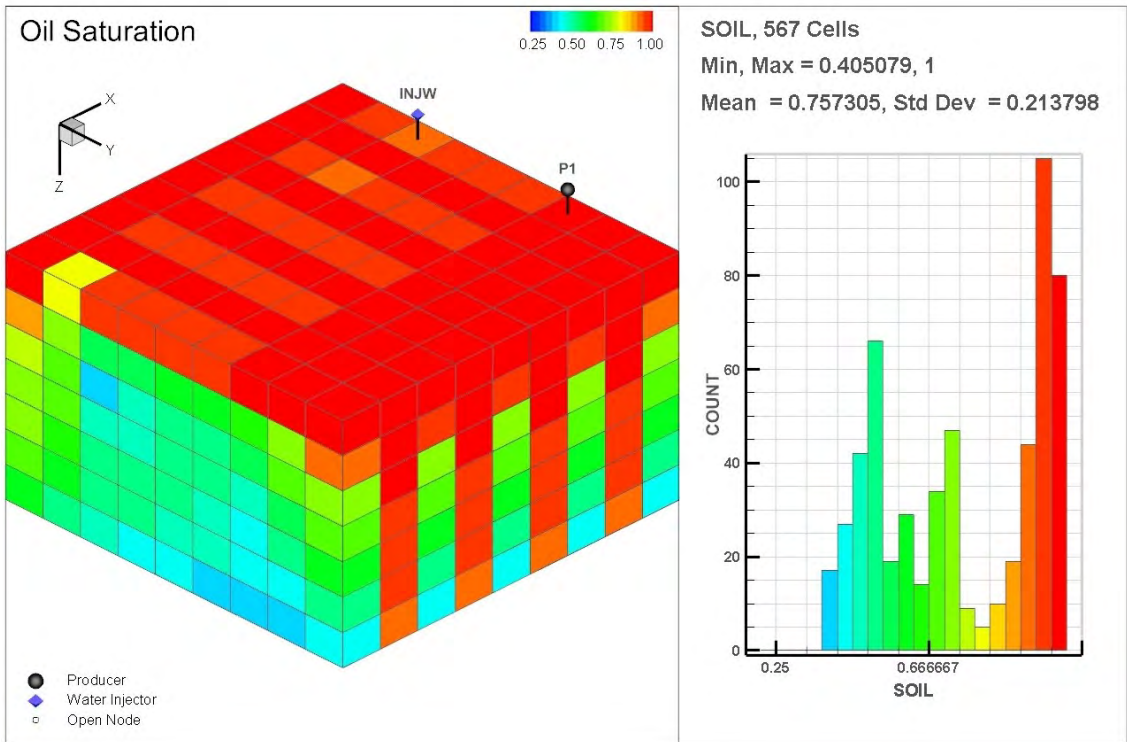
Injection rate of 1500m³/day: Heterogeneous case at the 3653rd day
 1 Jan 2026



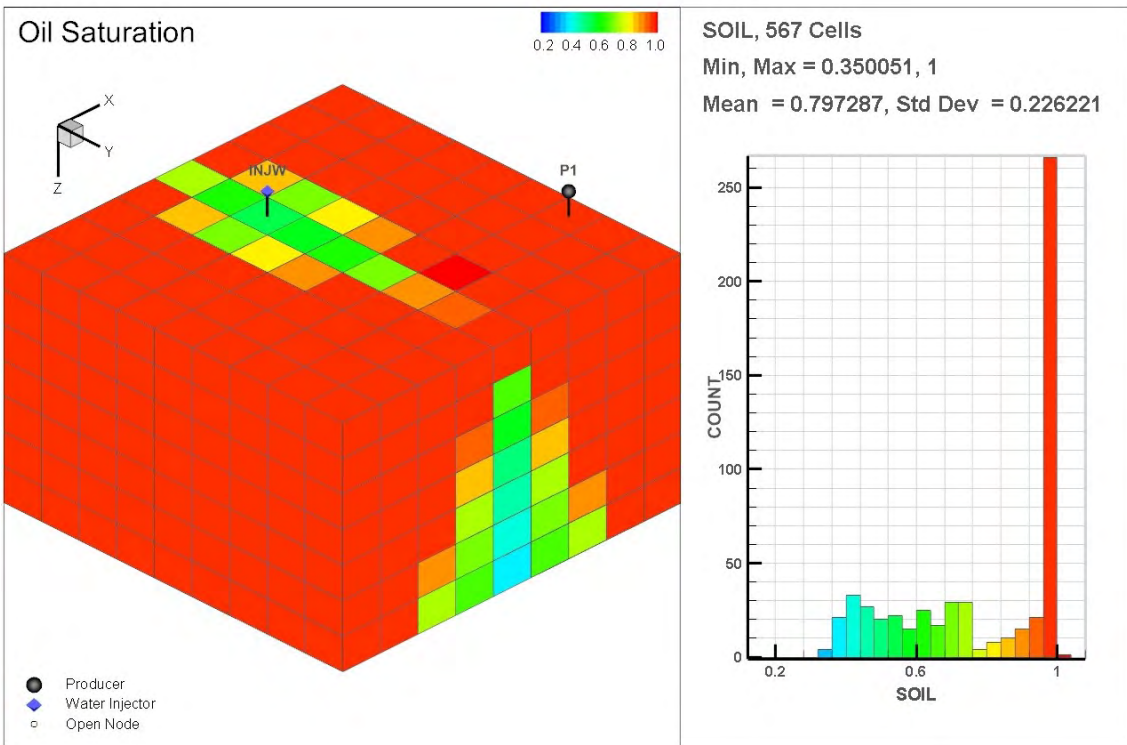
1 Jan 2026



Injection rate of 2000m³/day: Heterogeneous case at the 3653rd day
 1 Jan 2026

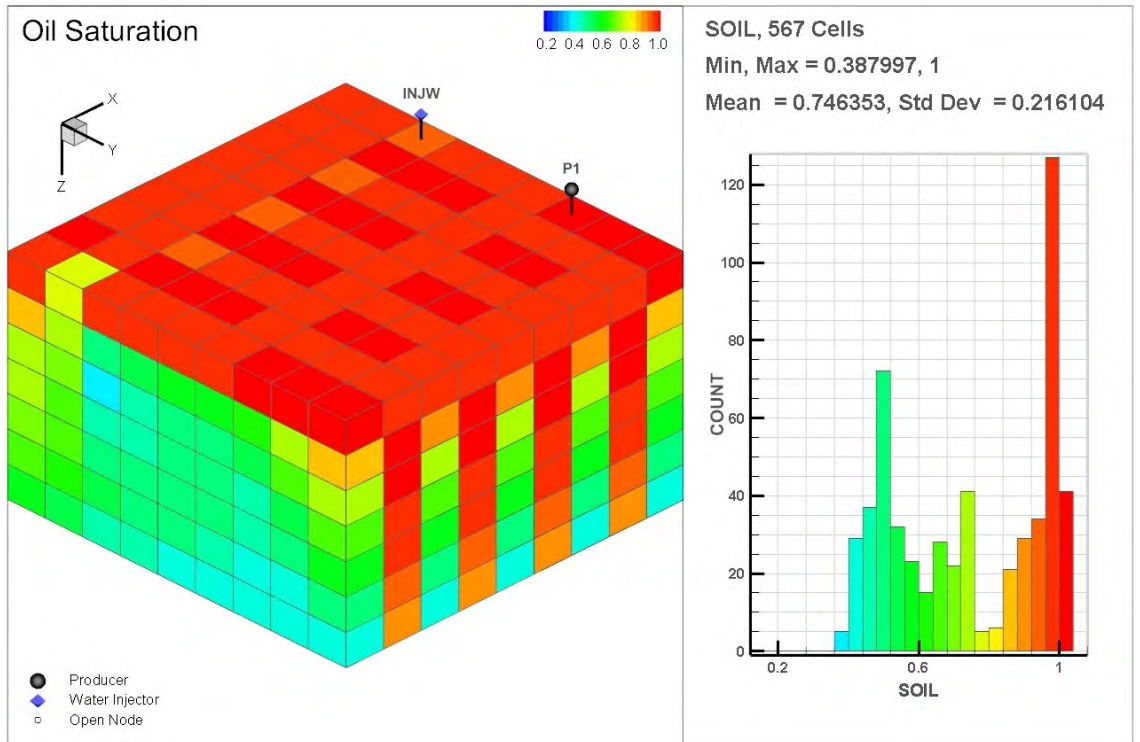


1 Jan 2026

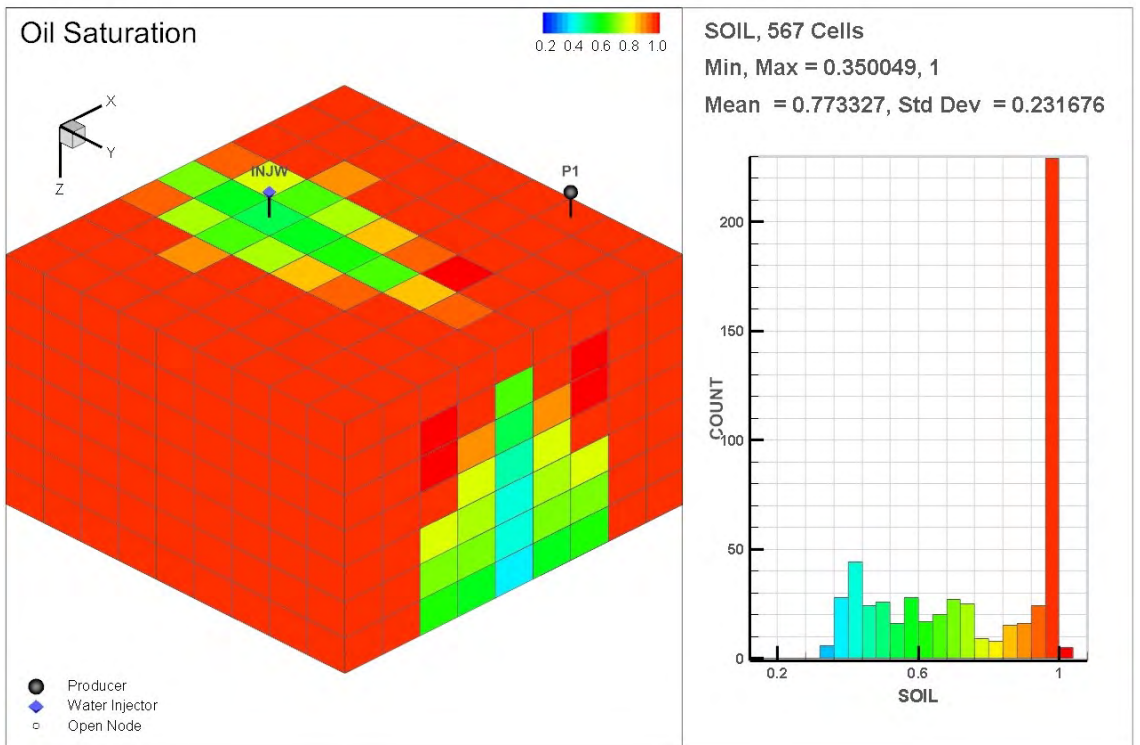


Injection rate of 2500m³/day: Heterogeneous case at the 3653rd day

1 Jan 2026



1 Jan 2026



Annex 9: Publications

Simulation of Horizontal and Vertical Water Flooding in a Homogeneous Reservoir Using ECLIPSE

Ambrose A. Ugwu and Britt M. E. Moldestad*
Department of Process, Energy and Environmental Technology
University College of Southeast Norway
Porsgrunn, Norway
Britt.Halvorsen@hit.no

Abstract— Over the recent years, several developments have been introduced within the field of oil and gas recovery, with the aim to maximize production. One of these developments is the use of water injection referred to as water flooding to improve oil and gas recovery. The objective of this work is to ascertain the optimal water injection arrangement between vertical and horizontal water flooding using ECLIPSE Reservoir simulation software. Within this work, analyses of oil production rate, water cut, reservoir pressure drop, accumulated oil production and recovery factor were made between horizontal and vertical water flooding in a homogeneous reservoir. Result shows that horizontal water flooding could be effective if water breakthrough is delayed. The increase in oil recovery achieved through this method varied between 6% and 36% while the delay in breakthrough varied between 459 days and 1362 days. This work also predicts production performance for ten years which would be useful for dynamic optimization of water flooding. However, reservoir heterogeneity would introduce geological uncertainty, which could bring mismatch between the simulated case and a real case.

Keywords— ECLIPSE; IOR; Waterflooding; Injection

I. INTRODUCTION

Water flooding is a secondary method of oil recovery where water is injected into the reservoir with the aim to increase the pressure and thereby increasing oil production [1]. Water flooding was first practiced for pressure maintenance after primary depletion and has since become the most widely adopted IOR technique [2]. It is now commonly applied at the beginning of reservoir development [2].

With water injection, the reservoir pressure is sustained and oil is pushed towards the production well. The oil-water front progresses toward the production well until water breaks through into the production stream. With the increasing water production, the oil production rate diminishes, until the time when the recovery is no longer profitable and the production is brought to an end [3]. Up to 35% oil recovery could be achieved economically through water flooding [3]. Fig. 1 depicts a typical horizontal and vertical water flooding arrangement respectively.

Water can be injected through a vertical or a horizontal well. Determining the optimal position and orientation of the wells has a potentially high economic impact [4]. One major difference between the horizontal and vertical water injection is the water breakthrough behavior. Asheim studied the

optimization of vertical well water flooding processes with fixed well locations [5] while Brouwer & Jansen studied the optimization of water flooding using a horizontal injection [6]. In both cases, delay in water breakthrough improves production rate. Also from literature, it has been shown that water breakthrough can be delayed by changing the position of the injection well profiles [6]. Studies also revealed that the use of horizontal well, delays the water breakthrough and improves the vertical sweep efficiency [7].

In this paper, computational study of water flooding in a homogenous reservoir was treated under 6 sections. Sections 1 and 2 deal with the introduction and the theory of water flooding. Section 3 describes the ECLIPSE mathematical model used in the simulations while Section 4 presents the reservoir model used for the simulations. The simulated results from the horizontal and vertical between water flooding are compared in Section 5 and finally some conclusions are drawn in Section 6.

II. THEORY

The principal reason for water flooding is to increase the oil production rate and improve oil recovery. This is achieved through voidage replacement to support the reservoir pressure and sweep or displace oil from the reservoir towards the production well [8]. The efficiency of such displacement depends on many factors like oil viscosity, density and rock characteristics. Reservoir screening is necessary for the technical and economic success of water flooding.

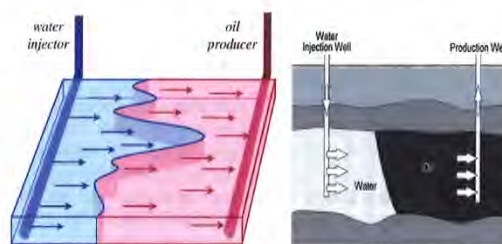


Fig. 1. Typical Horizontal[3] And Vertical Water Flooding [1]: left (Horizontal flooding) and right (Vertical flooding)

A. Residual Oil Saturation

Residual oil saturation and connate water saturation are very important numbers in water flooding. The connate water saturation is saturation is the lowest water saturation found in situ and determines how much oil is present initially, while the residual oil saturation indicates how much of the original oil in place (OOIP) will remain in the pores after sweeping the reservoir with injected water [8]. Equation (1a) represents the unit-displacement efficiency with the condition that the oil formation volume factor is the same at the start and the end of the water flooding [8].

$$E_D = 1 - \frac{S_{orw}}{S_{oi}} \quad (1)$$

$$S_{orw} = 1 - S_{wc} \quad (2)$$

where E_D is the unit displacement efficiency S_{oi} is the initial oil saturation, S_{orw} is the residual oil saturation and S_{wc} is the connate water saturation.

B. Wettability

The wettability of a reservoir rock can be defined as the tendency of a fluid to spread on, or to adhere to a solid surface in the presence of another immiscible fluid [9]. In an oil- water system it is a measure of the preference the rock has for either oil or water [10]. Changes in wettability influence the capillary pressure, irreducible water saturation, relative permeability and water flood behavior [10]. Maximum oil production rate by water flooding is normally achieved at water-wet conditions shortly after water breakthrough [11].

C. Capillary Pressure

Capillary pressure is the pressure difference existing across the interface separating two immiscible fluids in porous media. Capillary pressure determines the amount of recoverable oil for water flooding applications through imbibition process for water wet reservoir [8].

D. Relative Permeability

The Relative permeability is the ratio of the effective permeability to the absolute permeability of each phase. It is expressed for a specific saturation of the phases in (3):

$$k_{r,i} = \frac{k_i}{k} \quad (3)$$

where $k_{r,i}$ is the phase relative permeability, k is the total effective permeability and k_i is the phase effective permeability.

Relative permeability affects the unit displacement efficiency and how much of the OOIP will be recovered before the water flooding economic limit is reached. When the interfacial tension between oil and gas phases decreases, the relative permeability values change [12], which influences the oil and gas recovery as well as the reservoir pressure. Fig. 2 shows the plot of relative permeability curve used for the simulation.

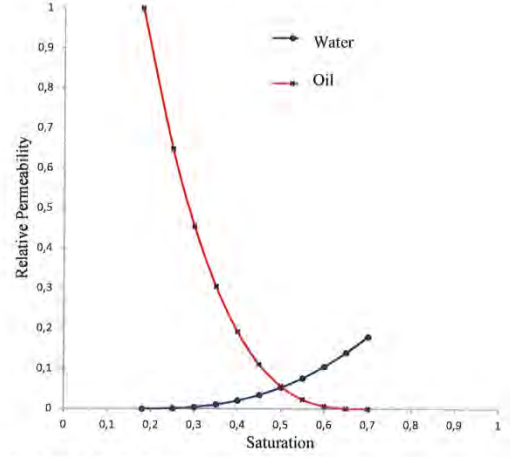


Fig. 2. Relative Permeability curve (water-wetted)

E. Mobility

Mobility, λ is described as the ratio between the endpoint effective permeability and the fluid viscosity, μ . It shows how easy the fluid is flowing through a porous medium [14]. Mobility ratio, M , plays an important role during water flooding. It can be defined as the ratio between the mobility of the displacing fluid (water) and the displaced fluid (oil) as expressed in (4) [14]:

$$M = \frac{\lambda_{(displacing)}}{\lambda_{(displaced)}} = \frac{K_{r(displacing)} \cdot \mu_{(displaced)}}{K_{r(displaced)} \cdot \mu_{(displacing)}} \quad (4)$$

where M is the mobility ratio, λ is the mobility, k_r is the relative permeability, μ is the viscosity. The subscripts displacing and displaced represent the displacing phase and the displaced phases respectively.

Mobility ratio is considered to be either favorable if the value is less than or equal to unity or unfavorable if the value is greater than unity [8]. Favorable mobility ratio means that the displaced phase (oil) can move more quickly than the displacing phase (water) through the reservoir rock.

III. COMPUTATIONAL MODEL

ECLIPSE Reservoir simulation is a form of numerical modeling used to quantify and interpret physical phenomena with the ability to predict future performance. The process involves dividing the reservoir into several discrete units in three dimensions, and modeling the progression of reservoir and fluid properties through space and time in a series of discrete steps [15]. Equations (5-11) are solved for each cell and each time step which are a combination of the material balance equation and Darcy's law [16].

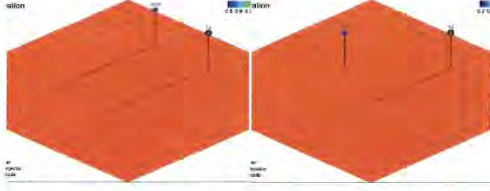


Fig. 3. Reservoir Geometry (3D): left (horizontal injection) and right (vertical injection)

1) Darcy's law (without gravity term) is expressed as:

$$q = -\frac{k}{\mu} \nabla P \quad (5)$$

where q is the flux, k is the permeability; μ is the viscosity and ∇P is the pressure gradient.

2) Material Balance is expressed as: (Mass Flux = Accumulation + Injection/Production):

$$-\nabla \cdot M = \frac{\partial}{\partial t} (\phi \rho) + Q \quad (6)$$

where M is the mobility ratio, ϕ is the porosity, ρ is density and Q is volume flow rate.

3) Simulator Flow Equation (with gravity term) is expressed as:

$$\nabla \cdot [\lambda (\nabla P - \gamma \nabla Z)] = \frac{\partial}{\partial t} \left(\frac{\phi}{\beta} \right) + \frac{Q}{\rho} \quad (7)$$

$$\lambda = -\frac{k}{\mu \beta} \quad (8)$$

where λ is mobility, t is time, β is momentum transfer coefficient, γ is relative gravity and Z is vertical position.

4) Well Model is expressed as:

$$q_{p,j} = T_{w,j} M_{p,j} (P_j - P_w - H_{w,j}) \quad (9)$$

$$M_{o,j} = \frac{K_{o,j}}{B_{o,j} \cdot \mu_{o,j}} + R_v \frac{K_{g,j}}{B_{g,j} \cdot \mu_{g,j}} \quad (10)$$

$$M_{g,j} = \frac{K_{g,j}}{B_{g,j} \cdot \mu_{g,j}} + R_s \frac{K_{o,j}}{B_{o,j} \cdot \mu_{o,j}} \quad (11)$$

where T is the transmissibility, P is the pressure, H is the pressure head, B is the formation volume factor, R_s is the gas-oil ratio and R_v is the oil-gas ratio. The subscripts p is phase, j is connection, w is well, o is oil and g is gas.

IV. ECLIPSE SIMULATION

Simulations were carried out for 10 years by injecting water at a constant rate through a horizontal and a vertical well respectively. In both cases, water was injected at the same depth as the production well. Also the same lateral distance was maintained between the injection well and the production

for both cases. Different simulations were performed by varying injection rate from 200m³/day to 2,500 m³/day for each case. A base case without water injection was considered for reference.

A. Geometry

Rectangular reservoir geometry was considered with the dimension 900m x 900m x 70m. Fig. 3 shows the reservoir geometry for the horizontal and the vertical water injection used in the simulation. The horizontal production (P1) and injection (INJW) wells are 800m long respectively while the length of the vertical injection well (INJW) is 40m.

B. Reservoir Conditions

The reservoir is homogeneous and consists of water-wetted rock. Although the reservoir fluid consists of live black oil, gas production was not considered for simplicity. The composition of oil components is assumed to be constant relative to pressure and time. It is also assumed that the reservoir fluid is Newtonian and that Darcy's law applies. The reservoir conditions used for the simulation are summarized in Table I.

C. Initial Conditions

Initially, the reservoir is assumed to be in hydrostatic equilibrium consisting of only oil. Table II shows the initial conditions considered during the simulation.

TABLE I. RESERVOIR CONDITIONS

Parameter	Value	Unit
Components	Oil, water and gas	-
Wettability	Water-wetted	-
Porosity	0.25	-
X Permeability	1	Darcy
Y Permeability	1	Darcy
Z Permeability	0.1	Darcy
Rock compressibility @ 10Bar	5.0E-5	/Bar
Oil gravity	35	°Api
Residual oil saturation	0.3	-
Oil viscosity @ 320Bar	3	cP
Water Density	1000	kg/m ³
Water viscosity	0.5	cP
Connate water saturation	0.2	-
Gas density	1	kg/m ³
Total simulation time	3653 (10 years)	days
No of Grids	567 (9x9x7)	-

TABLE II. INITIAL CONDITIONS

Initial condition	Value	Unit
Reservoir pressure	320	Bar
Bottomhole pressure	310	Bar
Bubble point pressure	182	Bar
Oil saturation	1	-
Water saturation	0	-
Gas saturation	0	-

V. RESULTS AND DISCUSSION

In this simulation, analysis of the oil production rate, water cut, reservoir pressure, accumulated oil production and recovery factor were made for the horizontal and vertical water flooding. A base case without water injection was also considered as reference.

A. Production Rate Trend

Fig. 4 shows the oil production rate for horizontal and vertical water injection respectively. The plot shows that horizontal water flooding maintains higher oil production rate for a longer period until water breaks through. After water breakthrough, the production rate drops more for horizontal water flooding than the vertical case. This may be attributed to rapid water production in all zones in the horizontal water flooding case, whereas for the vertical case water breakthrough occurs first in a few zones. The production rate for the base case is very low compared to the cases with water flooding. This is in agreement that water flooding improve the oil production rate [2].

B. Reservoir Pressure Trend

Fig. 5 shows the simulated reservoir pressure trend. For injection rates less than $1500\text{m}^3/\text{day}$, the pressure drop with horizontal injection is between 4% and 6% less than for the vertical case. For injection rates between $1500\text{m}^3/\text{day}$ and $2500\text{m}^3/\text{day}$, the pressure drop is between 9% and 14% less with horizontal flooding compared to vertical flooding.

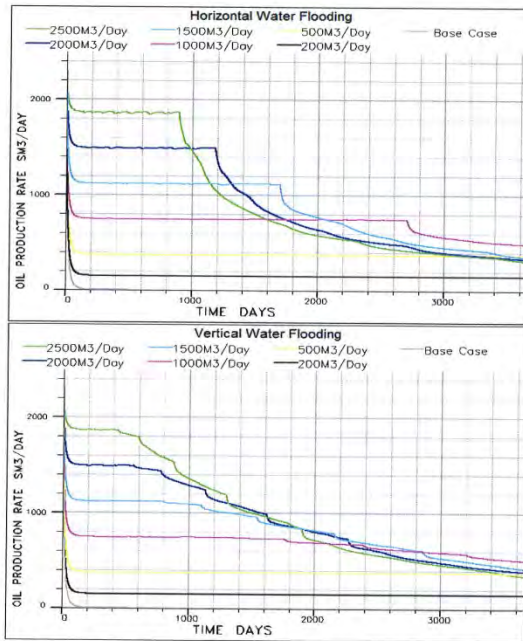


Fig. 4. Plot of oil production rate against time: upper plot (horizontal injection) and lower plot (vertical injection)

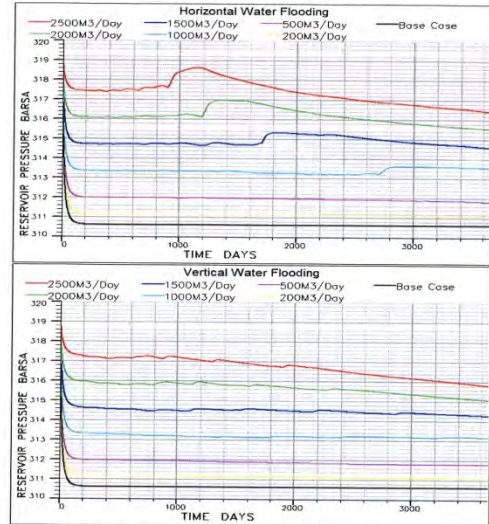


Fig. 5. Plot of reservoir pressure against time: upper plot (horizontal injection) and lower plot (vertical injection)

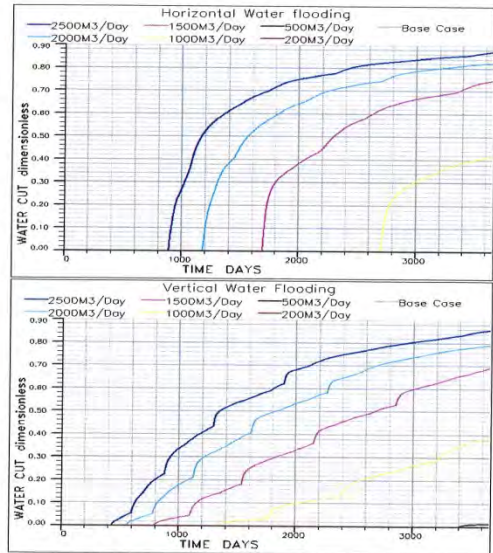


Fig. 6. Plot of watercut against time: upper plot (horizontal injection) and lower plot (vertical injection)

C. Watercut Trend

The water cut trend is shown in Fig. 6. It is observed that water breakthrough is delayed between 459 days and 1362 days with horizontal case compared with the vertical case. Despite of the late water breakthrough, the water cut after 3653 days is higher using horizontal flooding in all the cases.

D. Accumulated Oil Production

Fig. 7 shows the accumulated oil production trend. The plot shows that the accumulated oil production with horizontal flooding is higher for injection rates less than 1500m³/day due to lower pressure drop in the reservoir. For injection rates greater than 1500m³/day, accumulated oil production using horizontal flooding is less than for vertical flooding. This may be attributed to the rapid water production in horizontal flooding as opposed to vertical flooding.

The plot of the recovery factor against injection rate shown in Fig. 8 indicates that the recovery factor with horizontal flooding is less than for vertical flooding for injection rates greater than 1500m³/day. This may be due to rapid water breakthrough.

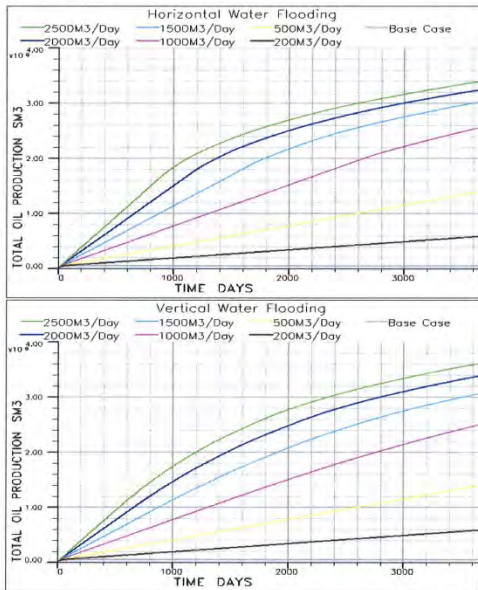


Fig. 7. Plot of accumulated oil production against time: upper plot (horizontal injection) and lower plot (vertical injection)

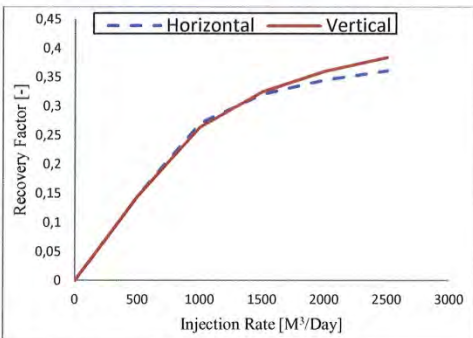


Fig. 8. Plot of recovery factor against injection rate

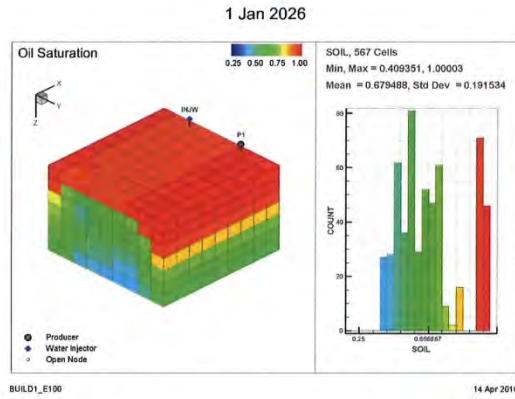


Fig. 9. Oil saturation distribution for horizontal injection after 10 years

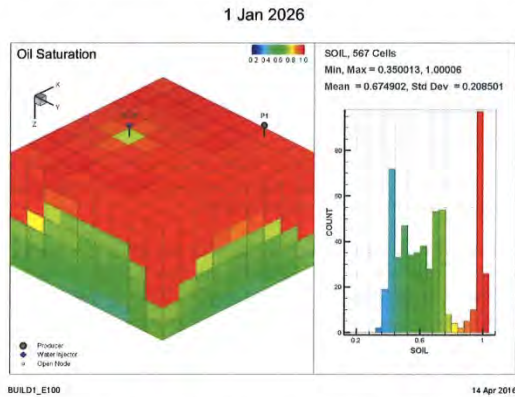


Fig. 10. Oil saturation distribution for vertical injection after 10 years

E. Oil Saturation distribution

The case for water injection at 1500m³/day is chosen to illustrate how oil saturation is distributed in the reservoir over time for horizontal and vertical water injection respectively. Initially, the oil saturation is 1 for both cases as shown in Fig. 3.

Fig. 9 shows the oil saturation distribution for horizontal injection after ten years. It can be seen that about 32% oil recovery was achieved through water flooding.

Fig. 10 shows the oil saturation distribution for vertical injection after ten years. About 33% oil recovery was achieved through water flooding.

F. Oil-Water Front Progression

The case for water injection at 1500m³/day is used to illustrate how water displaces oil and sweeps oil towards the production well in the reservoir. Fig. 11 shows the plan view of the oil-water front progression for the horizontal and vertical water injection after two years.

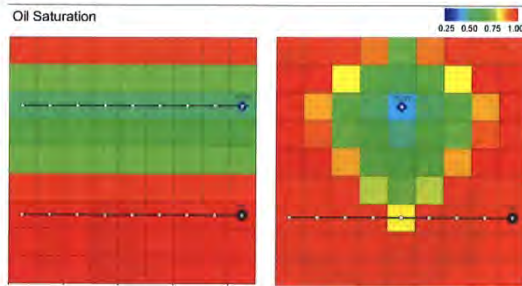


Fig. 11. Plan view of oil-water front progression after 2 years: left (horizontal injection) and right (vertical injection)

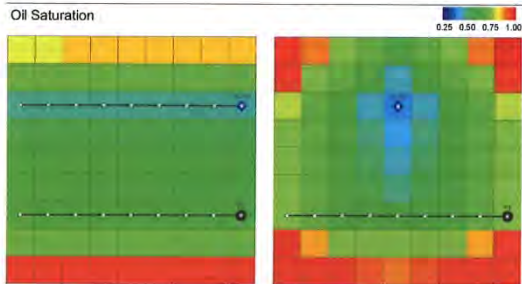


Fig. 12. Plan view of oil-water front progression after 10 years: left (horizontal injection) and right (vertical injection)

The oil-water front progression after ten years is shown in Fig. 12. From the plot, it can be seen that the oil saturation reduced due to more sweep by water injection. In general, result shows that oil-water front progresses laterally for horizontal flooding and radially for vertical flooding

VI. CONCLUSION

This paper compares oil production rate, water cut, reservoir pressure drop, accumulated oil production and recovery factor between horizontal and vertical water flooding in a homogeneous reservoir. The simulation was performed over ten years (3653 days) using ECLIPSE Reservoir simulator.

Result shows that horizontal water flooding maintains higher oil production rate for a longer period until water breakthrough. It is also observed that water breakthrough is earlier and water production increases gently with vertical flooding unlike the horizontal case where the water breakthrough comes late but water production increases rapidly with time.

The pressure drop is higher with vertical flooding in all cases compared with the horizontal flooding. This may be due to gravity effect and flow distribution in the reservoir. More difference in pressure drop is noticed between horizontal and vertical flooding with increase in injection rate.

Despite higher reservoir pressure and delay in water breakthrough, horizontal flooding accounts for less oil recovery due to rapid water production. With the implementation of inflow control device to reduce water production, oil recovery through horizontal water flooding would be optimal and more effective than vertical water flooding.

REFERENCES

- [1] G. E. P. LLC. (2016). Water Flooding. Available: <http://www.gtnenergypartners.com/technology/waterflooding>
- [2] N. Morrow and J. Buckley, "Improved oil recovery by low-salinity waterflooding," *Journal of Petroleum Technology*, vol. 63, pp. 106-112, 2011.
- [3] G. Van Essen, M. Zandvliet, J. Jansen, D. Hof, P. M. Van, and O. Bosgra, "Robust optimization of oil reservoir flooding," in *Computer Aided Control System Design, 2006 IEEE International Conference on Control Applications, 2006 IEEE International Symposium on Intelligent Control, 2006 IEEE*, 2006, pp. 699-704.
- [4] W. Bangerth, H. Klie, M. Wheeler, P. Stoffa, and M. Sen, "On optimization algorithms for the reservoir oil well placement problem," *Computational Geosciences*, vol. 10, pp. 303-319, 2006.
- [5] M. Zandvliet, M. Handels, G. van Essen, R. Brouwer, and J.-D. Jansen, "Adjoint-based well-placement optimization under production constraints," *SPE Journal*, vol. 13, pp. 392-399, 2008.
- [6] D. Brouwer, J. Jansen, S. Van der Starre, C. Van Kruijsdijk, and C. Berentsen, "Recovery increase through water flooding with smart well technology," in *SPE European Formation Damage Conference*, 2001.
- [7] R. Baker, "Reservoir management for waterfloods-Part II," *Journal of Canadian Petroleum Technology*, vol. 37, 1998.
- [8] S. o. P. Engineers. (2014). Microscopic Efficiency of Waterflooding. Available: <http://petrowiki.org/Waterflooding>
- [9] W. Owens and D. Archer, "The effect of rock wettability on oil-water relative permeability relationships," *Journal of Petroleum Technology*, vol. 23, pp. 873-878, 1971.
- [10] W. G. Anderson, "Wettability literature survey part 5: the effects of wettability on relative permeability," *Journal of Petroleum Technology*, vol. 39, pp. 1,453-1,468, 1987.
- [11] P. Jadhunandan and N. R. Morrow, "Effect of wettability on waterflood recovery for crude-oil/brine/rock systems," *SPE reservoir engineering*, vol. 10, pp. 40-46, 1995.
- [12] Y. Al-Wahaibi, C. Grattoni, and A. Muggeridge, "Drainage and imbibition relative permeabilities at near miscible conditions," *Journal of Petroleum Science and Engineering*, vol. 53, pp. 239-253, 2006.
- [13] T. Ydstebø, "Enhanced Oil Recovery by CO₂ and CO₂-Foam in Fractured Carbonates," 2013.
- [14] Schlumberger, "ECLIPSE Reservoir Simulation Software - Technical Description." vol. 2013.1, ed, 2013.
- [15] Schlumberger, ECLIPSE Blackoil Reservoir Simulation vol. 2.0, 2008.

The Application of Inflow Control Device for an Improved Oil Recovery Using ECLIPSE

Ambrose A. Ugwu and Britt M. E. Moldestad*
 Department of Process, Energy and Environmental Technology
 University College of Southeast Norway
 Porsgrunn, Norway
 Britt.Halvorsen@hit.no

Abstract— The rate of inflow to a horizontal well can vary along the completion length due to some reasons such as frictional pressure losses or heterogeneity in reservoir permeability. These variations reduce oil sweep efficiency and the ultimate recovery. Owing to this, it is necessary to manage fluid flow through the reservoir in order to maximize oil recovery along horizontal wells. One increasingly popular approach is to use inflow control devices that delay water and gas breakthrough into the well. Inflow control devices balance the inflow coming from the reservoir toward the wellbore by introducing an extra pressure drop. This paper presents the mathematical models used for the implementation of ICD in ECLIPSE. A case study using reservoir conditions similar to Troll offshore Norway was simulated to illustrate the effect of ICD in a heterogeneous reservoir. The simulation result shows that with ICD completion, water breakthrough was delayed for 262 day and water cut after 3000 days reduced by 11%. Despite the delay in water breakthrough, the oil production rate decreased. Although well productivity is reduced by approximately 42%, there is an improved degree of inflow equalization through ICD completion. Gas production was decreased by approximately 51% with ICD completion.

Keywords— ECLIPSE; IOR; ICD; Inflow

I. INTRODUCTION

The challenges introduced by reservoir heterogeneity with horizontal wells tends to increase with increasing well length [1]. Completions with long intervals often have significantly uneven specific inflow distribution along their length. These inflow variations cause premature water or gas breakthrough and should be minimized [2]. Advanced well completions have been demonstrated as solution to these challenges. Inflow Control Devices (ICDs) is an established type of advanced completions that provide passive inflow control [3]. ICDs are widely used and can be considered to be a mature well completion technology. One of the challenges is the variation in rock properties. Fluid specific inflow rate tends to increase with increasing well length [4]. The performance of ICDs can be analyzed in detail with the help of various reservoir simulation tool such as ECLIPSE [1, 5]. ECLIPSE includes basic functionality for ICD modeling [1] and also offer a practical means to capture the effect of annular flow. ICDs are static and usually installed at the beginning of the production life. An alternative technology is the use of autonomous inflow control device with the ability of closing off the flow interval in an event of water or gas breakthrough [1].

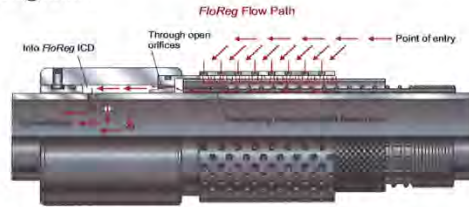


Fig. 1. Oriface ICD [1].

This paper presents ECLIPSE model for the application of ICD in heterogeneous reservoirs. From the mathematical models, the parameters that substantially reduce the inflow variation can be determined. A case study was simulated to illustrate the impact of a specific ICD completion on inflow performance at Troll offshore Norway.

II. ECLIPSE COMPUTATIONAL MODEL

In ECLIPSE, ICD is used to control the inflow profile along a horizontal well or branch by imposing an additional pressure drop between the sand face and the tubing. The device is placed around a section of the tubing and diverts the fluid inflowing from the adjacent part of the formation through a sand screen and then into a spiral before it enters the tubing [6].

A. Pressure drop

The pressure drop across the device is calculated from calibration data, adjusted to allow for the varying density and viscosity of the reservoir fluid flowing through the device. The pressure drop equation is shown in equation (1) below [7].

$$\delta P = \left(\frac{\rho_{cal} \cdot \mu_{mix}}{\rho_{mix} \cdot \mu_{cal}} \right)^{1/4} \cdot \frac{\rho_{mix}}{\rho_{cal}} \cdot K \cdot q^2 \quad (1)$$

Here ρ_{mix} is the density of the fluid mixture in the segment at local conditions and ρ_{cal} is the density of the fluid used to calibrate the ICD. μ_{mix} is the viscosity of the fluid mixture in the segment at local conditions and μ_{cal} is the viscosity of the fluid used to calibrate the ICD. K is the base strength of the ICD defined in equation (2).

$$K = \frac{a_{ICD}}{\rho_{cal} \cdot q}, \quad (2)$$

where a_{ICD} is defined as the strength of the ICD, q is the volume flow rate of fluid mixture through the ICD at local conditions, which is equal to the volume flow rate through the

ICD segment multiplied by a scaling factor that depends on the length of the device.

The density of the fluid mixture at local segment conditions is given in equation (3)

$$\rho_{mix} = \alpha_o \cdot \rho_o + \alpha_w \cdot \rho_w + \alpha_g \cdot \rho_g \quad (3)$$

where $\alpha_{o,w,g}$ is the volume fraction of the free oil, water, gas phases at local conditions and $\rho_{o,w,g}$ is the density of the oil, water, gas phases at local conditions[7].

The viscosity of the fluid mixture at local segment conditions is given in equation (4).

$$\mu_{mix} = (\alpha_o + \alpha_w) \cdot \mu_{emul} + \alpha_g \cdot \mu_g \quad (4)$$

where μ_{emul} is the viscosity of the oil-water emulsion at local conditions and μ_g is the gas viscosity at local conditions. The calculation of μ_{emul} is described in "Emulsion viscosity" section [7].

To include a series of these devices in a multi-segment well, the devices should be represented by segments branching off the tubing as shown in Figure 2. The grid block connections are located in the ICD segments instead of the segments representing the well tubing. The ICD segments should be given a very small length (of the order, say, of the wellbore radius). This length is not used in the pressure loss calculations, but it influences the location of the connections of the grid block in the reservoir. The ICD segments were given the same depth as their 'parent' tubing segments, so that there will be no hydrostatic head across them [8]. The pressure loss across an ICD segment is reported as the friction pressure loss; the acceleration pressure loss is set to zero.

B. Emulsion Viscosity

The emulsion viscosity is a function of the local phase volume fractions in the segment and has differing functional forms at low water in liquid fractions (when oil is the continuous phase) and high water in liquid fractions (when water is the continuous phase) [7]. A critical water in liquid fraction as shown in figure 3 is used to select between equations (5) and (6) below.

$$\mu_{wio} = \mu_o \cdot \left(\frac{1}{1 - \left(\frac{0.8415}{0.7480} \alpha_{wl} \right)} \right)^{2.5} \quad (5)$$

$$\mu_{oiw} = \mu_w \cdot \left(\frac{1}{1 - \left(\frac{0.6019}{0.6410} \alpha_{ol} \right)} \right)^{2.5} \quad (6)$$

where μ_{wio} is the water-in-oil emulsion viscosity (when oil is the continuous phase), μ_{oiw} is the oil-in-water emulsion viscosity (when water is the continuous phase) and μ_o is the oil viscosity at local conditions, α_{wl} is the local water in liquid fraction and α_{ol} is the local oil in liquid fraction.

The water-in-oil viscosity is subject to an upper limit expressed as a maximum ratio of water-in-oil viscosity to oil viscosity.

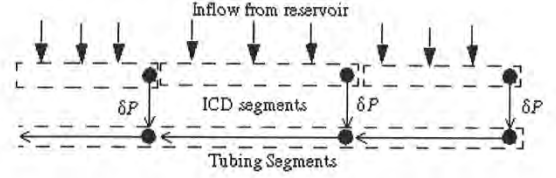


Fig. 2. Segments ICDs along the well.

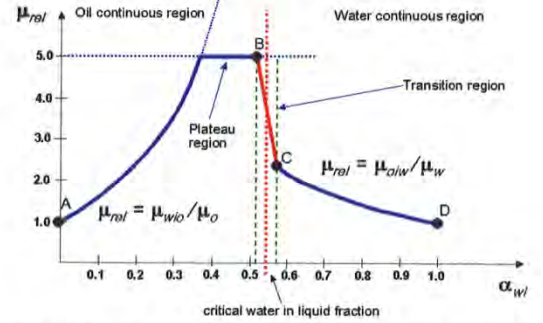


Fig. 3. Phase Transition region about the critical water in liquid fraction [7].

This usually results in a 'plateau' region within which the water-in-oil viscosity is at its maximum permitted value as shown schematically in Fig. 3, with the maximum viscosity ratio set at 5.0 [7]. This upper limit also applies to the oil-in-water viscosity, but is less commonly encountered. At the critical water in liquid fraction there is a jump in emulsion viscosity as the continuous phase changes. Such a discontinuity would cause stability problems in the simulator and a transition region is defined about the critical water in liquid fraction to avoid this. In this region the emulsion viscosity is linearly interpolated between the water-in-oil and oil-in-water viscosities at the edges of the region; the viscosity is thus a continuous function of the water in liquid fraction. This transition region is presented schematically in Fig. 3, with the linear interpolation shown in red between points B and C [7].

III. CASE STUDY

A study was considered with reservoir conditions similar to the Troll field, Norway to illustrate the effect of ICD on oil recovery, reservoir sweep, delay in water breakthrough and decrease in water cut. Troll is a large subsea offshore Norway. The challenge is to drill and complete well in a way that gas and water do not have easy access to the production well [3]. The main oil reservoir at Troll is the Late Jurassic Sognefjord Formation. This formation consists of Sandstone and siltstone with thickness of about 160m. The porosity vary between 30 - 35% and permeability between 1 - 20D. The reservoir driving mechanism is mainly gas expansion and water drive. Horizontal wells are located close to the oil-water contact in order to reduce gas breakthrough[3].

Simulation was carried out for 3000 days. Water drive was achieved by connecting analytical aquifer (Fetkovich aquifer) at the bottom of the reservoir. Frictional pressure drop and variation in permeability will lead to non-uniform inflow profile along the production well [9]. ICDs are set at two segments along the production open hole section to distribute downhole pressure to optimize fluid inflow along the entire production interval. Water saturation profile shown in Fig. 4 indicates that more water is produced at the 225m and 375m positions of the production well due to high permeability at these positions. To reduce water breakthrough, ICDs were placed at these positions. Each ICD joint is about 12m in length and about 3mm nozzle diameter. A base case without water ICD was considered for reference.

A. Geometry

Rectangular reservoir geometry was considered with the dimension 500m x 450m x 70m. The multi-segment horizontal production (PROD) well is of length 450m. The reservoir is heterogeneous with varying permeability from 1 to 20 Darcy. The areas of high permeability represents defeat in the reservoir see Fig. 5 and 6.

B. Reservoir Conditions

The reservoir is heterogeneous and consists of water-wetted rock. Although the reservoir fluid consists of live black oil, gas production was not considered for simplicity. The composition of oil components is assumed to be constant relative to pressure and time. It is also assumed that the reservoir fluid is Newtonian and that Darcy’s law applies. The reservoir conditions used for the simulation are summarized in Table I.

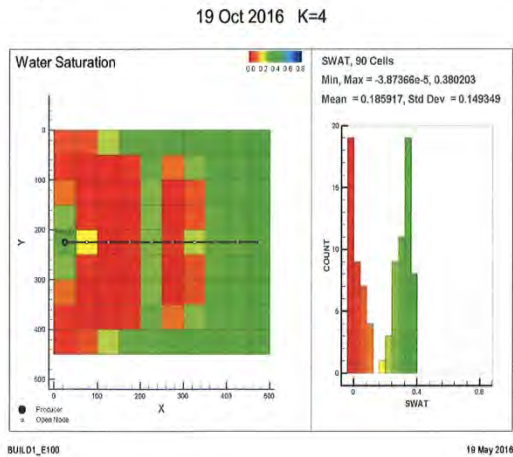


Fig. 4. ICD positions along the well

C. Assumptions

The following assumptions were made regarding the inflow:

1. Darcy’s law applies to the flow through the reservoir.
2. The flow into the well is at steady or pseudo-steady state.

3. The distance between the well and the reservoir boundary is longer than the length of the well length.

The following assumptions were made about the ICDs:

1. There is no flow in the annulus parallel to the base pipe. This means that fluid flows from reservoir directly through ICD screens into the base pipe [10].
2. ICDs installed are of the same strength. This is the most common type of ICD application due to the relative simplicity of its design and installation operation [3]. This is done in order to reduce the operational risks [5, 11].

D. Initial Conditions

Initially, the reservoir is assumed to be in hydrostatic equilibrium consisting of only oil. The the initial pressure is greater than the bubble point and water has much higher mobility than oil. Table II shows the initial conditions considered during the simulation.

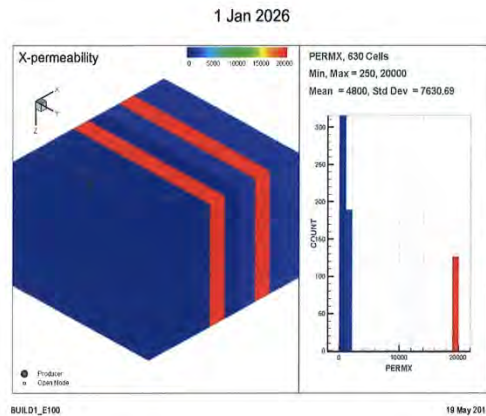


Fig. 5. Reservoir geometry showing the distribution of X and Y permeability

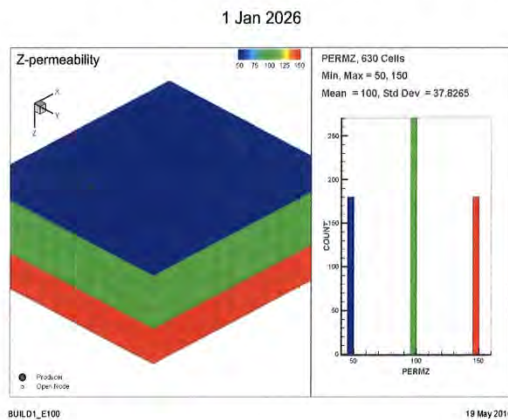


Fig. 6. Reservoir geometry showing the distribution of Z- permeability

TABLE I. RESERVOIR CONDITIONS

Parameter	Value	Unit
Components	Oil, water and gas	-
Wettability	Water-wetted	-
Porosity	0.30	-
X Permeability	0.1 - 20	Darcy
Y Permeability	0.1 - 20	Darcy
Z Permeability	0.1-1	Darcy
Rock compressibility @ 10Bar	5.0E-5	/Bar
Oil gravity	35	°Api
Residual oil saturation	0.3	-
Oil viscosity @ 320Bar	10	cP
Water Density	1000	kg/m ³
Water viscosity	0.5	cP
Connate water saturation	0.2	-
Gas density	1	kg/m ³
Well length	450	m
Target well flow rate	2000	Sm ³ /day
ICD Length	12	m
ICD Strength	0.00021	bar/(Rm ³ /day) ²
ICD nozzle diameter	3	mm
Total simulation time	3000	days
No of Grids	630 (10x9x7)	-

TABLE II. INITIAL CONDITION

Initial condition	Value	Unit
Reservoir pressure	320	Bar
Bottomhole pressure	310	Bar
Bubble point pressure	182	Bar
Oil saturation	1	-
Water saturation	0	-
Gas saturation	0	-

IV. RESULTS AND DISCUSSION

In this simulation, the effect of ICD completion on oil, water and gas production was investigated. Also the reservoir pressure trend recovery was discussed. A base case without ICD completion was considered as reference.

A. Reservoir Pressure

Fig. 7 shows the simulated reservoir pressure trend. The ratio of the total pressure drop without ICD completion to the total pressure drop with ICD is about 52. The high pressure drop for the case without ICD may be due to more reservoir depletion as a result of high water production. ICD tends to maintain the reservoir pressure by retaining water in the reservoir pore spaces.

B. Water Production

The water cut trend is shown in Fig. 8. It is observed that water breakthrough is delayed for 262 days (about 66%) with the installation of ICD. Also the water cut is reduced with about 11% after 3000 days with the ICD completion. This would be attributed to the restriction imposed on water flow due to the additional pressure drop with the ICD.

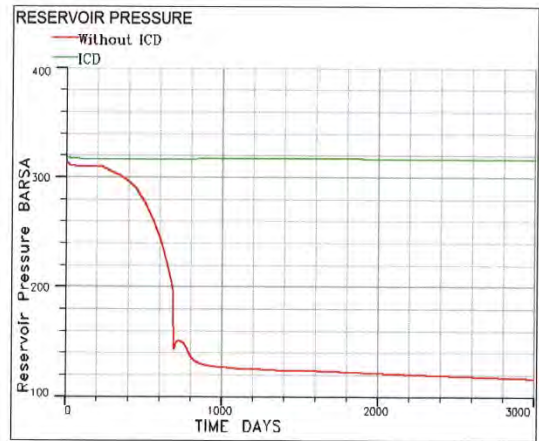


Fig. 7. Reservoir Pressure Trend

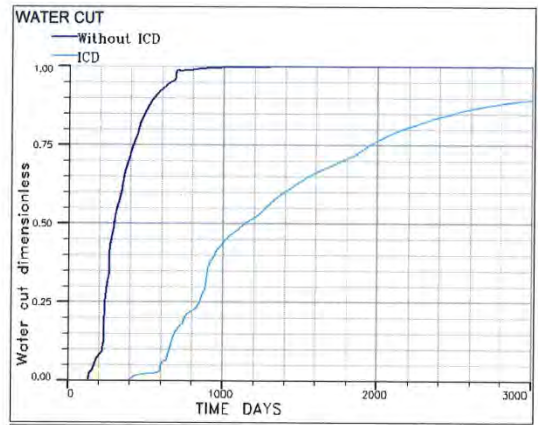


Fig. 8. Trend of water cut

C. Oil Production

Fig. 9 shows the oil production rate with and without ICD respectively. Although the water breakthrough is delayed with ICD, the oil production rate is lower compared with the case without ICD. After water breakthrough, the production rate drops more rapidly for the case without ICD. This may be attributed to rapid water production as there is no restriction towards water production. Shock wave was propagated at about 690th day due to sudden opening of valve to match up the production target for the case without ICD. This shock wave can lead to very high pressure buildup which could make the system to fail. With the ICD, this phenomenon is annulled through its equalization effect on flow variation making the system stable throughout the production life.

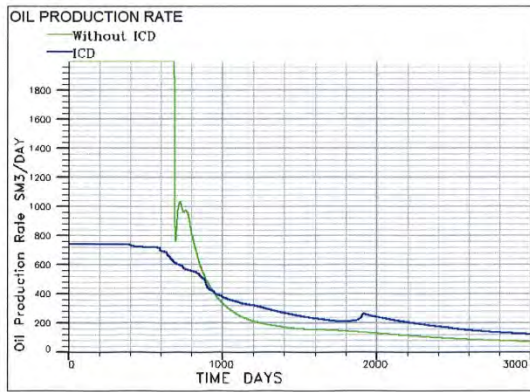


Fig. 9. Trend of Oil Production Rate

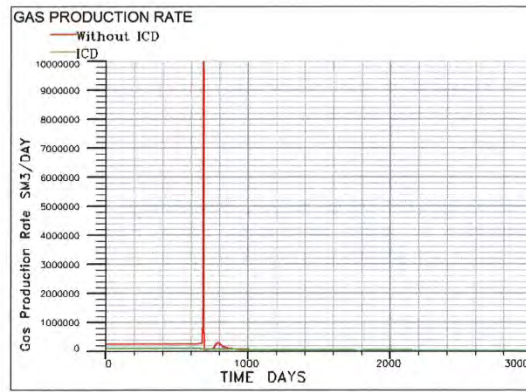


Fig. 11. Trend of Gas Production Rate

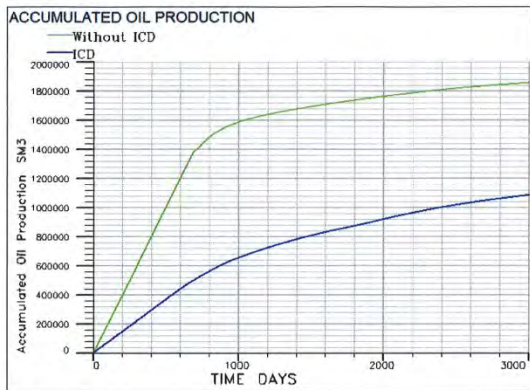


Fig. 10. Trend of Accumulated Oil Production

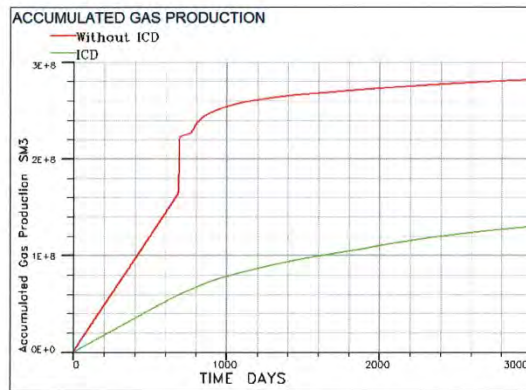


Fig. 12. Trend of the accumulated gas production

Although well productivity is reduced by approximately 42%, there is an improved degree of inflow equalization through ICD completion. The accumulated oil production is shown in Fig. 10. From the slope, production would be sustained more and the accumulated oil production expected to be higher over a long time with ICD completion.

D. Gas Production.

Fig. 11 shows the gas production rate with ICD and without ICD completions respectively. It can be seen that gas production rate is less with ICD completion throughout the production life. This may be attributed to rapid water production in the case without ICD as there is no restriction towards water production. Shock wave was propagated at about 690th day due to sudden opening of valve to match up production target for the case without ICD. This shock wave can lead to system failure as result of high pressure. This shock effect is not observed with ICD completion due to the restriction imposed by additional pressure drop and the equalization effect on flow variation.

With ICD completion, the system is stable throughout the production life. There is about 51% decrease in gas production as depicted in fig. 12 with ICD completion. This increase in gas production for the case without ICD may reduce well performance and recovery significantly as oppose to ICD completion.

V. CONCLUSION

This paper presents the mathematical models used for the implementation of ICD in ECLIPSE reservoir simulator. A case study using similar reservoir conditions as Troll offshore Norway was simulated to illustrate the effect of ICD in a heterogeneous reservoir. Analysis of oil, water and gas production was made within a simulation period of 3000 days.

Result shows that with ICD completion, water breakthrough was delayed with 262 day and water cut after 3000 days was reduced by 11%. Despite the delay in water breakthrough, the oil production rate was reduced due to flow restriction by additional pressure drop with ICD completion. A trade-off between well productivity and inflow equalization is important. Although well productivity is reduced by

approximately 42%, there is an improved degree of inflow equalization through ICD completion. Gas production was decreased by approximately 51% with ICD completion. With this reduction in gas production, well performance and ultimate recovery would improve. Result also indicates that the case with ICD completion sustains the reservoir pressure as water is forced to occupy the pore spaces of the reservoir.

It can be inferred that although ICD delays water and gas breakthrough, it could not stop the breakthrough. It would be appropriate to apply autonomous inflow control device instead, to stop gas and water breakthrough.


REFERENCES

- [1] V. Birchenko, A. I. Bejan, A. Usnich, and D. Davies, "Application of inflow control devices to heterogeneous reservoirs," *Journal of Petroleum Science and Engineering*, vol. 78, pp. 534-541, 2011.
- [2] J. Hallundbæk and P. Hazel, "Inflow control in a production casing," ed: Google Patents, 2010.
- [3] K. H. Henriksen, E. I. Gule, and J. R. Augustine, "Case Study: The Application of Inflow Control Devices in the Troll Field," in *SPE Europec/EAGE Annual Conference and Exhibition*, 2006.
- [4] D. Krinis, D. E. Hembling, N. J. Al-Dawood, S. A. Al-Qatari, S. Simonian, and G. Salerno, "SS-Optimizing Horizontal Well Performance In Non-Uniform Pressure Environments Using Passive Inflow Control Devices," in *Offshore Technology Conference*, 2009.
- [5] K. Muradov, V. Birchenko, and D. Davies, "Modeling of the Heel-toe Effect in a Horizontal Well with Inflow Control Devices," in *12th European Conference on the Mathematics of Oil Recovery*, 2010.
- [6] V. Mathiesen, B. Werswick, H. Aakre, and G. Elseth, "Autonomous Valve, A Game Changer Of Inflow Control In Horizontal Wells," in *Offshore Europe*, 2011.
- [7] Schlumberger, "ECLIPSE Reservoir Simulation Software - Technical Description," vol. 2013.1, ed, 2013.
- [8] C. D. Johnson and G. M. Oddie, "Flow control regulation method and apparatus," ed: Google Patents, 2004.
- [9] H. Aakre, B. Halvorsen, B. Werswick, and V. Mathiesen, "Smart well with autonomous inflow control valve technology," in *SPE Middle East Oil and Gas Show and Conference*, 2013.
- [10] L.-B. Ouyang, "Practical consideration of an inflow-control device application for reducing water production," in *SPE Annual Technical Conference and Exhibition*, 2009.
- [11] V. Birchenko, K. Muradov, and D. Davies, "Reduction of the horizontal well's heel-toe effect with inflow control devices," *Journal of Petroleum Science and Engineering*, vol. 75, pp. 244-250, 2010.

MASTER'S THESIS, COURSE CODE FMH606

Student: Ugwu Ambrose Anibueze

Thesis title: Improved Oil Recovery and The Study of CO₂ Storage in Oil/Gas Reservoirs and Aquifers

Signature:  ...02/06/2016

Number of pages: 148

Keywords: ECLIPSE, Waterflooding, ICD, IOR, CO₂, Water injection
.....

Supervisor: Prof. Britt M. E. Moldestad Sign.:

2nd supervisor: Vidar Mathiesen, Dr.ing Sign.:

Censor: Sign.:

External partner: InflowControl AS Sign.:

Availability: Open

Archive approval (supervisor signature): Sign.: **Date :**

Abstract:

As the world's energy needs grow, several techniques have been introduced for an improved oil recovery (IOR) and secured storage of CO₂. Such techniques include the use of water injection, CO₂ for Enhanced Oil Recovery (EOR) and the application of inflow control devices (ICD) with the aim to maximize production and improve well performance. To meet global energy demand with the instability in oil price, these IOR techniques through advanced well completion and stimulation techniques have enabled commercial production in reservoirs previously abandoned by traditional recovery methods. One of the objectives of this work is to ascertain the optimal water injection arrangement between vertical and horizontal water injection using ECLIPSE. Within this work, analyses of oil production, water breakthrough and pressure over simulation time were made. These analyses cover both cases of horizontal and vertical waterflooding in a homogeneous and a heterogeneous reservoir. In the results, it shows that the horizontal waterflooding provides longer delay in water breakthrough and increase in oil production. The increase in oil recovery achieved varies between 6% and 36% while the delay in breakthrough varies between 459 days and 1362 days. This work also presents the mathematical models used for the implementation of ICD in ECLIPSE. A case study using reservoir conditions similar to Troll offshore Norway was simulated to illustrate the effect of ICD in a heterogeneous reservoir. The simulation result shows that with ICD completion, water breakthrough could be delayed for 262 days and water cut after 3000 days reduced by 11%. Despite the delay in water breakthrough, the oil production rate decreased. Although well productivity is reduced by approximately 42%, there is an improved degree of inflow equalization through ICD completion. Gas production was decreased by approximately 51% with ICD completion. In addition to using CO₂ for EOR, it is crucial to store CO₂ to avoid the large contribution to global warming. It has been revealed that about 120 Giga tons of CO₂ would need to be captured and stored between 2015 and 2050 globally. Mature oil reservoirs and underlying aquifers are considered as the future solution for CO₂ storage. In this work, literature study was carried out to have a better understanding of the storage capacity and suitability for CO₂ storage in oil/gas reservoirs and aquifers. The study shows that residual gas trapping and the dissolution in water give greater contribution to CO₂ storage than the structure trapping mechanism.

University College of Southeast Norway accepts no responsibility for results and conclusions presented in this report.